MANNED SPACE-FLIGHT EXPERIMENTS

INTERIM REPORT

GEMINI V MISSION

AUDITORIUM OF THE FEDERAL OFFICE BUILDING-6
WASHINGTON, D. C.
JANUARY 6, 1966

NATIONAL AERONAUTICS AND SPACE ADMINISTRATION

FOREWORD

This compilation of papers constitutes an interim report on the results of experiments conducted during the Gemini V manned space flight. The results of experiments conducted on Gemini III and IV manned space flights have been published previously in a similar interim report, "Manned Space Flight Experiments Symposium, Gemini Missions III and IV," which is available upon request from MSC Experiments Program Office, Houston, Texas (Code EX, Attention of R. Kinard).

The Gemini V mission provided the greatest opportunity to date for conducting experiments; the increased mission duration of eight days provided this added capability. The total mission experiment complement was seventeen. Five experiments were designed to obtain basic scientific knowledge, five were medical, and seven were technological and engineering in nature. Six of the experiments had flown previously on Gemini IV, and eleven were new. The results of the experiments, including real-time modification to preflight plans made necessary by abnormal spacecraft system operation, are presented in the following papers.

In keeping with the primary purpose of this series of activities, which is the early reporting and dissemination of the results of Gemini flight experiments, it should be reiterated that some of the results presented are tentative. As Dr. Mueller pointed out by way of introduction to the previous symposium, the experimenters have in some cases not completed their analyses of the data. Moreover, a number of experiments will be repeated on future missions, and the total experiment will not be complete until all the missions have been conducted and the results correlated and analyzed.

CONTENTS

1. EXPERIMENT S-1, ZODIACAL LIGHT PHOTOGRAPHY

By E. P. Ney and W. F. Huch
University of Minnesota

The light of the moonless night sky as viewed from the ground consists principally of scattered light from cities, twilight and starlight, zodiacal light, airglow, and aurora.* All of these contributing sources vary with either time or position in the sky, or both. The quantitative observation of any of these from the ground is further complicated by the effects of scattering and absorption within the atmosphere. For several years, the University of Minnesota has carried out a program aimed at separating and understanding the individual contributions to the night sky brightness. In this study, we have used balloon-borne photometers, polarimeters, and special camera techniques. More recently, we have had the assistance of the manned space program in obtaining special photographs in earth-orbiting missions (MA-9 and Gemini V).

The principal purpose of this report is to describe the Gemini V observations in the context of their relation to ground-based and balloon experiments on dim-light phenomena.

Zodiacal light is the visible manifestation of dust grains in orbit about the sun. The brightness of the light at 20° elongation from the sun and on the ecliptic is about 2×10^{-12} of the sun's surface brightness, or about the same as the zenith sky observed from the ground at the time of full moon. At 60° elongation, the brightness is about 2×10^{-13} of the sun's surface brightness, or about one-half the brightness of the brightest milky way. At larger elongation angles, the zodiacal light becomes obscured by the terrestrial continuum airglow, which has an average surface brightness of about 2×10^{-14} of the sun's surface brightness. In the direction approximately opposite to the sun is the phenomenon of the gegenschein, which is believed to be about 2×10^{-14} of the sun's surface brightness. No previous attempts to photograph the gegenschein were successful.

---

*Although lightning is an important contributor and cerenkov light from cosmic-ray air showers is a detectable source, we confine ourselves here to slowly varying sources of light.

As observed from the ground, the zodiacal light is grossly distorted by the effects of atmospheric extinction. From balloons at 100 000 feet, the effects of atmospheric extinction may be essentially eliminated, even in the horizontal direction. Figure 1-1 shows a balloon photograph of the zodiacal light. The photograph was made with Ansco film 529, an f/0.8 lens, and a 1-minute exposure. The solar elongation in the horizontal direction is 21°. Figure 1-2 shows the star field, the horizontal, and the ecliptic appropriate for figure 1-1. The balloon photograph was made over Texas to eliminate aurora. The airglow shows in the photograph as a diffuse light increasing toward the horizontal, according to the Van Rijn variation of brightness with zenith angle. No twilight is evident in figure 1-1; however, measuring the zodiacal light from balloons is impossible at elongation angles of less than 19° because of the twilight. One of the objectives of the Gemini V experiment was to determine the minimum angle from the sun at which the zodiacal light could be studied without twilight contamination.

To estimate airglow contamination of zodiacal light measurements in the visible region of the spectrum, an experiment was performed in the MA-9 flight (ref. 1). Cooper carried a camera with an f/1 lens and photographed the airglow in profile from above, with exposures of 10 seconds, 30 seconds, and 120 seconds on Ansco film 529. Figure 1-3 shows one of these photographs. The moon had not risen, so the earth is dark, the horizon is delineated by very distant lightning strokes, and the airglow layer shows with a sharp line on top and a rather diffuse illumination below. These photographs showed that the majority of the light in the visible region of the spectrum arises in a layer 20 km thick and at an altitude of about 95 km. Although this result was not unexpected, it had not previously been demonstrated because height measurements of the airglow have been made for selected lines and small regions of the continuum. The principal brightness, however, is throughout the continuum, and broad-band spectral observations with the MA-9 photographs show that all the important illumination within the film bandwidth arises in a thin layer. This statement cannot, of course, be taken to include the 6300 line of oxygen or the infrared to which the film is not sensitive. Sensitometry of the MA-9 negatives showed that only 10 percent of the light was reaching the film and only third-magnitude stars could be identified because of the low transmission of the spacecraft window.

The MA-9 experiment had conclusively shown that experiments on extraterrestrial light could be performed without airglow contamination at altitudes above 90 km. The Gemini V experiments were addressed to the following questions: (a) What is the smallest elongation at which zodiacal light measurements can be made from an earth-orbiting spacecraft above the airglow layer? (b) Can the gegenschein be detected and measured from above the airglow layer?

The camera designed for the experiments had an f/1 lens, used Eastman Kodak Tri X film, and was programed with transistor circuits to take doubling exposures in sequence, starting at 1/2 second and finally reaching 3 minutes. Between successive exposures, 20 seconds of shutter-closed time was allowed for spacecraft maneuvering. The field of view of the camera was 50° by 130°, obtained by rotating the optical system during the exposure. With the camera mounted in the pilot's window, a photosensitive eye was arranged to start the programed sequence at sunset. In the actual experiment, the photo eye was not used because the camera was turned on by Conrad precisely at sunset.

The experiment, performed on August 24, 1965, during orbit 46, was composed of two parts. Before sunset, the command pilot (Cooper) acquired a definite spacecraft orientation in which he used his reticle and the Southern Cross as a reference. This placed the other window and the camera in the correct position to photograph the twilight and the zodiacal light. After 5 minutes of stepped exposures, the spacecraft was maneuvered to the Constellation Grus, where α and β Grus and Fomalhaut supplied the reference field for the reticle. The position opposite the sun was centered in the camera's field. In this orientation, spacecraft motions were stopped as far as possible (using the reference stars) to attempt an inertial fix. In all, 17 exposures were taken, and three of these are of special interest. Frames 1 through 5 are properly exposed, but the twilight was so bright that it obscured the zodiacal light. Frame 7 shows the zodiacal light with an 81-second exposure. Also visible in this negative is the illuminated horizon, with the airglow layer showing in profile above it. The frame represents approximately the smallest elongation at which zodiacal light may be studied without external occulting; the elongation is 16°.

This photograph may be studied quantitatively for airglow brightness and zodiacal light, but this study appears very difficult because of a photographic artifact. Figure 1-4 is a print of frame 7, which shows the zodiacal light; figure 1-5 is a sketch of the star field shown in figure 1-4. The top portion of frame 7 was printed with 40 times the exposure of the top. This ratio brings out the earth limb and the airglow layer which show in spite of the artifact. The airglow layer, viewed in profile, has about the same surface brightness as the zodiacal light at 16° elongation. The zodiacal light at this elongation (ref. 2) is 4×10^{-12} of the sun's surface brightness. The ratio of profile to zenith brightness of the airglow is about 40, so the inferred zenith airglow brightness is 10^{-13} of the sun's surface brightness. This is about three times brighter than the average nighttime airglow but within the range of variation commonly observed.

Frames 8 and 9 show exposure of the film by thruster light, and frames 10-14 excessive motion of the star field. However, frames

15 and 16 represent good celestial holds, and both of these negatives appear to show the gegenschein. Its center is about halfway between θ and ι Aquarius, and it appears to have an angular size of about 10°. It is within a few degrees of the direction opposite to the sun. Its brightness is estimated to be in the range of 1×10^{-14} to 9×10^{-14} of the sun's surface brightness. Figure 1-6 shows the star field photographed in the gegenschein experiment. Stars to the sixth magnitude may be identified. Figure 1-7 is a drawing which represents the star field shown in figure 1-6. The direction opposite to the sun should be the direction of the gegenschein if this phenomenon is produced by the backscattering of sunlight by dust. There is no evidence of the westerly displacement which might be expected if the gegenschein resulted from a comet-like dust tail of the earth.

REFERENCES

1. Gillett, F. C.; Huch, W. F.; Ney, E. P.; and Cooper, G.: J. Geophys. Res., vol. 69, no. 13, 1964, p. 2827.

2. Gillett, F. C.; Stein, W. A.; and Ney, E. P.: Astrophys. J., vol. 140, no. 1, 1964, p. 292.

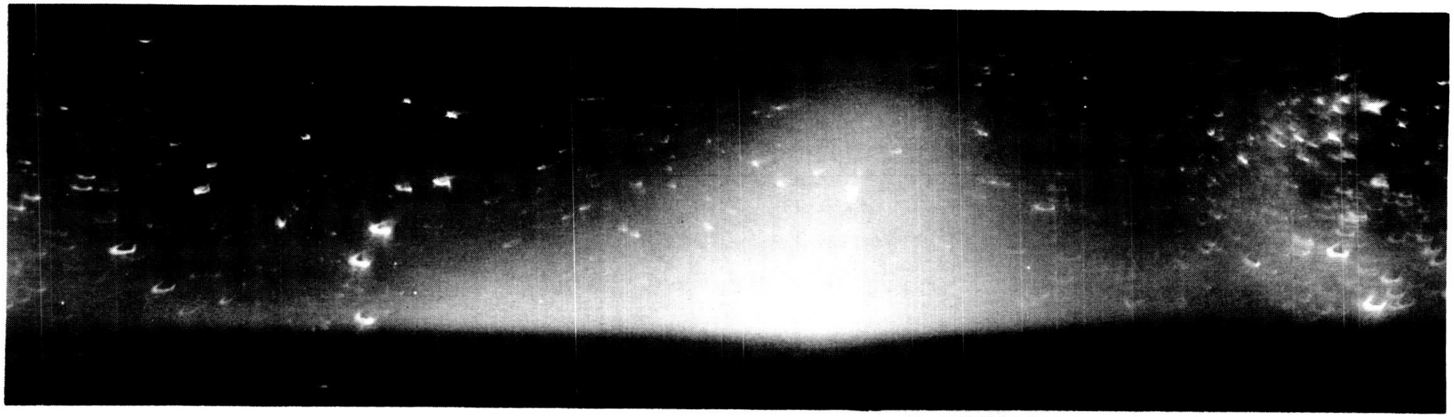

Figure 1-1.- Balloon-borne camera photograph of the sky taken on September 30, 1962. The zodiacal light is rising in the east. Also clearly evident are the Milky Way on the right and the airglow becoming brighter near the horizon.

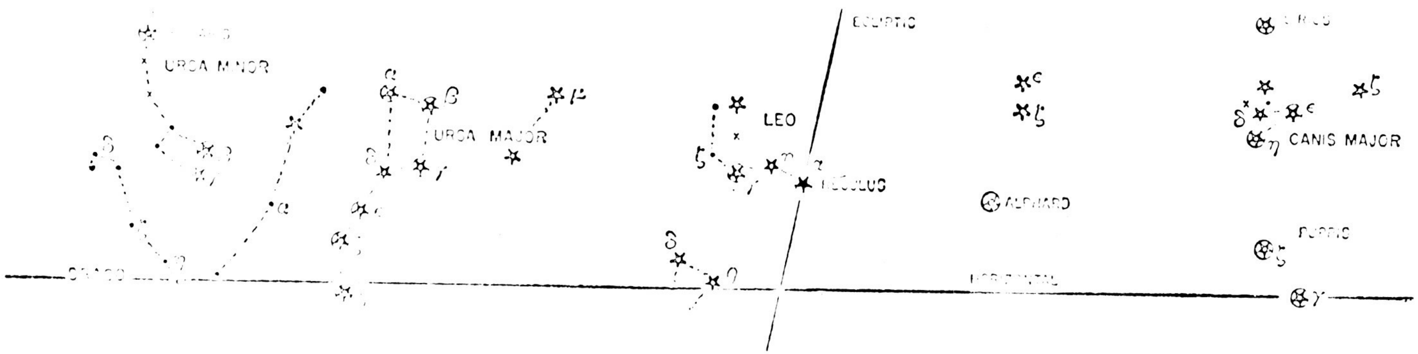

Figure 1-2.- Drawing of the star field shown in figure 1-1.

Figure 1-3.- Photograph of the airglow viewed in profile from above. This was one of the exposures taken in MA-9. The 30-second f/1 shows the airglow in spite of a factor of about 10 in attenuation through the spacecraft window. The lightning flashes in this picture are on the distant horizon, and the sky is moonless.

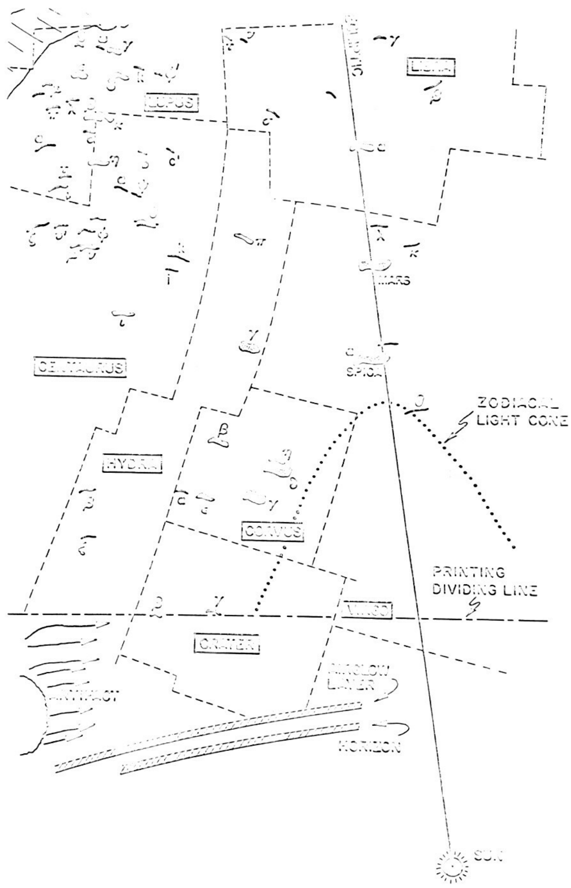

Figure 1-4.- Print of frame 7, from the Gemini V experiment. The upper portion of the print has been given 40 times the exposure of the bottom. The quality of the bottom portion is degraded by an artifact, but the airglow layer and the horizon lit by twilight can be clearly seen. The zodiacal light is centered on the ecliptic. In the original negative, the zodiacal light can be seen as far as the star α Libra. Because of the manner in which the field is exposed, the top and bottom portions of the frame have less exposure than the center.

Figure 1-5.- Sketch of the pertinent features of figure 1-4.

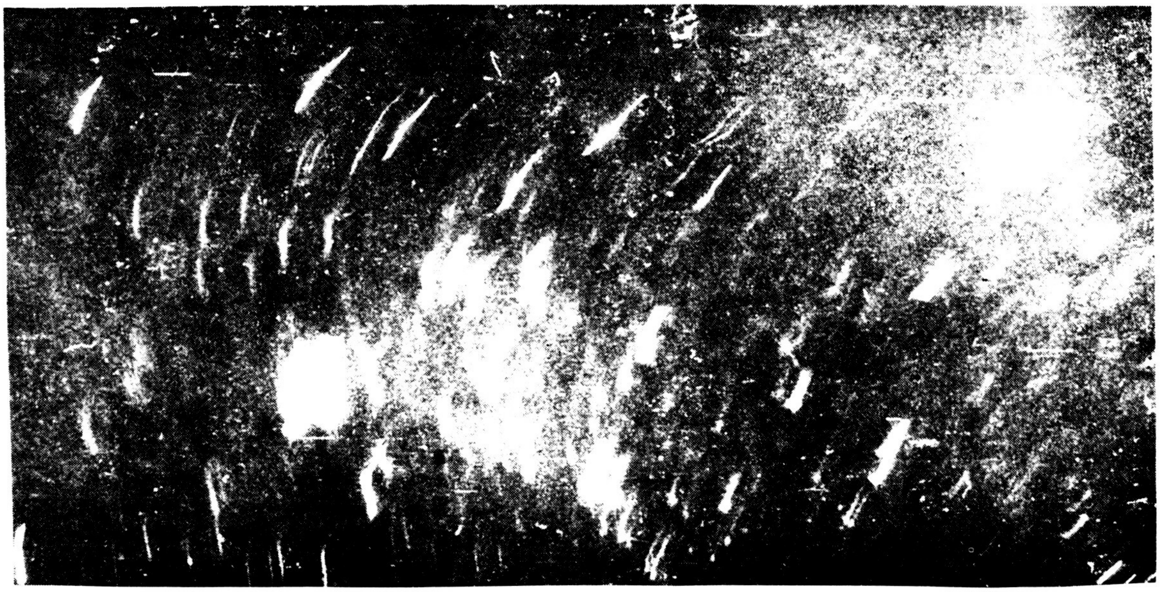

Figure 1-6.- Print of frame 15, from the Gemini V experiment. The contrast in this picture is enhanced by photographic reproduction, but the exposure in the gegenschein area is quite evident on the original negative. Two photographs of this area were obtained, and both show the enhanced exposure in the gegenschein direction.

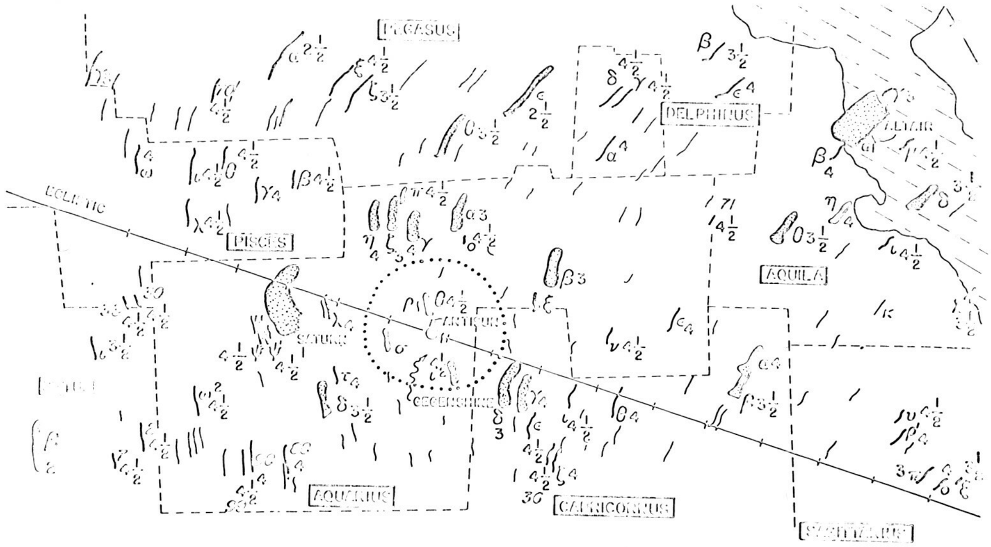

Figure 1-7.- Drawing of the star field shown in figure 1-6. The bright stars are identified, and their visual magnitudes are written next to the Greek letters. For example, θ Aquarius is fourth magnitude. Saturn and Altair are first magnitude. Sixth magnitude stars are identified in spite of the motion during this 160-second exposure.

2. EXPERIMENT S-5, SYNOPTIC TERRAIN PHOTOGRAPHY

Paul D. Lowman, Jr., Ph.D.
NASA Goddard Space Flight Center

The Synoptic Terrain Photography Experiment (S-5) was successfully conducted during the Gemini V mission, the second of the Gemini flights on which it was carried. This report summarizes briefly the methods and results of the experiment. Interpretation of the many excellent pictures obtained is in progress, and a full report is not possible at this time; instead, representative pictures will be presented and described.

The purpose of the experiment was to obtain a large number of high-quality color photographs of selected land areas for geologic and geographic study. Southern Mexico, eastern Africa, and Australia were given high priority, but it was stressed that good pictures of any cloud-free land area would be useful. The same camera (Hasselblad 500 C) and film (Ektachrome MS) used on the Gemini III and IV missions were carried on the Gemini V flight.

The experiment can be considered highly successful. Despite fuel and power limitations, which prevented spacecraft orientation, approximately 170 usable pictures of land areas were taken; a large proportion of these are of excellent quality, and a few are even usable for stereoscopic study. The locations and times of all 70-mm Hasselblad pictures are listed in reference 1.

Figure 2-1, taken over Iran, shows an area approximately 90 miles on a side of the Zagros Mountains, about 50 miles east of the city of Shiraz. The two large lakes, partly surrounded by salt flats, are the Daryacheh-ye Tashk (to the north) and the Daryacheh-ye Bakhtegan. The northwest-trending ranges are mostly Mesozoic and Tertiary sedimentary rocks folded into a series of anticlines and synclines. The dark hills at bottom center are composed of volcanic rock.

This picture appears to be potentially useful for refining existing maps of the area. It shows considerably more geologic and topographic detail than the Geological Map of Iran (ref. 2) whose scale (1:2 500 000) is close to that of the Gemini photograph. The picture would be especially useful in mapping Quaternary alluvium and evaporite deposits and in delineating major faults.

Figures 2-2 and 2-3, taken over southwestern Iran, show an area of great geologic interest. The mountain ranges are Cenozoic sedimentary rocks folded into anticlines and synclines of remarkable complexity. Of particular interest is the fault scarp at the left. This feature reflects a recent and probably still active fault of the "scissors" type in which movement has opposite directions at opposite ends. Toward the bottom of the picture, the right-hand fault block has moved up; toward the top, the left-hand side has moved up. The recency of the fault is shown by the virtually negligible amount of dissection of the scarp. The linear features to the left of the fault are probably truncated strata rather than sand dunes, since they can be seen to continue under the alluvium.

Figure 2-4 shows the mouth of the Yangtze River and the East China Sea, looking toward the east. This picture is typical of many taken during the Gemini V mission which show submarine topography and turbidity currents. Such photographs are believed to be of great potential value for hydrologic and oceanographic studies (ref. 3), since they permit a simultaneous view of large ocean areas, with the added advantage of color.

Figure 2-5, taken over New Mexico, is one of the most northerly pictures of the United States obtained on any of the Mercury or Gemini flights. It shows a wide variety of rock types and structures. The white patch at top center (marred by a flaw) is the gypsum sand of the White Sands National Monument. West of the Monument are the San Andres Mountains, which are bordered on the south by the Tertiary volcanics of the Organ Mountains. West of the Rio Grande, at the top left, a series of northerly-trending faults in the vicinity of Magdalena Peak are visible. Finally, at least two units can be distinguished in the Quaternary basalt flows west of the Rio Grande at the left, although the most recent geologic map of New Mexico (ref. 4) shows only one map unit.

The availability of a recent geologic map of this area makes this photograph of particular value for comparison purposes. Preliminary study indicates that many of the major lithologic units and structures (especially faults) shown on the 1:500 000 scale geologic map are visible on the photograph, whose original scale was about 1:2 000 000. The photograph, moreover, shows many features of Quaternary alluvium which are not shown on the map and permits rapid determination of the extent of the pediments surrounding the mountains, features which are not shown clearly on either topographic or geologic maps.

Because of daylight restrictions, photographing southern Africa was not possible during flights prior to Gemini V. However, a large number of excellent pictures of this area were obtained during this mission. One of these is shown in figure 2-6, taken over South West Africa. It includes a considerable part of the Namib Desert, which extends for several hundred miles along the coast of southern Africa, and part of the Precambrian shield. This picture demonstrates the potential value of hyperaltitude photography for studies of regional sand dune distribution and structural geology. The conspicuous fracture pattern at the right is covered more completely by an adjoining photograph. An interesting circular feature is shown at the top right, vaguely suggestive of the Richat structure photographed on the Gemini IV mission.

CONCLUDING REMARKS

This report covers only a very small part of the immense amount of geologic and geographic information contained in the terrain photographs taken during the Gemini V mission. Further detailed studies are in progress to evaluate the results of the experiment. The crew are to be commended for their interest and competence in carrying out the terrain photography under difficult conditions.

REFERENCES

1. Underwood, R. W.: Gemini V 70mm Photography Identification. NASA BL-111, Sept. 7, 1965.

2. National Iranian Oil Company: Geological Map of Iran (1:2,500,000). 1957.

3. Gettys, R. F.: Evaluation of Color Photos Exposed from the Gemini (GT-4) Flight over the Gulf of California. Unpublished manuscript, Technical Production Department, U. S. Naval Oceanographic Office, Washington, D.C., June 1965.

4. Dane, C. H.; and Bachman, G. O.: Geologic Map of New Mexico. U. S. Geological Survey, 1965.

Figure 2-1.- South-central Iran, showing the Zagros Mountains.

Figure 2-2.- South-eastern Iran, showing folded mountains cut by scissors fault (left).

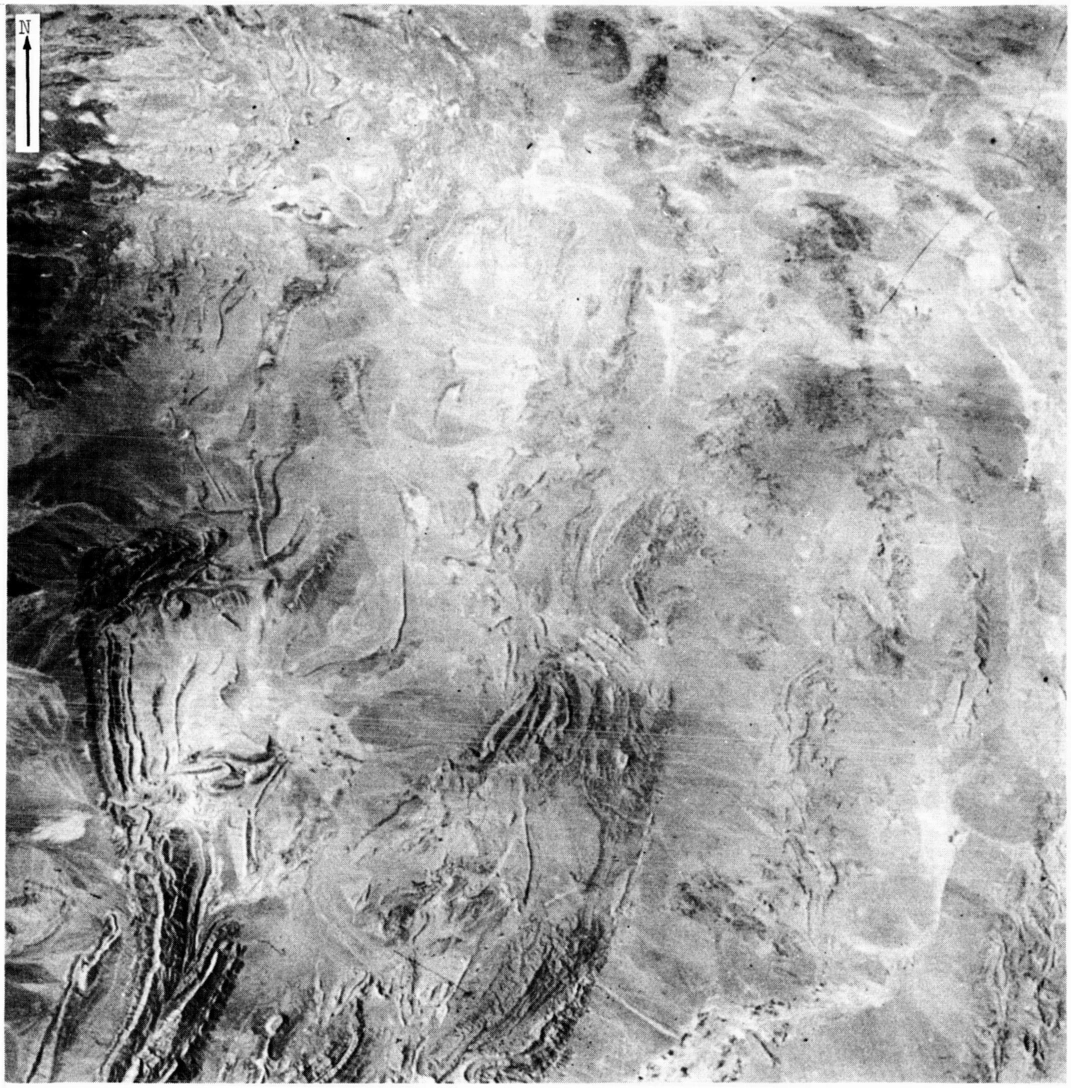

Figure 2-3.- South-eastern Iran, showing an area of folded mountains overlapping the area shown in figure 2-2.

Figure 2-4.- Mouth of the Yangtze River, showing bottom topography and/or turbidity currents.

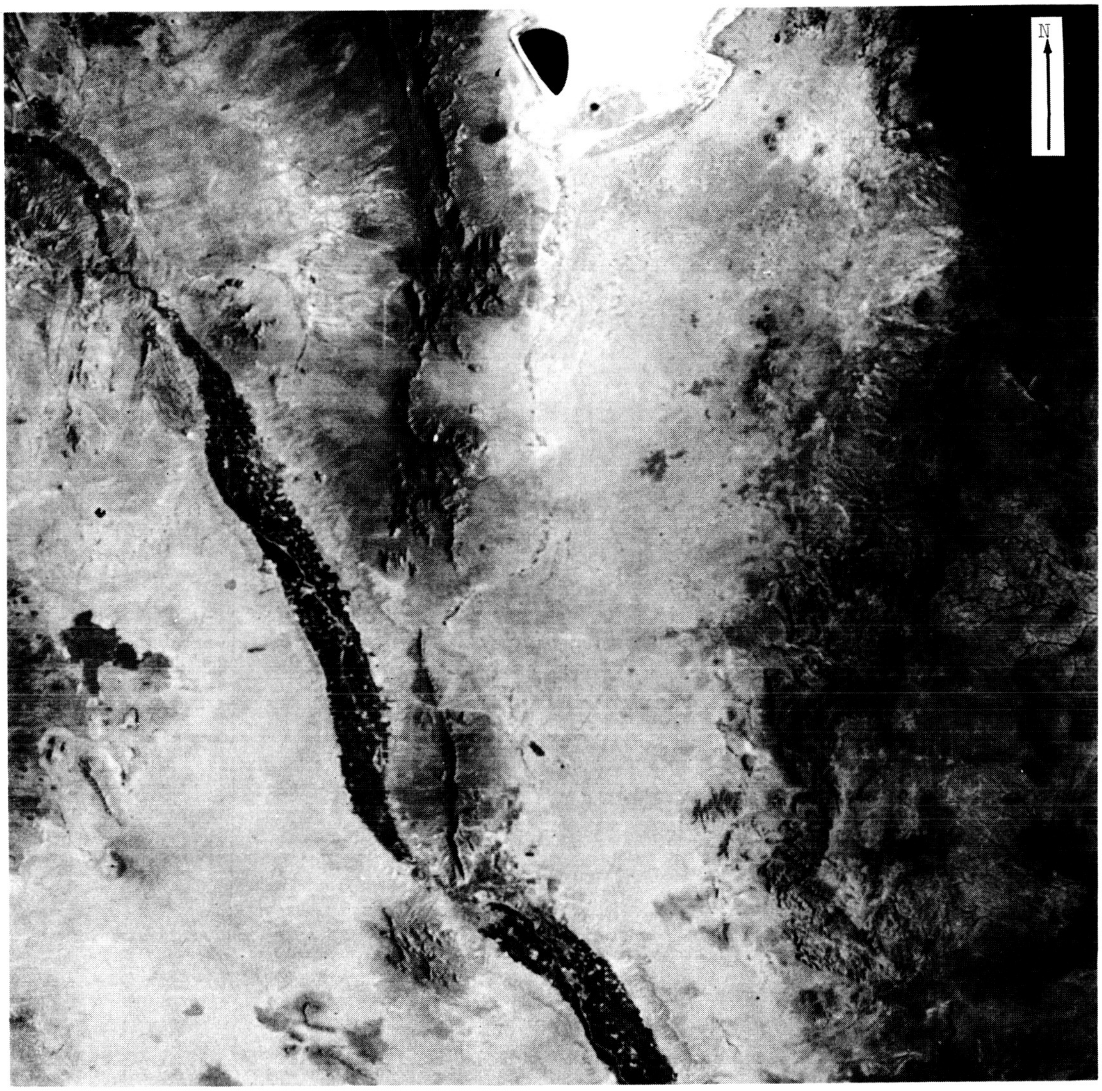

Figure 2-5.- South-central New Mexico, showing the Rio Grande valley, the San Andres and Organ Mountains, and the White Sands National Monument (top).

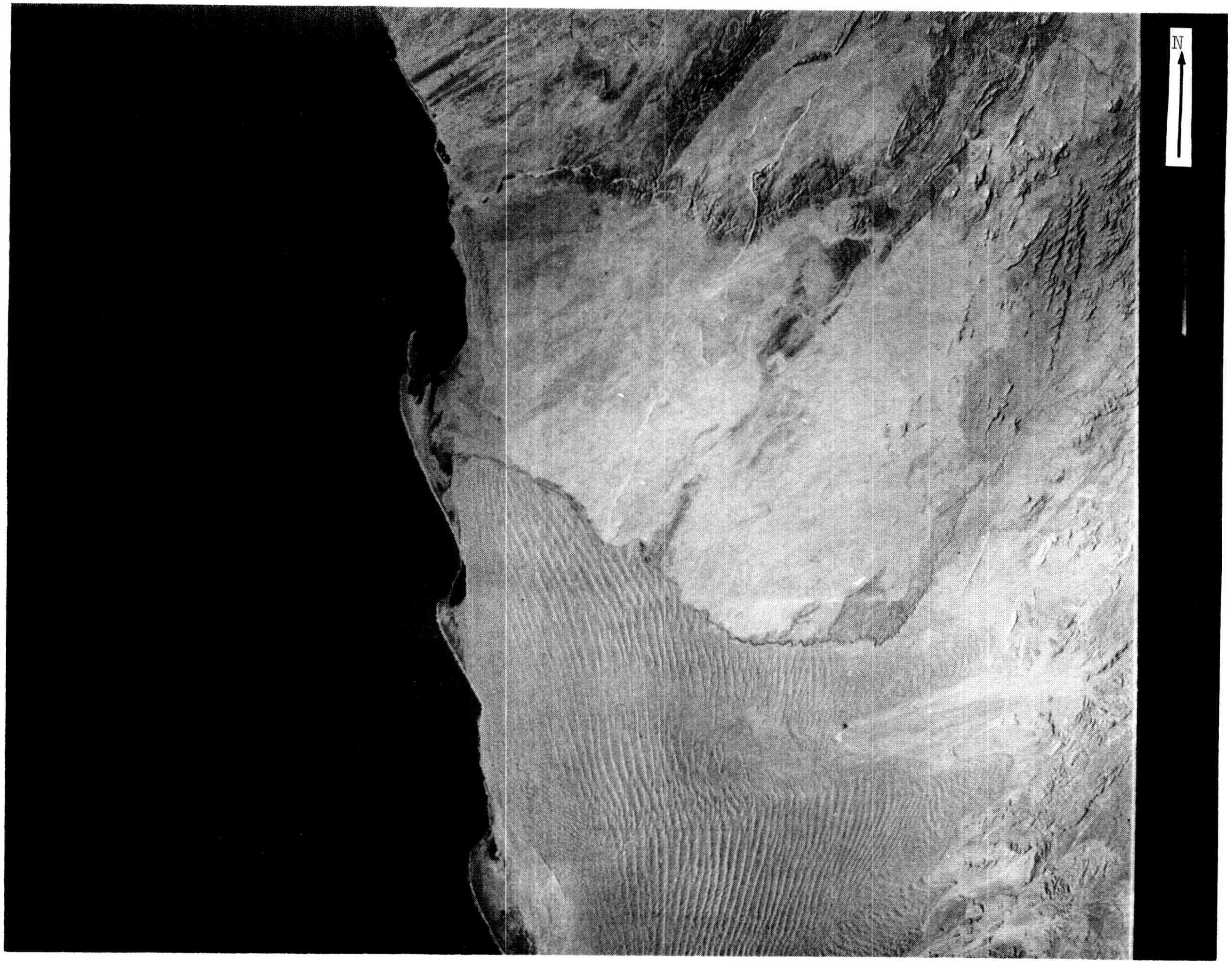

Figure 2-6.- South West Africa, showing part of the Namib Desert and structure in Precambrian rocks (right).

3. EXPERIMENT S-6, SYNOPTIC WEATHER PHOTOGRAPHY

By Kenneth M. Nagler
U. S. Weather Bureau, ESSA

Stanley D. Soules
National Environmental Satellite Center, ESSA

SUMMARY

As part of the continuing effort to obtain a selection of high-resolution color pictures of cloud systems, well over a hundred views of meteorological interest were obtained by the Gemini V crew. A number of these are being studied by various investigators.

DESCRIPTION

The S-6 weather photography experiment on Gemini V was a continuation of the effort to collect a selection of meteorologically interesting photographs. A number of cloud pictures were obtained on previous Gemini and Mercury flights--especially Gemini IV, the first flight on which weather photography was scheduled as a specific experiment.

Since weather is highly variable from area to area and day to day, there remain many cloud systems which meteorologists would like to see photographed in color on the scale obtainable from the Gemini flight altitudes.

The basic aims, procedures, and equipment for the weather photography effort are essentially the same as have been discussed previously (refs. 1, 2).

Briefly, for a variety of systems, one aim is to get pictures which help in interpreting meteorological satellite views. TIROS pictures cover much of the earth each day and are becoming an increasingly important part of the world's meteorological observation system. But with the requirement for extensive area coverage through televised pictures goes a limitation in resolution. Thus, the Gemini photographs can help the meteorologist interpret some of the features he sees on the operational meteorological satellite pictures.

Also, there are special meteorological and related phenomena which can be studied through pictures on the scale obtainable on the Gemini photographs.

Another aim is the obtaining of views of the same cloud pattern on two or more passes of the spacecraft on the same day in order to study movement and changes over fairly short time intervals.

The procedures for conducting the experiment were the same as for the Gemini IV flight. Well in advance of the flight, a number of meteorologists (primarily from the National Environmental Satellite Center and the Weather Bureau) were queried as to the types of cloud systems they would like to see and as to what particular geographical areas were of interest to them. Several months before the flight, the aims of the experiment were discussed in detail with the flight crew. A number of specific types of clouds were suggested as possibilities for viewing on their mission.

The mission plan was arranged so that the pilots could devote part of their time over the pre-selected areas to this cloud photography. At Cape Kennedy on the day preceding launch, the pilots were briefed on several interesting features likely to be seen on their mission. From time to time during the mission, areas of interest were selected from weather analyses and from TIROS pictures. Whenever operationally feasible, this information was communicated to the crew in time for them to locate and to photograph the clouds in question, provided this did not interfere with their other duties. As long as fuel was available for changing the attitude of the spacecraft for this purpose, the pilots were able to search for the desired locations. Otherwise, they could take pictures only of those scenes which happened to come into view.

The equipment consisted of the Hasselblad camera (Model 500 C, modified by NASA) with a haze filter on the standard Zeiss Planar, 80-mm f2.8 lens. The 70-mm film used on the flight--for the combined purposes of the S-6 weather photography experiment, the S-5 terrain photography experiment, and general purpose photography--included three rolls of Ektachrome MS SO-217 film and one roll of Anscochrome D-50 film, for a total of about 250 frames.

RESULTS

Astronauts Cooper and Conrad used all of the film and, with a very few exceptions, obtained photographs of excellent quality. Over half of the pictures showed clouds. A selection of views of special meteorological interest is shown here.

Always of interest are views of tropical storms. Figure 3-1 shows a small tropical storm near the Marshall Islands. The spiral cloud bands and the surrounding clouds associated with this immature disturbance can be seen in great detail. Figure 3-2 shows Tropical Storm Doreen in the eastern North Pacific, a larger storm of nearly typhoon intensity. In addition to getting pictures of this storm, the Gemini V crew twice provided timely information on its location, information which was used by the Weather Bureau in the preparation of advisories on Doreen.

Views of an area of Florida on successive passes of the spacecraft are shown in figures 3-3 through 3-5. Note in figure 3-3 (about 10:30 a.m. local time) that cumulus clouds had formed over most of the land areas, but, with a few exceptions such as the one over Merritt Island, the clouds did not have much vertical development. By about noon local time (fig. 3-4), a line of towering cumulus had formed some 20 to 30 miles inland from the east coast. By about 1:30 p.m. (fig. 3-5), some of these towering cumulus clouds had reached the thunderstorm stage, and their cirrus anvil tops had spread westward to central Florida.

Figure 3-6, overlapping the previous picture, completes the view of Florida and shows a large thunderstorm southwest of Miami. On the following day, about 24 hours after figures 3-5 and 3-6 were taken, the cloud pattern over Florida was as shown in figure 3-7. Again, the line of greater vertical development occurred - except over water areas - but with strong thunderstorm development confined to the western part of the Florida Keys. The cloud streets are particularly well formed and are alined with the easterly winds blowing straight across Florida.

These and other views of Florida are being studied relative to the location and timing of thunderstorm formation in the Cape Kennedy - Merritt Island region.

As was mentioned in the discussions of the cloud photography experiment on Gemini IV, some features besides clouds are of interest to meteorologists and scientists in related fields. Figure 3-8 illustrates a view of interest to oceanographers. The detail in the shallow water bottom configuration in the Bahama area as seen on this and other views is being studied. Also, because of certain similarities in the deposition of wind-borne and water-borne sand, the oceanographers as well as meteorologists are interested in the configuration of sand dunes shown in some of the pictures taken as part of the S-5 experiment.

In summary, the high-quality pictures taken by the Gemini V crew have made a definite contribution to the knowledge of cloud systems. They are very much in demand by the meteorological community and are being used or planned for use in a number of meteorological and related investigations.

REFERENCES

1. Nagler, K. M.; and Soules, S. D.: Cloud Photography from the Gemini IV Spaceflight. Bull. Am. Meteorol. Soc., vol. 46, no. 9, Sept. 1965.

2. Nagler, K. M.; and Soules, S. D.: Experiment S-6, Synoptic Weather Photography During Gemini IV. Manned Space Flight Experiments Symposium, Gemini Missions III and IV, Washington, D.C., October 18-19, 1965.

NASA
S-65-45494

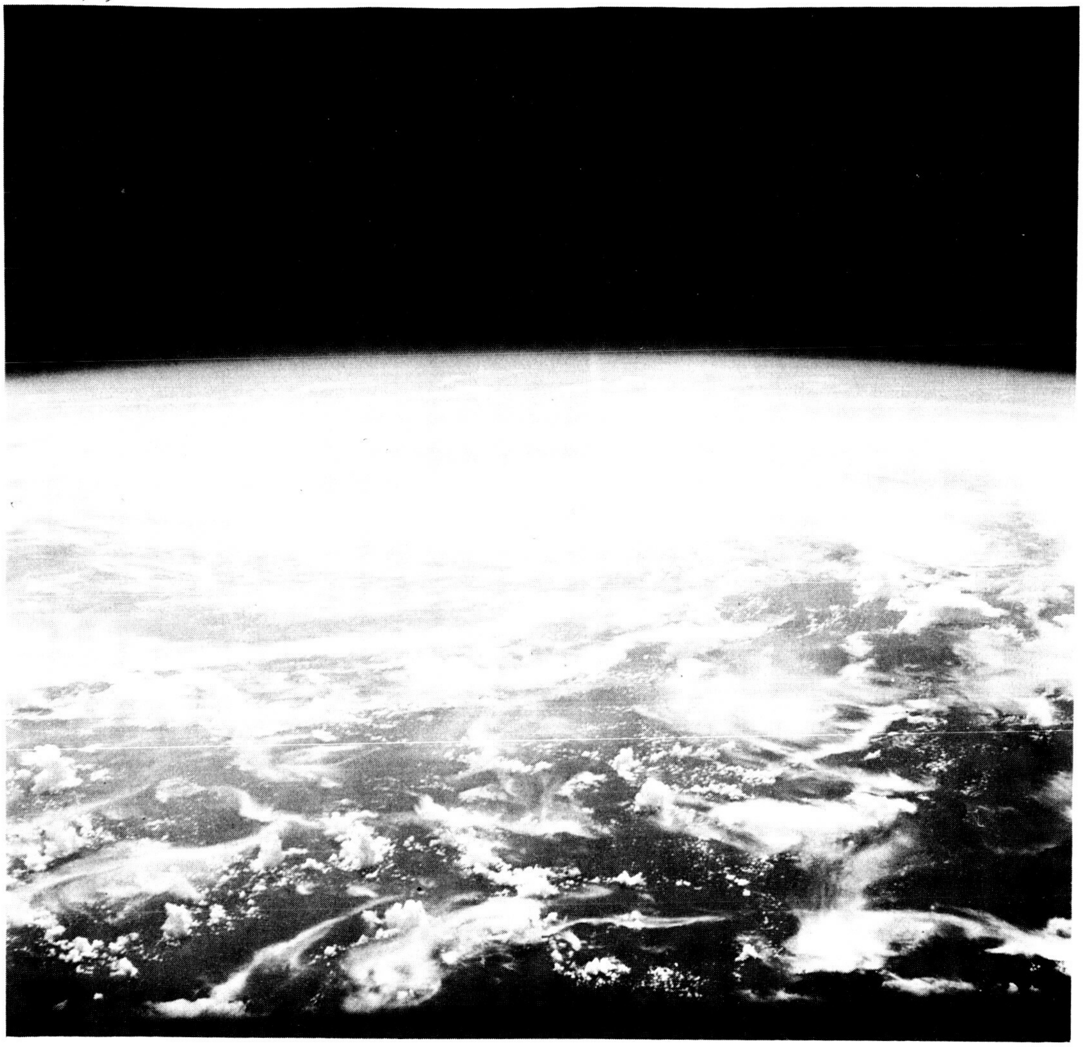

Figure 3-1.- A small tropical storm near the Marshall Islands, taken at 0125 GMT, August 23, 1965.

NASA
S-65-45424

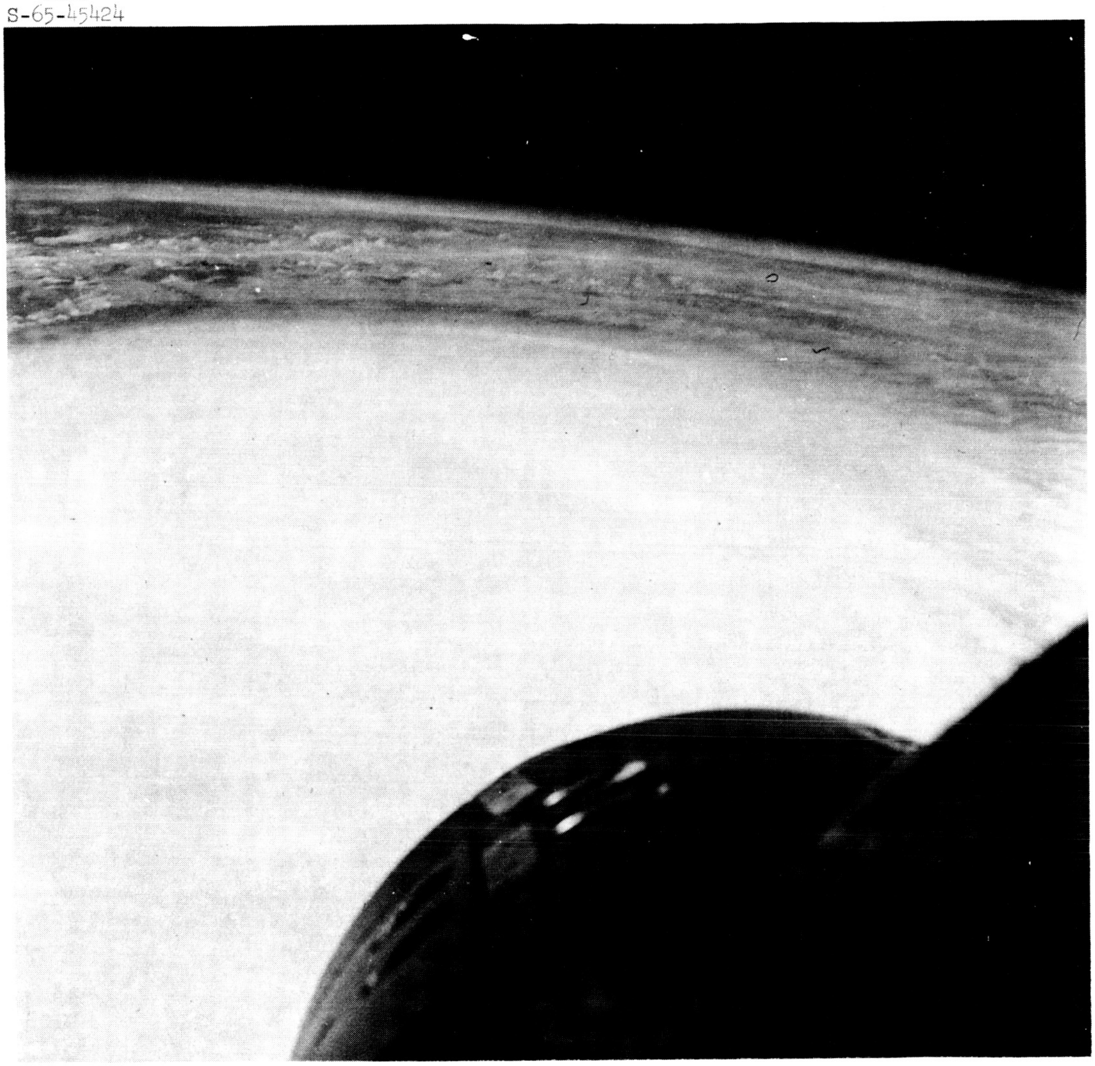

Figure 3-2.- Tropical Storm Doreen over the eastern North Pacific Ocean, taken at 2133 GMT, August 23, 1965.

NASA
S-65-45381

Figure 3-3.- View of Florida, taken at 1531 GMT, August 22, 1965; the first of three views of this area taken on successive passes.

NASA
S-65-45388

Figure 3-4.- View of Florida, taken at 1707 GMT, August 22, 1965; the first of three views of this area taken on successive passes.

NASA
S-65-45391

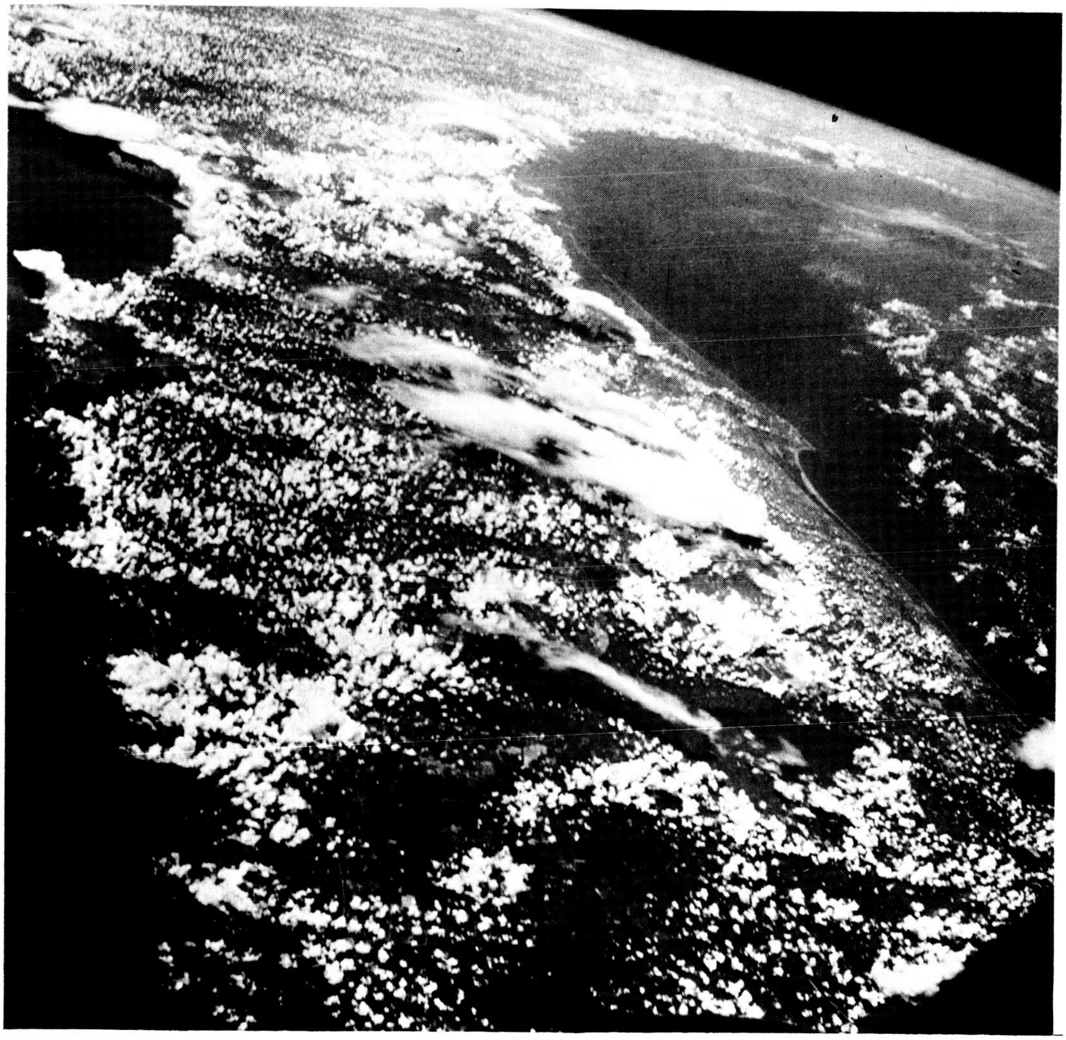

Figure 3-5.- View of Florida, taken at 1838 GMT, August 22, 1965; the third of three views of this area taken on successive passes.

NASA
S-65-45392

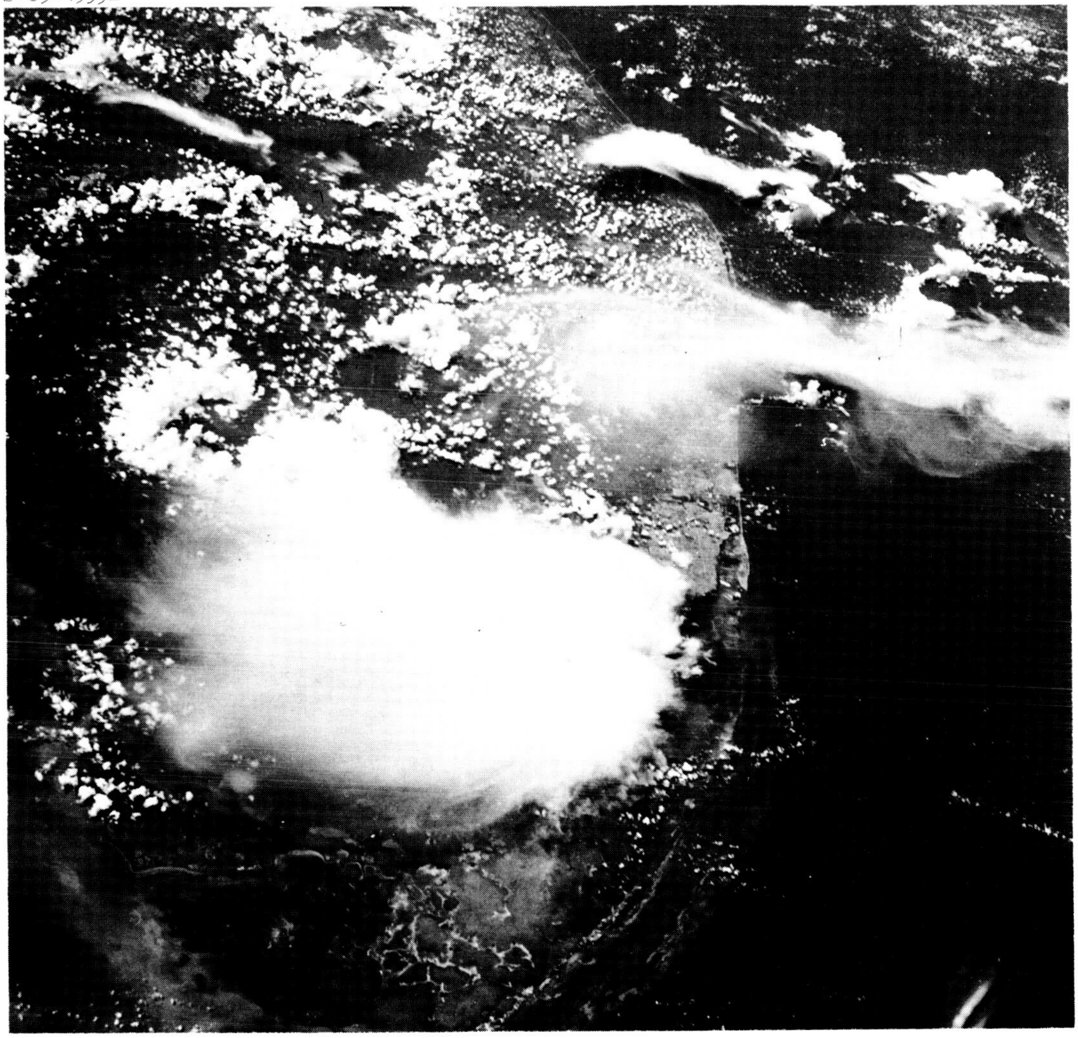

Figure 3-6.- View of large thunderstorm over southern Florida, taken at 1838 GMT, August 22, 1965.

NASA
S-65-45418

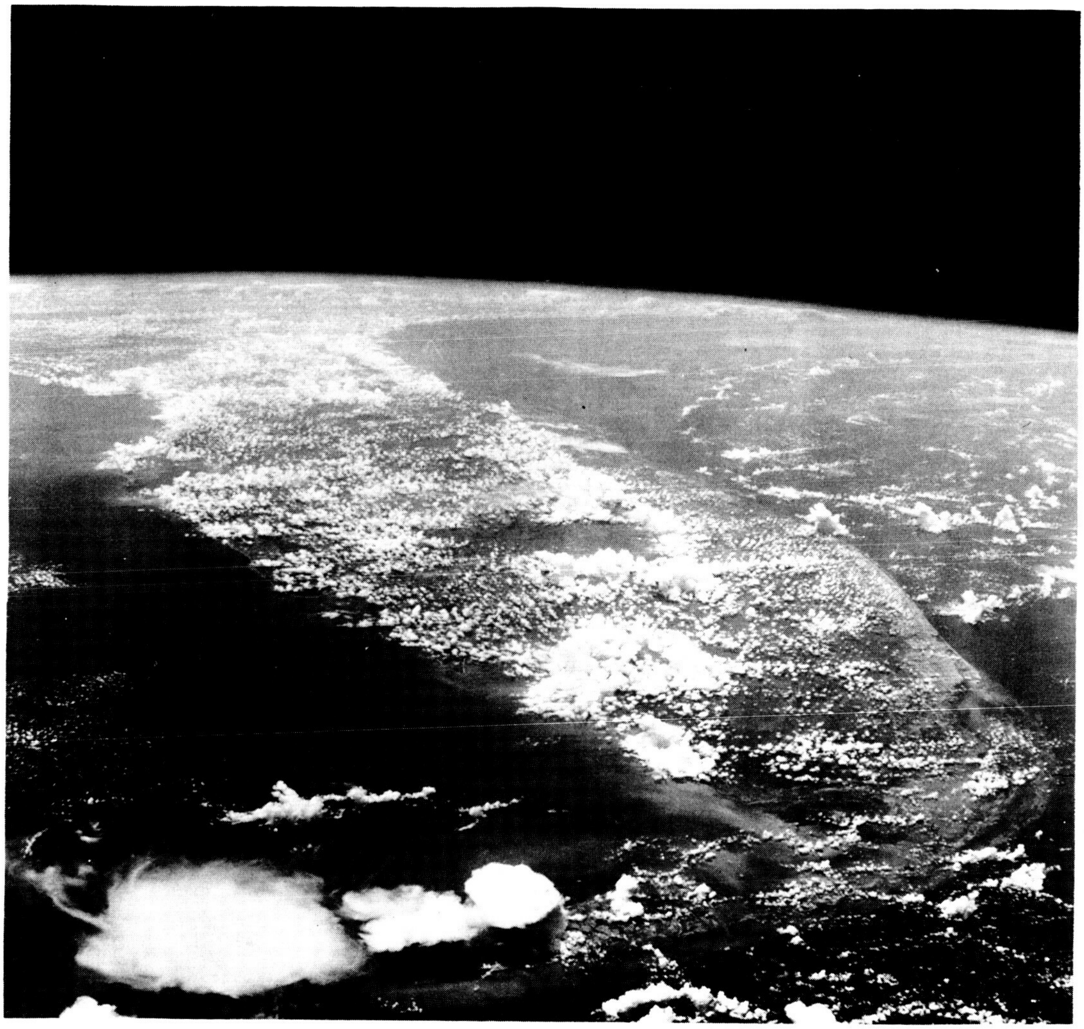

Figure 3-7.- View of Florida, taken at 1826 GMT, August 23, 1965, approximately 24 hours later than figures 3-5 and 3-6.

NASA
S-65-45395

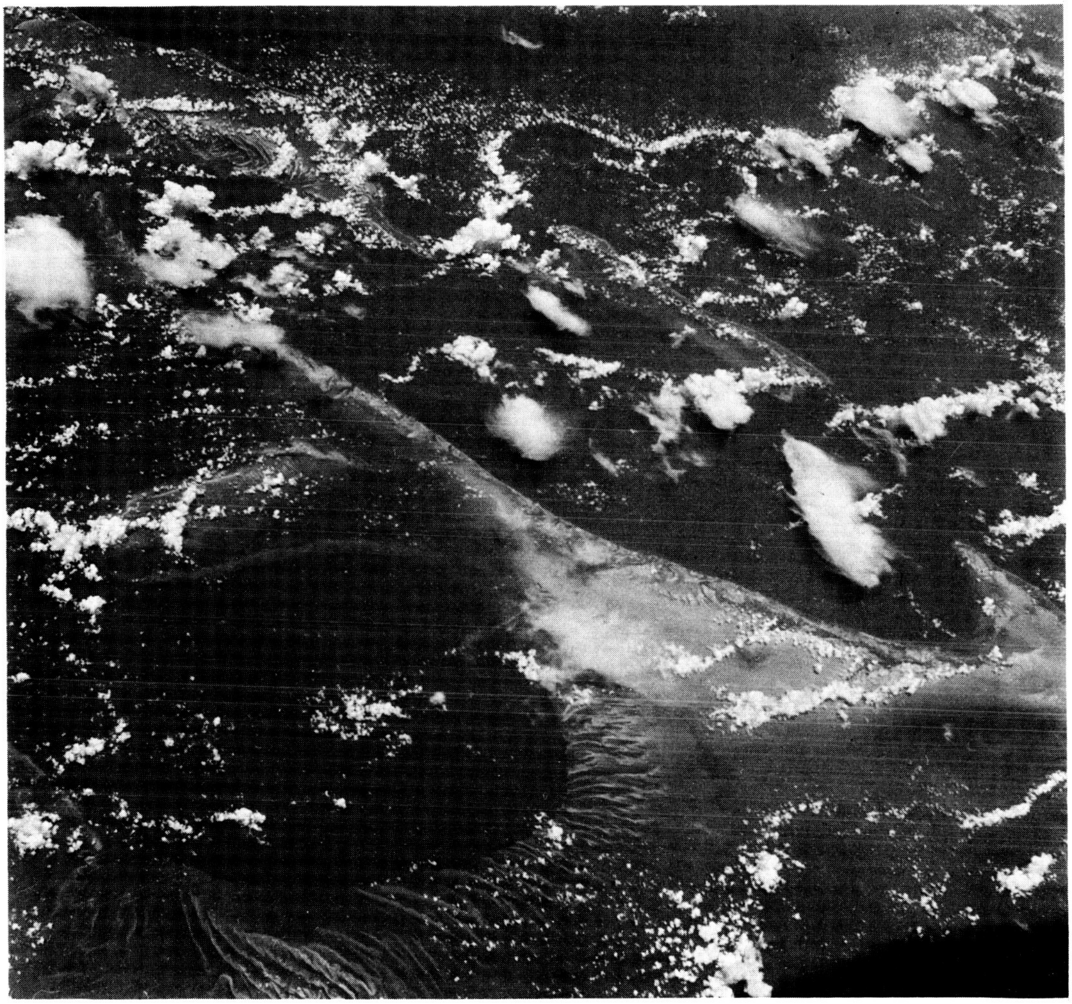

Figure 3-8.- Great Exuma and nearby islands in the Bahamas, showing the interesting bottom configuration in the shallow water, taken at 1839 GMT, August 22, 1965.

4. EXPERIMENT S-7, CLOUD-TOP SPECTROMETER

By F. Saiedy
University of Maryland

D. Q. Wark and W. A. Morgan
Environmental Science Services Administration

INTRODUCTION

TIROS weather satellites have presented meteorologists and weather forecasters with cloud pictures which show the geographic distribution of cloudiness and permit the qualitative judgment of cloud types. Cloud types are classified according to their altitudes. Meteorologists are interested in cloud altitudes because altitudes indicate the dynamic and thermodynamic state of the atmosphere upon which weather forecasts are based.

In 1961, Hanel suggested (ref. 1) the utilization of the absorption by the 2.0 μ CO_2 band in the sunlight reflected from the cloud for the determination of cloud altitude. The same year, Yamamoto and Wark pointed out (ref. 2) that the CO_2 band lies on the wing of the H_2O band at 1.87 μ. The accuracy of such determination would, then, be compromised by variations in the amount of water vapor in the atmosphere. They proposed the use of the oxygen A band at 7600 Å; measurements in this band would not be affected by water vapor.

METHOD

Basically the method of this experiment consists of comparing the cloud's radiance at a specified wavelength inside the band with its radiance in an atmospheric window outside the band. This ratio will show the absorption or transmission of oxygen in the atmosphere above the cloud top. Since oxygen is uniformly mixed with air, the transmission of oxygen is a function of the pressure altitude of the cloud and the atmospheric path traversed by light from the sun to the cloud top and, after reflection, from the cloud top to the measuring instrument (fig. 4-1). The mathematical representation is stated in the equation

$$\tau = f\left[p, (\sec z + \sec \alpha)\right] \quad (1)$$

where:

τ = oxygen transmission

p = pressure altitude

z = zenith angle of the sun

α = viewing angle.

The instrument used on the Gemini V mission was designed to test the feasibility of measuring the cloud altitude by this method. The wave length chosen inside the band is at 7631 Å for low clouds and 7607 Å for high clouds.

INSTRUMENT AND FILM CALIBRATION

A cross section of the instrument is shown in figure 4-2. The instrument is a small hand-held spectrograph which consists of a 3.2 by 3.2-cm replica grating with 1200 lines/mm blazed for 7500 Å in the first-order spectrum. A Schott RG8 filter (cutoff, 6700 Å) is used to eliminate higher order spectra. The entrance slit is 6.0 mm long and 0.1 mm wide, which corresponds to 5 Å resolution.

The spectrum from 7500 to 7800 Å, which includes the oxygen band, is recorded on a high-speed infrared film carried in the back of a camera equipped with a focal plane shutter. The instrument also photographs the cloud on the upper part of the film frame by means of another lens. Figure 4-3 shows the completed spectrograph. The capability of the spectrograph is shown in figure 4-4 which represents a densitometer trace of a photographed spectrum. The oxygen doublets are 5 Å apart and are just resolved. The variation in density of the flight film is carefully calibrated into variation in relative intensity by a method described in reference 3.

OBSERVATION FROM GEMINI V

One of the primary objects of the Gemini V cloud-top experiment was to obtain observations of the cloud from the spacecraft coincident with observations from aircraft. Consequently, a plan for the reporting of cloud height by civilian and military aircraft was initiated. The geographic areas were restricted by operational requirements to the southern United States, eastern Pacific, western Atlantic, and Guam-Philippines areas. An around-the-clock weather watch was established by a special meteorological staff on the day before the Gemini V lift-off. The geographic areas that coincided both with projected spacecraft orbits and promising cloud covers were selected, and the information was conveyed to Gemini control. When the selected areas were introduced into the Gemini V flight plan, civilian and military aircraft were notified of the place and time of observation. The U. S. Weather Bureau Research Flight Facility plane stationed in Miami was placed on the alert for cloud observation in the vicinity of Florida.

At the prescribed areas the astronaut pointed the spacecraft down, aimed the spectrograph through the viewfinder at the selected clouds, and operated the instrument. Then the astronaut recorded the time of observation to the nearest second, the spacecraft pitch and yaw angles, and a description of the cloud. The selective capability of the astronaut depended upon his background in meteorology. His knowledge of cloud types, derived from his aviation training, resulted in the improved efficiency of this experiment over that of an unmanned satellite. The cooperation of the participant organization in measuring cloud height from aircraft was good, but, due to the vast area covered, few of the aircraft observations were in near coincidence. The only coincident observation obtained was over Florida where the U. S. Weather Bureau Research Flight Facility plane was vectored to the area of Gemini V observation.

During the flight of Gemini V, twenty-six spectrographic observations were obtained on various cloud types - some for low cloud over the west coast of Baja California, some for fairly high cloud on a tropical storm in the eastern Pacific, and some on tropical storm Doreen. The instrument was operated correctly by the astronaut, and all pictures were correctly aimed and exposed.

RESULTS

An example of the type of spectrum and photograph is given in figure 4-5. It represents a cloud in the intertropical convergence zone. Figure 4-6 shows densimeter traces of the spectra of three types of cloud - high, medium, and low. It is quite apparent, qualitatively, that the transmission of radiation in the oxygen band for high cloud is much larger than that for low cloud. The results prove the feasibility of the cloud-altitude measurements from spacecraft by this method.

Table 4-I summarizes some of the Gemini V observations which have been studied. The measured oxygen transmission from Gemini V are compared with the calculated oxygen transmission from Wark and Mercer (ref. 4) to obtain the pressure altitude.

The values of pressure altitude calculated and presented in table 4-I do not include the required correction due to the multiscattering of radiation inside the clouds before it is reflected to the spacecraft. The multiscattering inside the clouds causes lower-than-actual altitude measurements. This problem has been discussed by Saiedy, Hilleary and Morgan (ref. 3). The magnitude of necessary correction depends mainly on the thickness of the cloud. Recent calculation on this problem shows that the thickness of the cloud can be determined, with accuracy adequate for correcting the cloud-top altitudes, from the measurements of the brightness of the cloud. Figure 4-7 shows the dependence of the brightness of the cloud on the thickness of the cloud, the zenith angle of the sun, and the viewing angle. An observation of a white card in sunlight was obtained during the mission. The angle between the card and the sun's rays was not recorded, however, preventing an absolute in-flight calibration of the spectrograph. Considering the relative brightness, we were able to make an estimate of the cloud thickness, which is shown in table 4-II. These results support to some extent our calculation between brightness and thickness.

DISCUSSION

In a planned second stage of this experiment on a subsequent flight, more emphasis will be placed on coincident observations by restricting the spacecraft observation to the southern United States. Aircraft coverage will be more complete, and two or possibly three aircraft will be available for vectoring into the selected cloud cover. The observation on white card to calibrate the spectrograph in orbit will be carefully planned for cloud brightness measuring, with the results of which the possibility of measuring cloud thickness can be tested.

Cloud thickness, besides being important for cloud-top measurements, is a valuable parameter by itself. If this experiment proves successful, we shall in the future, from unmanned spacecraft, have three-dimensional pictures of clouds with a geographic resolution of 6 by 6 miles. The National Environmental Satellite Center, capitalizing on the experience gained so far from the Gemini V flight, has successfully proved the feasibility of and determined the system design requirements for a sophisticated second-generation weather satellite instrument.

ACKNOWLEDGEMENTS

The authors wish to acknowledge with thanks the cooperation of the National Aeronautics and Space Administration and, particularly, the astronauts L. Gordon Cooper and Charles Conrad, Jr. We are indebted also to D. M. Mercer, H. Jacobowitz, and F. VanCleef of the Environmental Science Services Administration for their assistance, and to D. T. Hilleary who participated in the design and construction of the spectrograph.

REFERENCES

1. Hanel, R. A.: J. Geophys. Res., vol. 66, 1961, p. 1300.

2. Yamamoto, G. A.; and Wark, D. Q.: J. Geophys. Res., vol. 66, 1961, p. 3596.

3. Saiedy, F.; Hilleary, D. T.; and Morgan, W. A.: Applied Optics, vol. 4, 1965, p. 495.

4. Wark, D. Q.; and Mercer, D. M.: Applied Optics, vol. 4, 1965, p. 839.

TABLE 4-I.- RESULT FROM GEMINI-5 OBSERVATIONS OF CLOUD HEIGHT. THE ACTUAL HEIGHTS OF THE CLOUD ARE GIVEN WHERE POSSIBLE.

Date August 1965	Time	Cloud identification and location	Oxygen trans., percent		Calculated mean press. altitude, mb	Actual pressure altitude, mb
			7631Å	7607Å		
23	21:33:05	Tropical storm eastern Pacific	--	.48	290	--
24	21:20:08	Tropical storm Doreen eastern Pacific	--	.51	320	(350-220)
25	19:44:02	I.T.C. eastern Pacific	--	.39	440	--
25	16:37:00	Cumulo-nimbus Florida	--	.45	370	323
27	17:43:00	Stratus Baja California	0.32	--	980	960

TABLE 4-II.- APPROXIMATE RESULTS IN CLOUD THICKNESS

Cloud identification	Solar zenith angle, degrees	Relative brightness, percent	Estimated thickness, meters
Tropical storm	29°	≈ .85	> 3000
Tropical storm Doreen	13°	≈ .85	> 3000
Cumulo-nimbus	22°	.66	1000
I.T.C.	16°	.43	500
Stratus	34°	.47	600

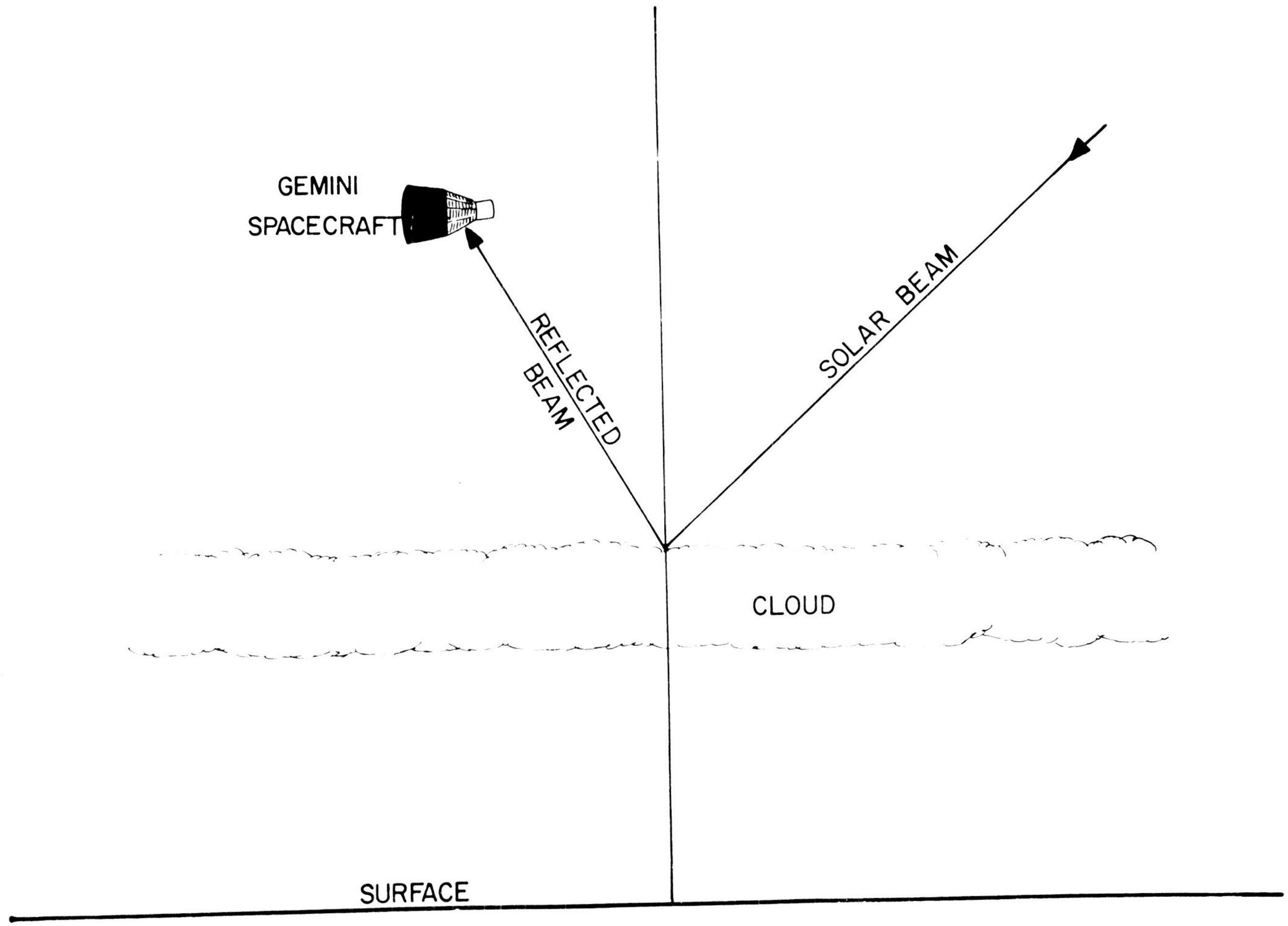

Figure 4-1.- Geometric representation showing the path of radiation from the sun to the cloud and up to the spacecraft.

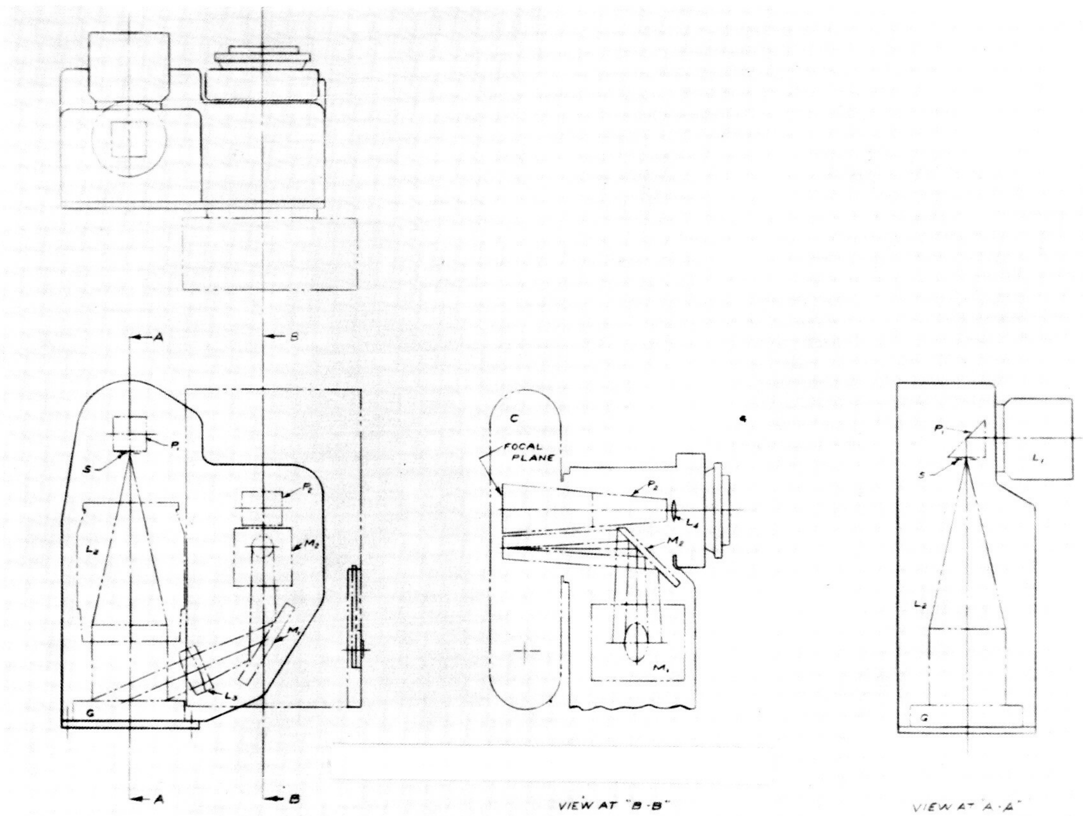

Figure 4-2.- Optical layout of the spectrograph.

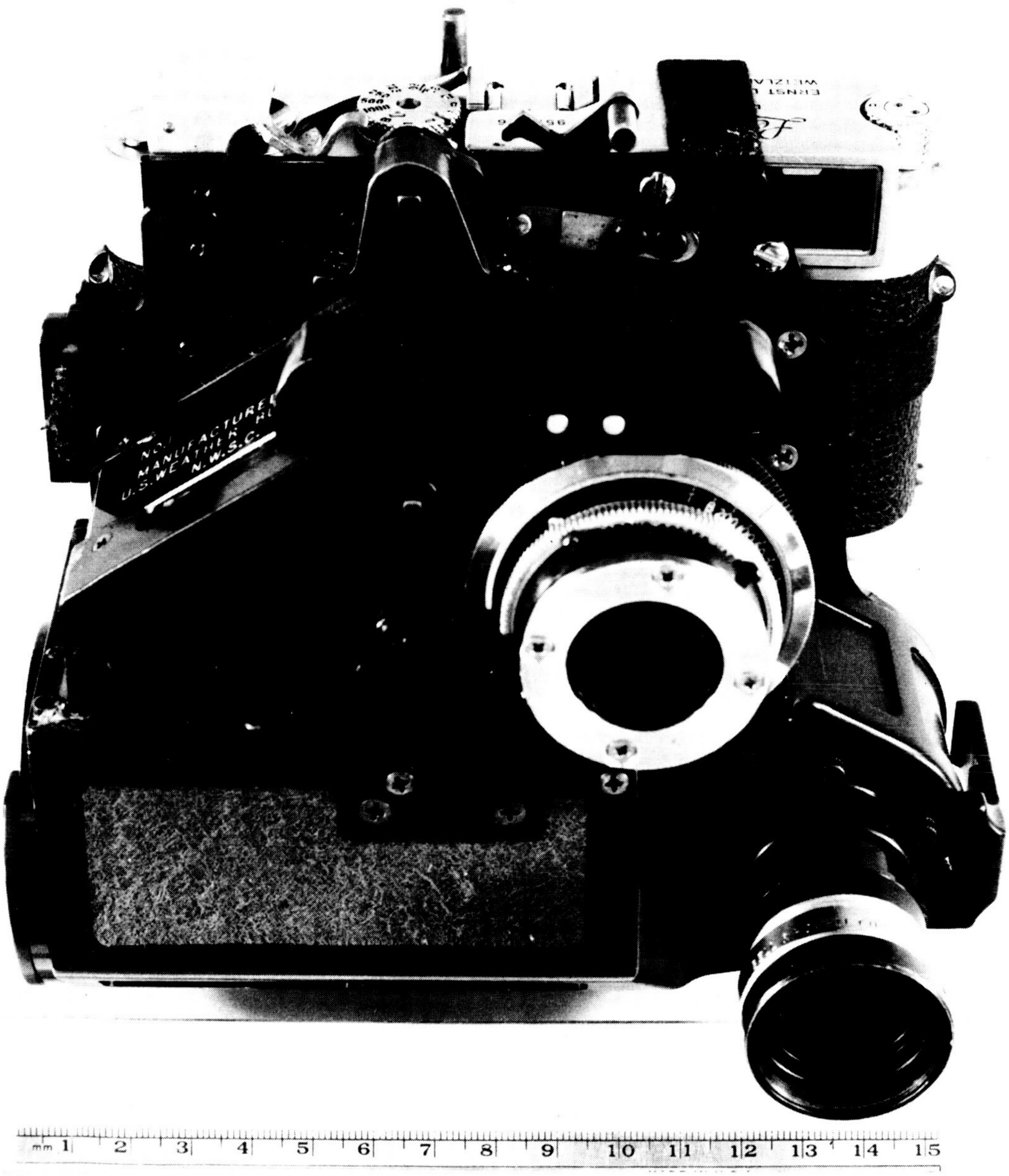

Figure 4-3.- View of the spectrograph showing the two objective lenses.

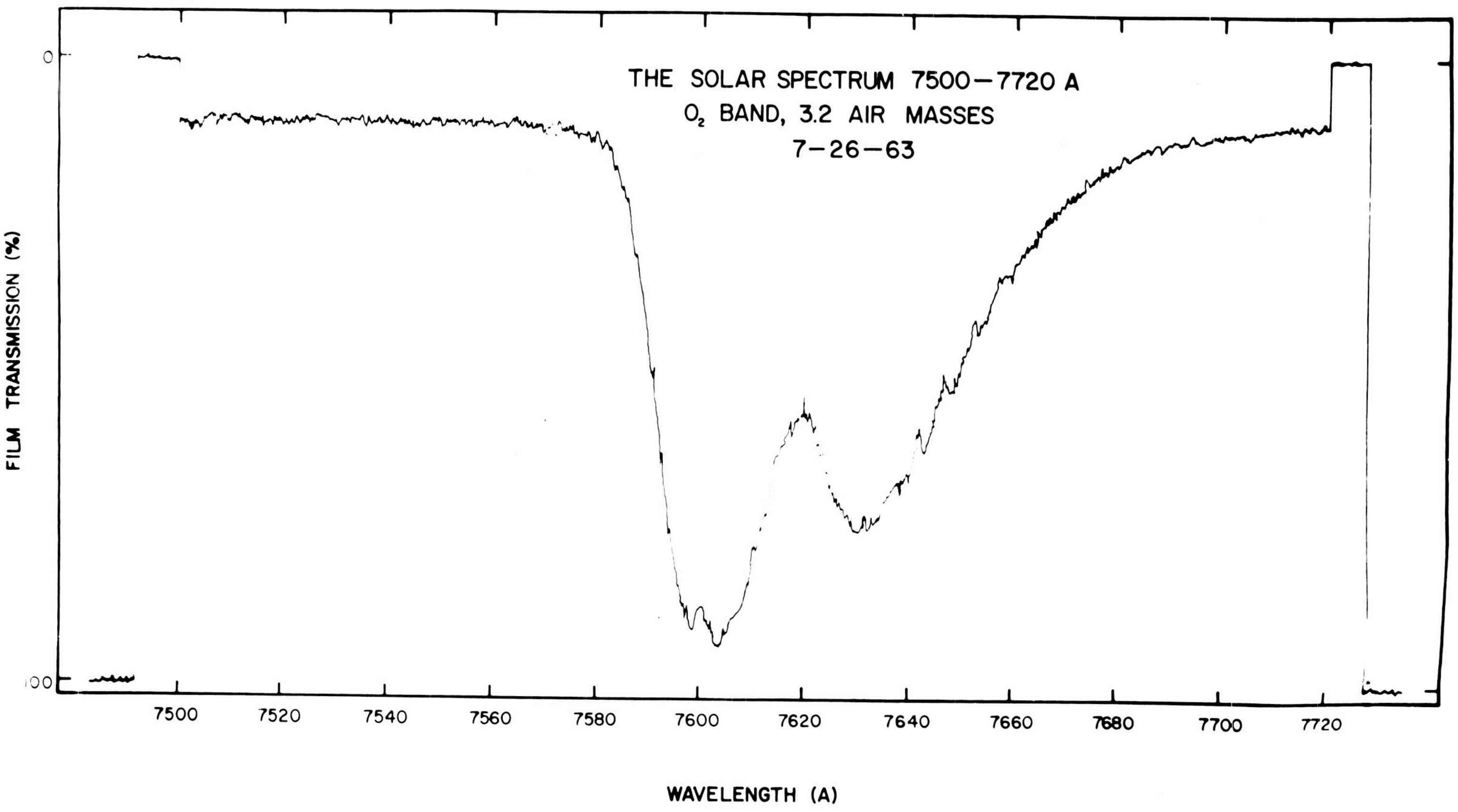

Figure 4-4.- Microdensitometer trace of the spectrum.

Figure 4-5.- Photograph and spectrogram taken from the Gemini V spacecraft. The spectrogram in the upper portion shows the oxygen "A" band near 7600 Å.

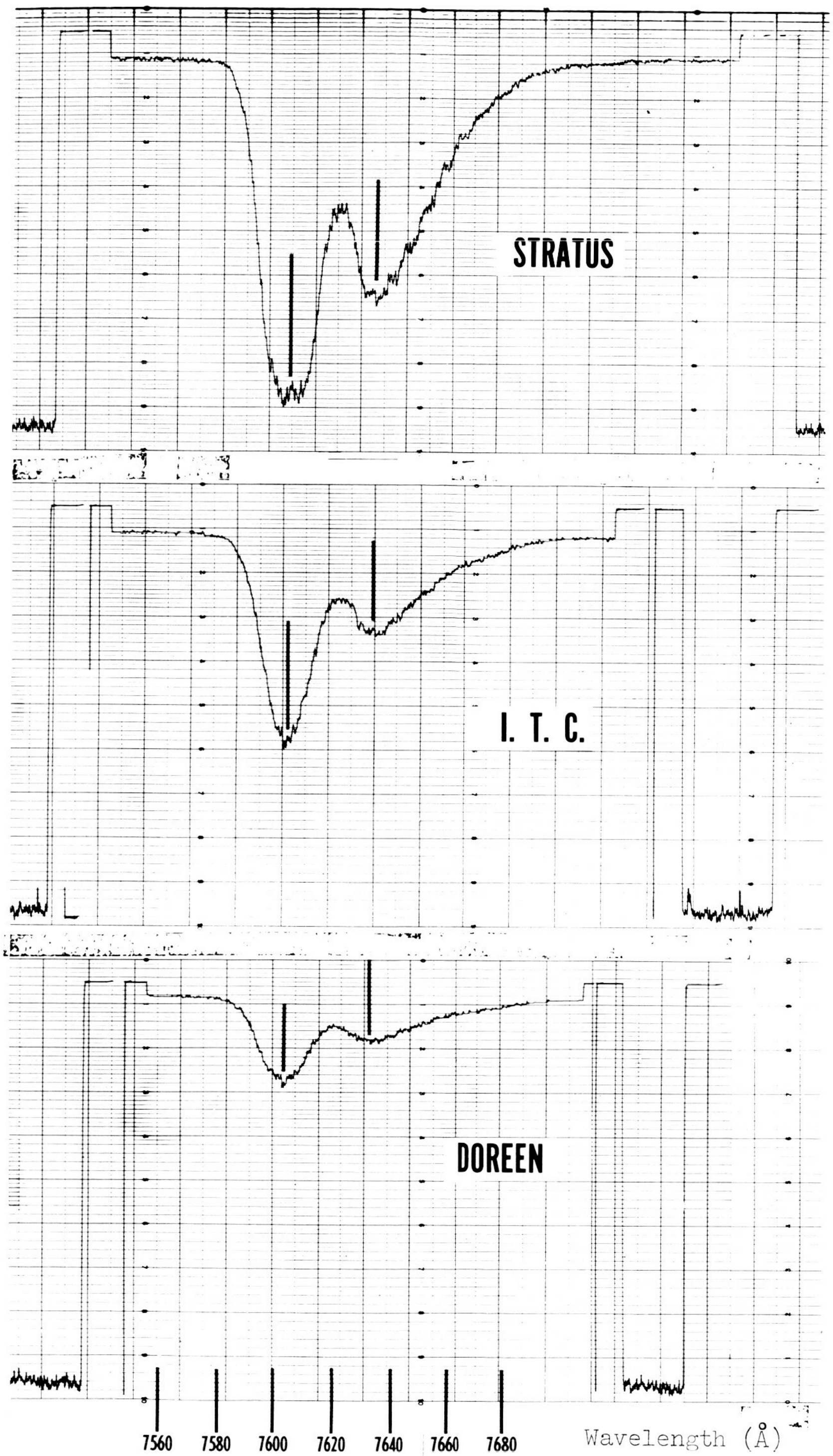

Figure 4-6.- Microdensitometer traces of three spectra obtained by the Gemini V astronauts. The vertical dashed lines are at 7607 Å and 7631 Å.

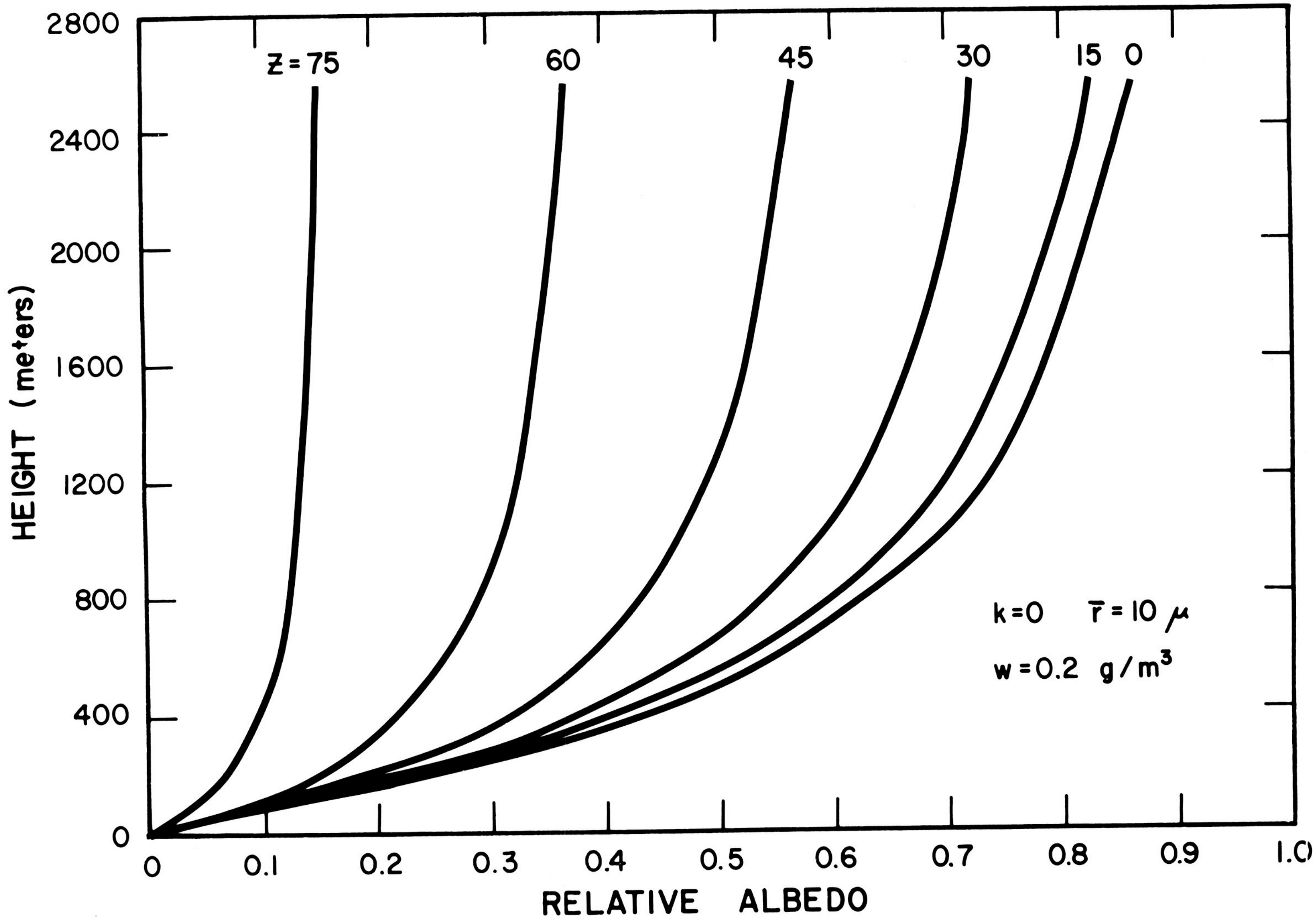

Figure 4-7.- The variation of the relative brightness of the cloud to cloud thickness and solar zenith angle.

5. EXPERIMENT S-8/D-13, VISUAL ACUITY AND ASTRONAUT VISIBILITY

By Seibert Q. Duntley, Roswell W. Austin,
John H. Taylor, and James L. Harris
Visibility Laboratory, Scripps Institute of Oceanography
University of California

SUMMARY

Preflight, in-flight, and postflight tests of the visual acuity of both the Gemini V crew members showed no statistically significant change in their visual capability. Observations of a prepared and monitored pattern of rectangles made at a ground site near Laredo, Texas confirmed that the visual performance of an astronaut in space was within the statistical range of his preflight thresholds, and that laboratory visual acuity data can be combined with environmental optical data to predict correctly man's limiting visual capability to discriminate small objects on the surface of the earth in daytime.

INTRODUCTION

Reports by Mercury astronauts of their sighting small objects on the ground prompted the initiation of a controlled visual acuity experiment which was first conducted in Gemini V. The first objective of Experiment S-8/D-13 was to measure the visual acuity of the crew members before, during, and after long-duration space flights in order to ascertain the effects of a prolonged spacecraft environment. The second objective was to test the use of basic visual-acuity data combined with measured optical properties of ground objects and their natural lighting, as well as of the atmosphere and the spacecraft window, to predict the flight crew's limiting naked-eye visual capability to discriminate small objects on the surface of the earth in daylight.

IN-FLIGHT VISION TESTS

In-flight Vision Tester

The visual performance of both crew members was tested one or more times each day by means of an in-flight vision tester. This was a small, self-contained, binocular optical device containing a transilluminated array of 36 high contrast and low contrast rectangles. Half of the rectangles were oriented vertically in the field of view and half were oriented horizontally. Rectangle size, contrast, and orientation were randomized; the presentation was sequential, and the sequences were nonrepetitive. Each rectangle was viewed singly at the center of a 30-degree adapting field, the apparent luminance of which was approximately 100 foot-lamberts. Both members of the flight crew made forced-choice judgments of the orientation of each rectangle and indicated their responses by punching holes in a record card. Optical alinement was accomplished by means of a biteboard equipped with the flight crew member's dental impression. Electrical power for illumination within the instrument was derived from the spacecraft.

The space available between the eyes of the astronaut and the sloping inner surface of the spacecraft window, a matter of 8 or 9 inches, was an important constraint on the physical size of the instrument. The superior visual performance of both crew members, as evidenced by clinical test scores of 20/10 and 20/12, made it necessary to use great care in alining the instrument with the observer's eyes, since the eyes and not the instrument must set the limit of resolution. In order to achieve this, the permissible tolerance of decentering between a corneal pole and the corresponding optical axis of the eyepiece was less than 0.005 of an inch. This tolerance was met by means of a biteboard equipped with a dental impression to take advantage of the fixed geometrical relation between the upper teeth and the eyes. Figure 5-1 shows a photograph of the in-flight vision tester.

Selection of the Test

The choice of test was made only after protracted study. Many interacting requirements were considered. If, for example, the visual capabilities of the astronauts should change during the long-duration flight, the readings should not go offscale. This requirement for a broad range of testing was not readily compatible with the desire to have fine steps within the test and yet have sufficient repetition to insure statistically significant results. If important changes occurred, moreover, it was of prime importance to measure the change in such a way that the limiting capability of astronauts to detect, recognize, classify, and identify unknown objects in space or on the ground would be predictable. This prediction requirement tended to eliminate the use of Snellen letters, Landolt rings, checkerboards, and virtually all of the conventional patterns used in testing vision. Both theory and experiment show that the higher order visual discriminations depend upon the quadratic content of the difference images between alternative objects, whereas all of the conventional test patterns yield low precision information on this important parameter. The same consideration also renders detection threshold tests undesirable.

It was also deemed desirable that the pattern chosen for the in-flight tester should be compatible with that used on the ground, where search contamination of the scores must be carefully avoided. This consideration also made any detection threshold test undesirable.

The optimum choice of test proved to be the orientation discrimination of a bar narrow enough to be unresolved in width but long enough to provide for threshold orientation discrimination. The solid angular subtense and the apparent contrast of all of the bars used in the test were sufficient to make them readily detectable, but only the larger members of the series were above the threshold of orientation discrimination. These two thresholds are more widely separated for the bar than for any other known test object. The inherent quadratic content of the difference image between orthogonal bars is of greater magnitude than the inherent quadratic content of the bar itself. Interpretation of any changes in the visual performance of the astronauts is, therefore, more generally possible on the basis of orientation discrimination thresholds for the bar than from any other known datum.

Rectangles in the Vision Tester

The rectangles presented for viewing within the in-flight vision tester were reproduced photographically on a transparent disc. Two series of rectangles were included, the major series being set at contrast-1 and the minor series being set at about one-third of this value. The higher contrast series constituted the primary test and was chosen to simulate the expected range of apparent contrast presented by the ground panels to the eyes of the astronauts in orbit. The series consisted of six sizes of rectangles, sizes which covered a sufficient range to guard against virtually any conceivable change in the visual performance of the astronauts during the long-duration flight. The size intervals were small enough, however, to provide a sufficiently sensitive test.

The stringent requirements imposed by conditions of space flight made it impossible to use as many repetitions of each rectangle as was desirable from statistical considerations. After much study it was decided to display each of the six rectangular sizes four times. This compromise produced a sufficient statistical sample to make the sensitivity of the in-flight test comparable to that ordinarily achieved with the most common variety of clinical wall chart. This sensitivity corresponds roughly to the ability to separate performance at 20/15 from performance at 20/20. It was judged that this compromise between the sensitivity of test and the range of the variables tested was the proper one for this exploratory investigation.

A secondary test at lower contrast was included as a safeguard against the possibility that visual performance at low contrast might change in some different way. With only twelve rectangles assignable within the in-flight vision tester for the low contrast array, it was decided to use only three widely different rectangle sizes, presenting each of these sizes four times.

Because of the accelerated launch schedule of Gemini V it was not possible to use the flight instrument for preflight experiments. These data were, therefore, obtained with the first of the in-flight vision testers (serial no. 1) while the last instrument to be constructed (serial no. 5) was put aboard the spacecraft. The two instruments were optically identical except for their twelve low contrast rectangles, which measured a contrast of -0.332 and -0.233, respectively.

Analysis of Correct Scores

A comparison of the correct scores made by the crew members on the ground (preflight) and in space (in-flight) can be used to ascertain whether their observed visual performance differed in the environments or changed during the 7-day mission. The correct scores from the low contrast and high contrast series in the vision tester are shown for both crew members in figure 5-2. The results of standard statistical tests applied to these data are shown in tables 5-I through 5-IV.

TABLE 5-I.- VISION TESTER (GROUND VERSUS SPACE)

Cooper	C = -1		C = -0.23	
	Ground	Space	Ground	Space
Number	7	9	7	9
Mean	17.6	18.4	8.6	8.3
S.d	2.3	0.96	1.3	1.4
t	0.96		0.31	
$t_{0.05}$	2.14		2.14	
F	6.12		1.02	
$F_{0.05}$	3.58		3.58	
$F_{0.01}$	6.37			

TABLE 5-II.- VISION TESTER (GROUND VERSUS SPACE)

Conrad	C = -1		C = -0.23	
	Ground	Space	Ground	Space
Number	7	9	7	9
Mean	20.7	20.7	9.7	8.6
S.d	2.7	1.7	1.2	2.0
t	0		1.13	
$t_{0.05}$	2.14		2.14	
F	2.79		2.43	
$F_{0.05}$	3.69		4.82	

TABLE 5-III.- VISION TESTER (IN-FLIGHT TREND)

Cooper	C = -1		C = -0.23	
	First 4	Last 4	First 4	Last 4
Number	4	4	4	4
Mean	18.2	18.8	8.5	8.5
S.d	0.83	1.1	0.87	1.8
t	0.68		0	
$t_{0.05}$	2.45		2.45	
F	1.73		4.33	
$F_{0.05}$	9.28		9.28	

TABLE 5-IV.- VISION TESTER (IN-FLIGHT TREND)

Conrad	C = -1		C = -0.23	
	First 4	Last 4	First 4	Last 4
Number	4	4	4	4
Mean	21.3	19.5	8.8	8.75
S.d	1.5	1.1	2.8	0.83
t	1.64		0	
$t_{0.05}$	2.45		2.45	
F	1.96		11.19	
$F_{0.05}$	9.28		9.28	
$F_{0.01}$			29.5	

Comparisons between preflight and in-flight data are given in tables 5-I and 5-II. All students' t tests show no significant difference in means. All Snedecor's F tests show no significant difference in variances at the 0.05 level, with the exception of Cooper's high contrast comparison which shows no significant difference at the 0.01 level.

Comparisons between the in-flight data at the beginning of the mission with that at the end are made in tables 5-III and 5-IV. All students' t tests and Snedecor's F tests show no significant difference at 0.05 level with the exception of the F test on Conrad's low contrast comparison which shows no significant contrast at 0.01 level.

These statistical findings support the null-hypothesis advanced by many scientists before the Gemini V mission was flown. Examination of the sensitivity of the test must next be considered, and this topic is treated in the following section.

Preflight Physiological Baseline

Design of the in-flight vision tester, as well as the ground sighting experiments described in a later section and the interpretation of the results from both experiments, required that a preflight physiological baseline be obtained for both crew members. For this purpose a NASA van was fitted out as a portable vision research laboratory, moved to the Manned Spacecraft Center at Houston, Texas, and operated by Visibility Laboratory personnel. Figure 5-3 is a cutaway drawing of this research van. The astronauts, seated at the left, viewed rear-screen projections from an automatic projection system located in the opposite end of the van. Each astronaut participated in several sessions in the laboratory van, during which they became experienced in the psychophysical techniques of the rectangle orientation discrimination visual task. A sufficiently large number of presentations were made to secure a properly numerous statistical sample. The astronauts' forced-choice visual thresholds for the discrimination task were measured accurately and their response distributions determined so that the standard deviations and confidence limits of their preflight visual performance were determined.

Figure 5-4 is a logarithmic plot of the pilot's preflight visual thresholds for the rectangle orientation discrimination task. In this figure the solid angular subtense of the rectangles is plotted along the horizontal axis because both the in-flight vision tester and the ground observation experiments used angular size as the independent variable. The solid line in this figure represents the forced-choice rectangle orientation threshold of the pilot at the 0.50 probability level. The dashed curves indicate the $-\sigma$, $+\sigma$, and $+2\sigma$ levels in terms of contrast. The six circled points in the upper row indicate the angular sizes of the high contrast ($C = -1$) rectangles presented by the in-flight vision tester. The three circled points of the middle and lower rows show the angular sizes of the low contrast rectangles used in the training unit (no. 1) and the flight unit (no. 5) respectively.

By means of figure 5-4, the separate discriminations recorded on the record cards in the in-flight vision tester can be used to determine a threshold of angular size. These thresholds are plotted for the high and low contrast tests of the command pilot in figures 5-5 and 5-6, and for the pilot in figures 5-7 and 5-8. In these four figures the horizontal solid line represents the forced-choice rectangular orientation threshold and the horizontal broken lines show statistical confidence limits in terms of angular size.

These four figures also support the null-hypothesis, and their quantitative aspect constitutes a specification of the sensitivity of the test. Thus, as planned, changes in visual performance comparable with those on a one line conventional clinical wall chart would have been detected. Preflight threshold data can, therefore, be used to predict the limiting visual acuity capabilities of astronauts during space flight provided adequate physical information concerning the object, its background, atmospheric effects, and spacecraft window exists. A test of such predictions was also carried out and is described in the following sections.

GROUND OBSERVATIONS

Ground observations were made of prepared and monitored rectangular patterns in order to test the use of basic visual acuity data combined with measured optical properties of ground objects and their natural lighting, the atmosphere, and the spacecraft window to predict the limiting naked-eye visual capability of the astronauts to discriminate small objects on the surface of the earth in daylight.

Equipment

The experimental equipment consists of an in-flight photometer to monitor the spacecraft window, test patterns at two ground observation sites, instrumentation for atmospheric, lighting, and pattern measurements at both sites, and a laboratory facility (housed in a trailer van) for training the astronauts to perform visual acuity threshold measurements and for obtaining a preflight physiological baseline descriptive of their visual performance and its statistical fluctuations. These equipments, except the last, are described in the following paragraphs.

Spacecraft window photometer.- A photoelectric in-flight photometer was mounted near the lower right corner of the pilot's window of the GT-V spacecraft, as shown in figure 5-9, in order to measure the amount of ambient light scattered by the window into the path of sight at the moment when observations of the ground test patterns were made. The photometer (fig. 5-10) had a narrow (1.2°) circular field of view, which was directed through the pilot's window and into the opening of a small black cavity a few inches away outside the window. The photometric scale was linear and extended from approximately 60 to 3000 foot-lamberts. Since the apparent luminance of the black cavity was always much less than 60 foot-lamberts, any reading of the in-flight photometer was ascribable to ambient light scattered by the window. Typical data during passes over the Laredo site are shown in figure 5-11. This information combined with data on the beam transmittance of the window and on the apparent luminance of the background squares in the ground pattern array enabled the contrast transmittance of the window at the moment of observation to be calculated. Uniformity of the window could be tested by removing the photometer from its positioning bracket and making a hand-held scan of the window, using a black region of space in lieu of the black cavity. A direct-reading meter incorporated in the photometer enabled the command pilot to observe the photometer readings while the pilot scanned his own window for uniformity. A corresponding scan of the command pilot's window could be made in the same way. Data from the photometer was sent to the ground by real-time telemetry. Electrical power for the photometer was provided entirely by batteries within the instrument.

Ground observation sites.- Sites were provided on the Gates Ranch, 40 miles north of Laredo, Texas (fig. 5-12), and on the Woodleigh Ranch, 90 miles south of Carnarvon, Australia, (figs. 5-13 and 5-14). At the Texas site, 12 squares of plowed, graded, and raked soil 2000 ft by 2000 ft were arranged in a 4 by 3 matrix. White rectangles of styrofoam-coated wallboard were laid out in each square. Their length decreased in a uniform logarithmic progression from 610 feet in the northwest corner (square number 1) to 152 feet in the southwest corner (square number 12) of the array. Each of the 12 rectangles was oriented in one of four positions (i.e., north-south, east-west, or diagonal), and the orientations were random within the series of 12. Advance knowledge of the rectangle orientations was withheld from the flight crew since their task was to report the orientations. Provision was made for changing the rectangle orientations between passes and for adjusting their size in accordance with anticipated slant range, solar elevation, and the visual performance of the astronauts on preceding passes. The observation site in Australia was somewhat similar to the Texas site, but, inasmuch as no observations occurred there during GT-V, the specific details are unnecessary in this report.

Instrumentation.- Instrumentation at both ground sites consisted of a single tripod-mounted, multipurpose, recording photoelectric photometer (figs. 5-15 and 5-16) capable of obtaining all the data needed to specify the apparent contrast of the pattern as seen from the spacecraft at the moment of observation. The apparent luminance of the background squares, needed for evaluation of the contrast loss due to the spacecraft window, was also ascertained by this instrument. A 14-foot high mobile tower, constructed of metal scaffolding and attached to a truck, supported the tripod-mounted photometer high enough above the ground to enable the plowed surface of the background squares to be measured properly. This arrangement is shown in figures 5-17 and 5-18.

Scheduled Observations

Observation of the Texas ground pattern site was first attempted on revolution 18, but fuel cell difficulties which denied the use of the platform was apparently responsible for lack of acquisition of the ground site.

The second scheduled attempt to see the pattern near Laredo was on revolution 33. Acquisition of the site was achieved by the command pilot but not by the pilot, and no read-out of rectangle orientation was made.

At the request of the experimenters, the third attempt at Laredo, scheduled originally for revolution 45, was made on revolution 48 in order to secure a higher sun and a shorter slant range. Success was achieved on this pass and is described below in the section on results.

Unfavorable cloud conditions caused the fourth scheduled observation at the Texas site, on revolution 60, to be scrubbed. Thereafter, lack of thruster control made observation of the ground patterns impossible, although excellent weather conditions prevailed on three scheduled occasions at Laredo (revolutions 75, 92 and 107) and once at the Australian site (revolution 88). Long range visual acquisition of the smoke markers used at both sites was reported in each instance, but the drifting spacecraft was not properly oriented near closest approach to the pattern to enable observations to be made. A fleeting glimpse of the Laredo pattern on revolution 92 enabled it to be successfully photographed with hand cameras. On revolution 107, roll rates were neutralized by use of thrusters prior to the pass over Laredo, and although the command pilot reported a fleeting glimpse of the pattern at closest approach, the viewing time was not sufficient for him to read the orientation of the rectangles successfully.

Results

Quantitative observation of ground markings was achieved only once during GT-V. This observation occurred during revolution 48 at the ground observation site near Laredo, Texas at 18:16:14 on the third day of the flight. Despite early acquisition of the smoke marker by the command pilot and further acquisition by him of the target pattern itself well before the point of closest approach, the pilot did not acquire the markings until the spacecraft had been turned to provide him with a going-away view. Telemetry records from the in-flight photometer shows that the pilot's window produced a heavy veil of scattered light until the spacecraft was rotated into the going-away position. Presumably, elimination of the morning sun on the pilot's window enabled him to make visual contact with the pattern in time to make a quick observation of the orientation of some rectangles. It may be noted that, during approach, the reduction of contrast due to light scattered by the window was more severe than that due to light scattered by the atmosphere.

An ambiguity exists between the transcription of the radio report made at the time of the pass and the written record in the flight log. The writing was made "blind" while the pilot was actually looking at the pattern; it is a diagram drawn in the manner depicted in the GT-V flight plan, the Mission Operation Plan, the Description of Experiment, and other documents. The orientation of the rectangles in the 6th and 7th squares appears to have been correctly noted. The verbal report given several seconds later correctly records the orientation of the rectangle in the 6th square if it is assumed that the spoken words describe the appearance of the pattern as seen from a position east of the array while going away from the site.

Despite the fleeting nature of the only apparently successful quantitative observation of a ground site during GT-V, there seems to be a reasonable probability that the sighting was a valid indication of the pilot's correctly discriminating the rectangles in the 6th and 7th squares. Since he did not give forced-choice responses to squares 8 through 12, presumably due to lack of viewing time, it can only be inferred that his threshold lay at square 6 or higher.

Tentative values of the apparent contrast and angular size of the 6th and 7th rectangles at the Laredo site at the time of the observation are plotted in figure 5-19. The solid line represents the preflight visual performance of Astronaut Conrad as measured in the training van. The dashed lines represent the 1- and 2-sigma limits of his visual performance. The positions of the plotted points indicate that his visual performance at the time of revolution 48 was within the statistical range of his preflight visual performance.

CONCLUSIONS

Experiment S-8/D-13 appears to have achieved successfully both of its stated objectives: data from the in-flight vision tester indicate that the visual performance of the astronauts neither degraded nor improved during the 8-day Gemini V mission. Results from observation of the ground site near Laredo, Texas appear to confirm that the visual performance of the pilot during space flight was within the statistical range of his preflight visual performance and that laboratory visual acuity data can be combined with environmental optical data to predict correctly the astronaut's limiting visual capability to discriminate small objects on the surface of the earth in daylight.

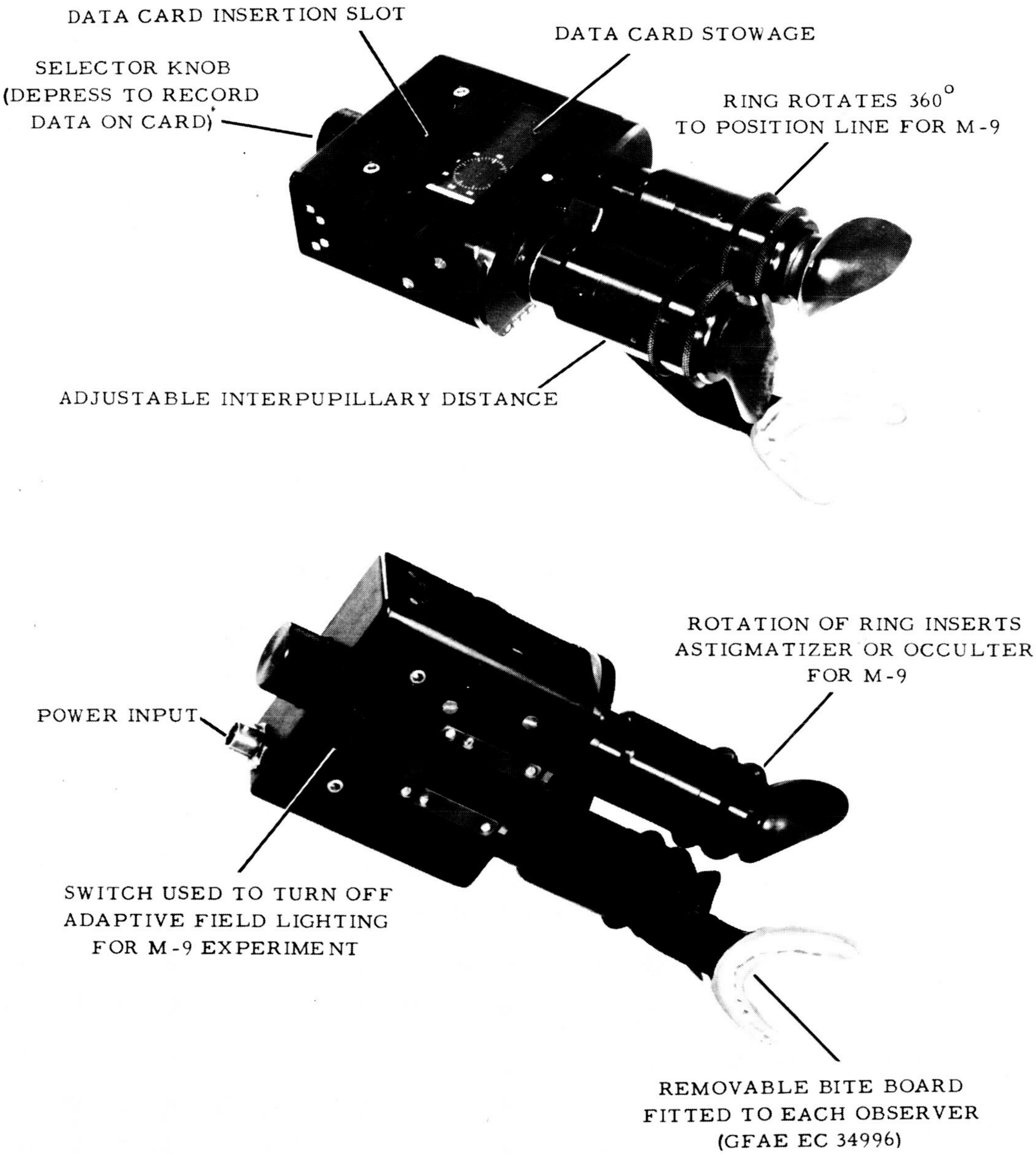

Figure 5-1.- In-flight vision tester.

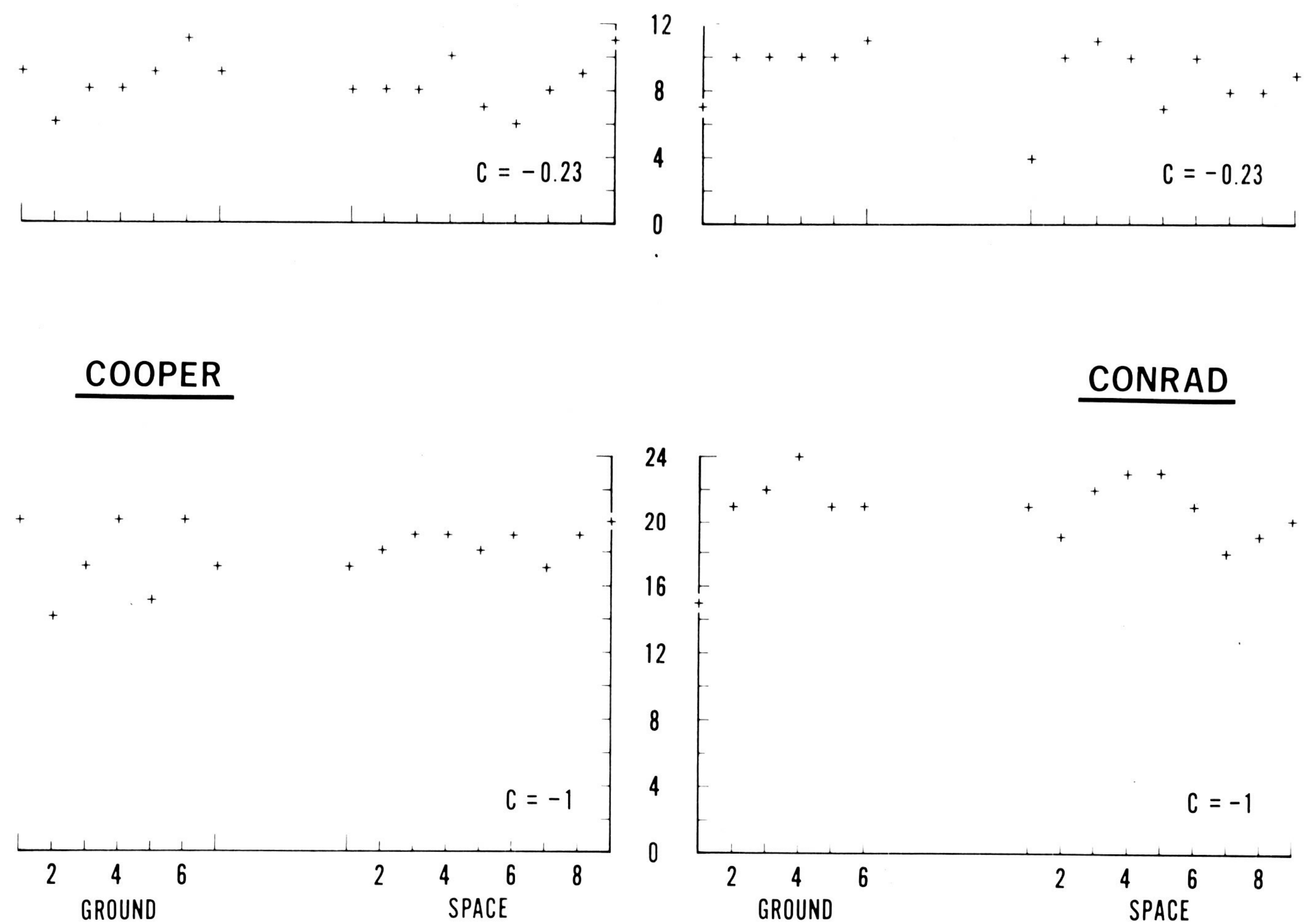

Figure 5-2.- Correct scores for the vision tester.

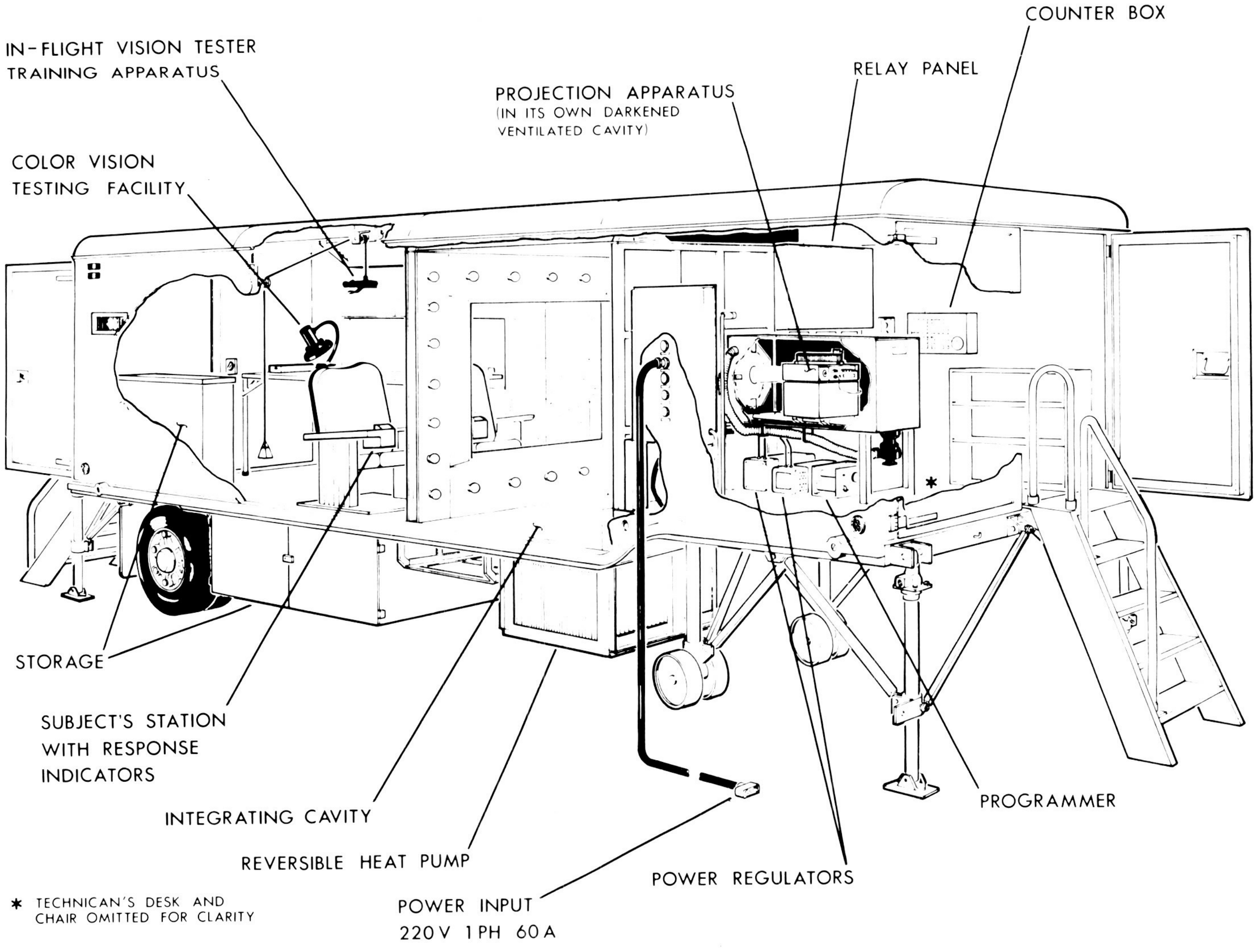

Figure 5-3.- Vision research and training van.

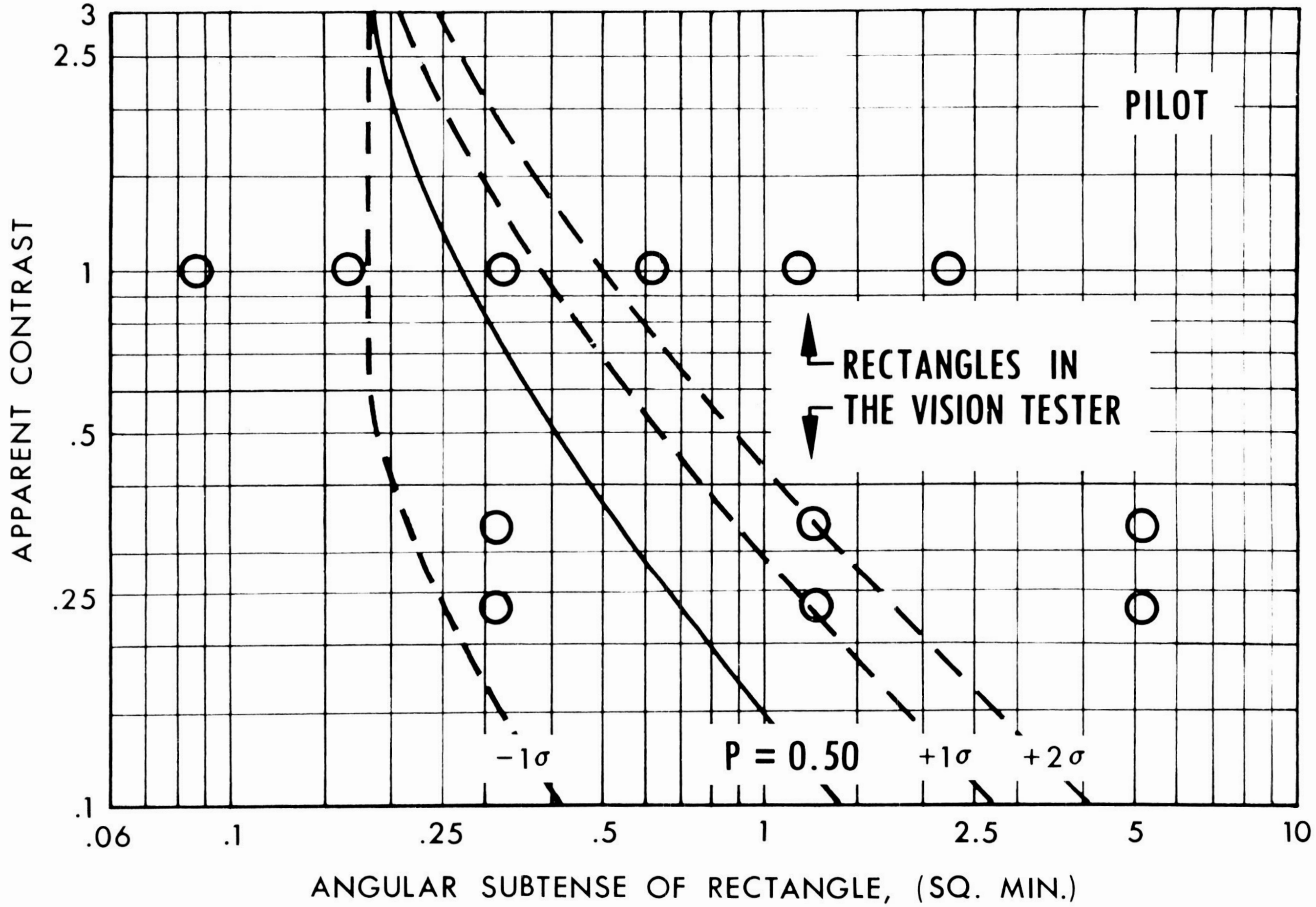

Figure 5-4.- Logarithmic plot of preflight visual thresholds.

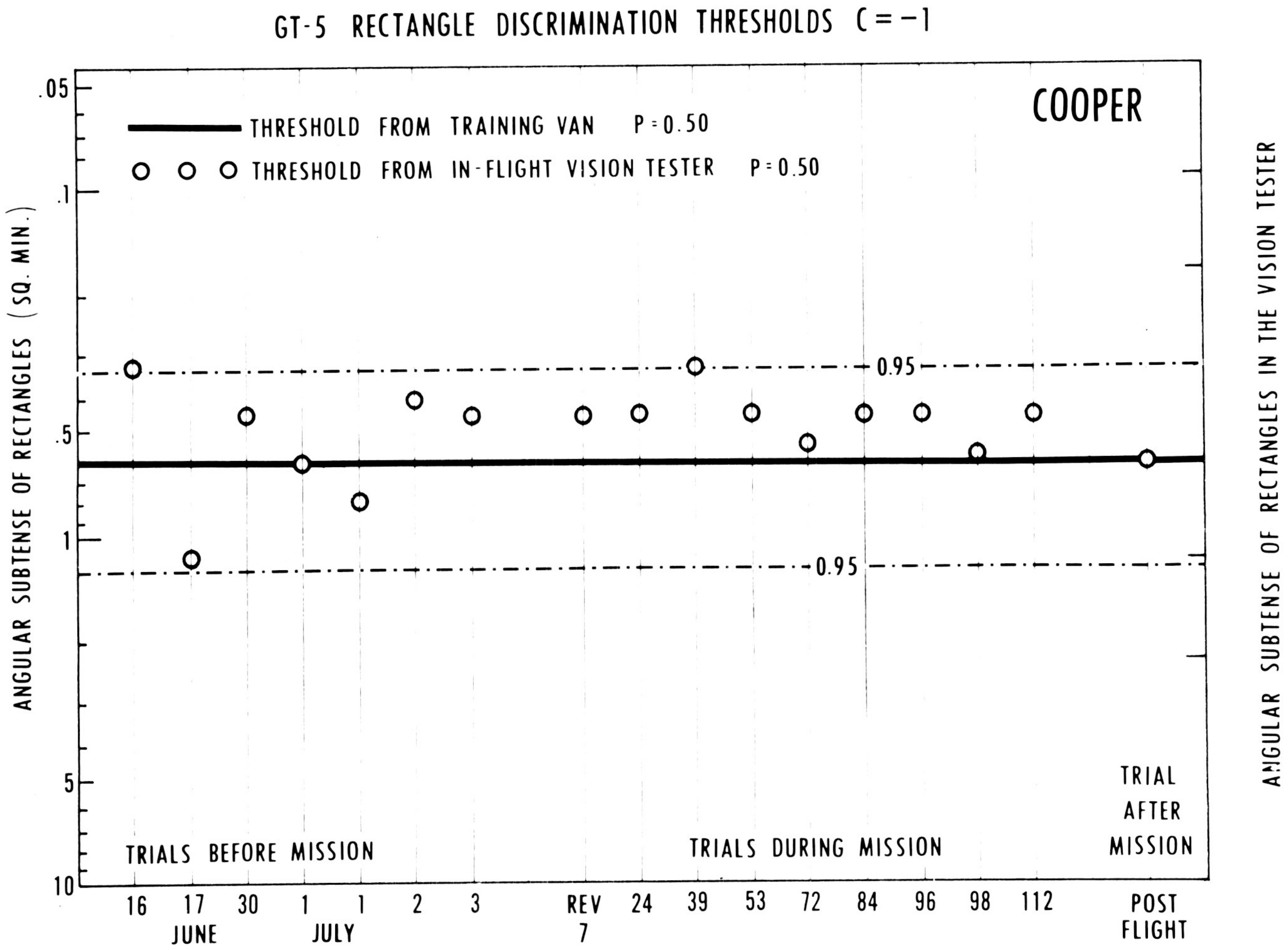

Figure 5-5.- Gemini V command pilot's rectangle discrimination thresholds C = -1.

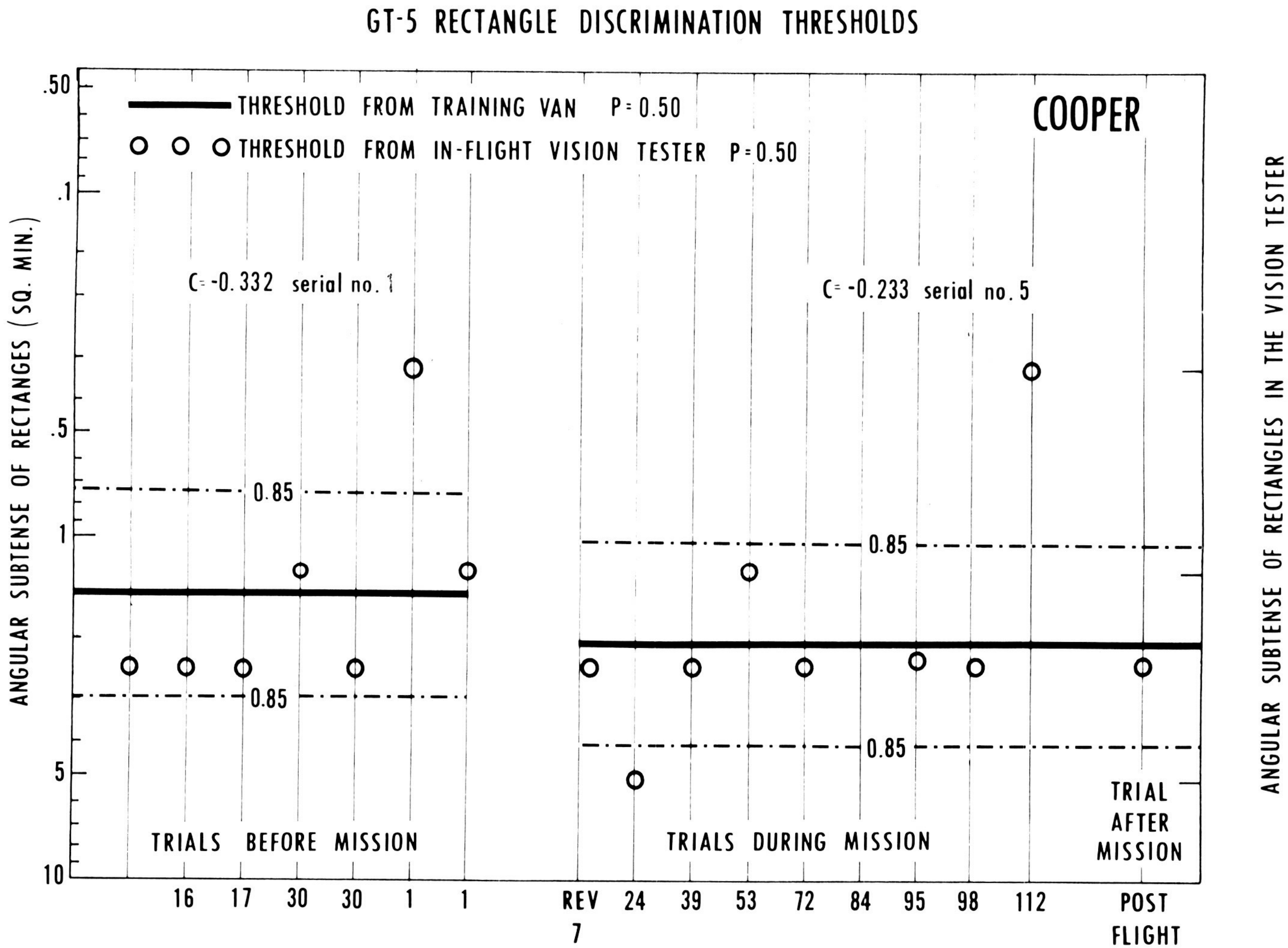

Figure 5-6.- Gemini V command pilot's rectangle discrimination thresholds.

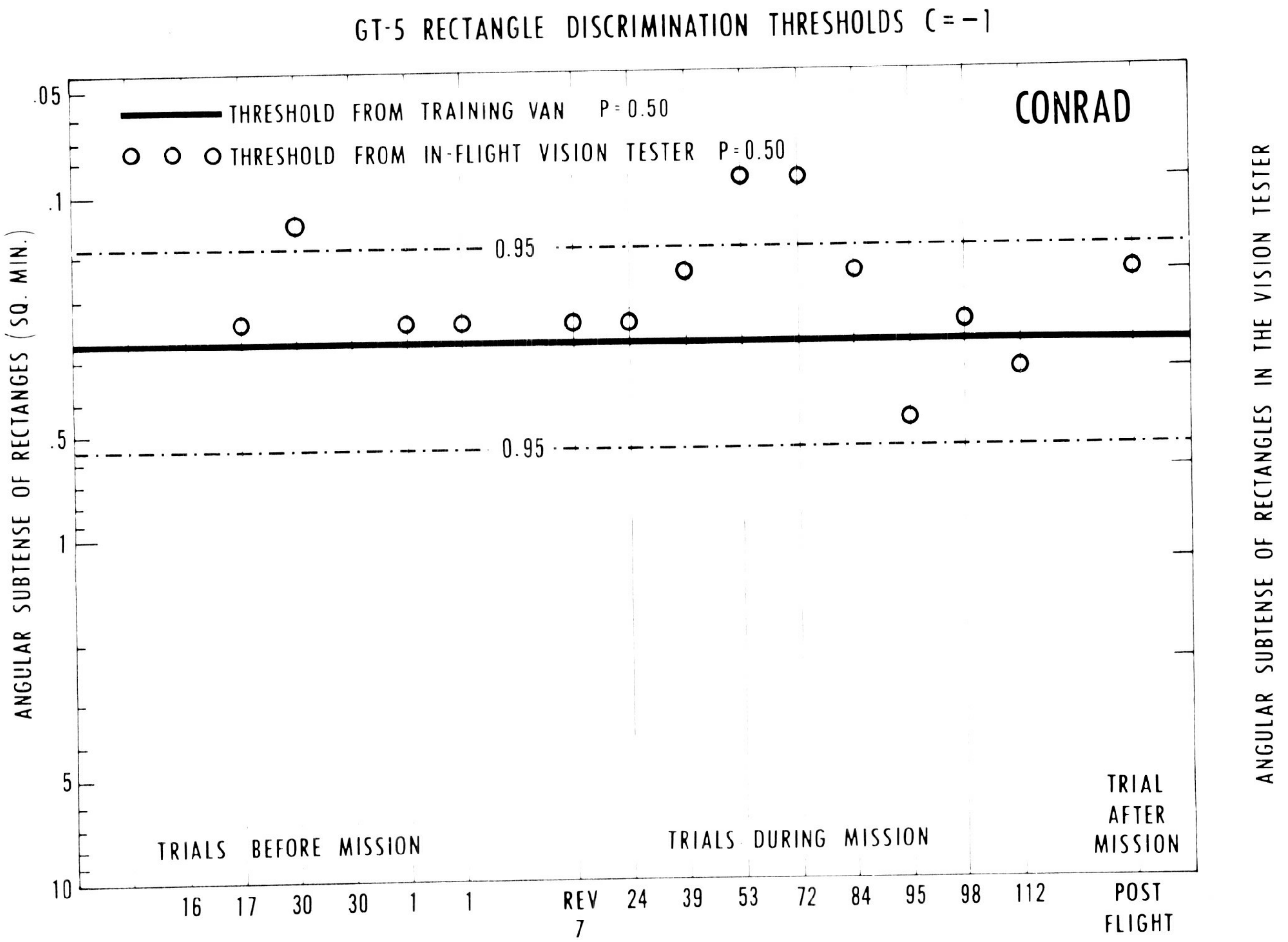

Figure 5-7.- Gemini V pilot's rectangle discrimination thresholds C = -1.

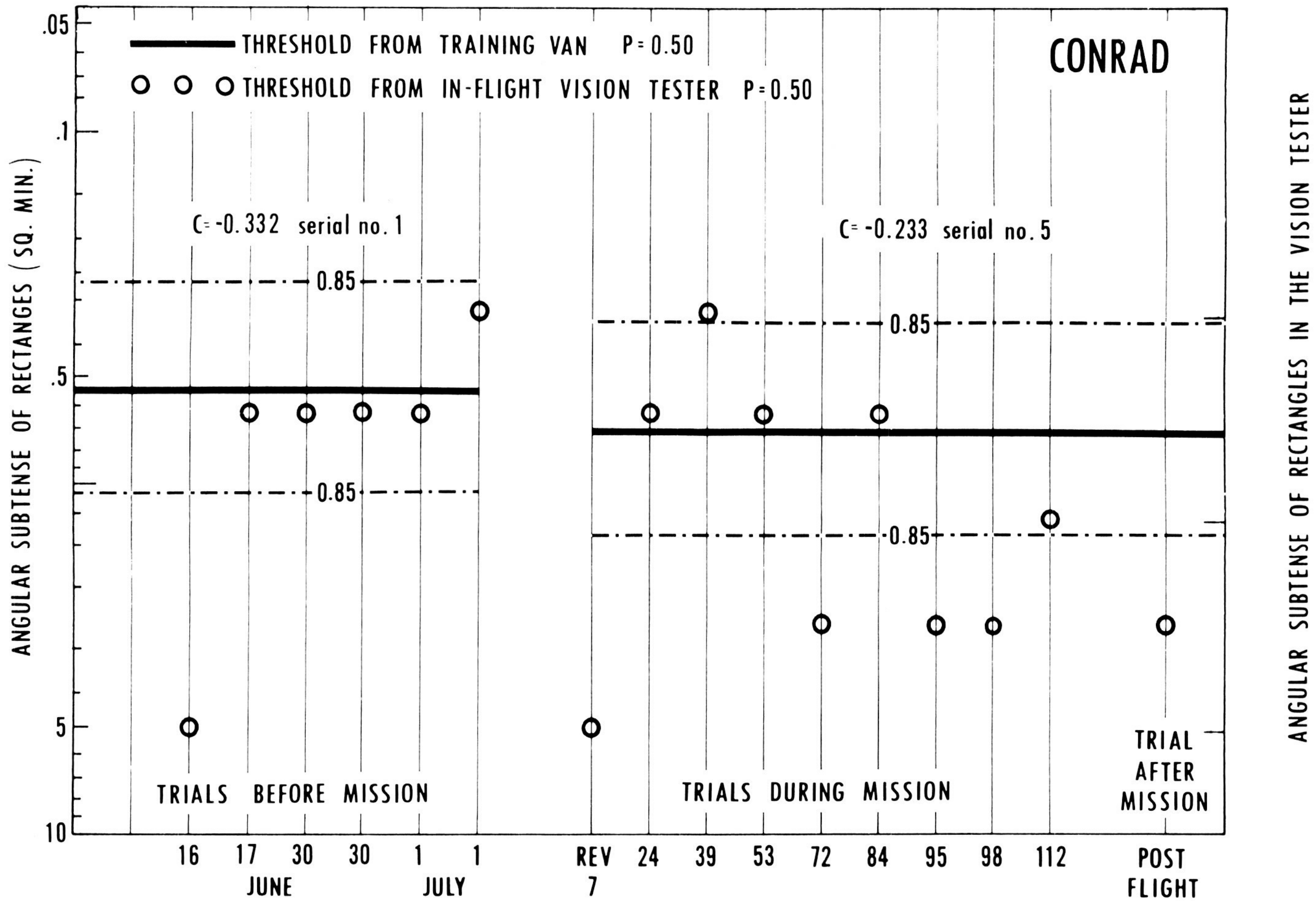

Figure 5-8.- Gemini V pilot's rectangle discrimination thresholds.

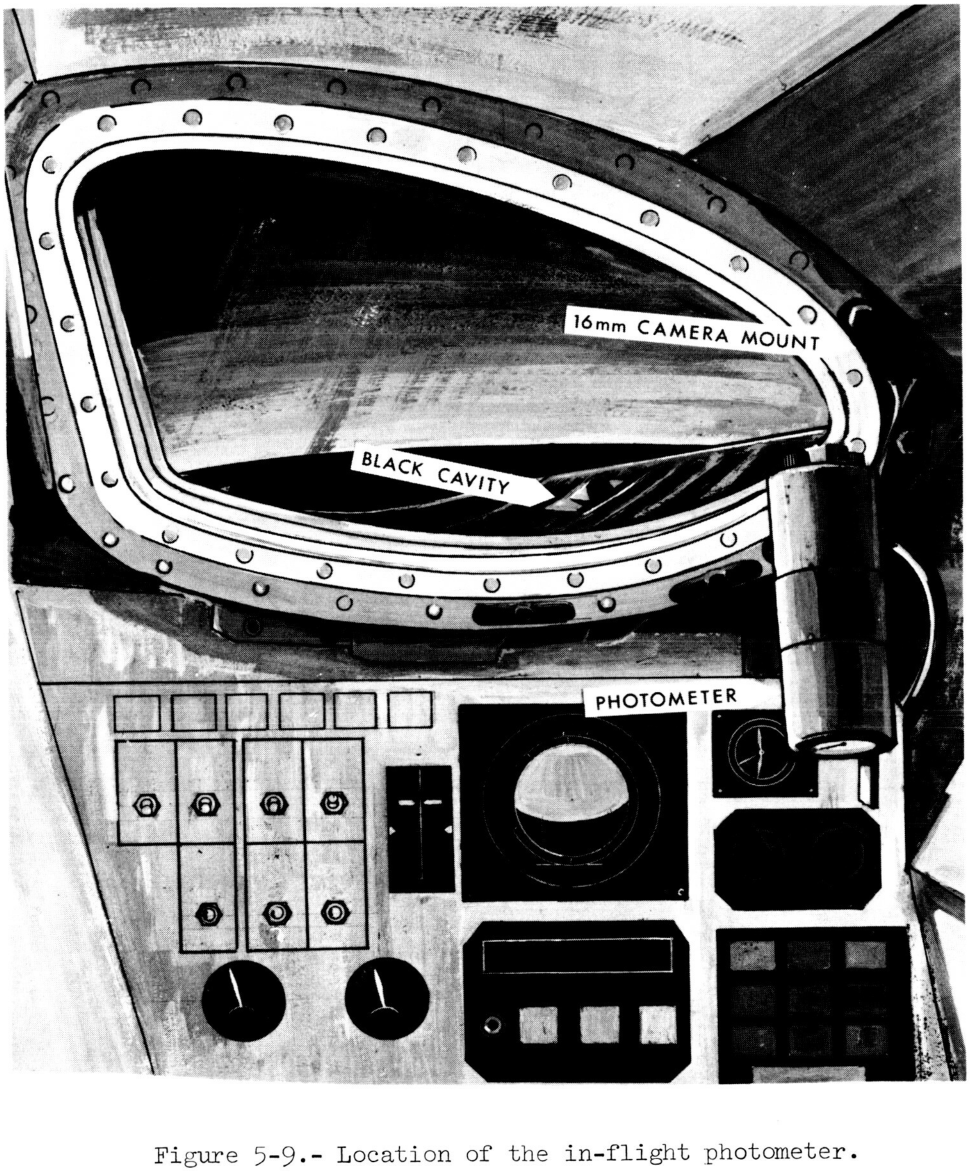

Figure 5-9.- Location of the in-flight photometer.

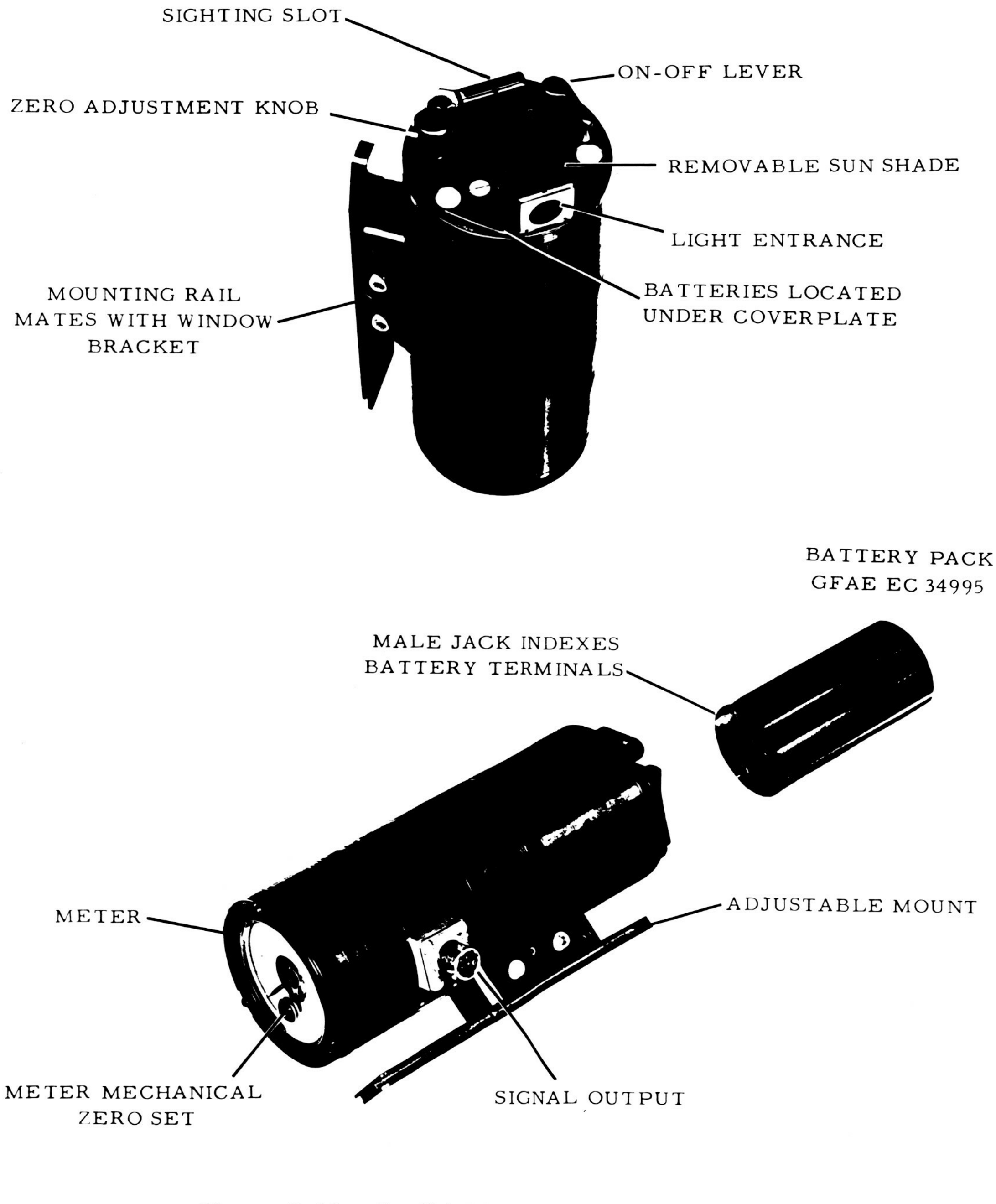

Figure 5-10.- In-flight photometer components.

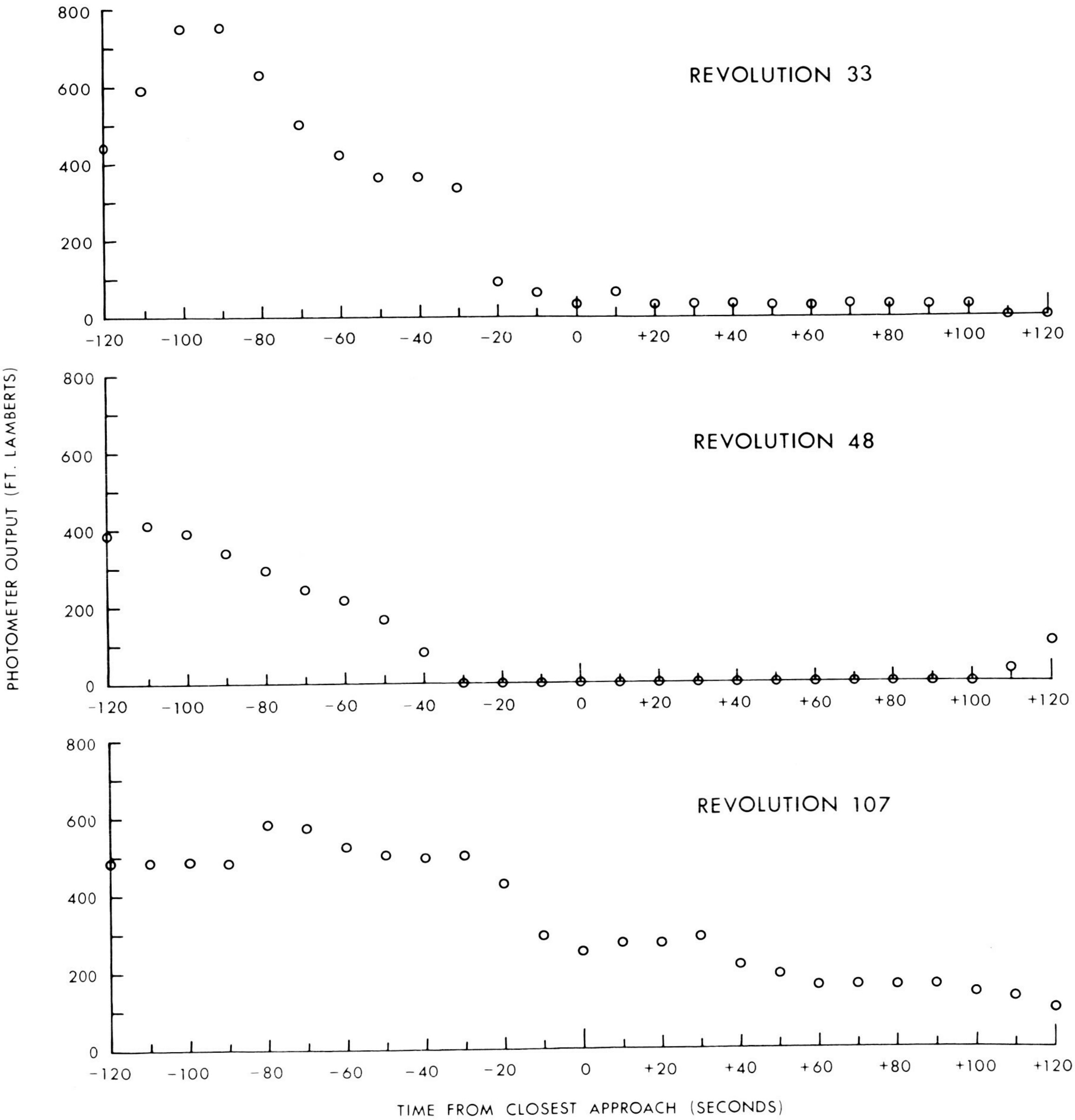

Figure 5-11.- Laredo site photometer data.

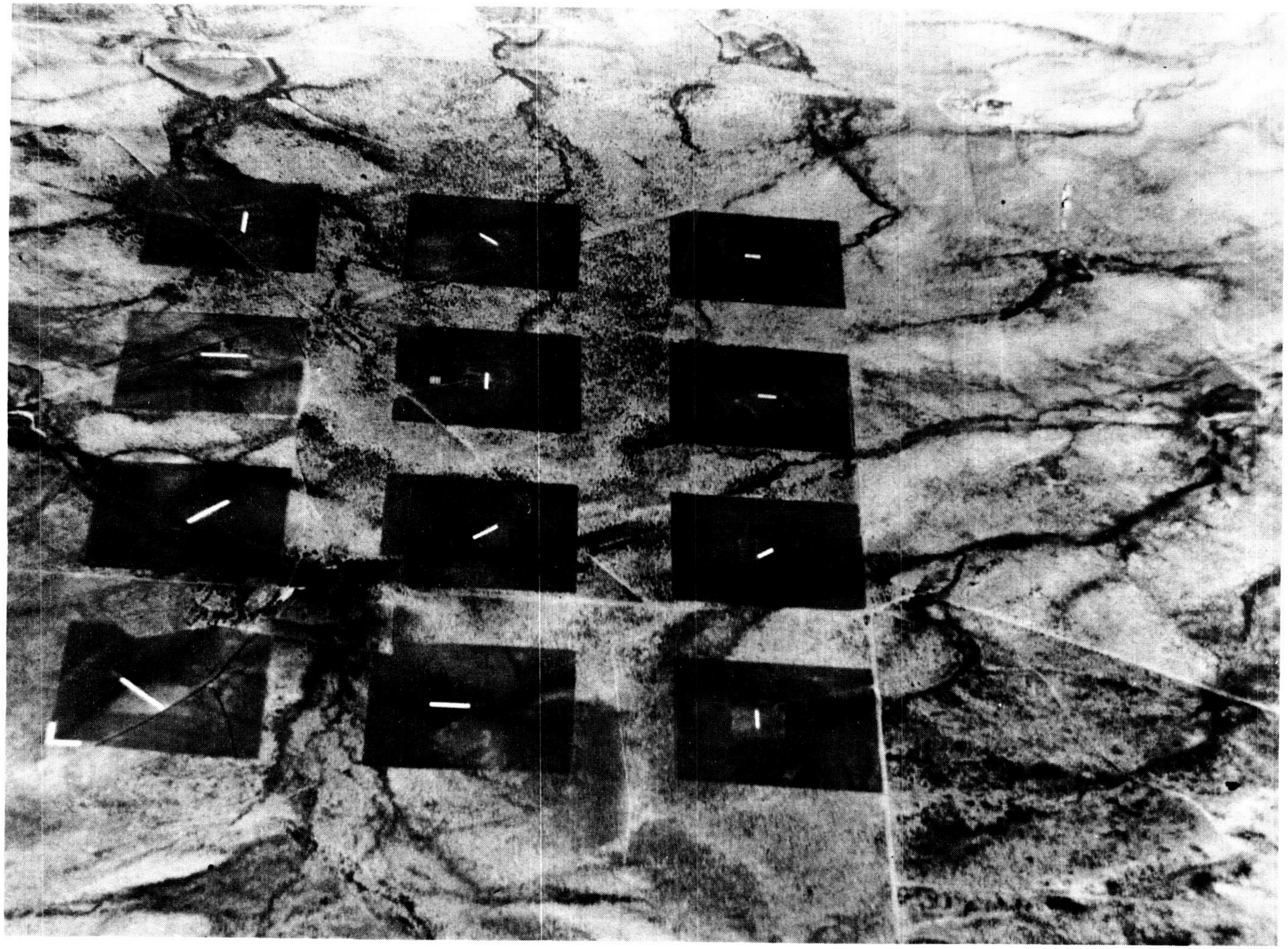

Figure 5-12.- Aerial photograph of the Gemini V visual acuity experiment ground pattern at Laredo, Texas.

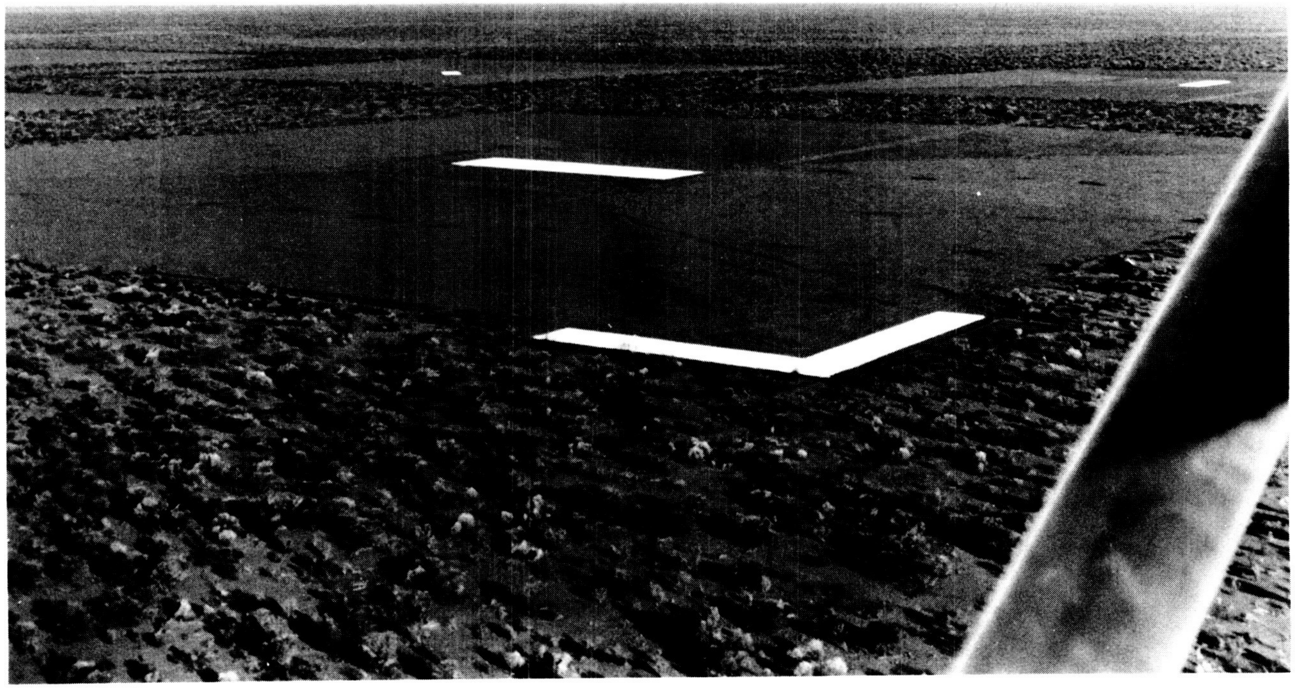

Figure 5-13.- Aerial photograph of the Gemini V visual acuity experiment ground pattern at Carnarvon, Australia.

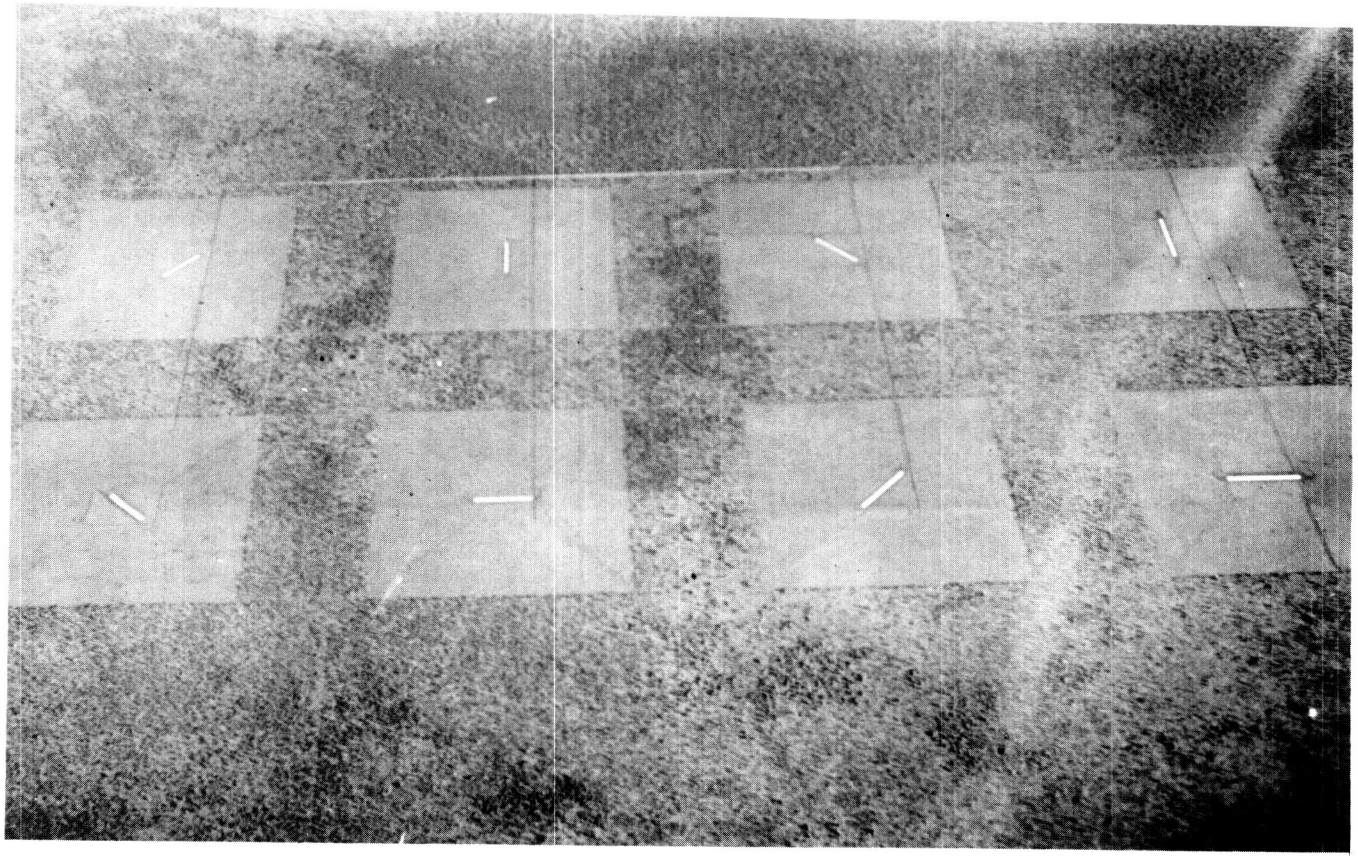

Figure 5-14.- Aerial photograph of the Gemini V visual acuity experiment ground pattern at Carnarvon, Australia.

Figure 5-15.- Ground site tripod-mounted photoelectric photometer.

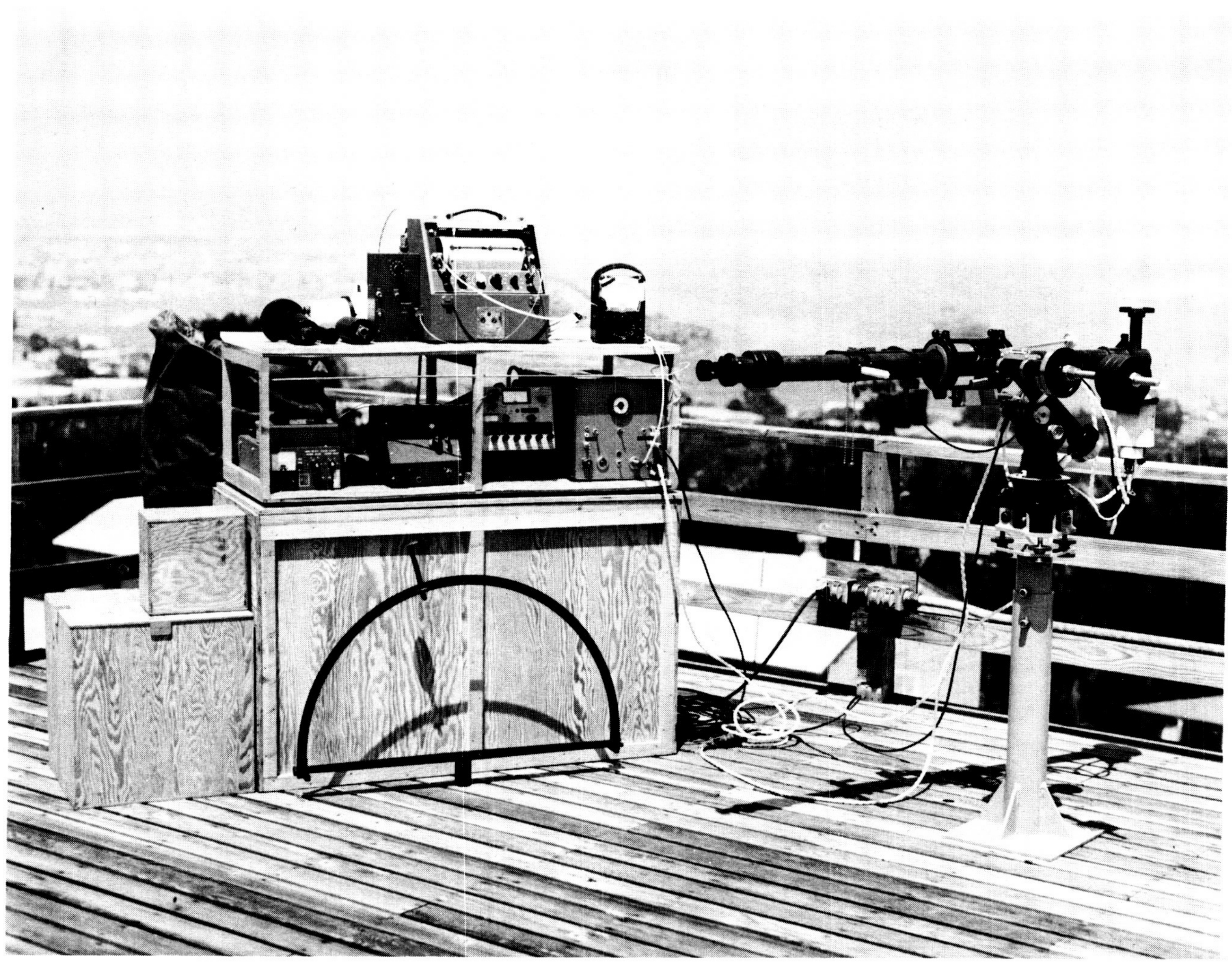

Figure 5-16.- Ground site photoelectric photometer with recording unit.

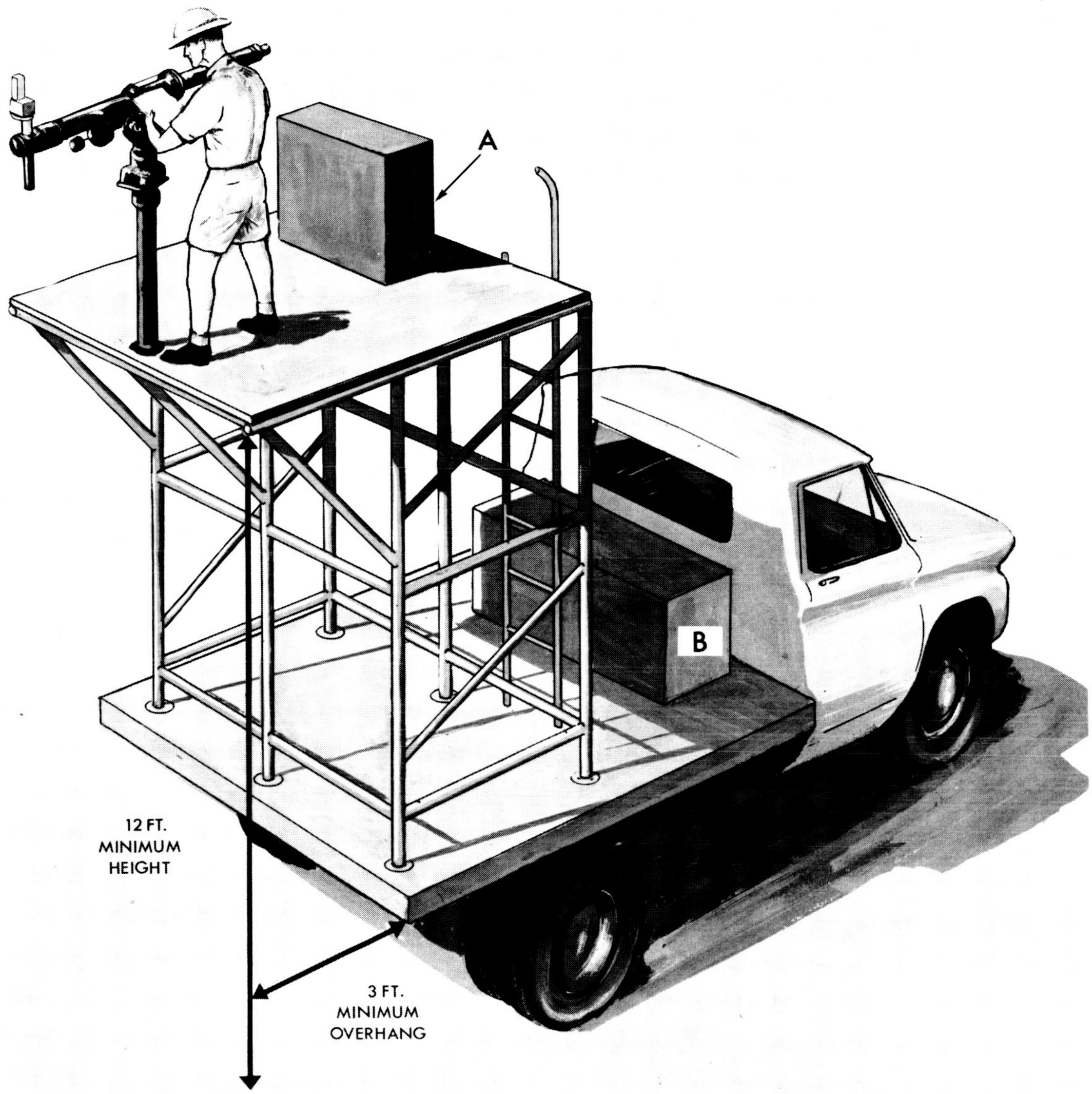

Figure 5-17.- Ground site photoelectric photometer mounted on a truck.

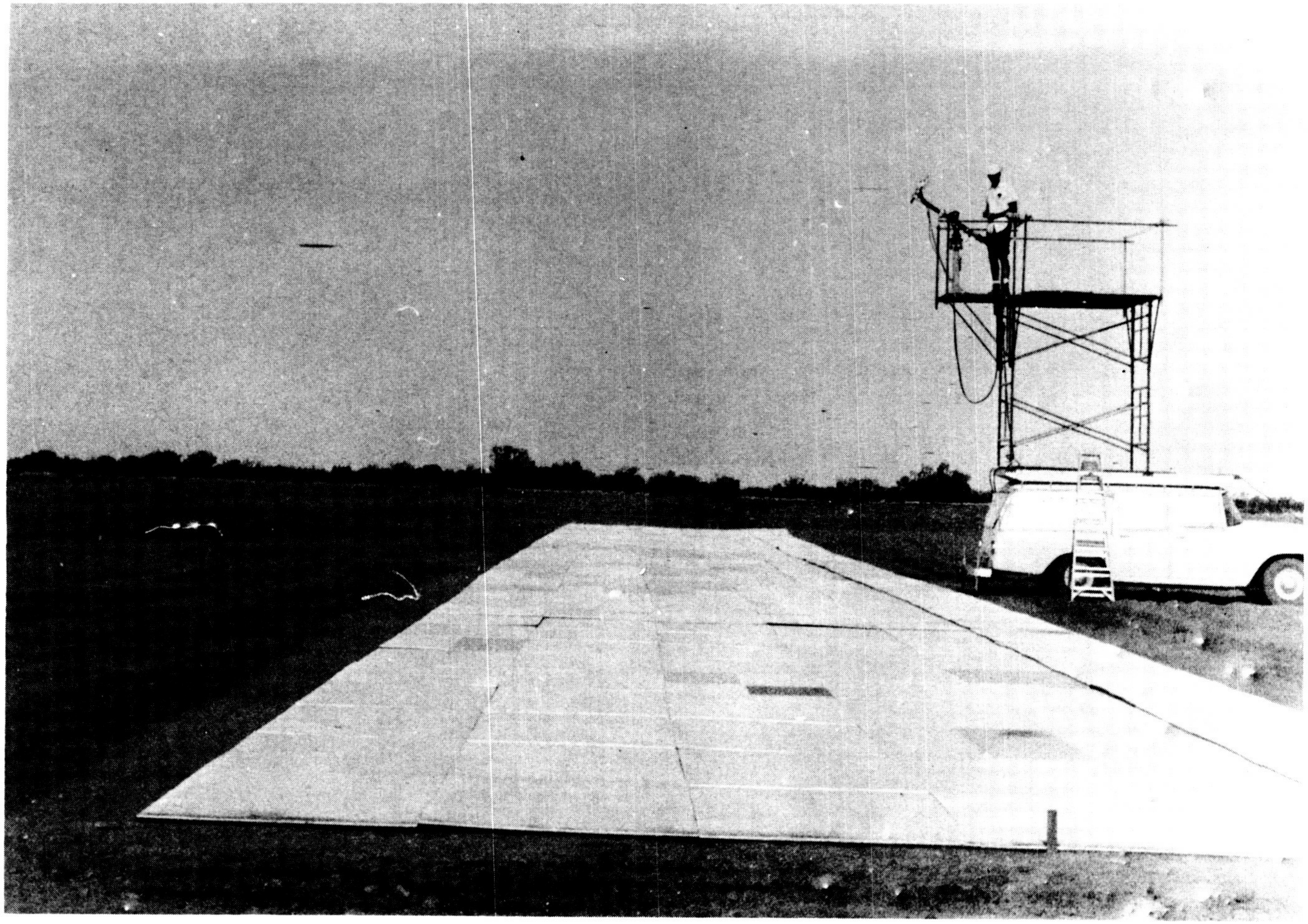

Figure 5-18.- Photograph of truck-mounted photoelectric photometer.

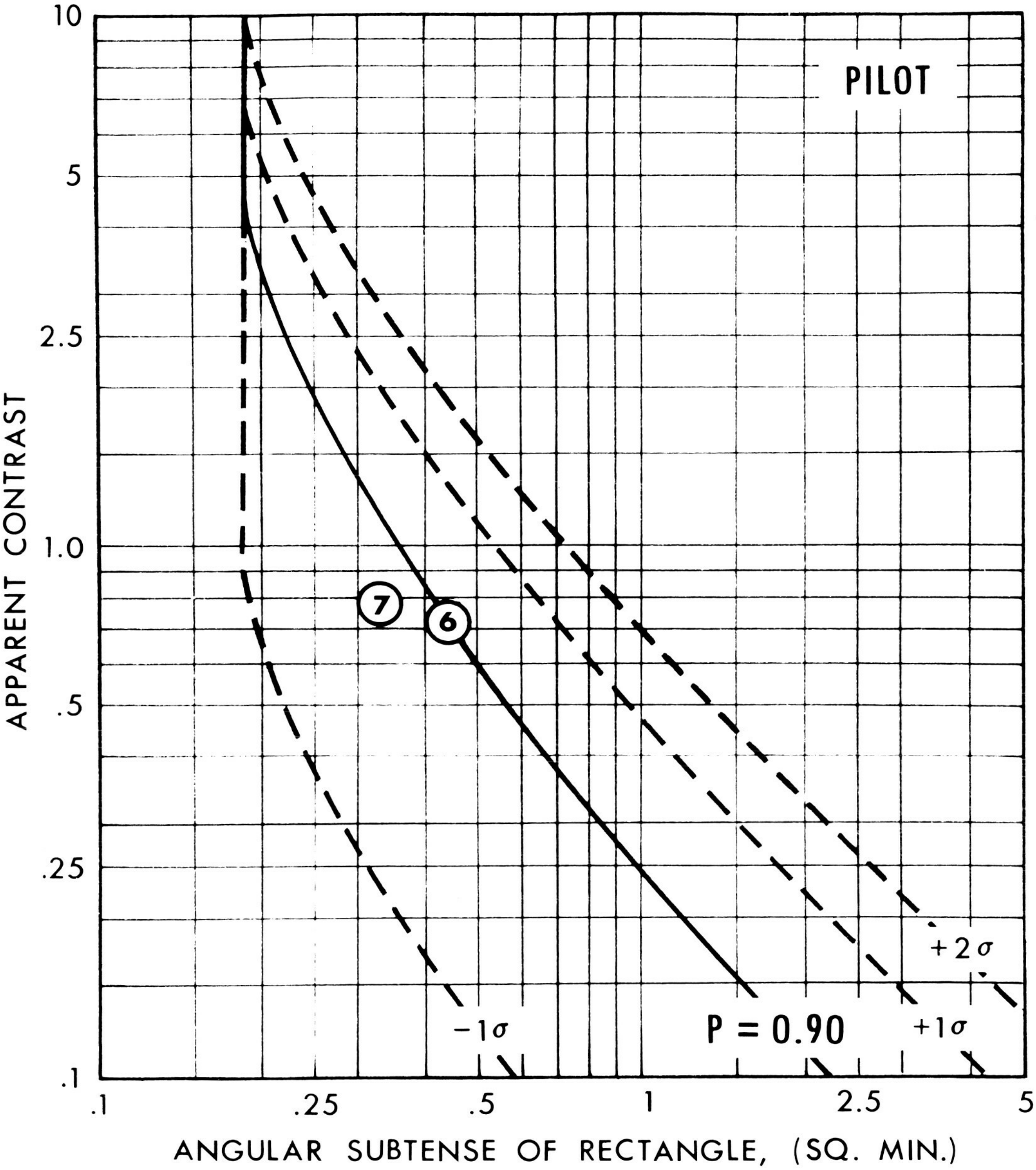

Figure 5-19.- Apparent contrast versus angular size of the sixth and seventh rectangles.

6(a). EXPERIMENT M-1, CARDIOVASCULAR CONDITIONING

Lawrence F. Dietlein, M.D. and William V. Judy
NASA Manned Spacecraft Center

SUMMARY

Intermittent venous occlusion of the extremities of man, during weightlessness simulation studies, has been demonstrated to be effective in preventing or mitigating the orthostatic hypotension observed following such simulations (refs. 1-3). A similar preventive measure was employed on the pilot of Gemini V with a view to determining the efficacy of pulsatile leg cuffs in preventing or lessening the orthostatic hypotension observed following previous space flights (refs. 4 and 5). Unfortunately, the cuff device was operative continuously during only the first 4 days of the 8-day mission. Postflight tilt-table responses of the command pilot and the pilot were considerably different, but the data cannot be construed as a conclusive demonstration that the observed differences were the result of the action of the pulsatile cuffs. The differences in the tilt responses of the Gemini V flight crew may be only a reflection of individual variability so commonly observed in biological experimentation. More data shall be required before a judgment can be rendered as to the efficacy of the pulsatile-leg-cuff technique in lessening postflight postural or orthostatic hypotension.

INTRODUCTION

Ground baseline studies in support of Experiment M-1 indicated that leg cuffs alone, inflated to 70-75 mm Hg for 2 minutes out of every 6, provided protection against cardiovascular deconditioning resulting from 6 hours of water immersion (ref. 6). Four healthy male subjects were immersed in water to neck level for a 6-hour period on two separate occasions, 2 days apart. Leg cuffs were utilized during the second immersion period. Referral to figures 6(a)-1 through 6(a)-4 reveals that 6 hours of water immersion did indeed result in cardiovascular deconditioning, as evidenced by cardio-acceleration in excess of that observed during the control tilt and by the occurrence of syncope in two of the four subjects. The tilt responses after the second period of immersion, during which leg cuffs were utilized, revealed that a definite protective effect was achieved; cardio-acceleration was lessened, and no syncope resulted.

During the postflight tilts, both crewmen sustained an increased pulse rate and a narrowed pulse pressure. The command pilot exhibited an increase of 78 beats/min in heart rate above his postflight resting level during the first tilt (4-hours postflight), and a 54 beat/min increase during the second tilt (8-hours postflight). The pilot exhibited a 46 beat/min increase during the first tilt and a 33 beat/min increase on the second tilt. Both crewmen revealed a marked decrease in both supine and upright heart rates 24 hours after recovery (supine rate decrease - 22 beats/min; upright rate decrease - 34 beats/min for each crew member). During the third, fourth, and fifth day after recovery, both crew members exhibited progressively decreasing supine and upright pulse rates, although these were still above preflight values.

During the first postflight tilts, the pulse pressure of each crew member exhibited narrowing as compared with preflight tilt and postflight resting values. During the second, third, and fourth postflight tilts, the command pilot continued to maintain a lower systolic pressure during tilt, whereas the pilot had returned to his normal preflight levels.

During the first postflight tilts, the command pilot and pilot exhibited an 89 and 87 percent increase, respectively, in leg blood volume. During the second tilt, however, the command pilot had increased this value to 149 percent over the preflight reading and the pilot to only 73 percent. Table 6(a)-II indicates the postflight changes in leg volume observed in the crews of Gemini IV and V:

TABLE 6(a)-II.- POSTFLIGHT LEG PLETHYSMOGRAPHIC VALUES

Days post recovery	Postflight change in volume per minute percent (a)			
	GEMINI V		GEMINI IV	
	Command pilot	Pilot	Command pilot	Pilot
1	[b]+119	+80	+22	+131
2	+44	+25	+27	+61
3	+73	+57	-38	+126
4	+78	+117		
5	+111	+97		

[a]Percent change in volume = cc/100 cc tissue/minute.

[b]+ indicates percent above preflight value; - indicates percent below.

The physiological mechanism responsible for the observed efficacy of the cuff technique remains evasive. One might postulate that the cuffs prevent thoracic blood volume overload, thus not activating the so-called Gauer-Henry reflex with its subsequent diuresis and diminished effective circulating blood volume. Alternatively, or perhaps additionally, one might postulate that the cuffs induce an intermittent artificial hydrostatic gradient across the walls of the leg veins by increasing venous pressure distal to the cuffs during inflation. This action simulates the situation that occurs in a one g environment and thereby maintains venomotor reflexes or "tone." Theoretically, this action should aid in preventing the pooling of blood in the lower extremities and increase the effective circulating blood volume in a subject standing upright in a one g environment. The precise mechanism or mechanisms of action must await further study.

EQUIPMENT AND METHODS

The cardiovascular-conditioning experiment equipment consisted of a pneumatic timing or cycling system and a pair of venous pressure cuffs (figs. 6(a)-5 through 6(a)-7). The cycling system was entirely pneumatic and alternately inflated and deflated the leg cuffs attached to the pilot's thighs to approximately 80 mm Hg pressure. The system consisted of three basic components:

(1) A pressurized storage vessel charged with oxygen to 3500 psig.

(2) A pneumatic control system for monitoring the pressurized storage vessel.

(3) A pneumatic oscillator system for periodically inflating and deflating the cuffs.

The pneumatic venous pressure cuffs were form-fitted to the proximal thigh area of the pilot. These consisted essentially of a 3 in. by 6 in. bladder enclosed in a soft nonstretchable fabric. The bladder was positioned on the dorsomedial aspect of each thigh. The lateral surface of the cuff consisted of a lace-type adjustor to insure proper fit.

Only the pilot wore the leg cuffs during the Gemini V mission. Upon activation of the manual shutoff valve, the cuffs were automatically pressurized to 80 mm Hg for 2 minutes of each 6-minute time interval. The system could operate continuously during flight, but it could be switched off for sleep periods. The experiment imposed no operational requirements other than activation of the device after insertion into orbit and deactivation prior to reentry.

RESULTS

The cardiovascular responses to three preflight 70-degree tilts for each crew member are summarized in table 6(a)-I (mean values):

TABLE 6(a)-I.- CARDIOVASCULAR RESPONSES TO PREFLIGHT 70-DEGREE TILTS

	Pretilt, supine		70-degree tilt		
	Heart rate, beats/min	Blood pressure, mm Hg	Heart rate, beats/min	Blood pressure, mm Hg	Percent blood volume change in legs (cc/100 cc tissue/min)
Command pilot	58	109/72	75	111/79	3.01
Pilot	59	117/68	78	120/79	2.70

Thus, during tilt, a slight increase in heart rate, a relatively constant blood pressure with a slight increase in diastolic values, and a slight increase in leg volume were noted. These values reverted to the pretilt levels following return to the horizontal position.

The cuffs were programed in the flight plan to operate continuously for the full 8-day mission. After 4 days, however, the pneumatic programer stopped cycling when the oxygen pressure of the storage vessel dropped below operational levels.

The results of six consecutive postflight tilt procedures are indicated in figures 6(a)-8 through 6(a)-13 for the command pilot and in figures 6(a)-14 through 6(a)-19 for the pilot. Both crew members exhibited increased resting pulse rates during the first 2 days after recovery. Maximum increases in resting pulse rate over preflight resting values were observed on the first day after recovery (command pilot increase - 27 beats/min; pilot increase - 50 beats/min). Postflight resting blood pressure was below preflight values for the command pilot. His systolic pressure remained 10 mm Hg below preflight values for 3 days after recovery. His diastolic pressure readings were 8 mm Hg below preflight resting values for 4 days after recovery. The pilot exhibited an increased resting diastolic pressure (3 to 9 mm Hg) for 4 days postflight, whereas his systolic values were essentially identical with the preflight readings.

CONCLUSIONS

(1) The pilot's pulse rate and pulse pressure returned to normal within 2 days after recovery, whereas the command pilot required a somewhat longer period to return to preflight values.

(2) The pilot's narrowing of pulse pressure was less pronounced than that of the command pilot.

(3) The pilot's decrease in measured plasma volume was -5 percent; the command pilot's was -9 percent.

(4) The pilot's body weight loss was 8 1/2 pounds; the command pilot lost 7 1/2 pounds.

(5) The pilot's pooling of blood in the legs generally was less than that observed in the command pilot.

On the basis of the preflight and postflight data presented, one is tempted to conclude that the pulsatile cuff device was at least partially successful in lessening the severity of the postflight orthostatic responses observed in the pilot. But individual variation in response must be reckoned with when dealing with biological systems, and, although the data appear attractive and perhaps reflect a measure of protective "trend" in the use of the cuff technique, we cannot make such a conclusion on the basis of the data available from a single experiment. The differences observed in the tilt responses of the Gemini V crew may well be only a reflection of physiological variance in human subjects. More conclusive data shall be required before the pulsatile leg cuff can be judged a useful device or technique in mitigating the cardiovascular-deconditioning effects of space flight.

REFERENCES

1. Graveline, D. E.; and Balke, B.: The Physiologic Effects of Hypodynamics Induced by Water Immersion. USAF School of Aviation Medicine Report No. 60-88, Sept. 1960.

2. Graybiel, A.; and Clark, B.: Symptoms Resulting from Prolonged Immersion in Water: The Problem of Zero G Asthenia. Aerospace Medicine, vol. 32, 1961, p. 181.

3. Vogt, F. B.: Effect of Extremity Cuff-Tourniquets on Tilt Table Tolerance after Water Immersion. Aerospace Medicine, vol. 36, 1965, p. 442.

4. Berry, C. A.; Minners, H. A.; McCutcheon, E. P.; and Pollard, R. A.: Aeromedical Analysis. Results of the Third United States Orbital Space Flight, NASA SP-12, Oct. 3, 1962.

5. Catterson, A. D.; McCutcheon, E. P.; Minners, H. A.; and Pollard, R. A.: Aeromedical Observations. Mercury Project Summary Including the Results of the Fourth Manned Orbital Flight, NASA SP-45, May 15-16, 1963.

6. Vogt, F. B.: Personal Communication. Study to be published.

NASA
S-65-7381

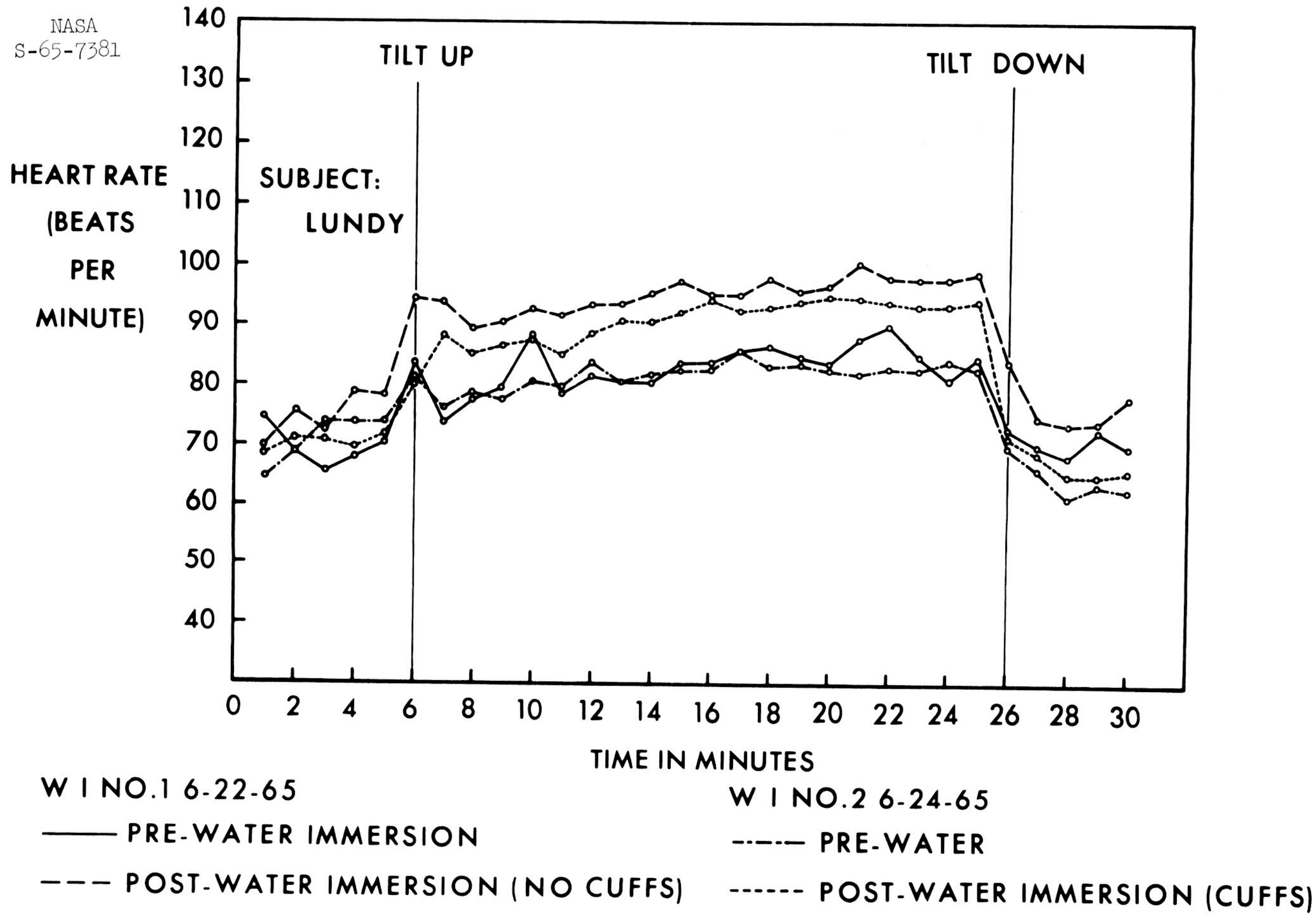

Figure 6(a)-1.- Six-hour water immersion study, test subject Lundy.

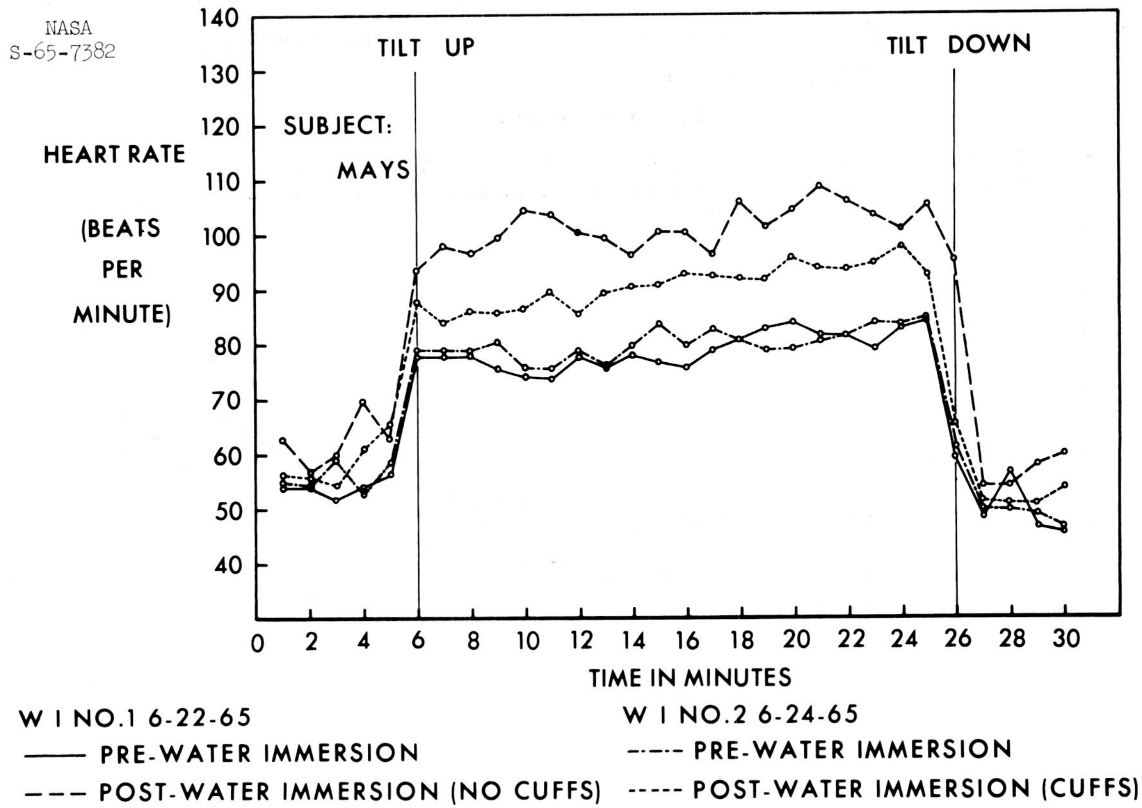

Figure 6(a)-2.- Six-hour water immersion study, test subject Mays.

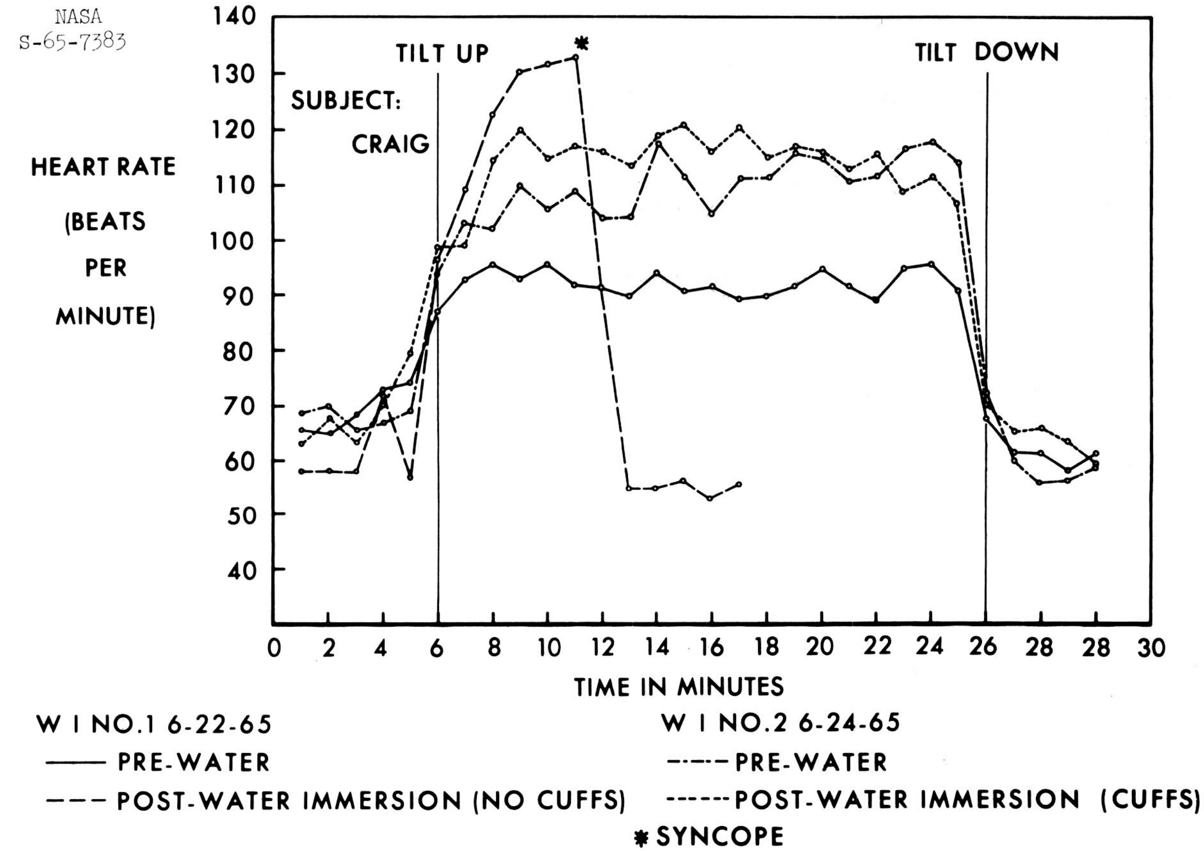

Figure 6(a)-3.- Six-hour water immersion study, test subject Craig.

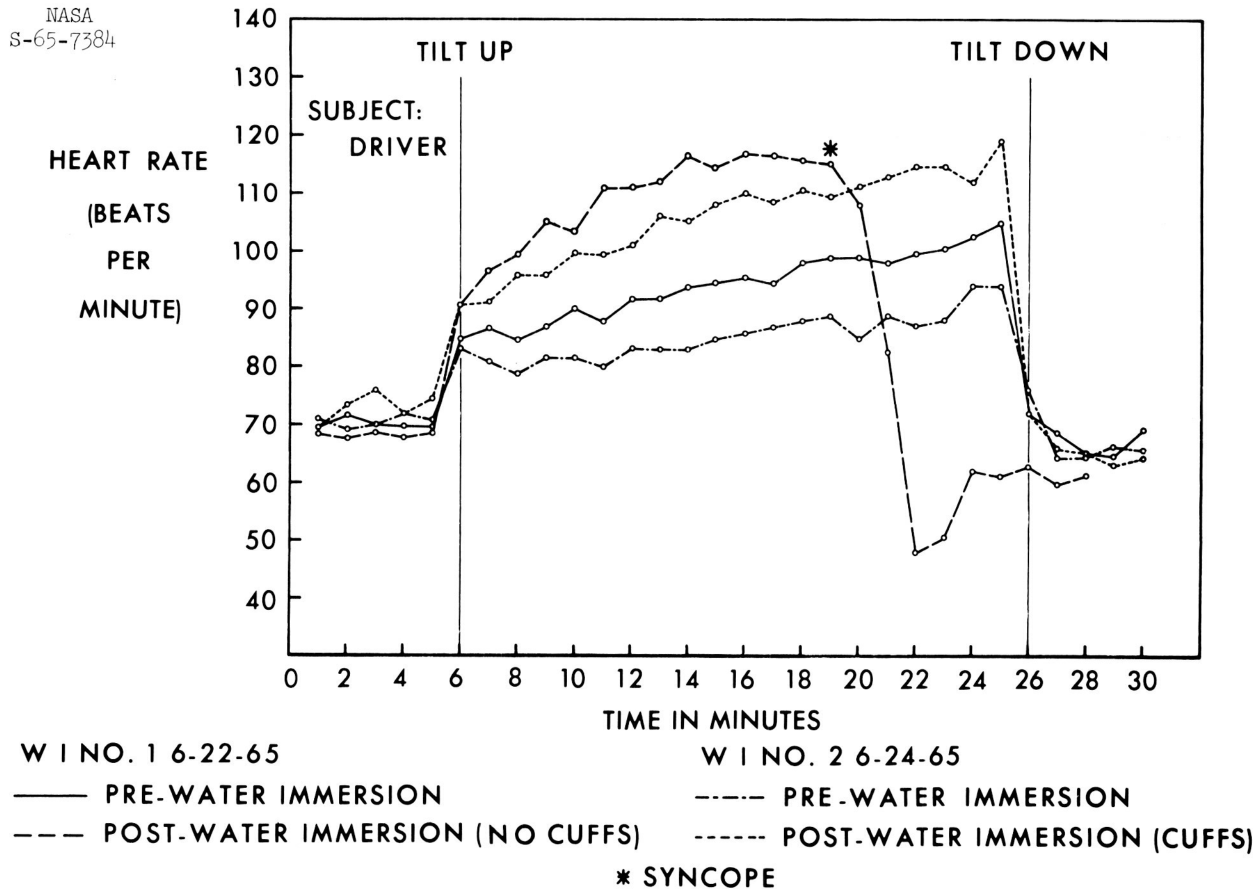

Figure 6(a)-4.- Six-hour water immersion study, test subject Driver.

NASA
S-65-3256

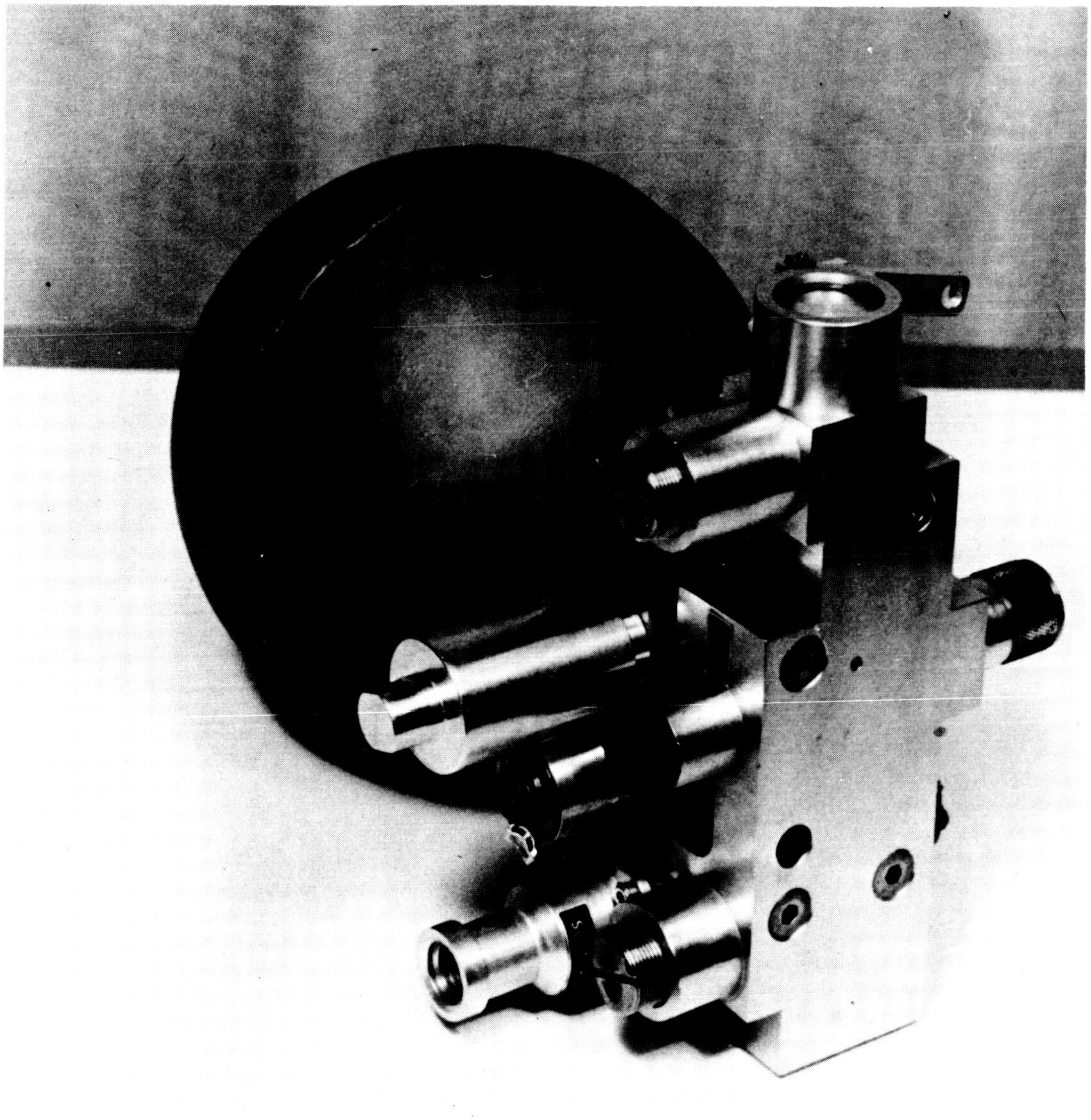

Figure 6(a)-5.- Cardiovascular reflex conditioning system.

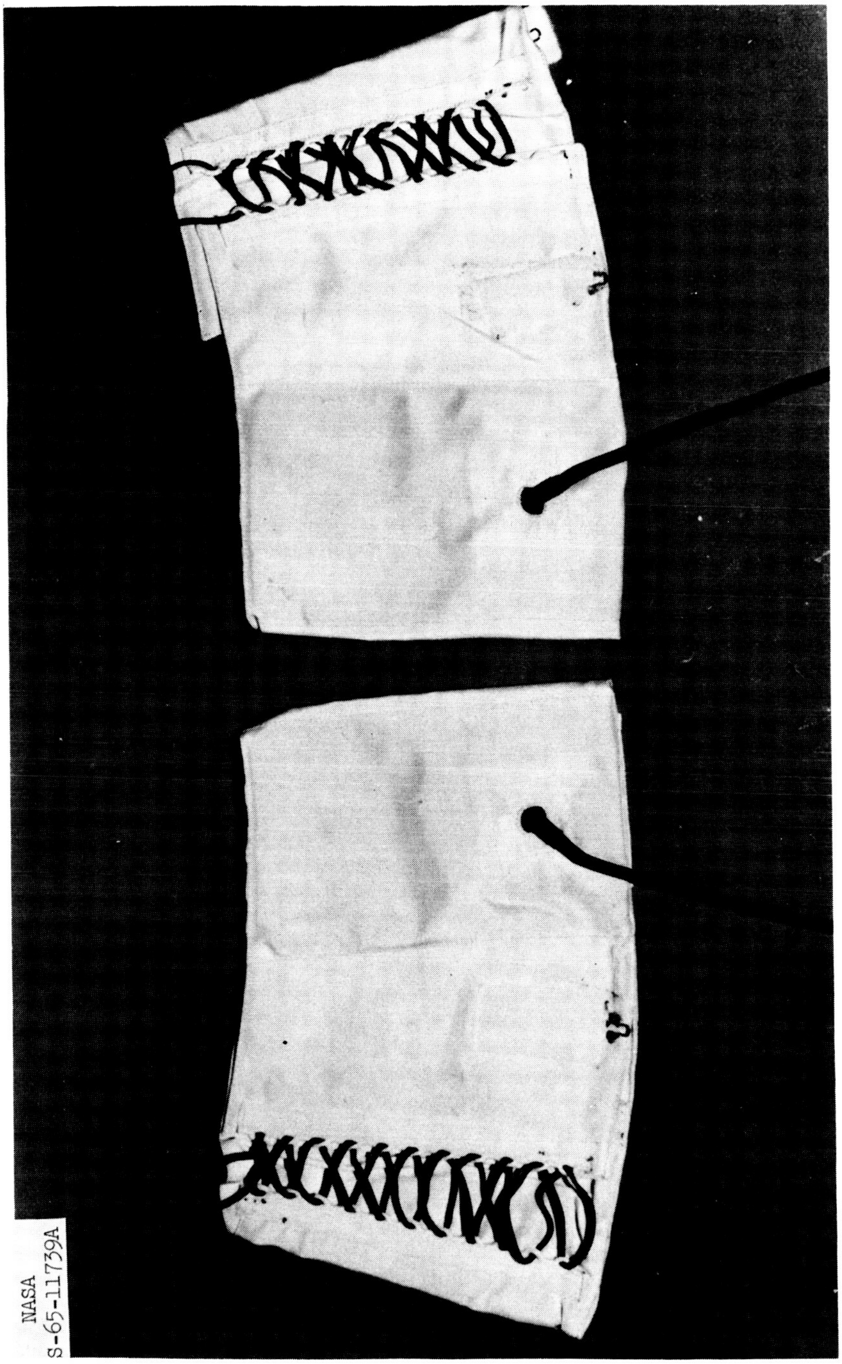

Figure 6(a)-6.- Pneumatic cuffs, cardiovascular continuing.

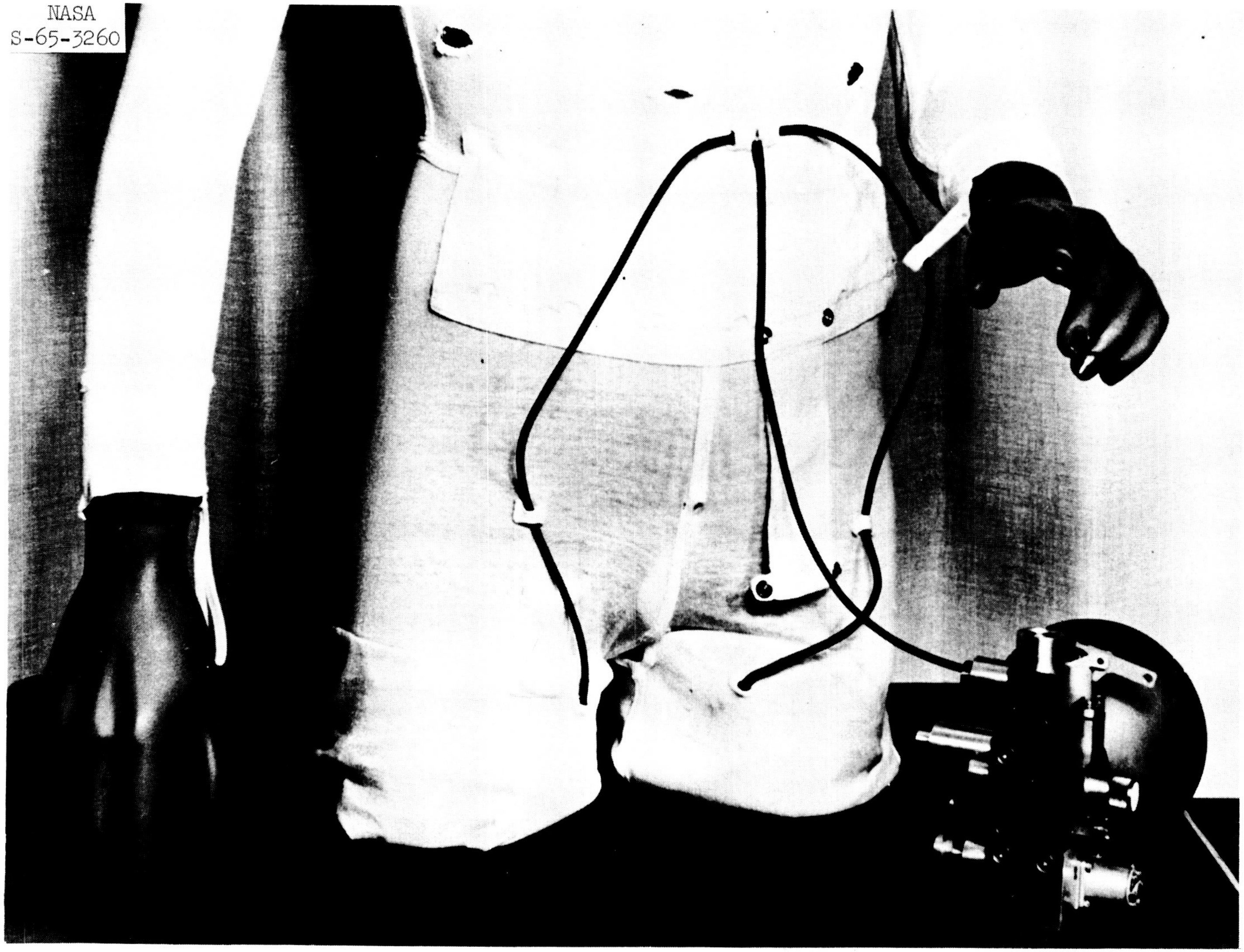

Figure 6(a)-7.- Cardiovascular reflex conditioning system and suit undergarment with pressure cuffs.

NASA
S-65-9634

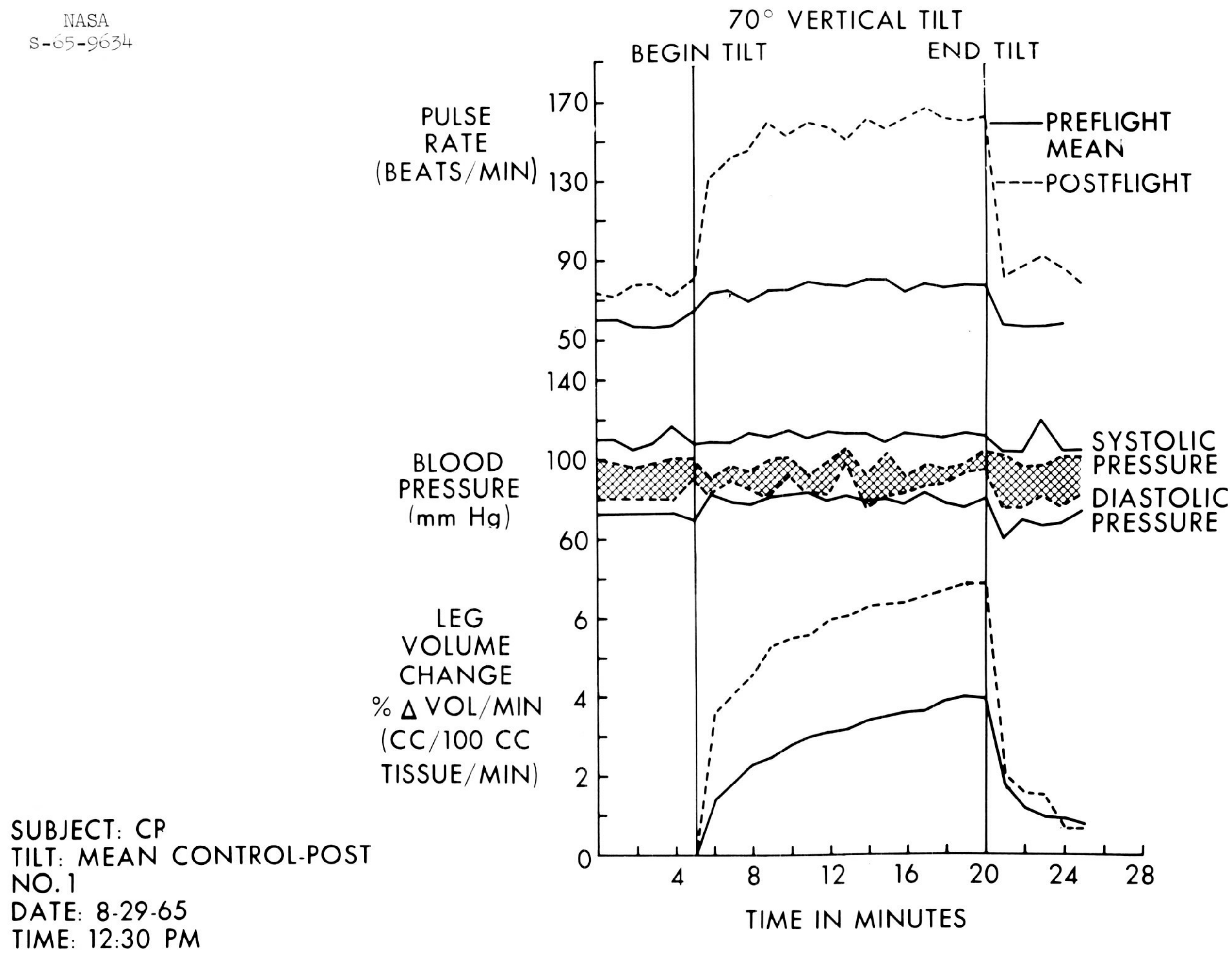

Figure 6(a)-8.- Command pilot tilt-table data.

NASA
S-65-9642

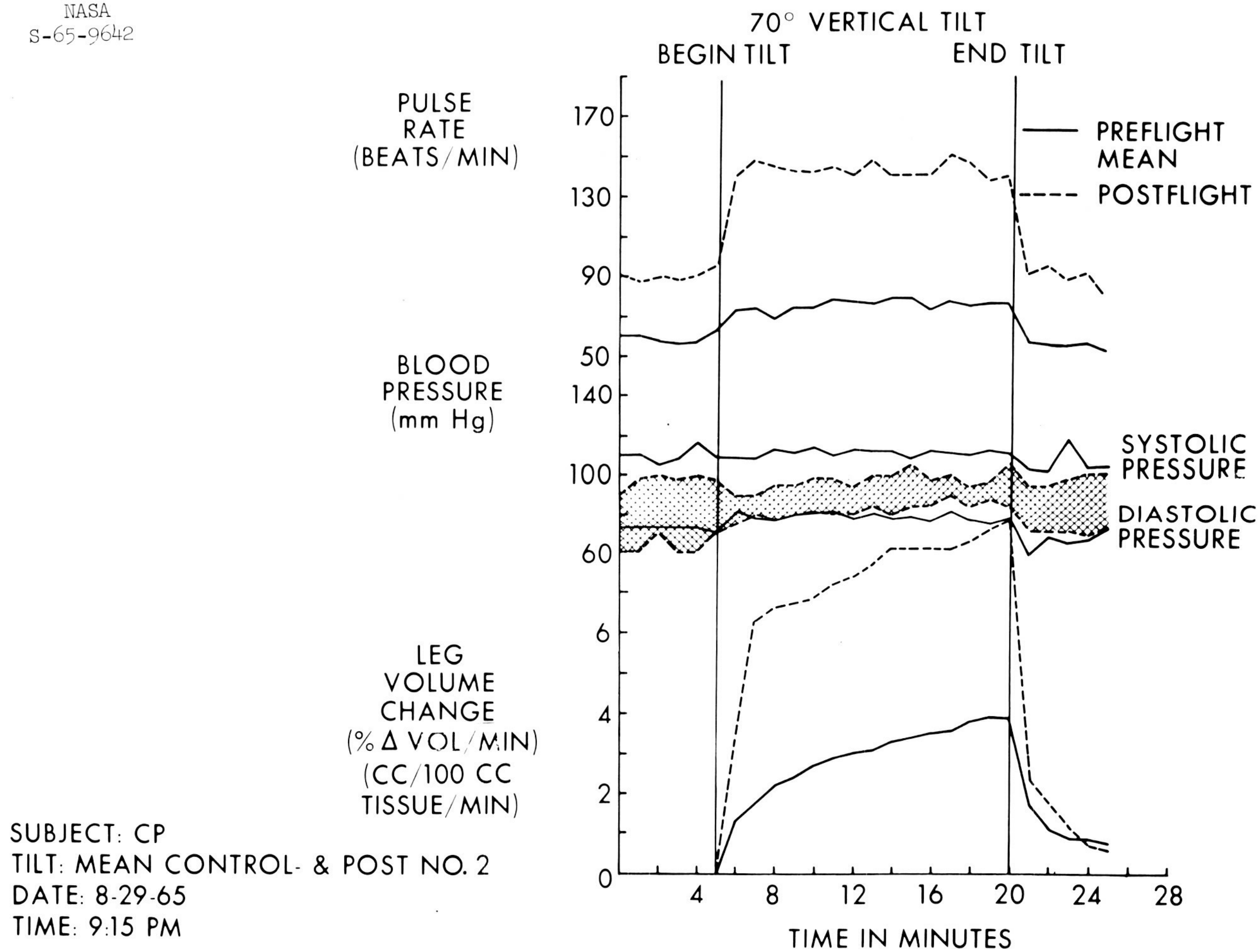

Figure 6(a)-9.- Command pilot tilt-table data.

NASA
S-65-9645

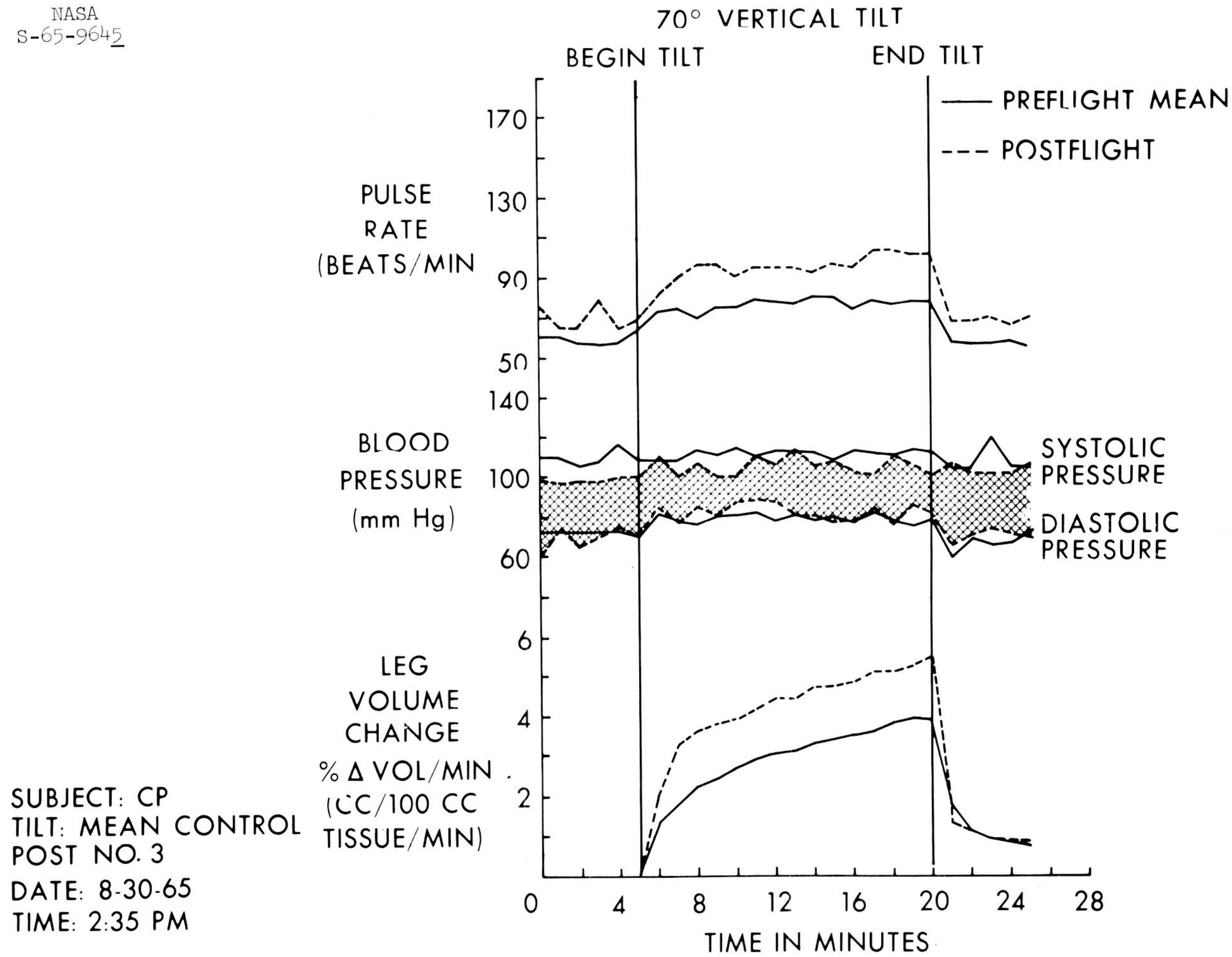

Figure 6(a)-10.- Command pilot tilt-table data.

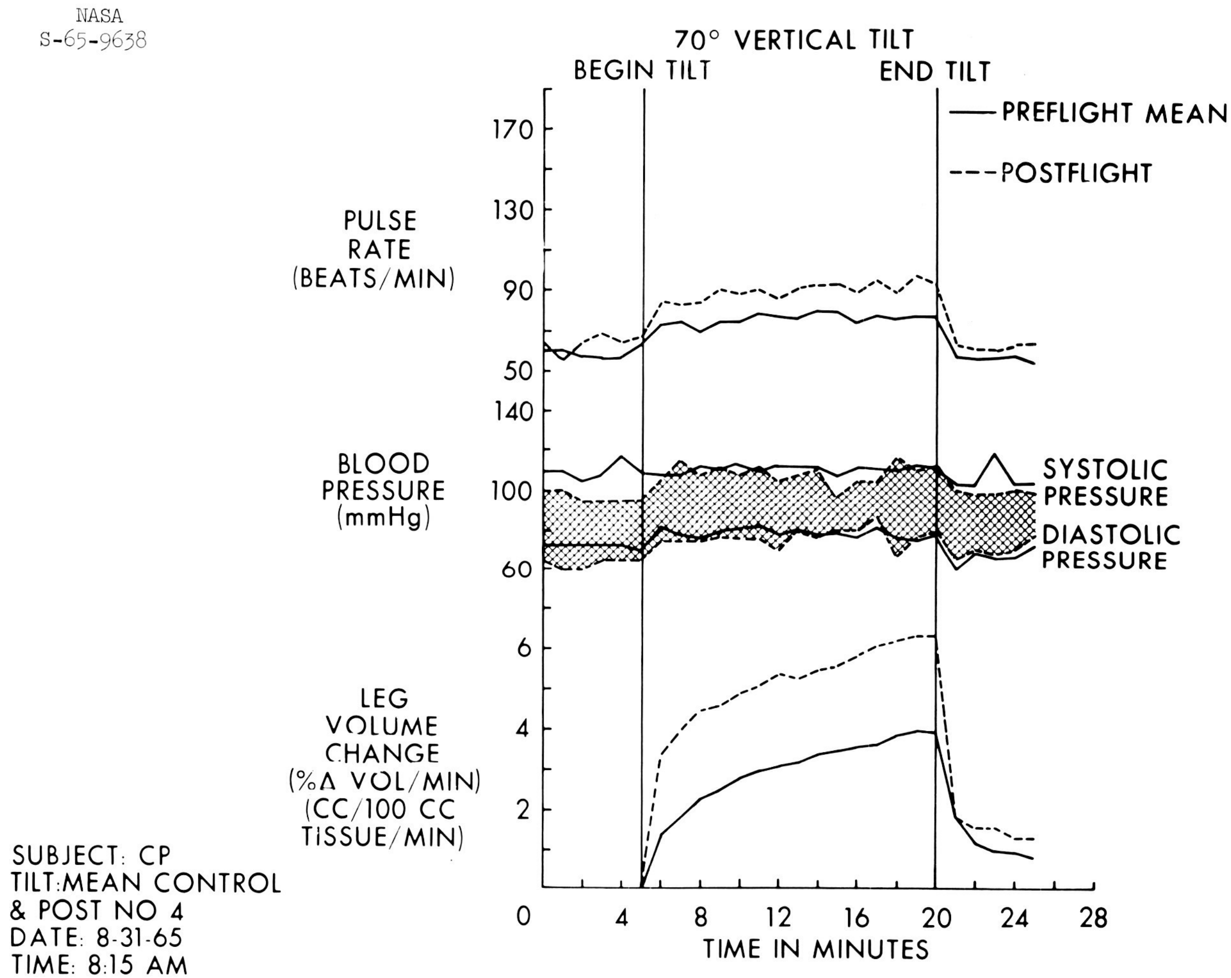

Figure 6(a)-11.- Command pilot tilt-table data.

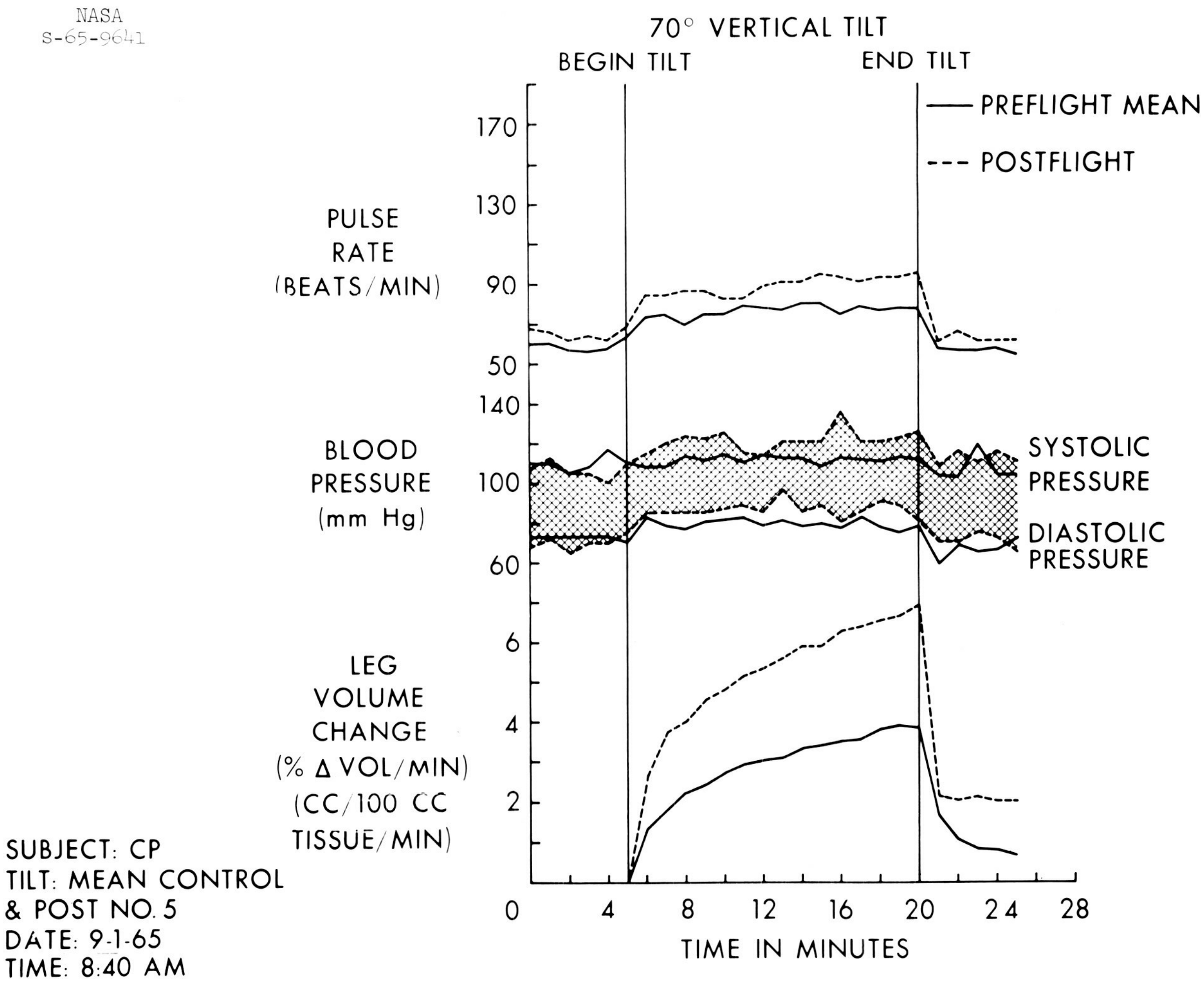

Figure 6(a)-12.- Command pilot tilt-table data.

NASA
S-65-9635

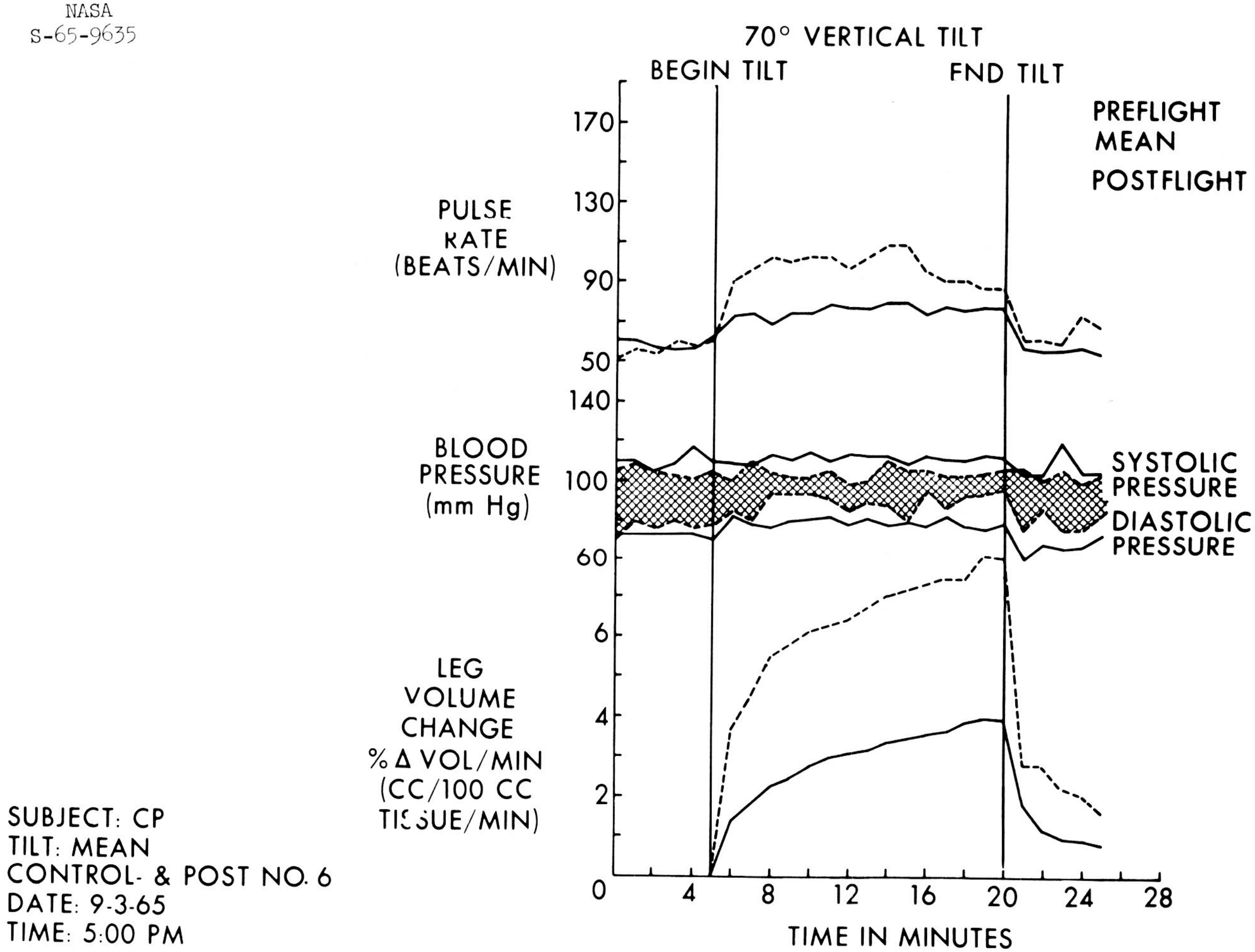

Figure 6(a)-13.- Command pilot tilt-table data.

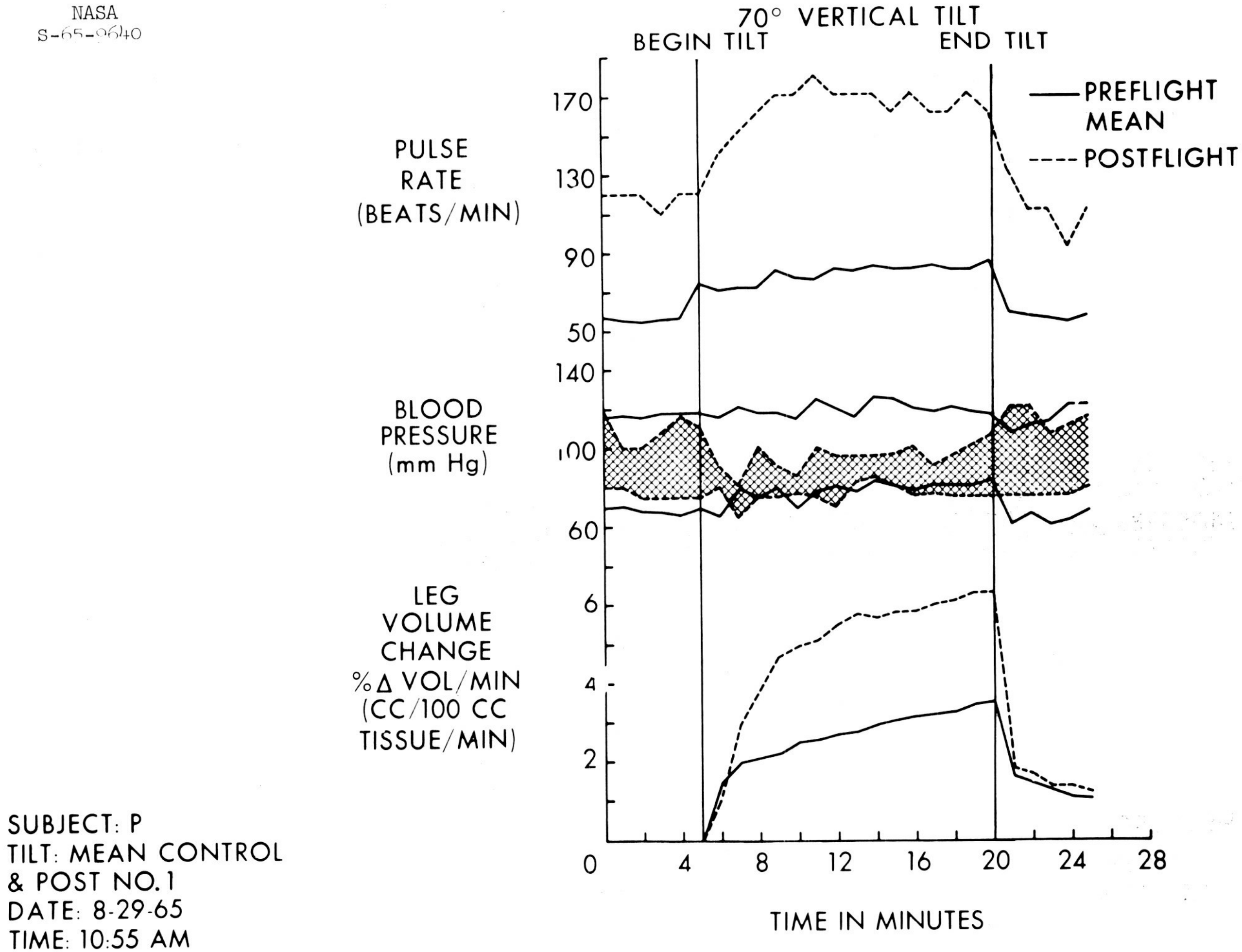

Figure 6(a)-14.- Pilot tilt-table data.

NASA
S-65-9643

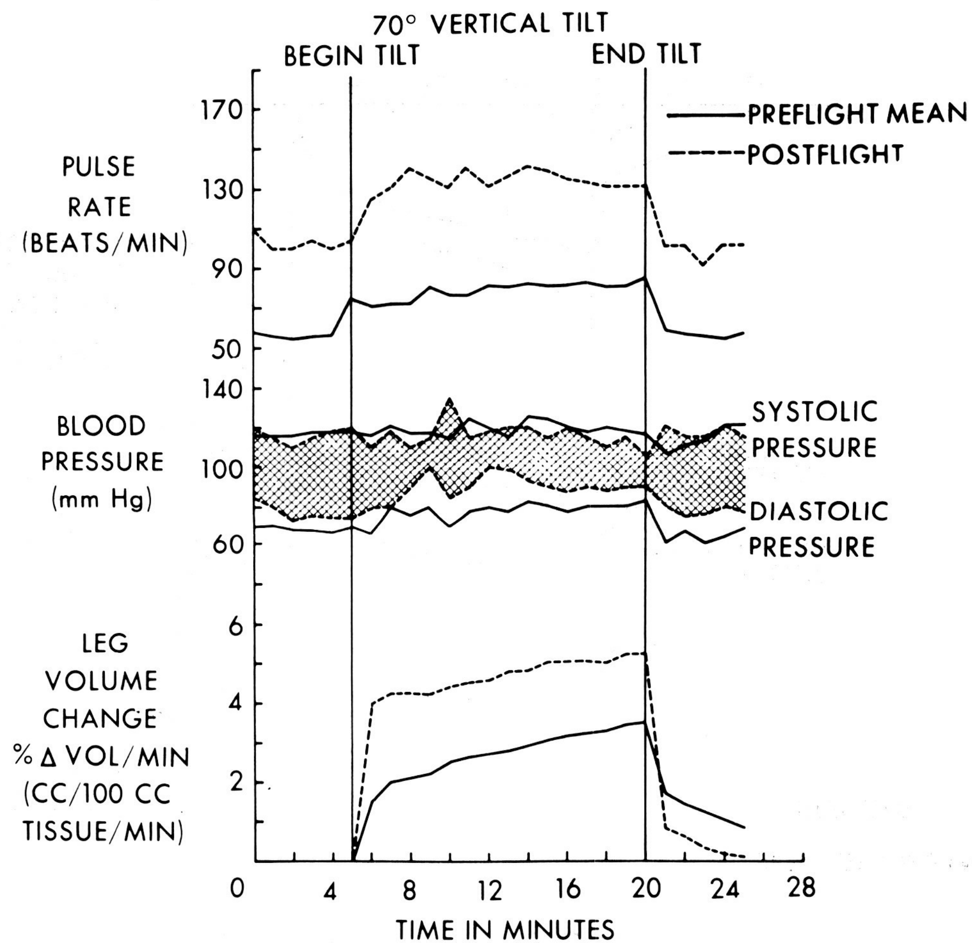

SUBJECT: P
TILT: MEAN
CONTROL & POST
NO. 2
DATE: 8-29-65
TIME: 8:15 PM

Figure 6(a)-15.- Pilot tilt-table data.

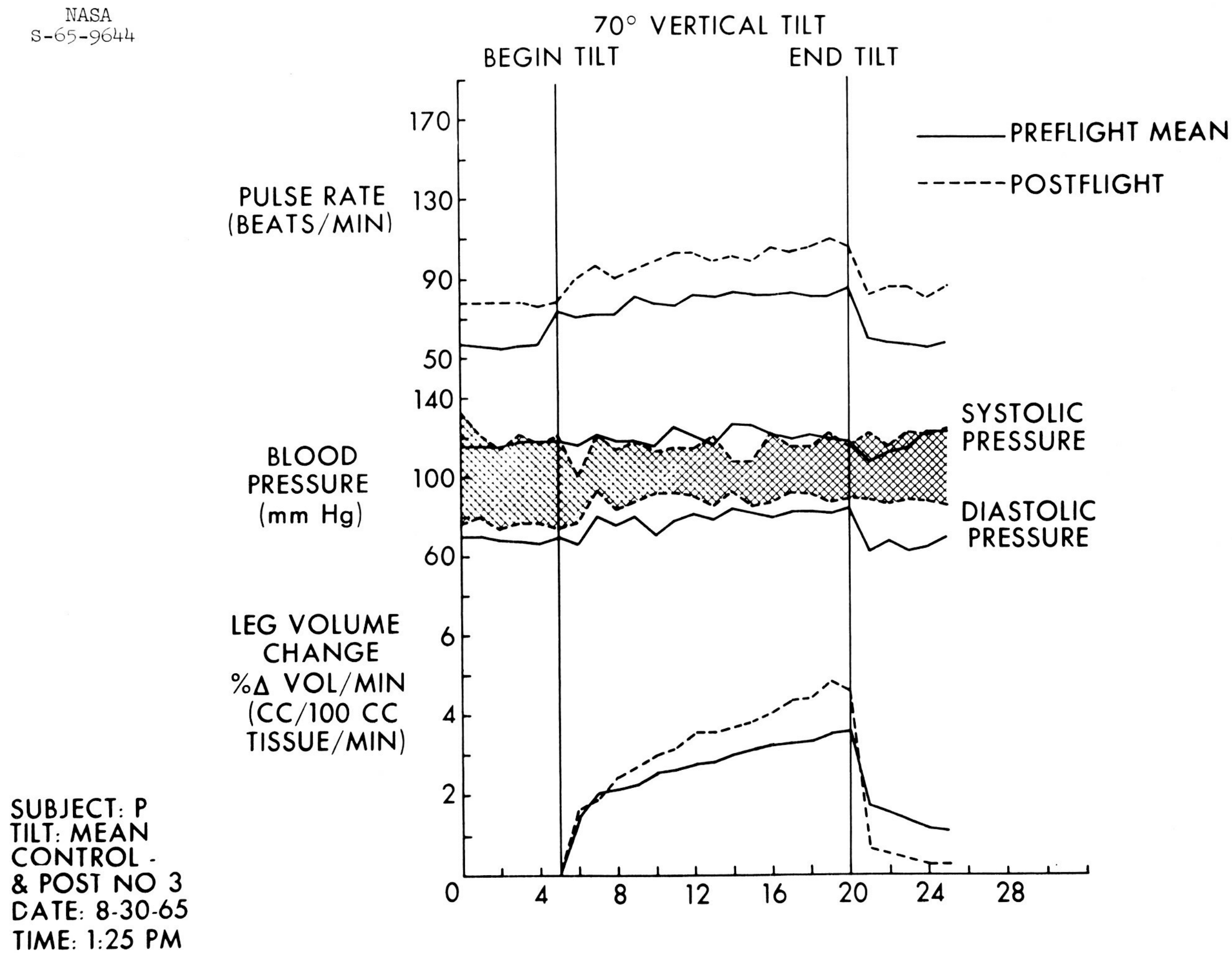

Figure 6(a)-16.- Pilot tilt-table data.

NASA
S-65-9639

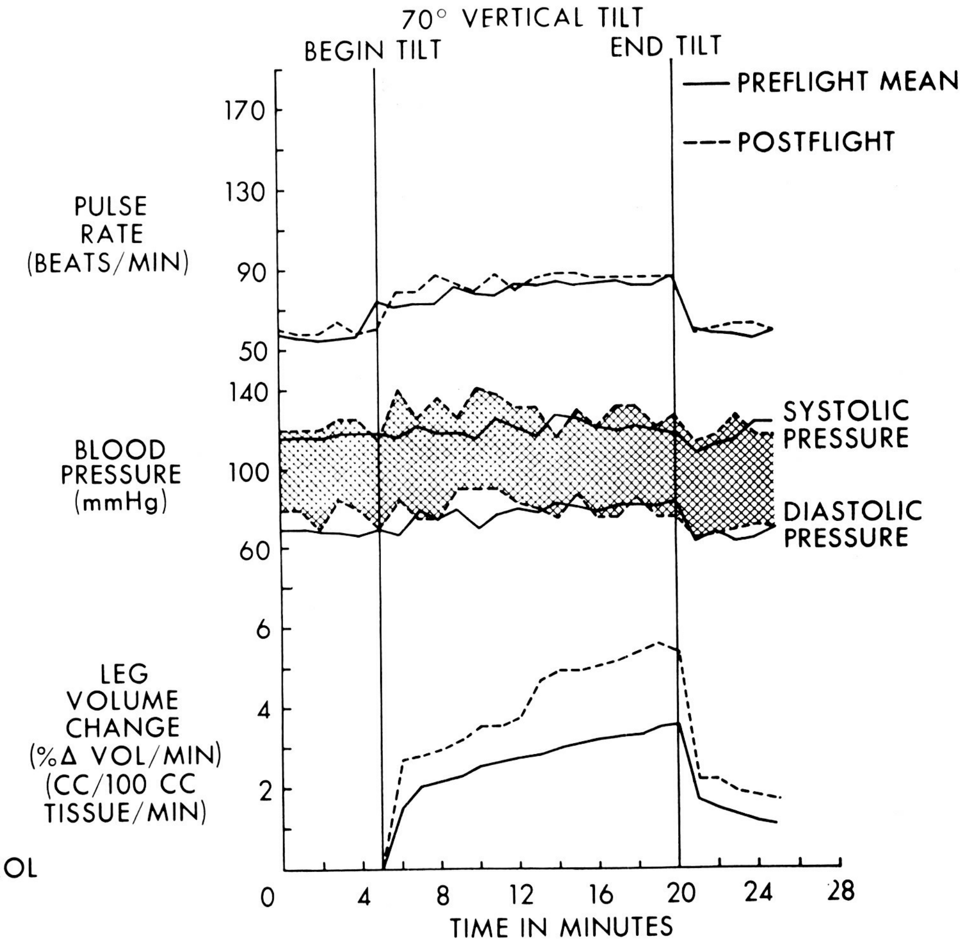

SUBJECT: P
TILT: MEAN CONTROL
& POST NO 4
DATE: 8-31-65
TIME: 9:30 AM

Figure 6(a)-17.- Pilot tilt-table data.

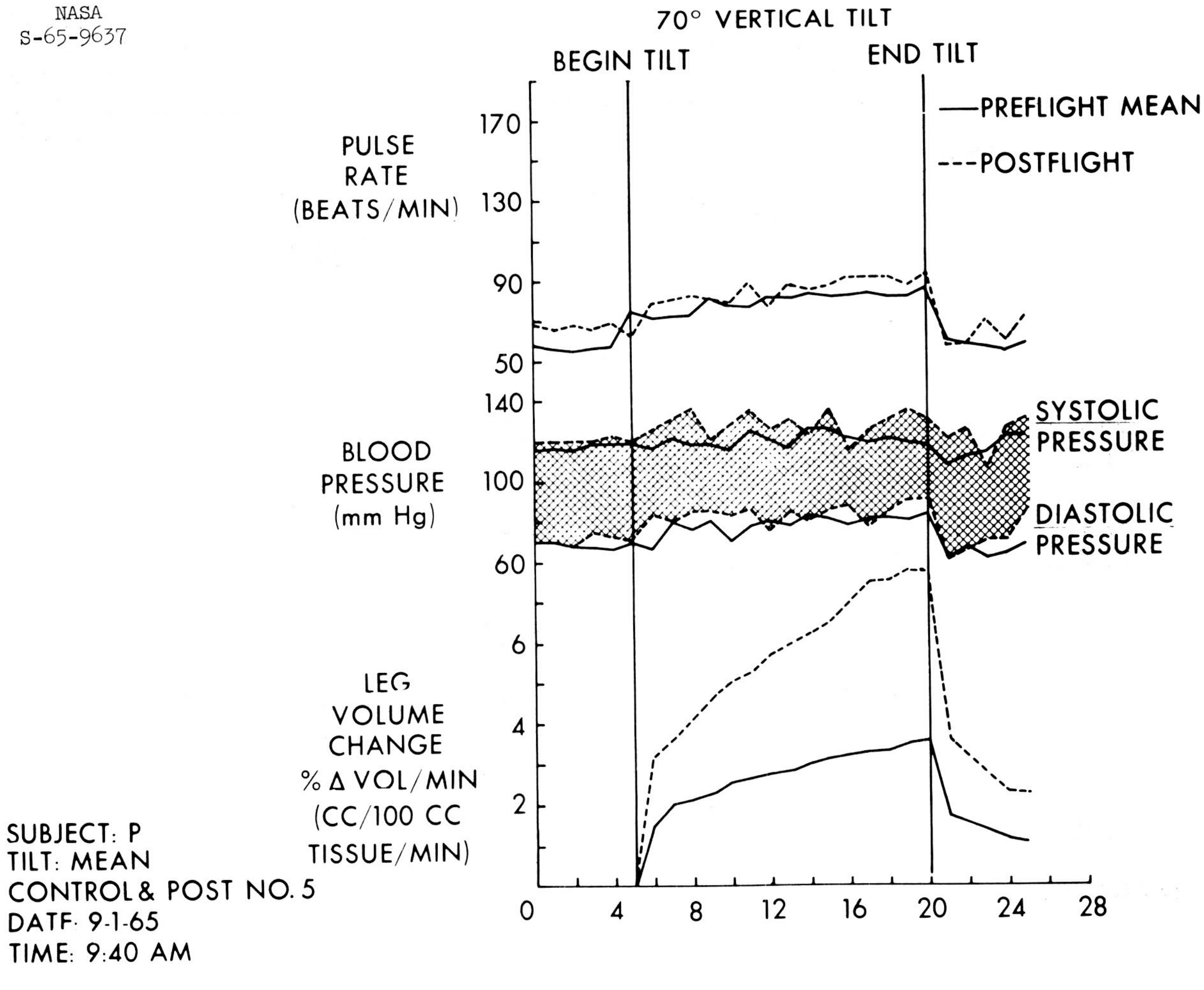

Figure 6(a)-18.- Pilot tilt-table data.

NASA
S-65-9636

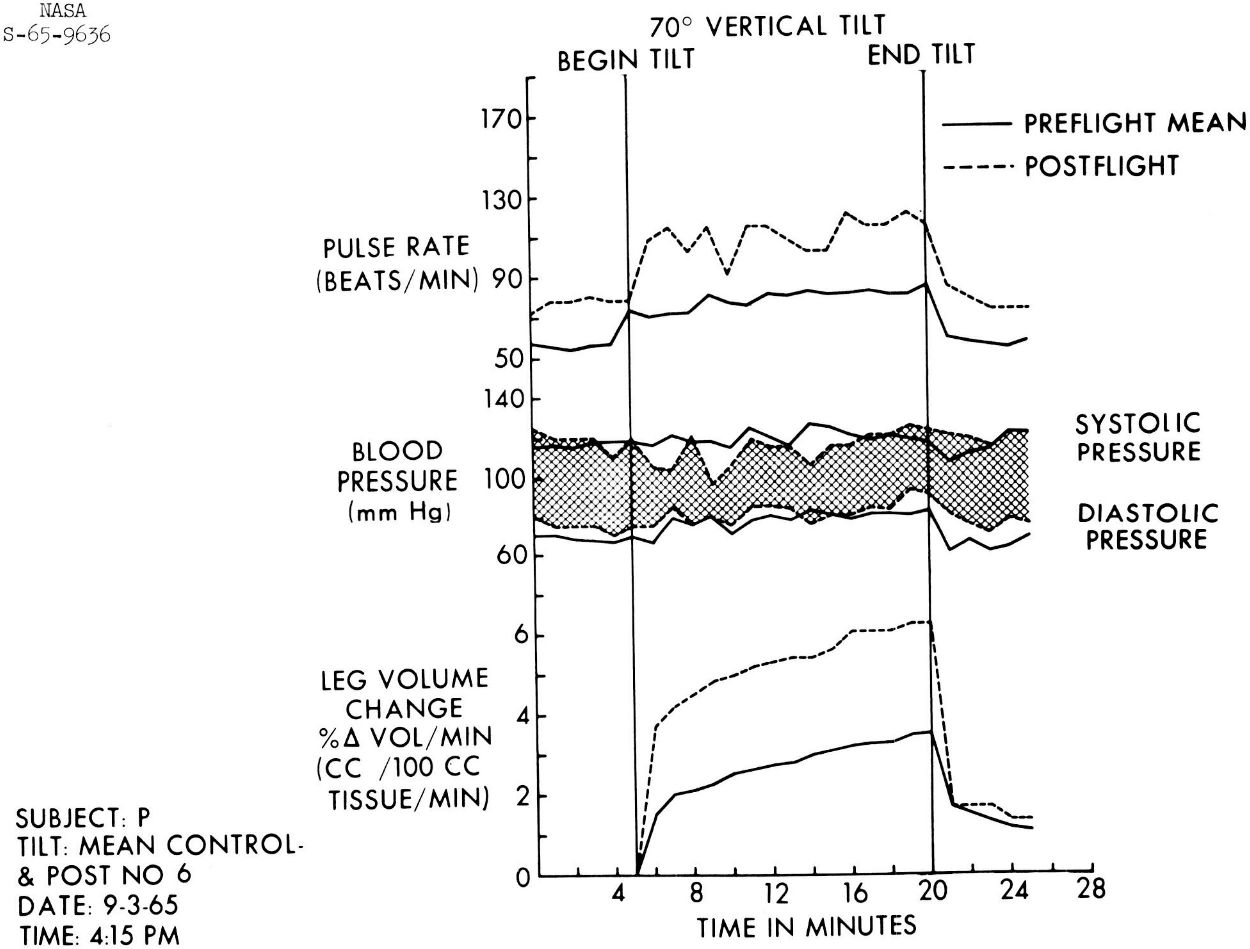

Figure 6(a)-19.- Pilot tilt-table data.

6(b). EXPERIMENT M-3, IN-FLIGHT EXERCISER

Lawrence F. Dietlein, M. D. and Rita M. Rapp
NASA Manned Spacecraft Center

SUMMARY

The response of the cardiovascular system to a quantified workload is an index of the general physical condition of an individual. Utilizing mild exercise as a provocative stimulus, no significant decrement in the physical condition of either of the two astronauts could be detected during the Gemini V mission. The rate of return of the pulse rate to pre-exercise levels, following in-flight exercise periods, was essentially the same as that observed during preflight baseline studies.

OBJECTIVE

The objective of Experiment M-3 was the day-to-day evaluation of the general physical condition of the flight crew with an increase in time under conditions of space flight. The basis of this evaluation was the response of the cardiovascular system (pulse rate) to a calibrated workload.

EQUIPMENT

The exercise device (figs. 6(b)-1 and 6(b)-2) consisted of a pair of rubber bungee cords attached to a nylon handle at one end and to a nylon foot strap at the other. A stainless steel stop-cable limited the stretch length of the rubber bungee cords and fixed the isotonic workload of each pull. The device can be utilized to exercise the lower extremities by holding the handle fixed and pushing with the feet, or to exercise the upper extremities by holding the feet fixed and pulling on the handle. The flight bioinstrumentation system (fig. 6(b)-3) was utilized to obtain pulse rate, blood pressure, and respiration rate. These data were recorded on the onboard biomedical tape recorder and simultaneously telemetered to the ground monitoring stations.

PROCEDURE

The device used in the Gemini V mission required 70 pounds of force to stretch the rubber bungee cords maximally through an excursion of 12 inches. Exercise periods lasted for 30 seconds, during which time the astronaut pulled the handle of the exerciser through a full excursion once per second. Exercise periods (medical data passes) were scheduled approximately three times a day for each crew member. Blood pressure measurements were made before and after each exercise period. In addition, the command pilot, who was without pulsatile leg cuffs (Experiment M-1), was encouraged to exercise his legs between the scheduled periods.

RESULTS

The flight crew performed the exercise periods as scheduled. Heart rates were determined by counting 15-second periods for 2 minutes before and after exercise, and the first and last 15-second periods during exercise. Comparison of one-g preflight exercise periods with those obtained during flight indicated little difference in heart-rate response. Comparison of the in-flight exercise periods from the first to the last day also indicated little difference in heart-rate response. In-flight heart-rate responses are graphically illustrated in figure 6(b)-4 for the command pilot, and in figure 6(b)-5 for the pilot. Blood pressure measurements, before and after exercise periods, were generally not remarkable. In both the command pilot and the pilot, postexercise systolic pressures tended to be higher than the pre-exercise values. Postexercise diastolic pressures were generally slightly higher than or identical to pre-exercise values; rarely, they were slightly lower. The pulse pressure of the pilot tended to be significantly wider (160-130/60-70) than that of the command pilot (130-110/70-80). After the fourth day of flight, both crew members used the exerciser frequently between scheduled medical data passes. Both felt that exercise is essential and beneficial on flights of long duration.

CONCLUSIONS

The M-3 experiment on Gemini V was successfully performed. On the basis of the data obtained during this mission, the following conclusions appear warranted:

(1) The response of the cardiovascular system to a calibrated workload is relatively constant for a given individual during space flights lasting 8 days.

(2) The crew are able to perform mild to moderate amounts of work under the conditions of space flight and within the confines of the Gemini spacecraft, and this ability continues essentially unchanged for missions up to 8 days.

(3) Using a variant of the "Harvard Step Test" as an index, no decrement in the physical condition of the crew was apparent during an 8-day mission, at least under the stress of the relatively mild workloads imposed in this experiment.

NASA
S-65-2993

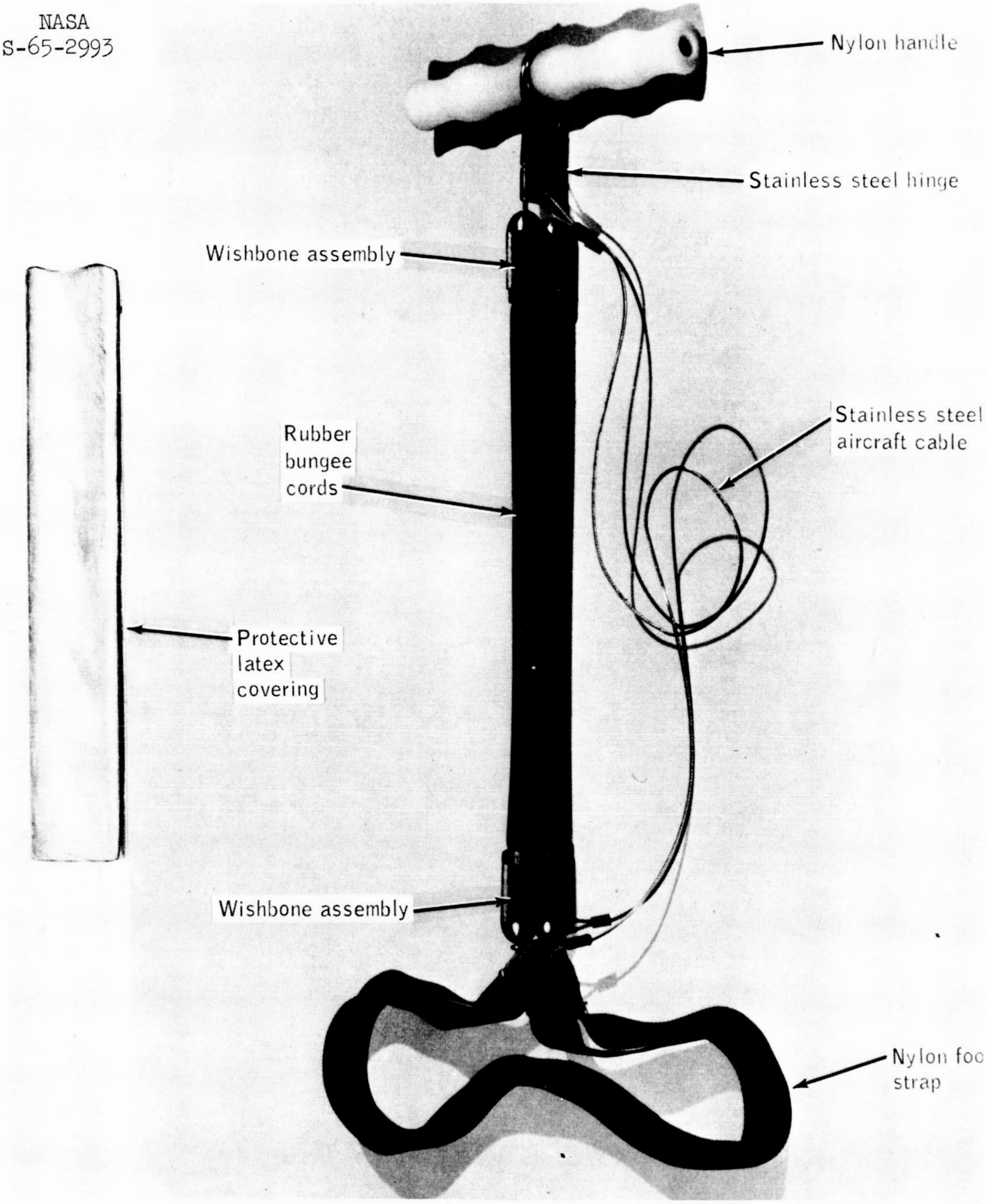

Figure 6(b)-1.- In-flight exerciser major components.

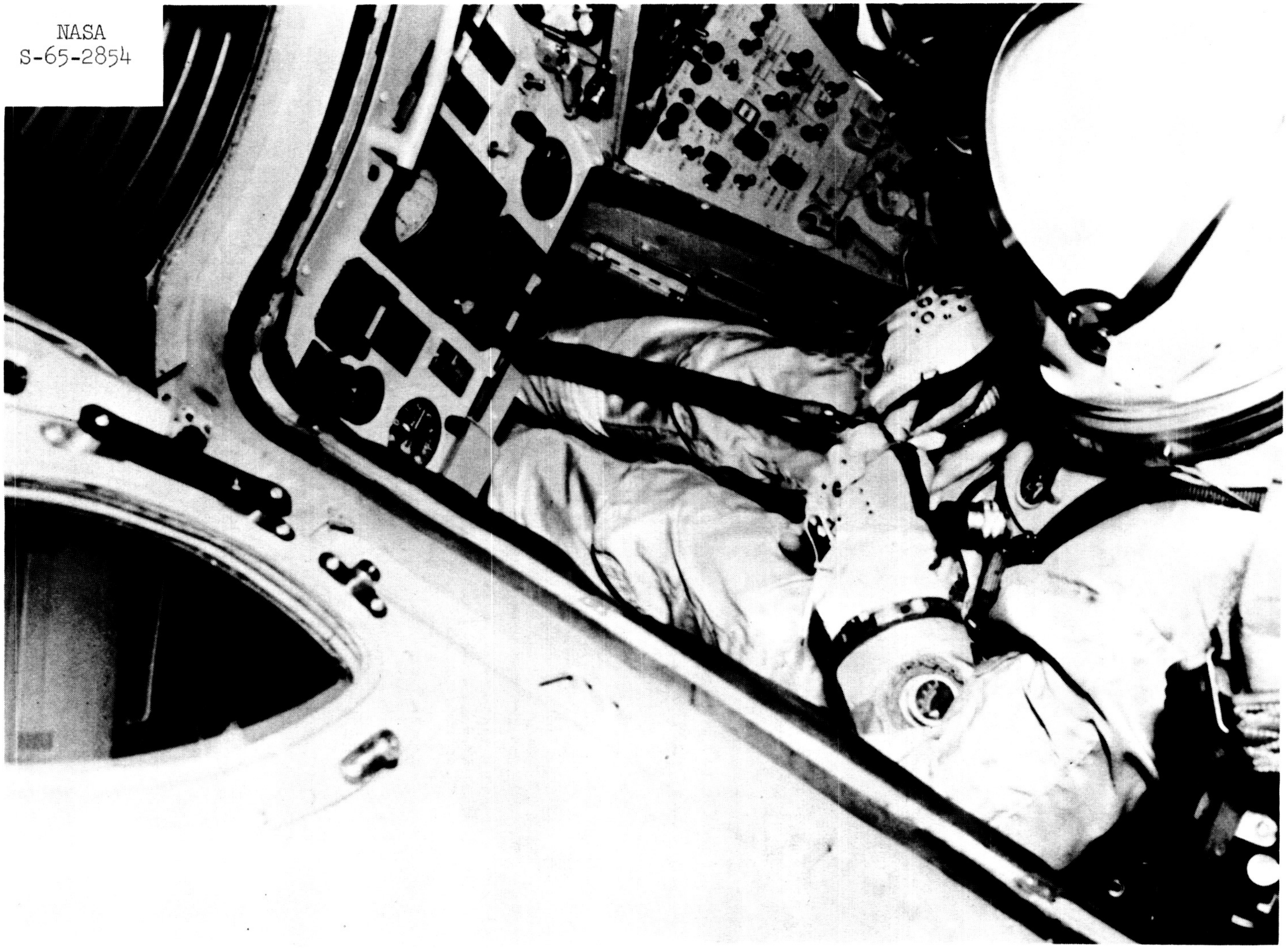

Figure 6(b)-2.- In-flight exerciser in use by an astronaut.

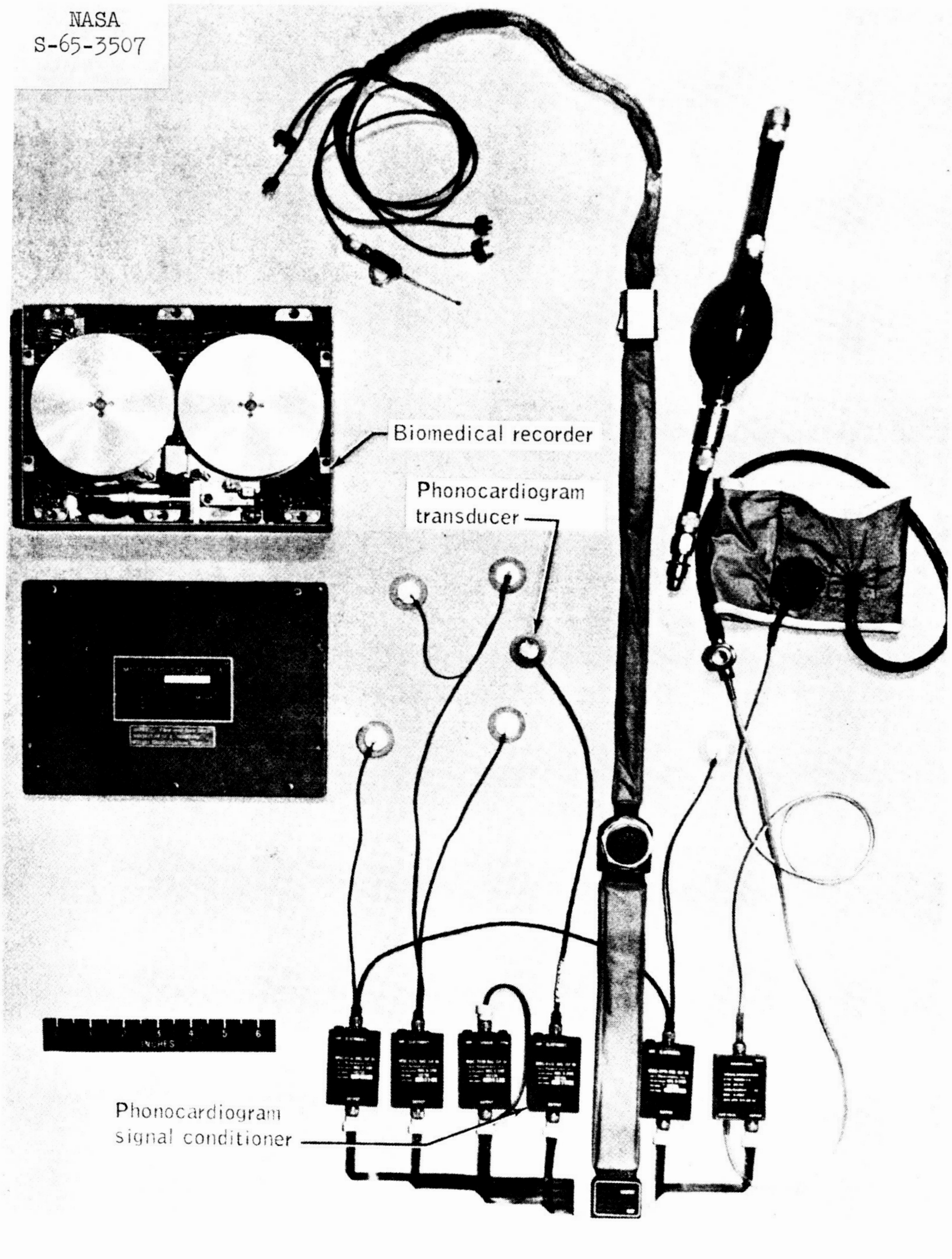

Figure 6(b)-3.- Gemini V biomedical and communications harness.

NASA
S-65-8568

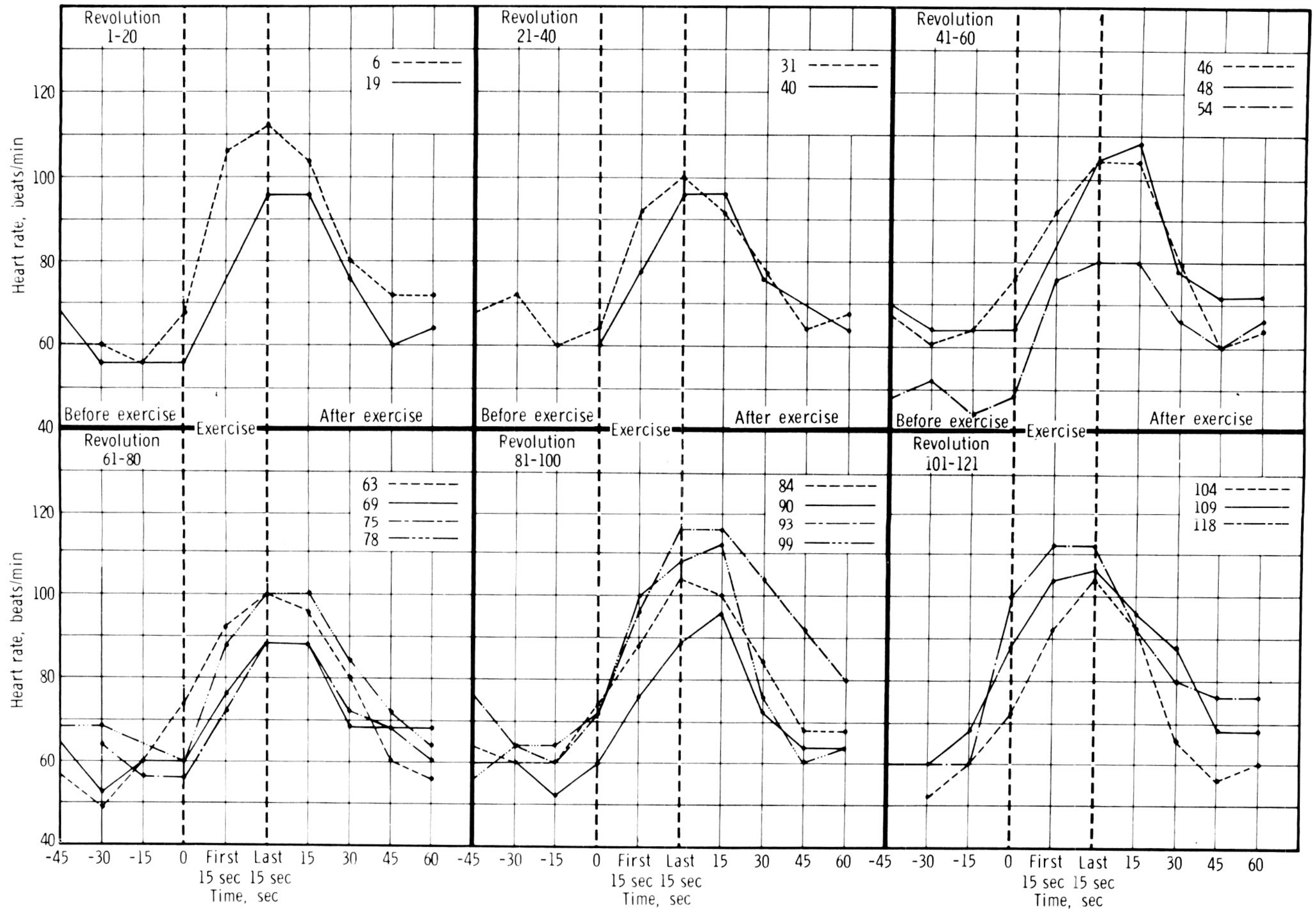

Figure 6(b)-4.- Command pilot in-flight heart-rate responses.

NASA
S-65-9210

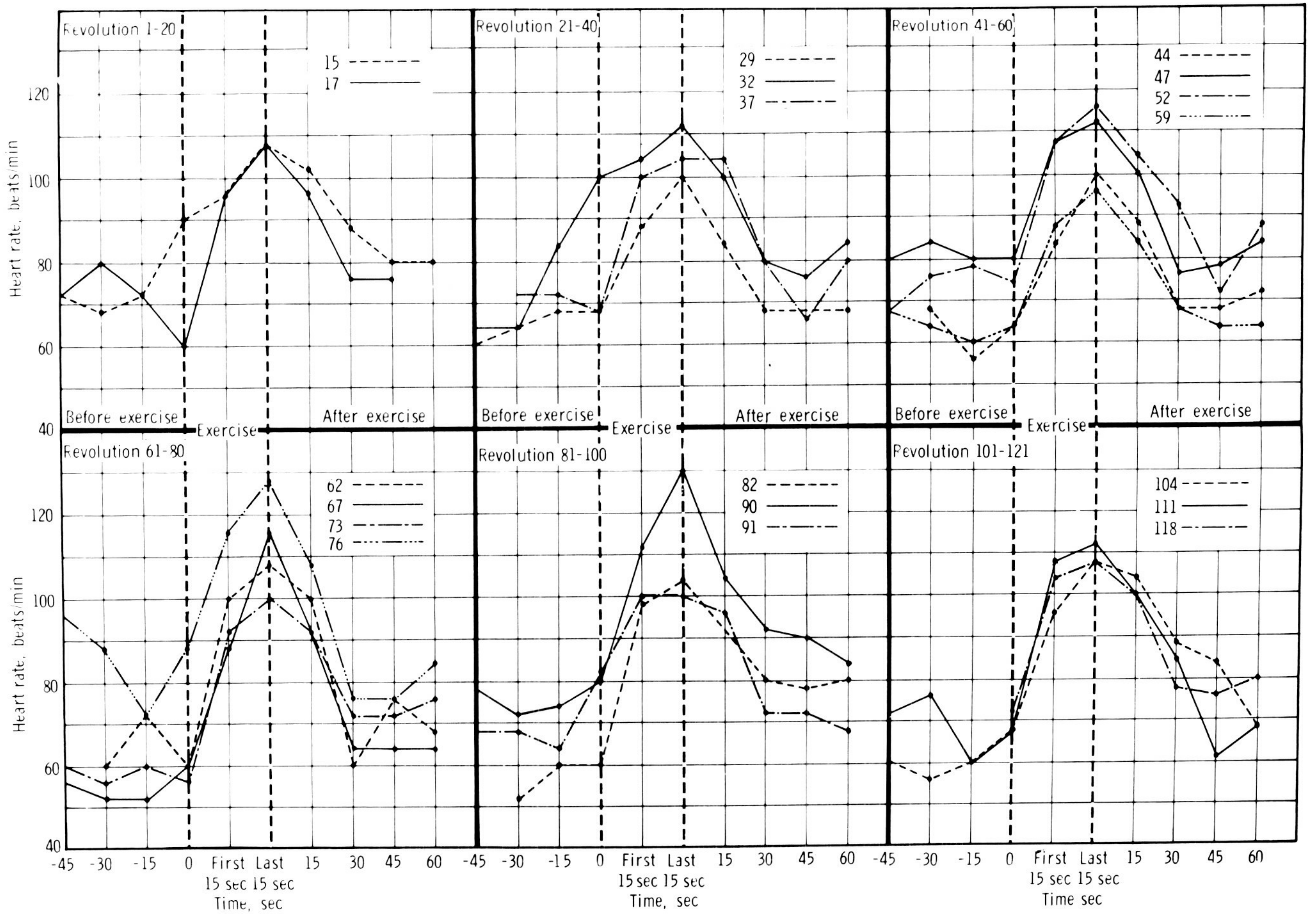

Figure 6(b)-5.- Pilot in-flight heart-rate responses.

7. EXPERIMENT M-6, BONE DEMINERALIZATION

By Pauline B. Mack, Ph.D.
Nelda Childers Stark Laboratory for Human Nutrition Research

George P. Vose, M.S.
Texas Woman's University

Fred B. Vogt, M.D.
Texas Institute for Rehabilitation and Research

Paul A. LaChance, Ph.D.
NASA Manned Spacecraft Center

SUMMARY

Experiment M-6 was designed to determine the effect upon the skeletal system of prolonged weightlessness and immobilization associated with the cockpit of the Gemini V spacecraft. Accordingly, a bone demineralization study was conducted on both the primary and backup crews of the 8-day Gemini V mission utilizing the same method of radiographic bone densitometry as that of the Gemini IV flight. Radiographs were made preflight and postflight of the left foot in lateral projection and the left hand in posterior-anterior projection of each astronaut at (a) 10 days, 4 days, 2 days and on the morning of lift-off at Cape Kennedy; (b) on the aircraft carrier U.S.S. Lake Champlain immediately after recovery and again after 24 hours; and (c) at the Manned Spacecraft Center at 10 days and 58 days following recovery.

Since different X-ray units were used at the separate locales, the radiographs prepared for densitometry were standardized by three methods: (a) by the use of an aluminum alloy wedge exposed adjacent to the bone; (b) by use of a roentgen meter to determine the calibrated kilovoltage producing identical beam qualities in each of the three X-ray units; and (c) by exposing at each testing site a standard absorber composed of bone ash in an organic matrix (casein) and enclosed in a tissue-simulating absorber (plexiglass) to detect possible technique variations at the three locations involved.

Losses in X-ray absorbence between radiographs made immediately preflight and postflight (in terms of X-ray equivalent aluminum alloy mass) at the conventional os calcis tracing path were 15.1 percent in the command pilot and 8.2 percent in the pilot. When the immediate postflight value was compared with the average of the four preflight values the

losses were 19.3 percent for the command pilot and 9.0 percent for the pilot.

Losses in X-ray wedge mass equivalency in the distal radius - a bone not examined in Gemini IV - were -25.3 percent and -22.3 percent for the command pilot and pilot, respectively. In the talus of the left foot, also not examined in previous flights, a decrease of 13.2 percent occurred in the command pilot and a decrease of 9.8 percent in the pilot.

In interpreting these data, it should be understood that changes in X-ray absorbency of bone involve not only calcium, but also other mineral constituents of calcium hydroxyapatite (the chief mineral component of bone), as well as interstitial and over- and underlying protein.

METHODS

Bone Densitometer Assembly

The instrumentation used in the photometric evaluation of bone density is a special analog computer consisting of a series of subassemblies, all designed to operate together as a completely integrated system. The theoretical aspects and instrumentation have been described in detail in references 1 and 4. The history of the development of the method and some specific applications of the method have been reported in references 2, 3 and 7.

Standard Radiographic Exposure Technique

The three diagnostic X-ray units used in the study were standardized with a central unit at Texas Woman's University by means of a calibration curve relating kilovoltage with the X-ray transmittance in milliroentgens through a standard 2-millimeter aluminum filter under a specific X-ray intensity. Under the exposure conditions utilized, all units yielded a beam quality equivalent to 60 kilovolts to assure a constant relationship among the mass absorption coefficients of hydroxyapatite, water, protein, fat, and aluminum alloy.

Evaluations of Wedge Mass Equivalency

In the previous investigation of bone mass changes before, during, and after the Gemini IV flight, two bones were examined: (a) the left os calcis or heel bone, and (b) phalanx 5-2 of the left hand. In the current study the same two bones were examined with the addition of phalanx 4-2, the distal end of the left radius, and the left talus. The anatomical sites examined are discussed in the following part, and are illustrated in figures 7-1 through 7-4.

Central os calcis section.- This anatomical site was used in the M-6 experiment in the Gemini IV flight and has been repeated in the Gemini V mission. The tracing path across the left os calcis in lateral projection (fig. 7-1) runs diagonally between conspicuous posterior and anterior landmarks which, by superimposing successive radiographs, can be accurately reproduced in serial films of the same individual. This single path (1.3 mm in width) is known as the "conventional scan."

Multiple parallel os calcis evaluations.- Approximately 60 percent of the total os calcis mass is evaluated in the parallel path system. After making the conventional scan, a series of parallel paths 1.0 millimeter apart were scanned beginning 1 millimeter above the conventional path and continuing to the lowest portion of the bone. The total number of paths scanned is therefore proportional to the size of the bone which, of course, has individual variations. For the command pilot 34 paths were required to cover the os calcis portion examined, while 35 parallel scans were needed for the pilot. Figure 7-2 illustrates the alinement of parallel paths through the os calcis portion examined although not every path is shown in the illustration.

Sections of the phalanx 4-2 and 5-2.- The second phalanx of the fourth and the fifth finger of the left hand was scanned by parallel cross-sectional paths 1 millimeter apart alined tangentially with the longitudinal axis and covering the entire bone area (fig. 7-3).

Distal end of radius.- A single scanning path was made through the diaphysis of the left radius parallel to the distal surface (fig. 7-4).

The talus.- A single scanning path was made through the talus of the left foot originating at the inferior surface and projecting anteriorly to the conspicuous landmark shown in figure 7-1.

INTERPRETATION OF THE TERM, "X-RAY ABSORBENCE" BY BONE

The term "X-ray absorbence" by bone as used in this report refers to the beam attenuation resulting from the hydroxyapatite and water-organic contents in their relative weight concentrations together with the over- and underlying soft tissue. Although changes in composition or thickness of the overlying soft tissue could account for slight changes in total X-ray absorption, our tests have shown that in the case of the os calcis, errors accountable to changes in soft tissue mass are slight, with changes in thickness of one millimeter accounting for X-ray absorption changes of approximately one percent.

RESULTS

X-ray Absorption Changes in the Central Os Calcis Section

(Conventional Path)

The X-ray absorption values (in terms of calibration wedge equivalency in grams) obtained from the central os calcis section during the Gemini V study are shown in figure 7-5 and table 7-I. Based on an average of all four preflight wedge equivalency values, the command pilot showed a change of 19.3 percent in this section of bone, with a 15.1 percent change when the immediate postflight film was compared with that made immediately before launch. The corresponding values for the pilot were 9.0 and 8.2 percent. Recovery was substantially complete in both astronauts on the 28th day (10 days postflight), and full recovery had occurred by the 75th day (58 days postflight).

Changes in Multiple Sections of the Os Calcis

Thirty-four parallel scans were made of each os calcis radiograph of the command pilot and 35 scans were made of the radiograph of the pilot covering approximately 60 percent of the total bone mass in each astronaut (fig. 7-2).

Figure 7-6 indicates that the values immediately following the flight and 24 hours after were lower than any of the preflight values with a 10.3 percent decrease in the command pilot and an 8.6 percent decrease in the pilot. Complete recovery had occurred by the 75th day (58 days postflight).

Comparison of Four Groups of Os Calcis

(Parallel Sections)

In an effort to determine which regions of the os calcis are the most sensitive reflectors of changes on bone mass, the multiple scans were divided into four groups each represented by a longitudinal section of bone approximately 9-10 millimeters wide. The changes between the preflight and postflight values of four sections for each astronaut were the following:

(1) Superior section (segments 1 millimeter above the scan through segment 8 below)

Command pilot	-12.8 percent
Pilot	- 8.5 percent

(2) Second section (segments 9 through 18 below the conventional scan)

Command pilot	-11.8 percent
Pilot	- 9.1 percent

(3) Third section (segments 9 through 18 below the conventional scan)

Command pilot	- 4.4 percent
Pilot	- 7.5 percent

(4) Inferior section (segments 28 to inferior surface of os calcis)

Command pilot	- 4.7 percent
Pilot	- 7.5 percent

As expected, there is some inconsistency in the magnitude of changes from section to section. However, it is apparent that the bone mass decreased somewhat more in the superior sections than in the inferior sections in both astronauts. This effect may be attributed to the greater proportion of cancellous to cortical bone in the superior regions than in the inferior regions of the os calcis, explaining the fact that changes of greater magnitude are often seen in the conventional scanning path than in multiple scans of the entire bone.

Changes in the Distal Area of the Radius

During the 8-day Gemini V flight, the X-ray wedge mass equivalency of the distal end of the left radius decreased by -25.3 percent in the command pilot and by -22.3 percent in the pilot. The preflight values were regained in both astronauts by the 75th day (fig. 7-7).

Changes in the Talus

The X-ray wedge mass equivalencies at the talus scanning site made immediately postflight was 13.2 percent lower than the final preflight value in the command pilot, and 9.8 percent lower in the pilot. Recovery was faster in the talus than in the radius, however, with both astronauts exhibiting almost full recovery on the 27th day (18 days postflight) and full recovery by the 75th day (58 days postflight).

Bone Mass Changes in Hand Phalanges 4-2 and 5-2

As in the case of the os calcis, multiple parallel scans were made across hand phalanges 4-2 and 5-2 so that the entire area of each phalanx in posterior-anterior projection was evaluated (fig. 7-3). Decreases in wedge mass equivalency were noted in both phalanges during the 8-day orbital phase of the study, although in both astronauts the decrease in phalanx 5-2 was greater than that in 4-2. In the command pilot a 22.6 percent decrease in wedge mass equivalency occurred when the immediate postflight value was compared with the average of the four preflight films, and the pilot decreased by 24.5 percent. In hand phalanx 4-2, decreases of -6.2 and -6.4 percent occurred in the command pilot and pilot, respectively (figs. 7-9 and 7-10).

RELATION OF SPACE FLIGHT FINDINGS TO FINDINGS FROM TWU BED-REST STUDIES

In this Gemini V study, an amount of 845 milligrams of calcium was provided per day for each man during the orbital flight. On the other hand, a mean of only 373 milligrams daily was consumed by the command pilot, and a mean of 333 milligrams by the pilot.

In the TWU bed rest, one group of men was placed on an extremely low level of calcium, with mean daily levels consumed tending to be even slightly below those of the Gemini V astronauts. Table 7-II summarizes the comparative wedge mass equivalency changes in the central os calcis section for both astronauts and for four bed-rest subjects on similar average levels of calcium for similar periods of time.

DISCUSSION

Densitometric evaluations of serial radiographs of "normal" subjects have often shown rather frequent changes in bone mass within relatively short periods of time. For this reason it was decided to make two preflight and two postflight radiographs of the Gemini V backup crew. In comparing the changes observed preflight and postflight as the conventional os calcis scanning site between the two crews, it was found that no changes greater than 4 percent were evident in either member of the backup crew. This is in contrast to the 15.1 and 8.9 percent losses observed in the prime crew.

It has long been known that the skeletal system experiences a general loss of mineral under immobilization or extended bed rest. However, in both Gemini IV and Gemini V studies, bone mass losses were greater in both the os calcis and phalanx than were shown by the TWU bed-rest subjects during the same period of time.

Although the bone mass losses in the 8-day Gemini V flight were generally greater than in the 4-day Gemini IV flight, the information to date is still insufficient to conclude that the losses tend to progress linearly with time, or whether a form of physiological adaptation may occur in longer space flights.

BIBLIOGRAPHY

1. Mack, Pauline Beery; Vose, George P.; and Nelson, James Donald: New Developments in Equipment for the Roentgenographic Measurement of Bone Density. American Journal of Roentgenology, Radium Therapy, and Nuclear Medicine, vol. 82, 1959, p. 647.

2. Mack, Pauline Beery: Radiographic Bone Densitometry. Conference under sponsorship of the National Aeronautics and Space Administration and the National Institutes of Health, Washington D.C., March 25-27, 1965.

3. Mack, Pauline Beery; O'Brien, Anne T.; Smith, Janice M.; and Bauman, Arthur W.: A Method for Estimating the Degree of Mineralization of Bones from Tracing of Roentgenograms. Science, vol. 89, 1939, p. 467.

4. Mack, Pauline Beery; Brown, Walter N.; and Trapp, Hughes Daniel: The Quantitative Evaluation of Bone Density. American Journal of Roentgenology and Radium Therapy, vol. 61, 1949, p. 808.

5. Mack, Pauline Beery; Klapper, Elsa A.; Pyke, Ralph E.; Alford, Betty B.; and Gauldin, Ruth: Fourth Semiannual Report to the National Aeronautics and Space Administration, Mar. 31, 1965.

6. Ibid: Fifth Semiannual Report to the National Aeronautics and Space Administration, Sept. 30, 1965.

7. Vogt, F. B.; Mack, P. B.; Beasley, W. G.; Spencer, W. A.; Cardus, D.; and Valbonna, C.: The Effect of Bedrest on Various Parameters of Physiological Functions, Part XII. The Effect of Bedrest on Bone Mass and Calcium Balance. Texas Institute of Rehabilitation and Research. Report to the National Aeronautics and Space Administration, Apr. 1965.

TABLE 7-I.- EVALUATION OF CENTRAL OS CALCIS POSTERIOR-ANTERIOR "CONVENTIONAL" SEGMENT

(a) Command pilot

Radiographs	X-ray absorption values in terms of aluminum wedge equivalency, grams
Mean of values from preflight films	2.0205
Film taken immediately before lift-off	1.9193
Film taken immediately after end of flight	1.6295
Film taken 10 days after end of flight	1.9215
Film taken 58 days after end of flight	2.0101

(b) Pilot

Mean of values from preflight films	1.8214
Film taken immediately before lift-off	1.8169
Film taken immediately after end of flight	1.6574
Film taken 10 days after end of flight	1.7762
Film taken 58 days after end of flight	1.8160

TABLE 7-II.- COMPARISON OF WEDGE MASS EQUIVALENCY LOSSES IN CENTRAL OS CALCIS OF GEMINI V CREW AND OF TWU BED-REST SUBJECTS ON SIMILAR DAILY INTAKES OF DIETARY CALCIUM FOR SIMILAR PERIODS OF TIME

Subjects	Number of days	Average calcium consumed/day, milligrams	Central os calcis wedge mass equivalency change, percent	
			Based on mean of preflight values	Based on last value before launch
Command pilot	8	373	-19.3	-15.1
Pilot	8	333	-9.0	-8.2
TWU Bed rest				Based on value before bed rest
Subject 1	8	307	X	-8.65
Subject 2	8	292	X	-5.06
Subject 3	8	303	X	-7.89
Subject 4	8	308	X	-8.06

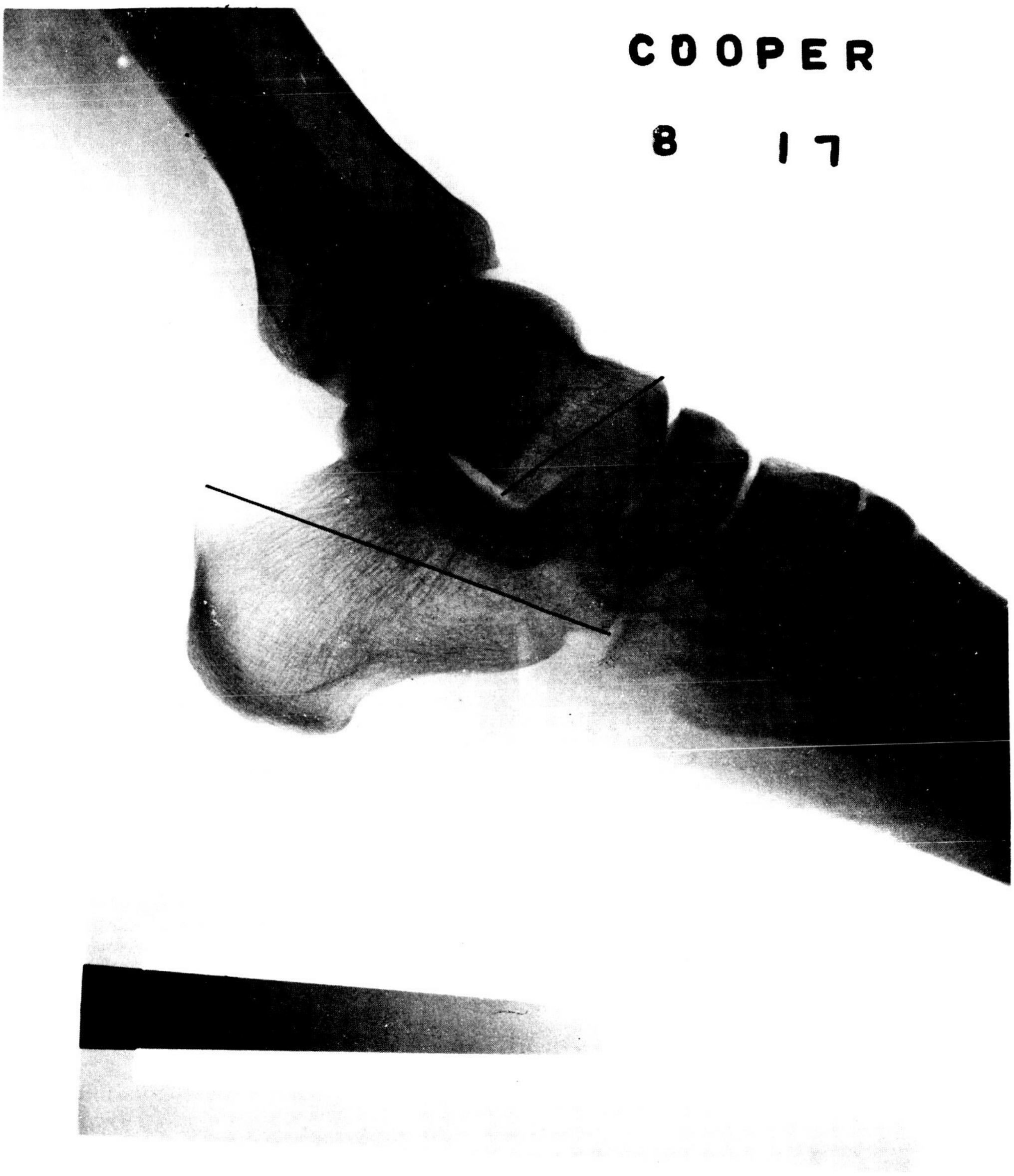

Figure 7-1.- Reproduction of positive of the lateral radiograph of the left foot of the Gemini V command pilot indication conventional scanning paths of os calcis and talus.

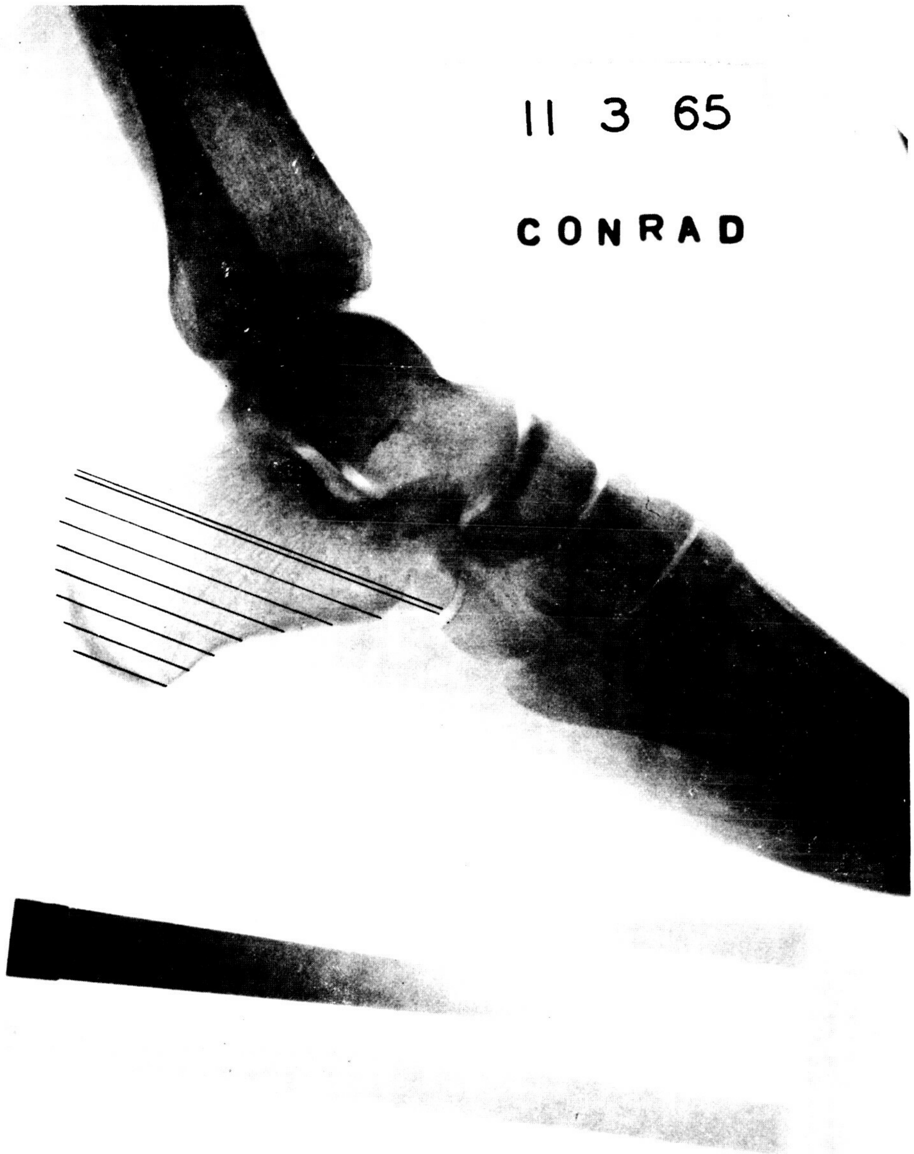

Figure 7-2.- Reproduction of the positive of the radiograph of the left foot of the Gemini V pilot indicating multiple parallel paths.

Figure 7-3.- Reproduction of the positive of the radiograph of the left hand of the Gemini V pilot indicating parallel paths of phalanges 4-2 and 5-2.

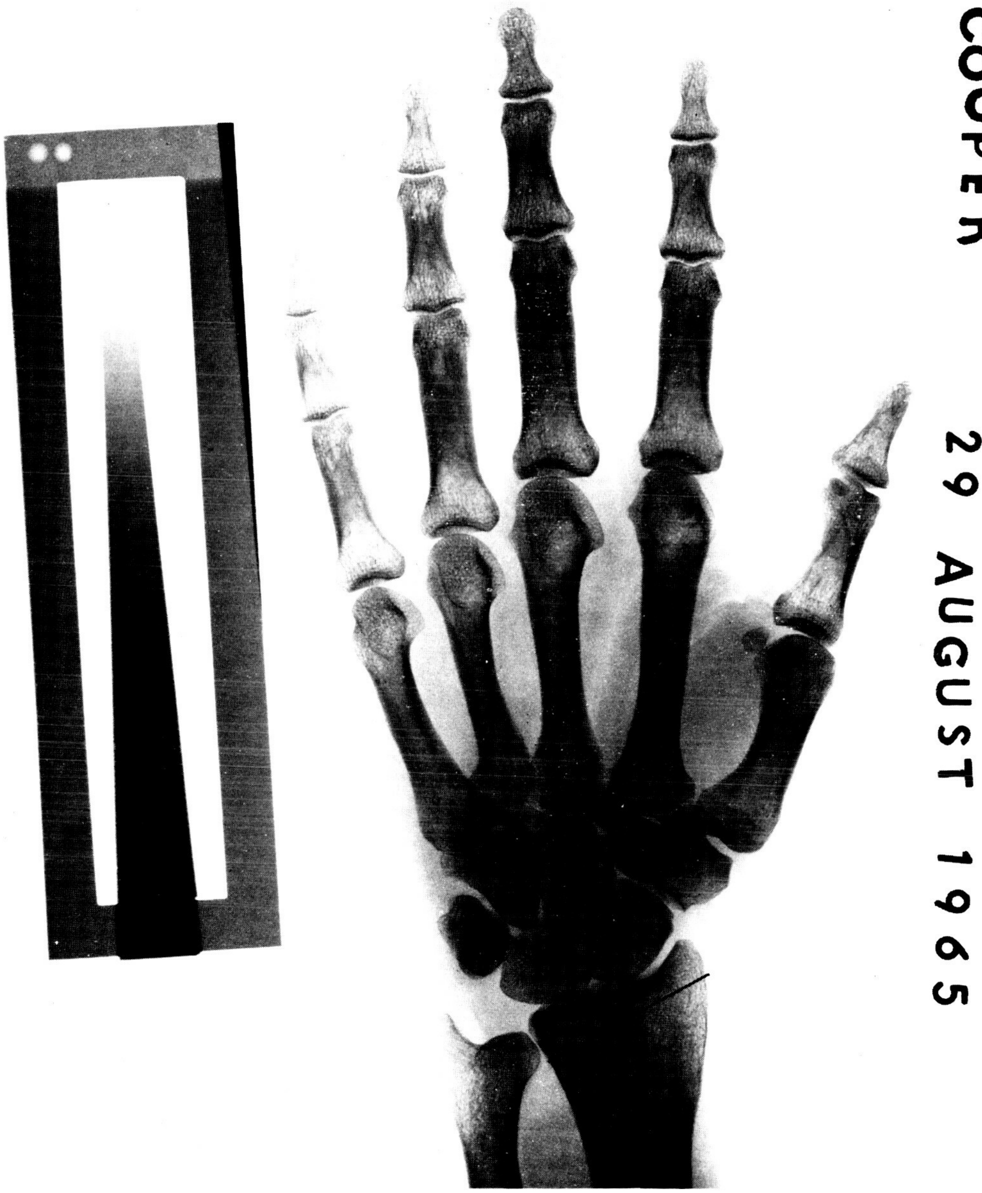

Figure 7-4.- Reproduction of the positive of the radiograph of the left hand of the Gemini V command pilot indicating the scanning path of the distal radius.

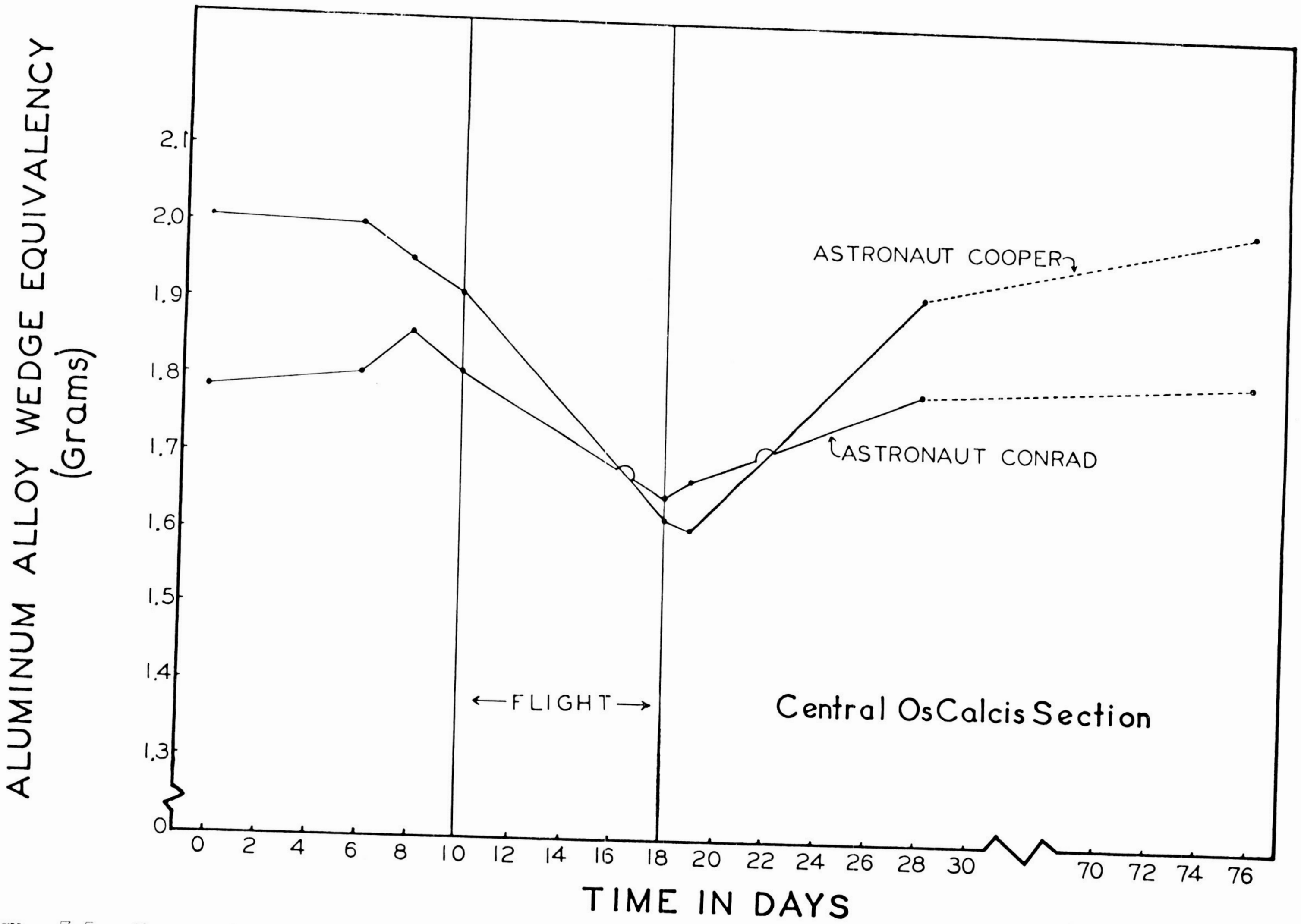

Figure 7-5.- Changes in aluminum alloy wedge mass equivalency of the central os calcis segment ("conventional path") of the Gemini V command pilot and pilot throughout the Gemini V program.

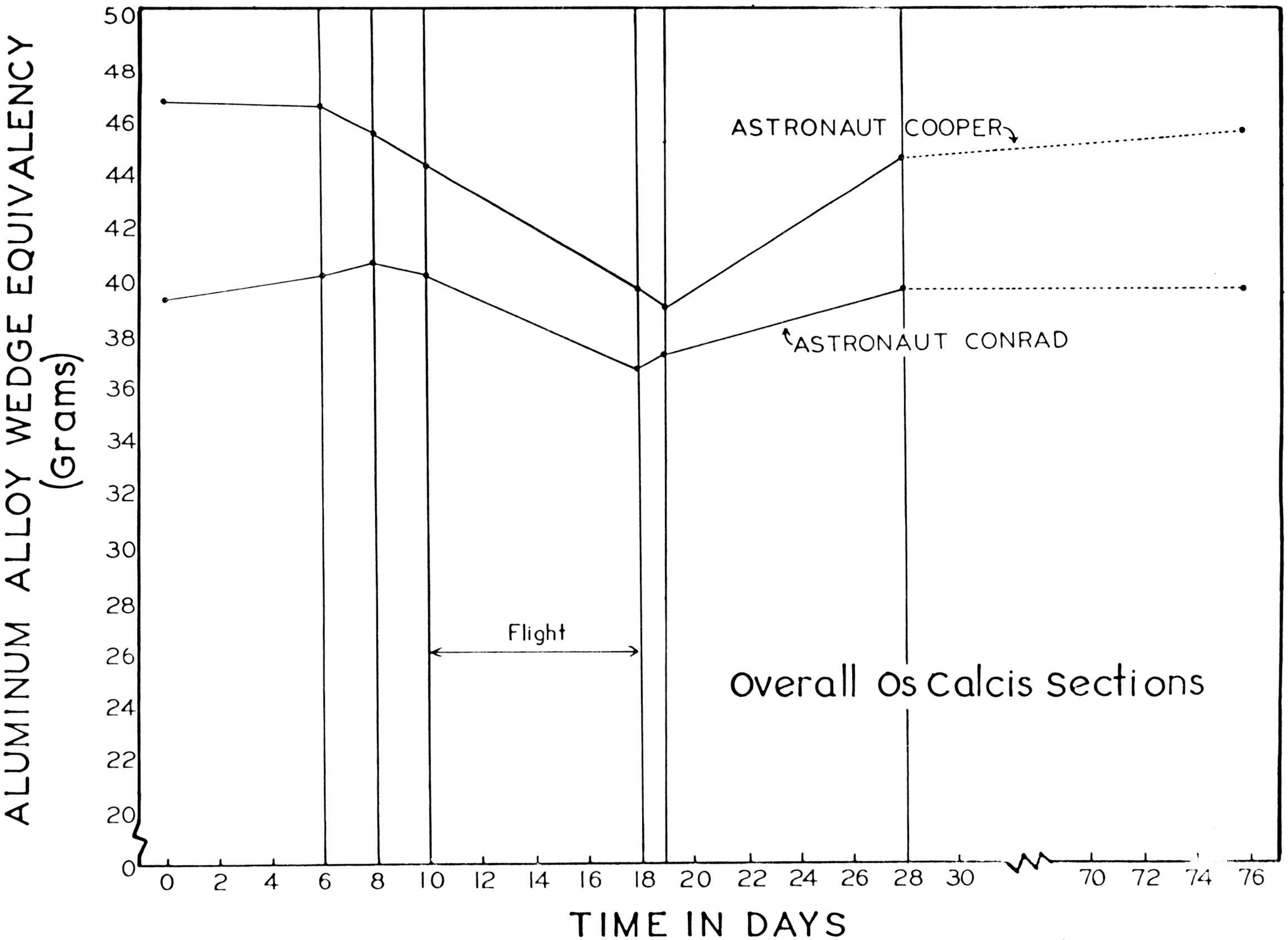

Figure 7-6.- Changes in aluminum alloy wedge mass equivalency of the entire series of parallel scans of the os calcis of the Gemini V command pilot and pilot.

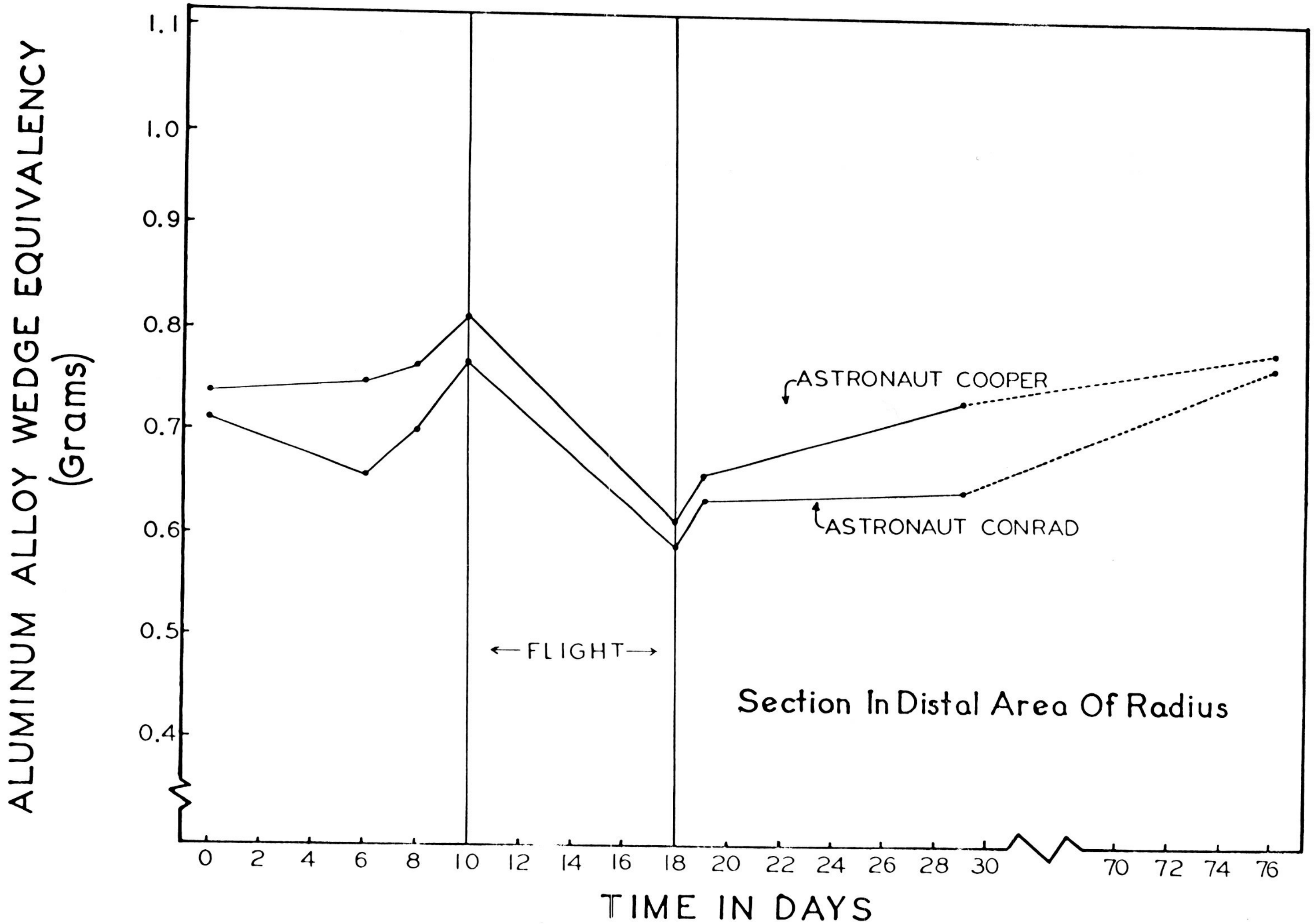

Figure 7-7.- Changes in aluminum alloy wedge mass equivalency of the distal end of the radius of the Gemini V command pilot and pilot.

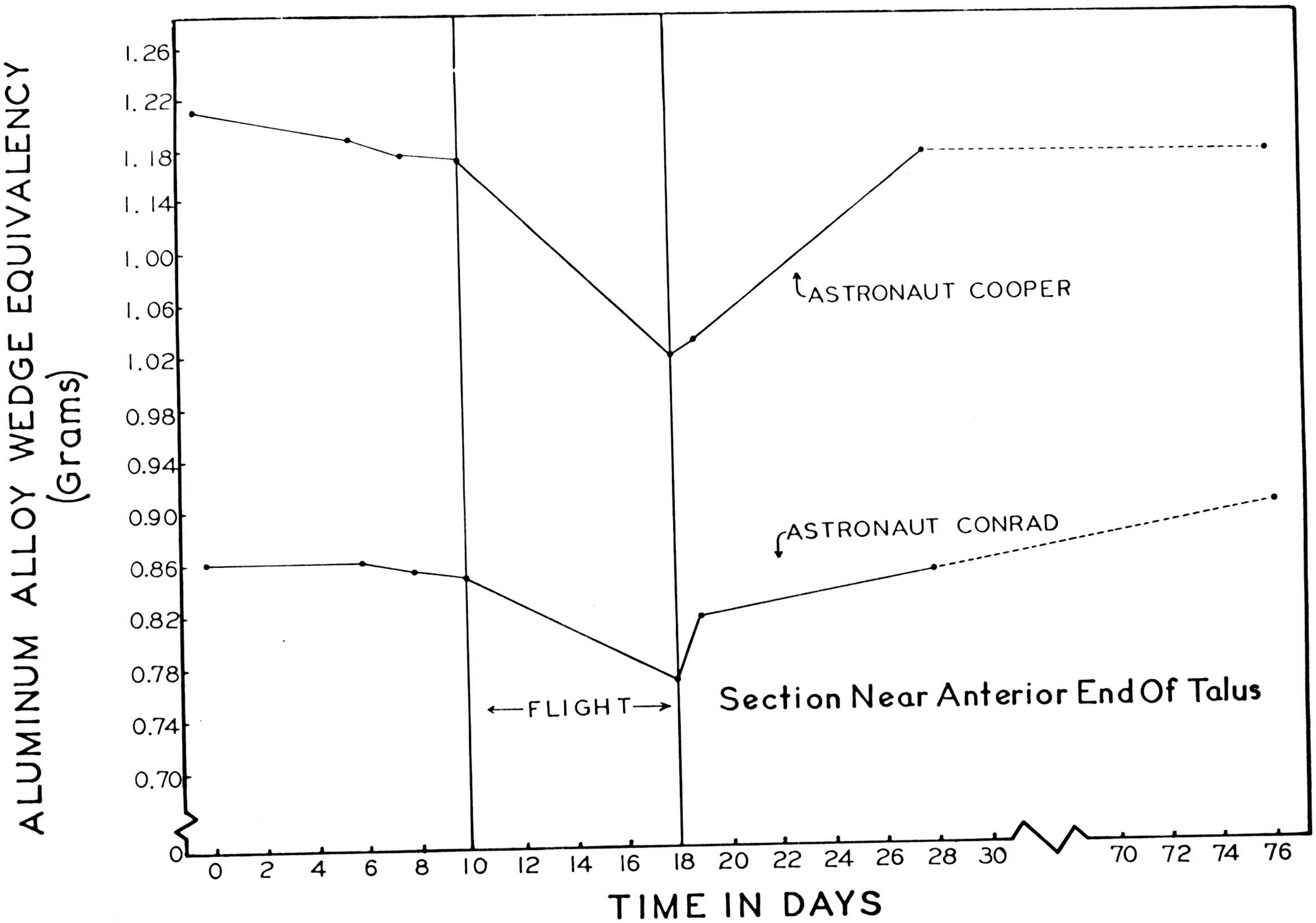

Figure 7-8.- Changes in aluminum alloy wedge mass equivalency of the talus of the Gemini V command pilot and pilot.

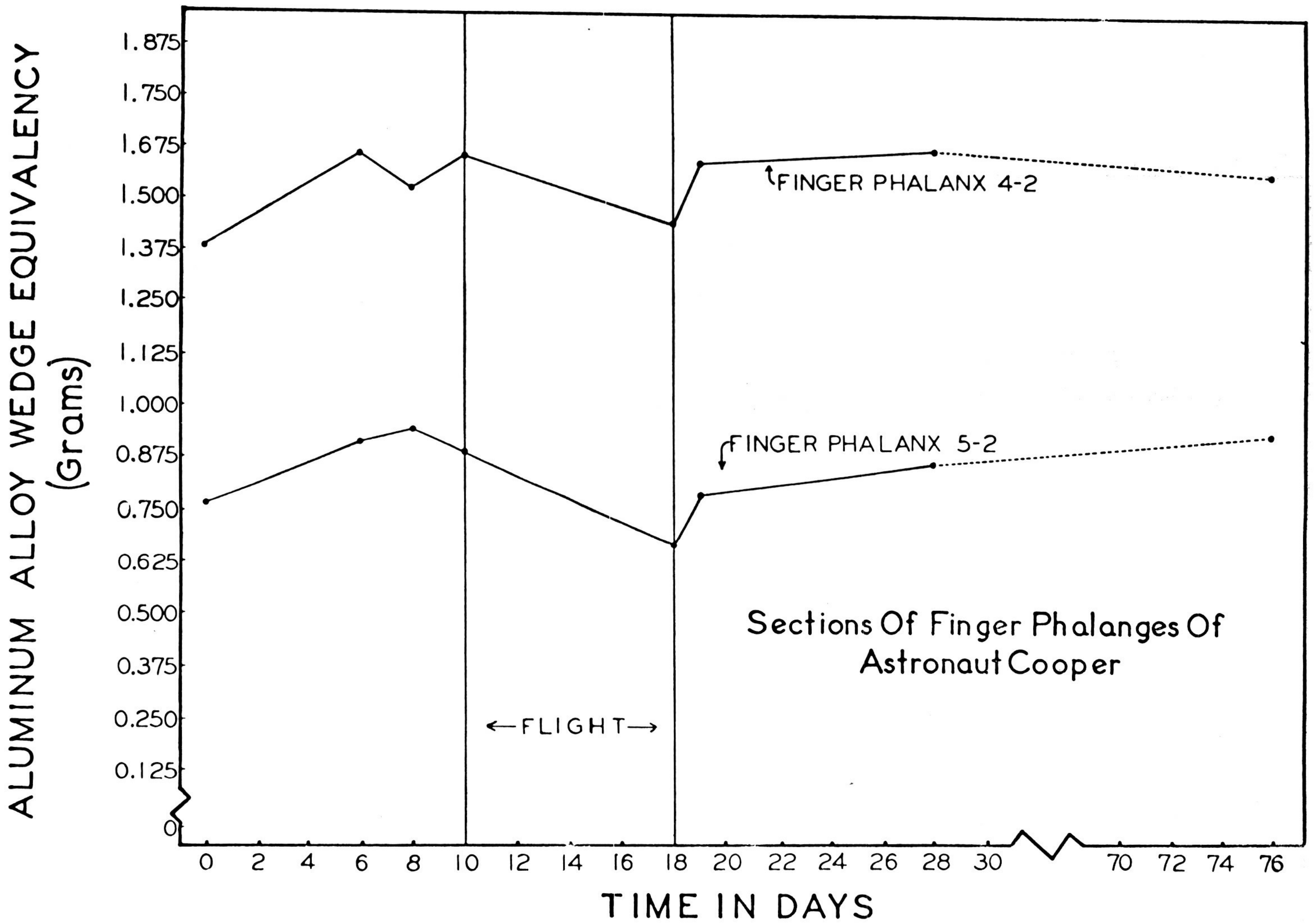

Figure 7-9.- Changes in aluminum alloy wedge mass equivalency of hand phalanges 4-2 and 5-2 of the Gemini V command pilot.

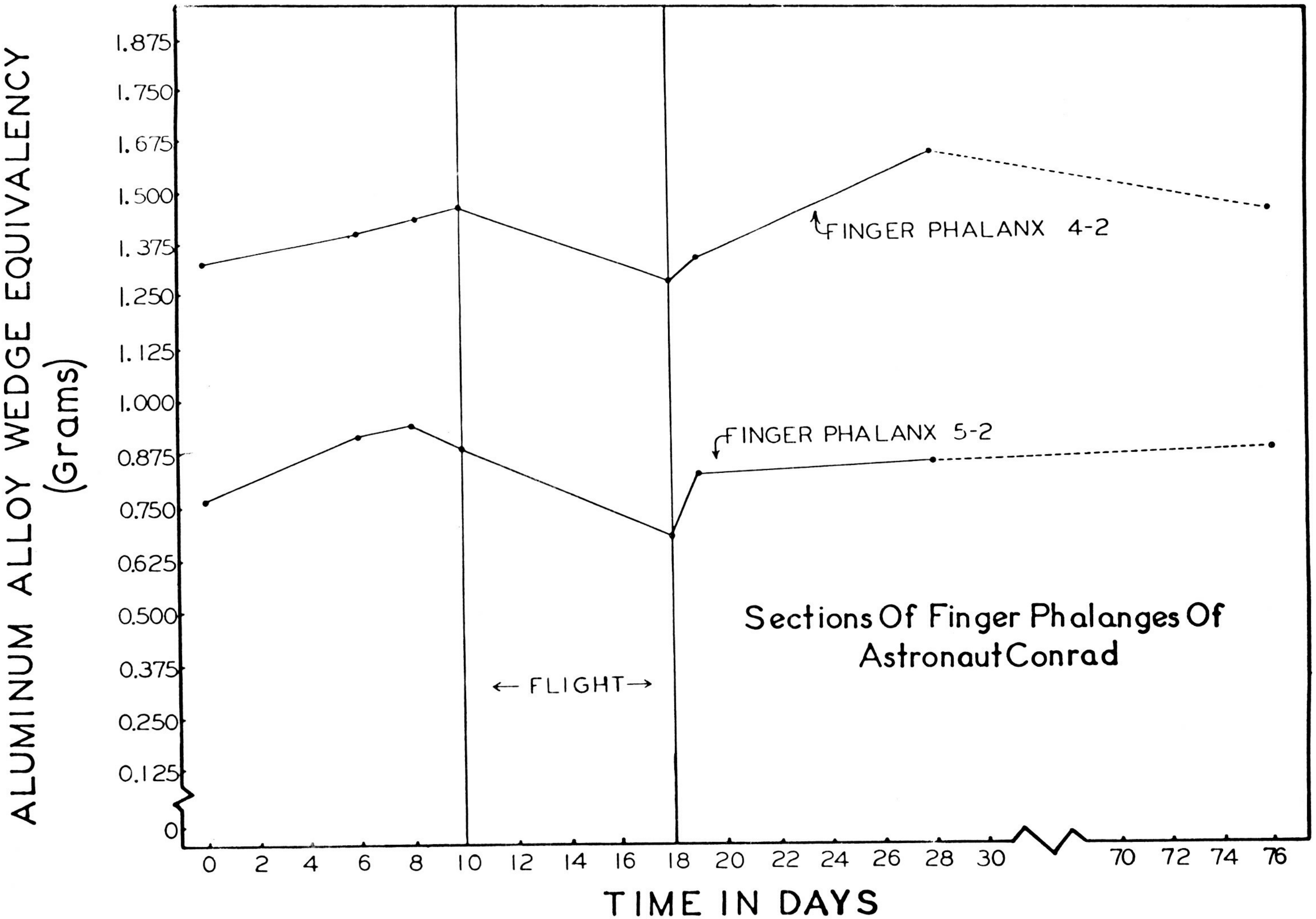

Figure 7-10.- Changes in aluminum alloy wedge mass equivalency of hand phalanges 4-2 and 5-2 of the Gemini V pilot.

8. EXPERIMENT M-9, HUMAN OTOLITH

By A. Graybiel
U. S. Naval Aviation Medical Center

INTRODUCTION

The purpose of this experiment was to obtain two types of information during orbital space flight. One type of information desired was to determine the ability of the astronauts to estimate horizontality with reference to the spacecraft in the absence of visual and primary gravitational cues. The other type was to determine the possible effect of prolonged weightlessness on otolith function.

Egocentric visual localization of the horizontal (EVLH) was the test chosen to measure "horizontality." It may best be described by means of an illustration (fig. 8-1). If an observer regards a dim line of light in darkness (while seated upright under ordinary conditions), he is able to set a line in the dark to the horizontal with great accuracy (ref. 1). If, under proper conditions, he is exposed to change in the gravitoinertial vertical with respect to himself, he is able to set the line approximately perpendicular to the changing direction of the mass acceleration (ref. 2). This confirms that, in the absence of visual cues (the line itself being an inadequate cue), the ability of the observer to estimate the vertical and horizontal is due to the influence of primary and secondary gravitational cues. Persons with bilateral loss of the organs of equilibrium (otolith apparatus) are inaccurate in carrying out this task, indicating the important role of the otolith apparatus in signaling the upright. In weightlessness, primary gravitational cues are lost and the otolith apparatus is physiologically deafferented (ref.3); that is to say, it has lost its normal stimulus. A unique opportunity is created to investigate the role of secondary gravitational cues in orientation to the environment with which a person is in contact. The astronaut in orbital flight is cued to his spacecraft even with eyes closed by virtue of tactile cues. Consequently, as a first step in exploring the loss of primary gravitational cues in space flight, it was deemed worthwhile to obtain serial EVLH measurements.

This test is based upon the observation that when a person is tilted to the right or to the left, his eyes tend to rotate in the opposite direction. Preflight and postflight otolith function was measured by means of ocular counterrolling (ref. 3). If proper technique is used, the amount of the counterroll can be measured accurately. Persons with bilateral loss of otolith function do not manifest counterrolling or any roll is minimal, possibly indicating slight residual function. In its present form, this test cannot be carried out in a small spacecraft; hence, the test is limited to preflight and postflight measurements. The object of the test was to determine whether prolonged physiological deafferentation of the otolith apparatus had changed its sensitivity of response.

APPARATUS

The apparatus for measuring the EVLH of the spacecraft was incorporated into the onboard vision tester, which was part of the S-8/D-13 Experiment. This incorporation was made to save weight and space and represented only a physical interface; in all other respects the two experiments were separate entities. The in-flight vision tester is a binocular instrument (fig. 8-2) with an adjustable interpupillary distance (IPD), but without any focusing adjustment. The instrument device is held at the proper position, with the lines of sight coincident with the optic axes of the instrument, by means of a biteboard individually fitted to the subject. The biteboard insured that, at each use, the instrument was similarly located with respect to the subject's axes, providing the proper IPD adjustment had been made. In this position, the eyecups connected to the eyepieces of the instrument excluded all extraneous light from the visual field. The dc power regulated by the instrument was supplied by the spacecraft.

The use of a bracket to fix the device about the roll axis of the spacecraft was not feasible. Parenthetically, it may be stated that the bracket was used for the Gemini VII mission.

The apparatus used represented a modification and miniaturization of a target device previously described (ref. 2). The apparatus consisted, essentially, of a collimated line of light in an otherwise dark field. This line could be rotated about its center by means of a knurled knob. A digit readout of line position was easily seen, and was accurate within $\pm 0.25^\circ$.

The device was monocular and fabricated in duplicate so that, for example, when the astronaut in the left-hand seat used the right eye, the readout was visible to the astronaut in the left-hand seat. The readout was adjusted so that horizontality to the apparatus was 61.25° for the astronaut on the left, and 98.75° for the astronaut on the right. The instrument's zero was represented by a value other than zero or 180° to eliminate or reduce the possible influence of knowledge of the settings upon subsequent judgments.

The apparatus used for measuring ocular counterrolling (CR) is essentially a tilt device on which a camera system is mounted (ref. 4). The main supporting part of the CR device acts as a carrier for the stretcher-like section. This section contains Velcro straps and a saddle mount to secure the subject in a standing position within the device. The device can be rotated laterally to 90° about the optic axis of the camera system as well as about the visual axis of his right or left eye, when the subject is properly adjusted. A custom fitted biteboard was also used in CR testing to fix the subject's head with respect to the camera recording system.

The camera system used to photograph the natural iris landmarks includes a motor driven 35-mm camera with bellows extension and an electronic flash unit. A console located at the base of the tilt device contains a bank of power packs which supply the electronic flash, a timer control mechanism, and controls for the round, flashing, fixation light which surrounds the camera lens. A triaxial accelerometer unit, which senses and relays signals of linear acceleration to a Consolidated Electrodynamics Corporation galvanometer recorder, was mounted to the head portion of the device.

A test cubicle, 12 by 16 by 10 feet, insulated against outside sounds, light, and temperature was constructed for carrying out the postflight tests of EVLH and CR onboard the recovery carrier.

Procedure

The preflight testing of CR and EVLH for both subjects was accomplished at Cape Kennedy 16 days prior to the flight.

Immediately prior to the preflight and postflight testing of EVLH, one drop of 1 percent pilocarpine hydrochloride ophthalmic solution was instilled in the eye which would not be used for making visual orientation judgments. The subject was then placed in the CR tilt device, properly adjusted, and secured. The method of conducting the preflight and postflight EVLH test was as follows: (1) the IPD of the vision tester was adjusted, and the device was brought into its proper position by inserting the biteboard into the mouth of the subject; (2) the experimenter initially offset the line target presented to one eye only (the other eye observed a completely dark field); (3) by means of the knurled wheel, the subject rotated the target clockwise or counterclockwise until it appeared to be alined parallel to the gravitational horizontal. This procedure was repeated in each test session until eight settings had been made in the upright position.

The method of testing EVLH inflight was as follows. Immediately after completion of the S-8/D-13 experiment, the instrument was readied for EVLH testing by occluding the left eyepiece (command pilot) or right eyepiece (pilot) by means of the ring on the eyepiece, and turning on the luminous target before the other eye. Pilot B was tested first. The target, appearing against a completely dark background, was initially offset at random by the observer pilot. The subject pilot's experimental task was to adjust the target until it appeared horizontal with respect to his immediate spacecraft environment. The subject, when satisfied with each setting, closed his eyes and removed his hand from the knurled ring. This served as a signal to the observer pilot to record the setting and offset the target. This procedure was planned to be repeated five times during each of the daily test sessions. The vision tester was then handed to pilot A, and the same sequence was carried out before completion of the visual acuity test. Finally, the readings for each pilot were to be tape recorded by voice. In lieu of the bracket for fixing the head and therefore the test instrument, the pilots were requested to maintain an erect position by alinement with the headrest.

The preflight and postflight measurements of ocular CR were accomplished according to the standard procedure used at the U. S. Naval Aerospace Medical Institute. Following the EVLH test, the subject remained in the upright position in the tilt device, the vision tester and its biteboard were removed, and preparations made for photographically recording the eye position associated with a given position of body tilt. The CR biteboard was inserted in the subject's mouth, and the position of his appropriate eye was adjusted so that it coincided with the optic axis of the camera system when he fixated the center of the flashing, red ring of light. Six photographic recordings were made at this position. The subject was then slowly tilted in his lateral plane to each of four other positions (±25°, ±50°), and the same photographic procedure was repeated.

The accelerometer system was used postflight to record continuously, during the EVLH and CR tests, motions of the recovery ship around its roll, pitch, and yaw axes.

During the EVLH and CR tests, readings of blood pressure, pulse rate, and EKG were monitored by NASA Manned Spacecraft Center medical personnel. Postflight examinations were begun for pilot B and pilot A approximately 5 and 6 hours, respectively, following their recovery at sea.

RESULTS

Ocular Counterrolling

Preflight.- Preflight measurements of ocular CR (fig. 8-3) indicated that the basic otolithic function of pilot A as well as pilot B fell at the low normal level but remained within the range of counterrolling response found among a random population of 100 normal subjects (represented in fig. 8-4 by the shaded area). The possibility existed that the lower response manifested by these pilots might be typical for the highly select population of astronauts and represent some byproduct of their pilot experience. The results of the testing of six additional astronauts (fig. 8-4) indicate, however, that this magnitude of response is not typical of this select population.

Postflight.- As indicated in figure 8-3, postflight measurements also revealed a reduced CR response which was not significantly different from the comparable preflight data. The slight differences in the CR curves can be accounted for by the small rotary oscillations (physiological unrest) of the eye about a mean position of the eyes associated with any given body tilt.

Egocentric Visual Localization of the Horizontal (EVLH)

Preflight and postflight.- The deviations from the instrument's zero of the pilot's discrete EVLH settings are summarized in figure 8-5. The judgments of each pilot in the location of the gravitational horizontal for an upright position were quite accurate and stable prior to the flight. On the day of recovery, the pattern of response was similar to that of preflight but was less accurate and consistent. Although the seas were relatively calm, the fact that judgments were made on an unstable platform could account for these differences.

Inflight.- Inflight EVLH measurements were not made in the early part of the flight, probably in the interest of conserving spacecraft power. During revolution 24 and two succeeding revolutions (39 and 54), only one EVLH judgment was made by each subject. Beginning on revolution 72, and continuing through several subsequent revolutions during the mission, five EVLH judgments were recorded. Evaluation of the inflight data indicates that pilot B rendered accurate and consistent visual estimations, while pilot A, although no less consistent than pilot B, made judgments which were markedly (greater than 30°) deviant from the absolute horizontal of his immediate spacecraft environment. A summary of the EVLH data is given in figure 8-5 which portrays the EVLH settings for each pilot preflight, during specific in-flight revolutions, and postflight. Lack of data for the initial part of the flight mission prevents any statement regarding the possible time of onset of the apparent change in visual orientation of pilot A.

DISCUSSION

The most significant findings requiring discussion are the EVLH measurements on astronaut A during actual flight. A systematic technical error seems to be ruled out for the following reasons: (1) the same device was used in obtaining, shortly after impact, the postflight measurements, and these were within the expected range; (2) the device was tested postflight, as it was preflight, and the digital readout was found to be accurate in both instances; (3) the possibility that the astronaut, lacking a device to fix the head, used head position as a frame of reference was ruled out since, by actual test, the astronaut could not incline his head 32°; and (4) the procedure was reviewed with the astronauts postflight, and there was no lack of understanding in carrying out the task. In the absence of gravity and with eyes closed, the cues furnished by virtue of contact with the spacecraft apparently did not allow correct perception of the cabin vertical in the case of astronaut A. The uniformity of the settings after the 24th revolution suggests that learning did not occur in the absence of any knowledge of the accuracy of the estimates.

If the observations on astronaut A are confirmed, either under operational or artifically contrived conditions in orbital flight, it will suggest one approach to the further investigation of secondary or indirect gravitational cues to our nonvisual perception of the upright position. The feasibility of this experimental approach was confirmed by the results of the present experiment since the Gemini V astronauts demonstrated that, if contact cues are adequate, a coordinate space sense with respect to the spacecraft exists even in weightlessness. With respect to the influence of these secondary gravitational cues upon perception, it is tempting to draw an analogy with what has been termed the aviators' leans. Here, with restricted cues, but in relative abundance in comparison with those in a spacecraft, there is a tendency either to fly with one wing low or, in straight and level flight using instruments, to feel inclined away from the upright.

REFERENCES

1. Miller, E. F., II; and Graybiel, A.: Role of the Otolith Organs in the Perception of Horizontality. Amer. J. Psychol., In press, 1965.

2. Graybiel, A.: Oculogravis Illusion. Arch Ophthal., vol. 48, pp. 605-615, 1952.

3. Miller, E. F., II; Graybiel, A.; and Kellogg, R. S.: Otolith Organ Activity Within Earth Standard, One-half Standard, and Zero Gravity Environments. NSAM-943, 1965. (NASA Order No. R-93.)

4. Miller, E. F., II; and Graybiel, A.: A Comparison of Ocular Counter-rolling Movements Between Normal Persons and Deaf Subjects with Bilateral Labyrinthine Defects. Ann. Otol., vol. 72, pp. 885-893, 1963.

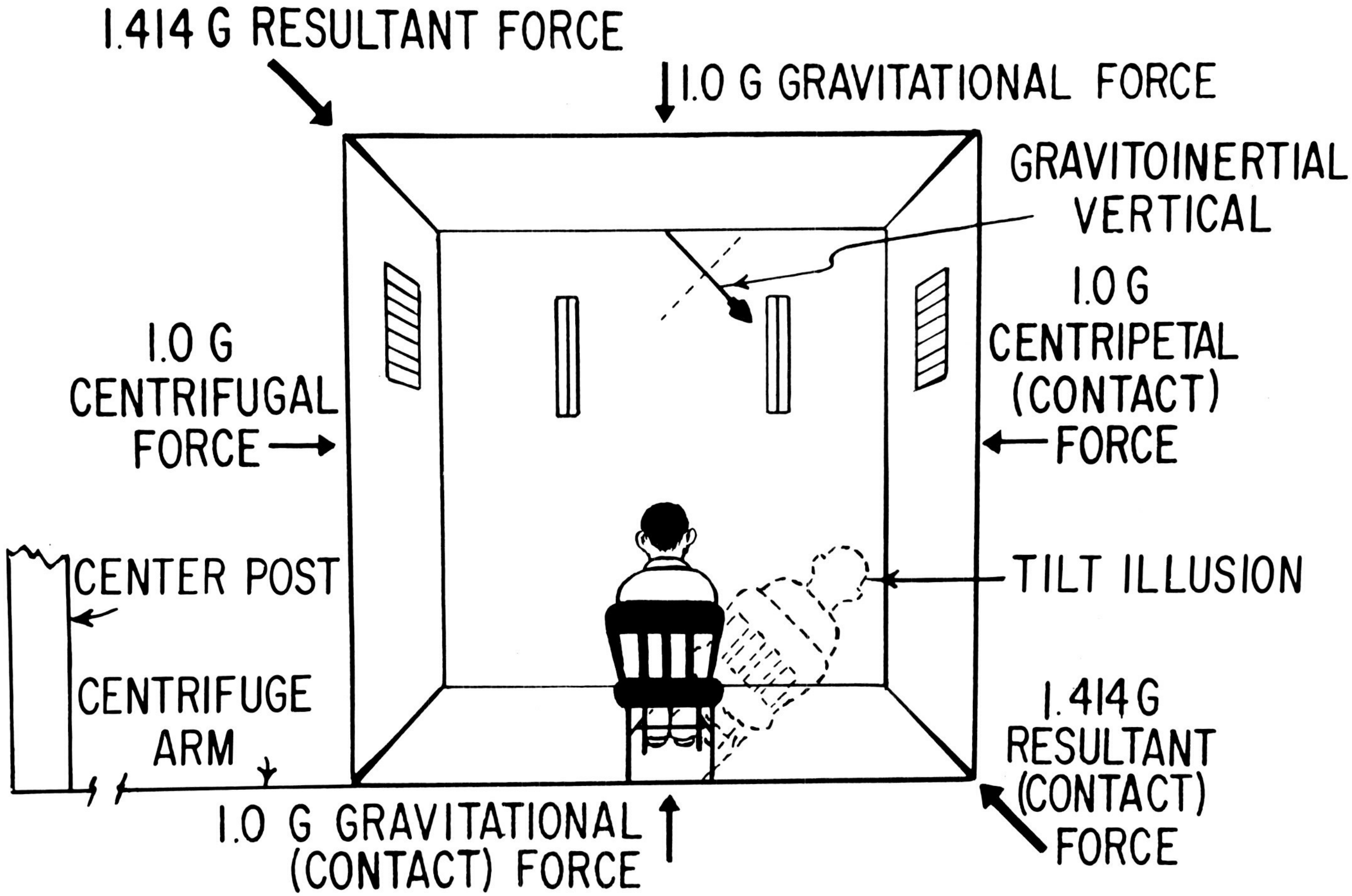

Figure 8-1.- Egocentric visual localization of the horizontal in response to and in accord with the direction of the acting gravitational or gravitoinertial force. The normal subject seated upright under one-g conditions accurately localizes the visual horizontal even in the absence of empirical visual cues. When an inertial force - for example, a centrigugal force of one g - is added to the existing one-g gravitational force, the normal subject feels tilted approximately 45° to his right, and he sets the line target (dotted line) at approximately right angles with the resultant force in order for the target to appear horizontal.

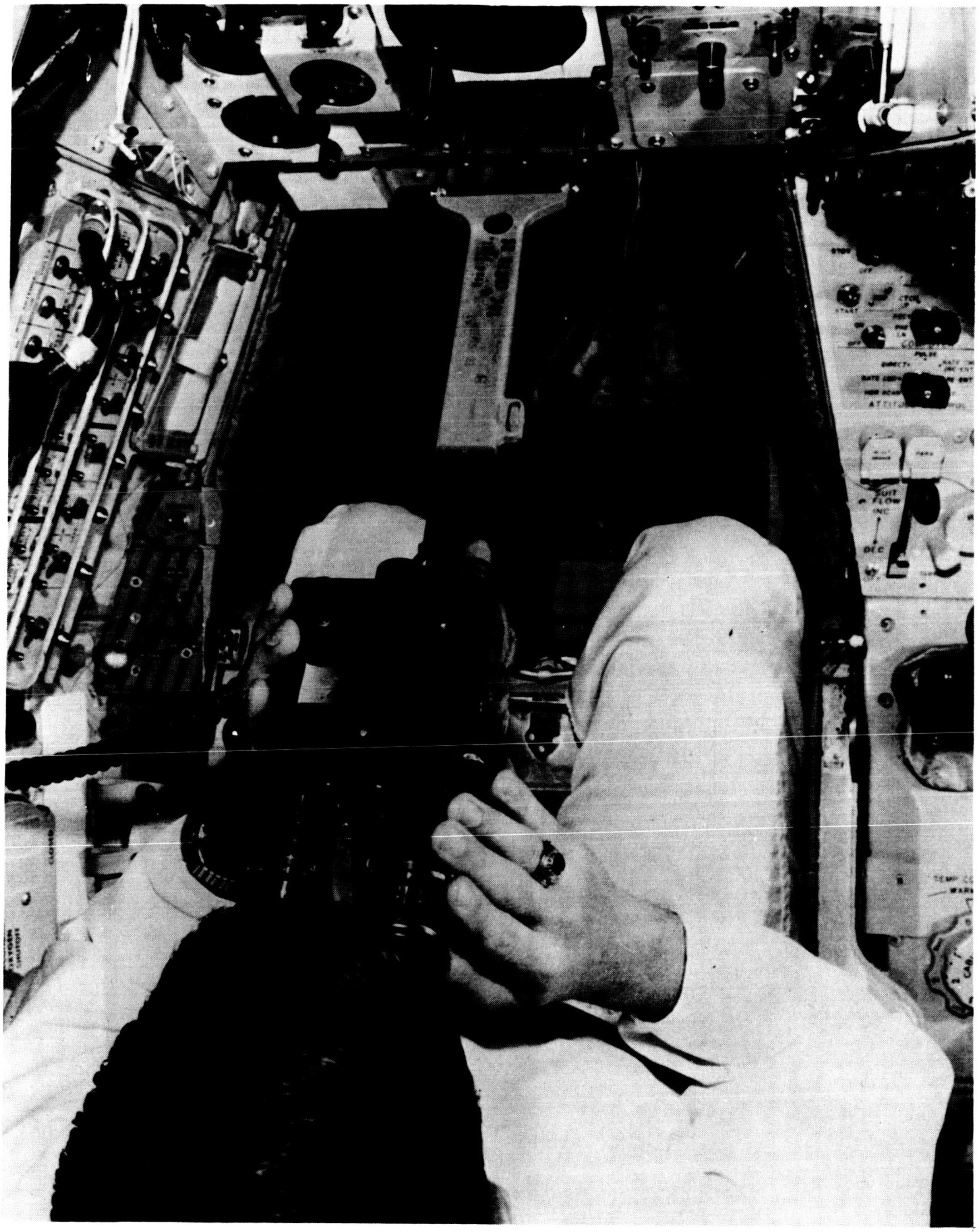

Figure 8-2.- Subject using the vision tester within the spacecraft. The head brace connecting the vision tester to the instrument panel was not used on the Gemini V flight.

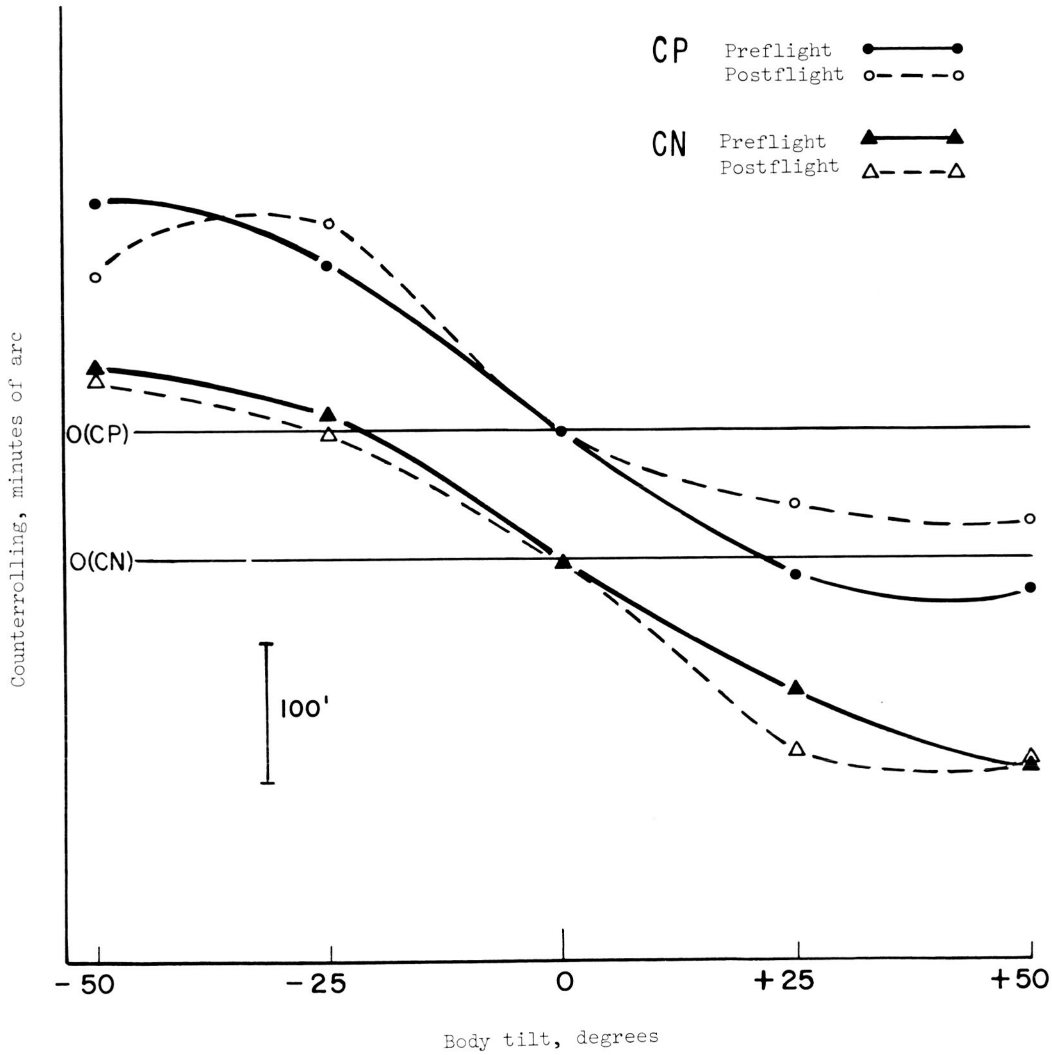

Figure 8-3.- Mean counterrolling (CR) response of each pilot (subject tilted up to ±50°) measured prior to the flight and several hours after recovery. For easier reading, the empirical data points and resultant curves were separated by vertically displacing the zero CR level between subjects.

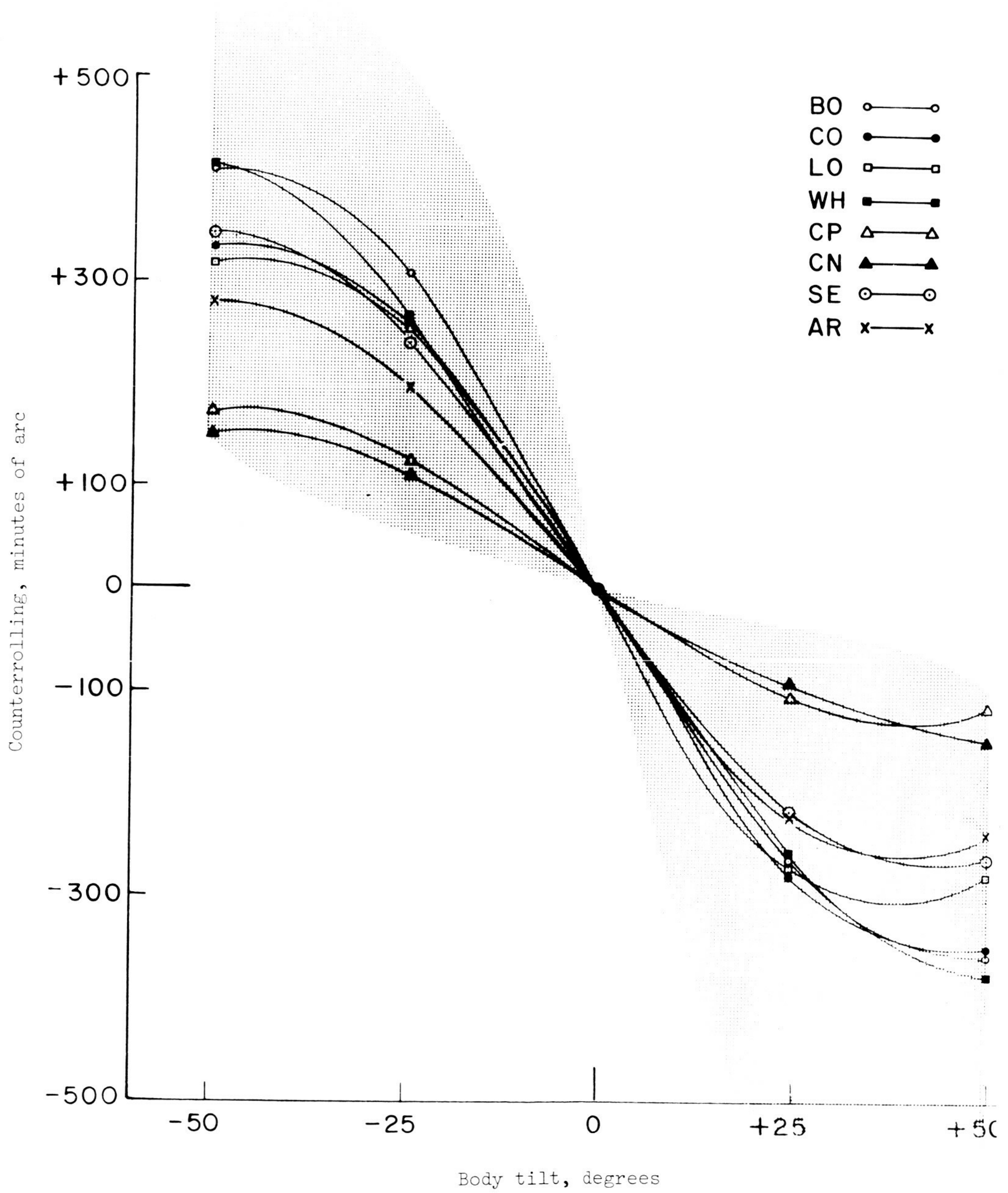

Figure 8-4.- Counterrolling response curves of the Gemini V pilots (CN, CP) compared with those of six other Gemini astronauts and the range of response among a randomly selected group of 100 normal subjects (shaded area).

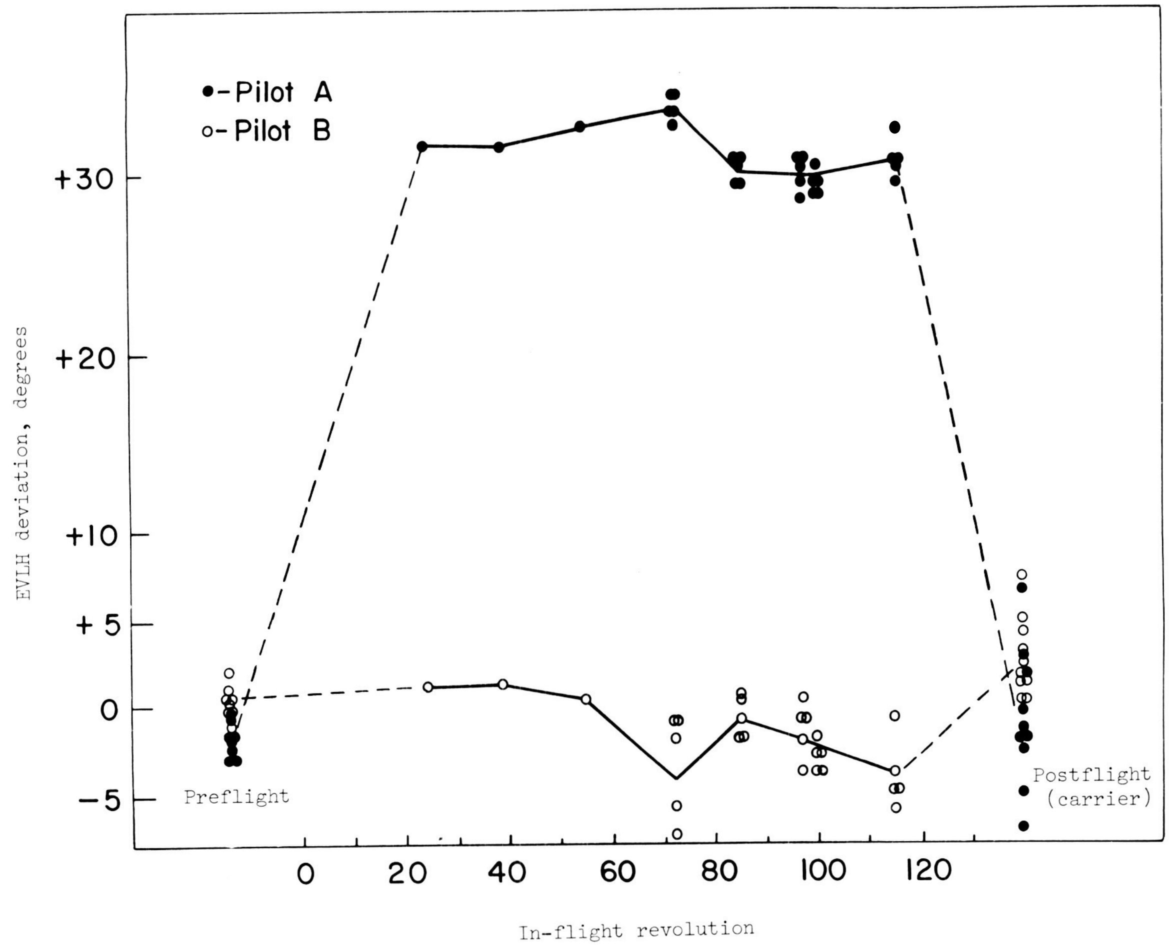

Figure 8-5.- Deviation of individual settings (closed circles, pilot A; open circles, pilot B) of EVLH from the instrument's absolute zero as recorded preflight and postflight. The postflight test was conducted onboard the recovery carrier.

9. EXPERIMENT D4/D7, CELESTIAL RADIOMETRY AND SPACE-OBJECT RADIOMETRY

By Major B. Brentnall
Air Force Systems Command Field Office

SUMMARY

The study of the spectral irradiance of natural phenomena and man-made objects has been of increasing interest in recent years both to the scientific community and to the Department of Defense. The purpose of the Air Force D4/D7 Experiment has been to obtain accurate measurements from space of emitted and reflected radiance from a comprehensive collection of subjects. The determination of threshold sensitivity values in absolute numbers, and the separation and correlation of specific targets with various backgrounds have been prime objectives.

This report is intended to provide a description of the equipment used on Gemini V, its operation, and a discussion of the measurements made. Results will be discussed generally on a quantitative basis.

EXPERIMENT DESCRIPTION

There were two interferometer spectrometers and a three-channel spectroradiometer used as the sensing instruments in this experiment. The selection of the instruments and of the particular detectors in the instruments was based upon the spectral bands to be investigated (fig. 9-1) and the nature of the intended measurements. The instrument characteristics (field of view and resolution, for example) were a compromise among optimization for a particular type of measurement, a need for a broad selection of spectral information, and the performance and other influencing characteristics of the spacecraft.

Since the D4/D7 experiment is contained in several units, the equipment will be reviewed first by component and then integrally as an experimental system aboard Gemini V. After the system has been defined, operational aspects will be discussed.

D4/D7 FLIGHT EQUIPMENT

Radiometer

One of the three measuring instruments used in this experiment was a tri-channel, dc spectroradiometer. In this radiometer (fig. 9-2), the impinging energy is focused by the collecting optics, mechanically chopped, filtered to obtain specific bands of interest, and then received by the three detectors. The detector signals are then amplified and demodulated. The resultant signals are a function of energy intensity in a given spectral band.

The D4/D7 radiometer (fig. 9-3), was made by Block Engineering Associates, Cambridge, Mass. The radiometer instrument parameters are set forth in table 9-I.

Table 9-I.- RADIOMETER INSTRUMENT PARAMETERS

Weight	17.5 lb		
Power input	14 watts		
Field of view	2°		
Optics	4 in. Cassegrain		
Detectors	Photomultiplier tube (IP 28)	PbS	Bolometer
Spectral band, μ	0.2-0.6	1.0-3.0	4-15
Nominal filter width, μ	0.03	0.1	0.3
Filters used, μ	.22 .24 .26 .28 .30 .35 .40 .50 .60	1.053 1.242 1.380 1.555 1.870 2.200 2.820	4.30 4.45 6.00 8.0 9.6 15.0
Dynamic range	10^5 in 4 discrete steps	10^3 log compressed	10^3 log compressed

A total of thirteen signals was provided from the radiometer. The signals included detector temperatures, gain, filter wheel position, and analog signal output from the detectors.

Interferometer Spectrometer

The second sensing instrument is a dual-channel interferometer spectrometer (fig. 9-4). The interferometer section is patterned after the Michelson interferometer (fig. 9-5).

The beam splitter splits the optical path, sending part of the beam to the movable mirror M_1 and the other part to a fixed mirror M_2. As a result of the optical path changeability, the waves returning from the mirrors may be in phase (additive) or may be out of phase to some degree and have a canceling effect. The total effect is to produce cyclic reinforcement or interference with the wave amplitude at the detector at any given frequency. The frequency at the detector of this alternate cancellation and reinforcement is a function of the particular spectral energy wave length λ, the optical retardation B of the mirror, and the time it takes to move the mirror (scan time) T. Thus $F_\lambda = \frac{B}{\lambda T}$.

The detector puts out an ac signal which is the sum of the ac signals corresponding to all the wavelengths from the source. The amplitudes of the signals will vary directly with the source brightness at each wavelength. The output of the interferometer is then a complex waveform called an interferogram which is the Fourier transform of the incident radiation frequencies (fig. 9-6(a)). This transform is reduced to a plot of wavelength versus intensity by taking the inverse transform of the interferogram (fig. 9-6(b)). An interferogram made with the D4/D7 instrument is shown in figure 9-6(c) and an actual measurement on the California coast shown in figure 9-6(d).

The D4/D7 interferometer spectrometer discussed here (and referred to non-technically as the "uncooled" or "IR" Spectrometer) contained a lead sulfide detector and a bolometer detector, thus providing correlative information to that of two of the channels of the spectroradiometer. This, too, was a Block Engineering instrument. Its parameters are as follows:

TABLE 9-II.- PARAMETERS OF THE IR SPECTROMETER

Weight	18.5 lb	
Power input	8 watts	
Field of view	2°	
Optics	4 in. Cassegrain	
Detectors	PbS	Bolometer
Spectral band, μ	1-3	3-15
Dynamic range	10^3 auto gain changing	10^3 auto gain changing

Data output from the instrument included the signals from the two detectors, gain settings, detector temperatures, and automatic calibration source data. PbS signal data were handled on a data channel-sharing basis with the detector output from the cryogenic spectrometer.

Cryogenic Interferometer Spectrometer

The cryogenic interferometer spectrometer is similar in operation to the IR Spectrometer, although dissimilar in appearance (fig. 9-7). The principal difference is that the highly sensitive detector must be cryogenically cooled to make measurements in the region of interest, 8 to 12 microns. The cooling is accomplished by immersing a well containing the detector, optics, and some of the electronics in liquid neon.

The cryogenic subsystem was made for Block Engineering by AiResearch Division of Garrett Corporation. It was an open cycle, sub-critical, cryogenic cooling system which maintained the instrument well at a temperature of -397° F for a period of approximately 15 hours. Figure 9-8 shows an X-ray view of the cryogenic tank and instrument well. The parameters for the instrument are as follows:

TABLE 9-III.- PARAMETERS OF THE CRYOGENIC INTERFEROMETER SPECTROMETER

Weight (with neon)	33.5 lb
Power input	6 watts
Field of view	2°
Optics	4 in. Cassegrain
Detector	Hg doped Ge
Spectral band	8-12 microns
Dynamic range	10^3 automatic gain changing
Coolant	liquid neon

Electronics Unit

The electronics unit (fig. 9-9, interior view) was used in conjunction with the three sensing devices. The unit contained various electronic circuits necessary to the experiment. The circuitry includes an electronic commutator, filter motor logic, variable control oscillators, mixer amplifier, clock pulse generator, and other secondary electronic circuitry.

Recorder Transport and Electronics

The D4/D7 experiment tape recorder was separated into two modules, the tape transport and the recorder electronics. This was done so that the recorder would fit into the available space on the Gemini reentry vehicle (fig. 9-10). The recorder provided 56 minutes of tape for three channels of data. It was not capable of dump, so data were stored and retrieved with the spacecraft.

FM Transmitter and Antenna

In parallel with the recorder, the D4/D7 transmitter provided three channels of real-time FM data to selected ground stations located around the earth. The transmitter, operating through an antenna extended from the pilot's side of the spacecraft, transmitted 2 watts on an assigned UHF frequency. Figure 9-11 shows the spacecraft electronics module with the transmitter, the electronics unit, and the antenna.

Control Panel

The majority of the switches associated with the experiment was located on the pilot's main console (fig. 9-12). Additional functions were provided by a meter and some sequencing switches.

D4/D7 Experiment System

The experiment system comprised of the foregoing components was mounted in Gemini V (fig. 9-13). The radiometer and spectrometers were mounted in the Gemini retro adapter section on swingout arms (fig. 9-14). After Gemini V was in orbit, doors in the adapter were pyrotechnically opened, and the three sensing units swung through the openings into boresight alinement with the spacecraft optical sight. After the sensing units had been erected, the spacecraft was then pointed at the desired area for measurement. Figure 9-15 shows the Gemini VII with the instruments extended. Gemini V was similar in appearance.

The data from the radiometer were telemetered through the spacecraft PCM system. The data from the spectrometers were telemetered through the transmitter, to the recorder, or a combination of both, as desired.

D4/D7 MISSION PLAN

The desired objectives for the D4/D7 measurements included the following:

Earth backgrounds	0.2 to 12 microns
Sky backgrounds	.2 to 12 microns
Rocket exhaust plumes	.2 to 3 microns
Natural space phenomena (stars, moon, sun)	.2 to 8 microns
Artificial satellites	.2 to 12 microns
Weather phenomena (clouds, storms, lightning)	.2 to 10 microns
Equatorial horizon spectral calibrations	8 to 10 microns

Since lifetime of the cryogenic neon in the cooled spectrometer was limited to 15 hours, of which 5 would be spent on the launch pad, the measurements requiring the use of the cooled spectrometer were planned for the first few revolutions. The rocket-plume measurements were planned for those revolutions which brought the spacecraft closest to the firing site, yet as early in the day as feasible to minimize background radiation. The sun measurement was planned to be the final measurement, since calibration of the detectors might be affected. The remainder of the measurements, requiring real-time updating, were interspersed throughout the flight.

RESULTS

Approximately 3 hours and 10 minutes of D4/D7 data were gathered during the Gemini V flight. Twenty-one separate measurements were made, covering thirty designated subjects. The PCM and FM transmitted data amount to 125 000 feet of magnetic tape.

Data processing is lengthy. The interferometer spectrometer data must be run through a wave analyzer or a high-speed computer. The wave analyzer integrates 35 interferograms and gives the results in the form of Fourier coefficients in about 30 minutes. The computer takes about 2 hours to perform the transform on 1 interferogram. Over 10 000 interferograms were made during the Gemini V flight.

The PCM data are reduced in terms of filter settings and gain; then, calibration coefficients are applied. Both PCM and FM data are correlated with astronaut comments and photography, where applicable.

From the foregoing, the magnitude of the data-reduction task can be seen. The data from D4/D7 on Gemini V are still in the process of reduction and, at the present time, are not available in sufficient amounts to report on qualitatively to any significant extent.

The following is a list of the D4/D7 measurements made during the Gemini V flight:

Rev	Location	Measurement
1	Canarvon, Australia	Operational readiness check of cryogenic spectrometer
2	Africa-Australia	REP measurements during darkness
14	Australia	Night water and night land measurements

Rev	Location	Measurement
16	Africa	Mountains and land with vegetation
16	Madagascar	Night land, water
16	Australia	Star measurement, Vega
16	Australia	Equipment alinement check
17	Australia	Moon irradiance measurement
31	Africa	Cloud blanket sweep, nadir to horizon
31/32	Florida	Land with vegetation
45	Australia	Night void sky measurement
47	Australia	Zodiacal light
47	Australia	Star measurement, Deneb
47	California	Minuteman missile launch
51	Hawaii	Island measurement
61	New Mexico	Rocket sled firing
62	California	Minuteman missile launch
74	Africa	Water, land, mountains, desert
88	Africa	Desert
89	Africa	Mountains
103	Australia	Horizon to nadir scan

The equipment was erected and operationally verified over Carnarvon, Australia, during the first revolution.

During the second revolution, the rendezvous evaluation pod (REP) was ejected and measurements were made of its separation from the spacecraft during the spacecraft darkness period. The primary instrument for this measurement was the cryogenic spectrometer. The cover on the spectrometer was jettisoned when the REP was approximately 2500 feet away from Gemini V, and measurements were made through the remainder of the darkness period.

After fifteen minutes of operation, the filter wheel on the radiometer ceased working and remained on filter settings of 4000 Ångstroms, 2.2 μ, and 4.3 μ for the remainder of the flight. Since the interferometers still functioned satisfactorily, the restriction in radiometer data was not of major concern. The main loss of data was in the UV region - not covered by the spectrometers - where only the 4000 Å information was available. In playing the onboard D4/D7 recorder after its retrieval, it was discovered that no REP measurement data were recorded on the tape. This limited the information from the cryogenic spectrometer to FM data received during the pass over Canarvon. Review of the interferograms made at Canarvon indicates that the signal was well above the noise level. Reduction is in process, and attempts are being made to separate background signal and spacecraft radiance from the signal of the REP. This task is made more difficult by the lack of data from the onboard recorder.

Due to the date of launch of Gemini V, the moon measurements had to be made on a partially illuminated moon. The radiometer data from this measurement can be seen in figures 9-16(a) and 9-16(b).

Quick-look information on the 4000 Å radiometer data on Vega and Deneb is excellent. The values on that spectrum band were slightly higher than those theoretically predicted; for example, the value for Vega was 1.2×10^{-11} watts/cm^2/μ at 4000 Å.

An example of the IR spectrometer data can be seen in figure 9-17. This shows the return at 1.88 microns on the California land background.

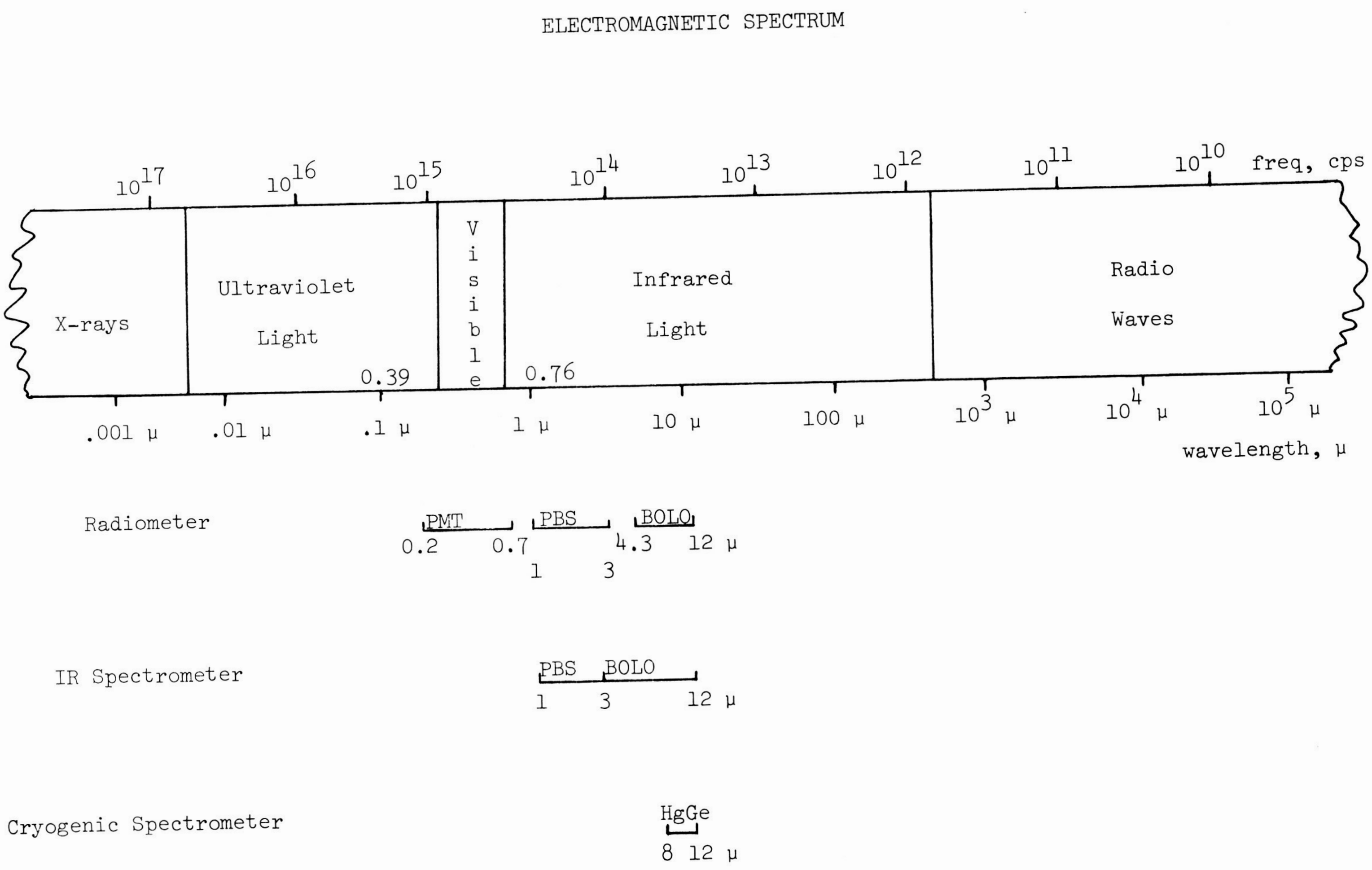

Figure 9-1.- Equipment spectral bands coverage.

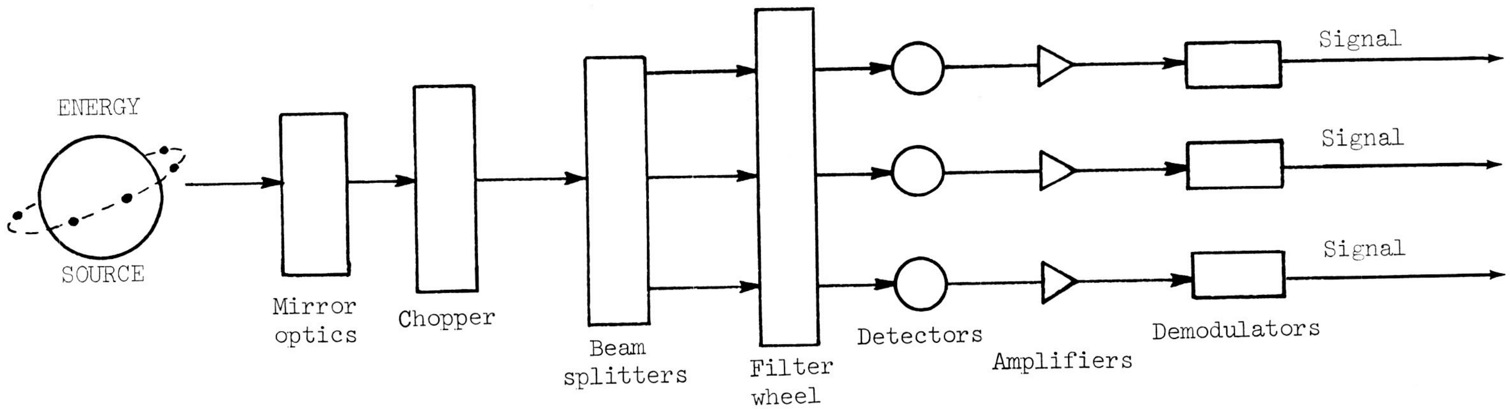

Figure 9-2.- D4/D7 radiometer functional diagram.

NASA
S-65-12328A

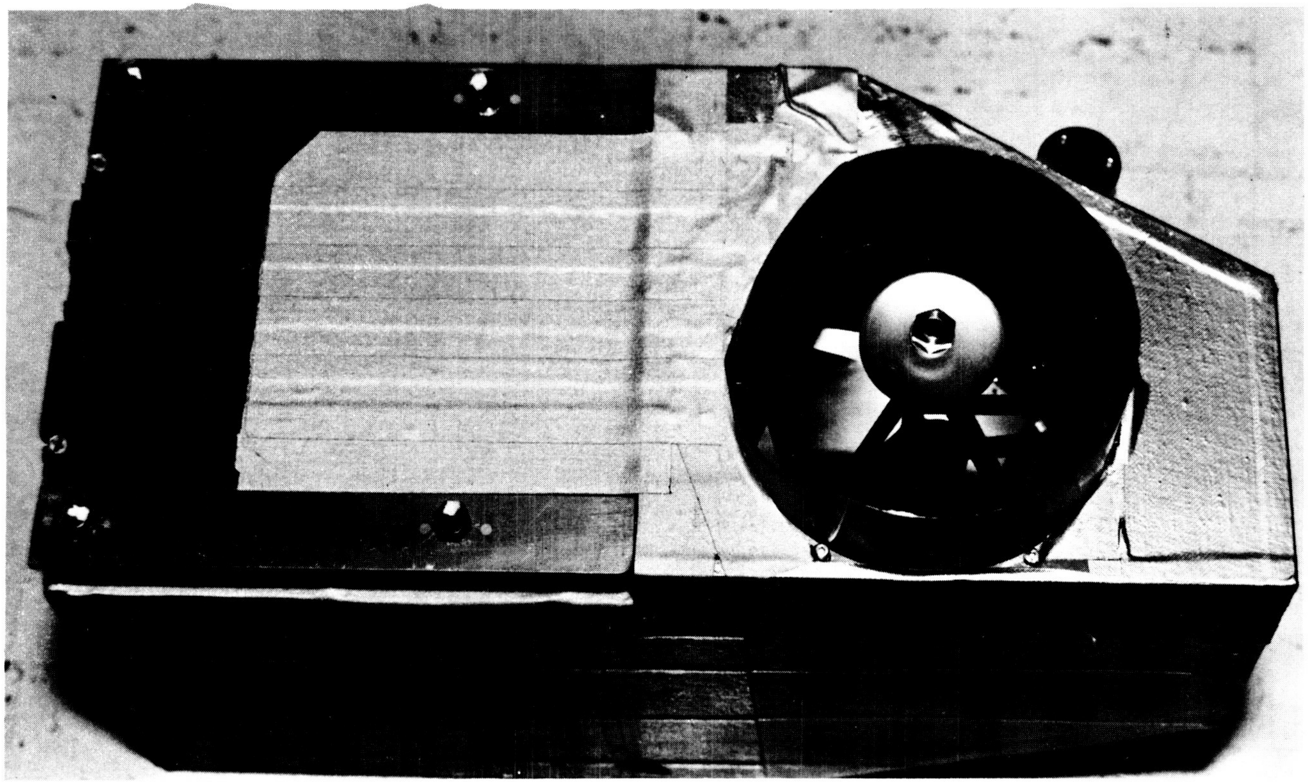

Figure 9-3.- Tri-channel spectroradiometer.

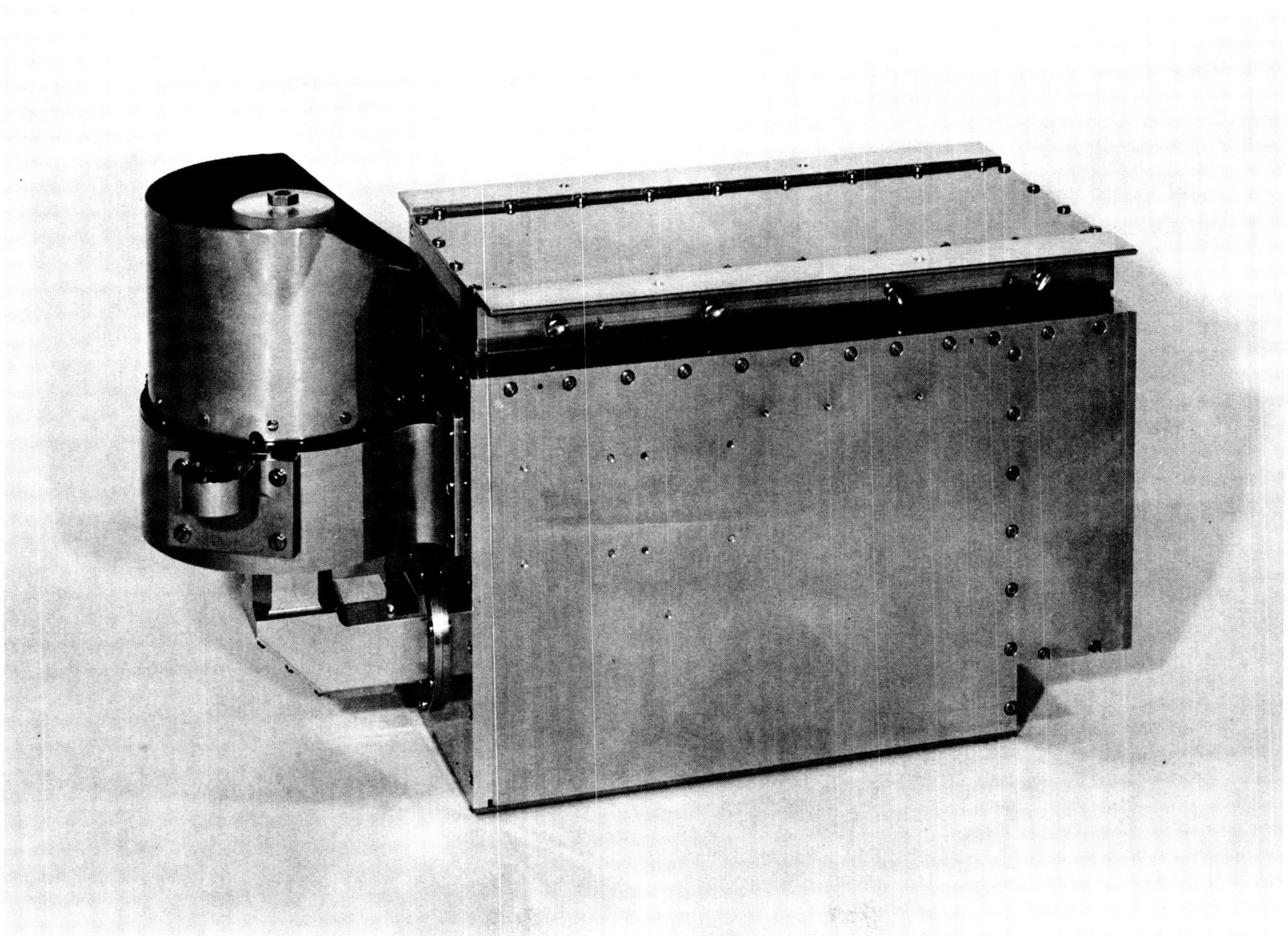

Figure 9-4.- Dual-channel interferometer spectrometer.

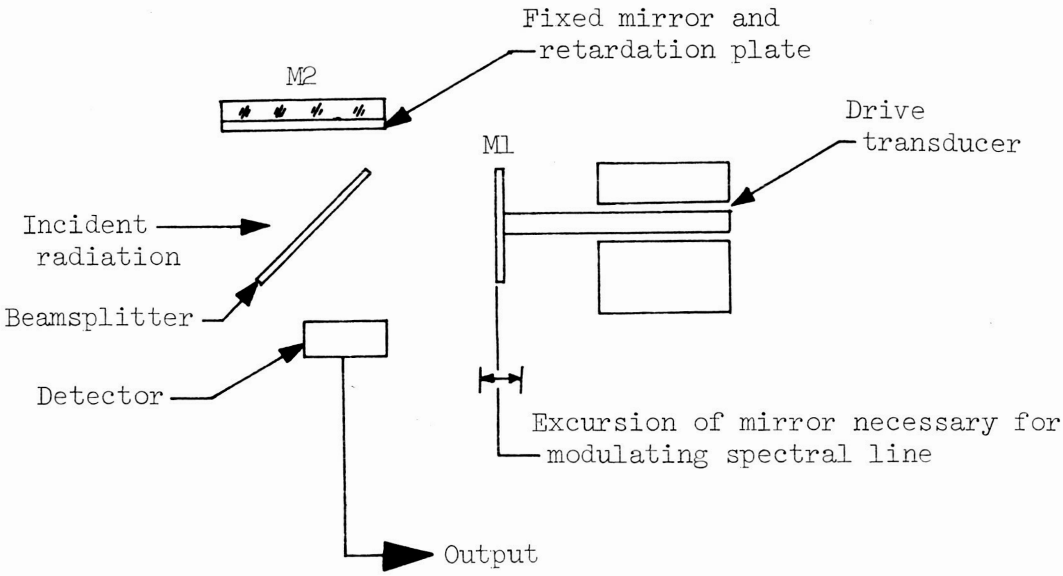

Figure 9-5.- Schematic section of Michelson interferometer.

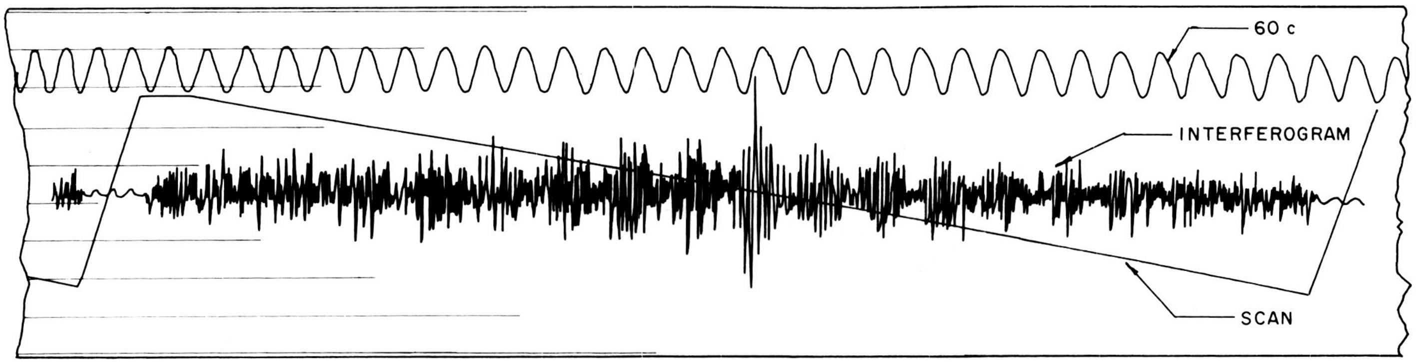

(a) Representation of an interferogram.

Figure 9-6.- Interferometer measurements.

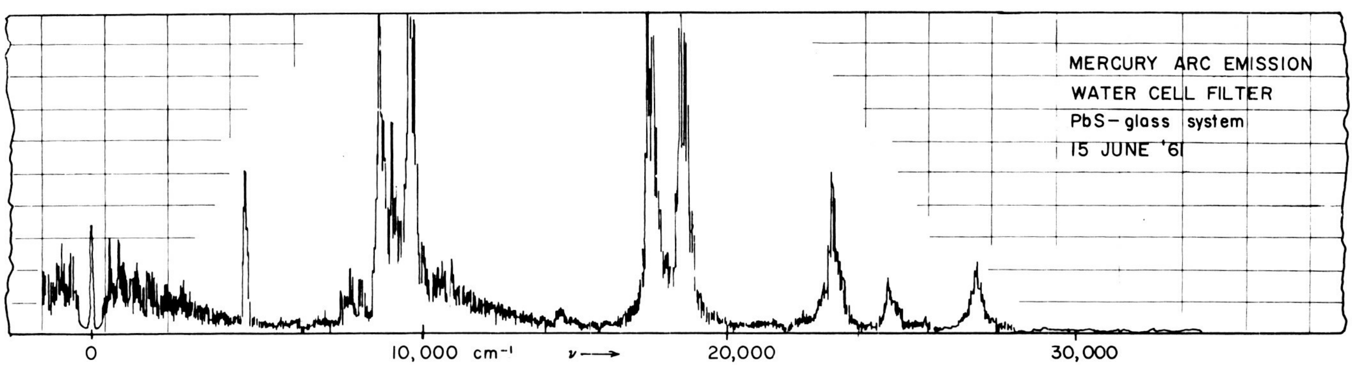

(b) Representation of an interferogram reduced to a spectrum.

Figure 9-6.- Interferometer measurements.

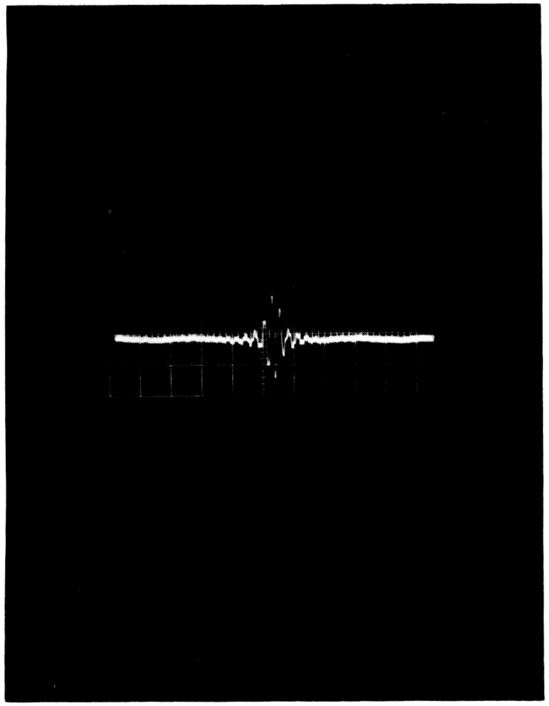

(c) Spectrometer interferogram on a 2100° C calibration source.

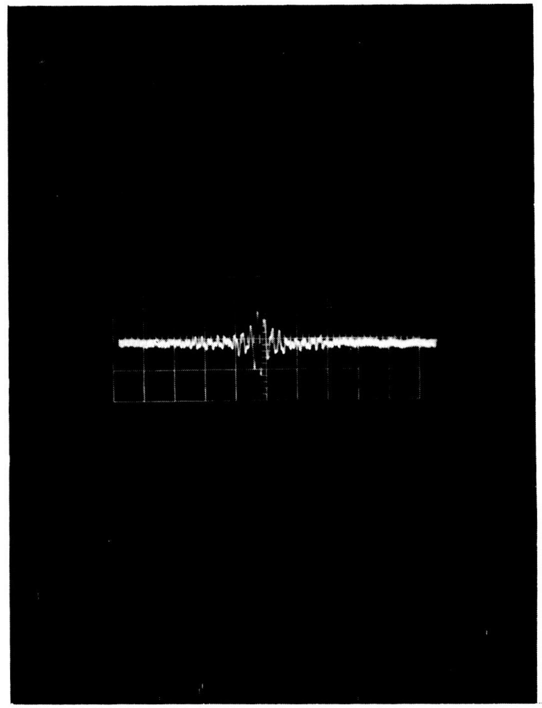

(d) IR spectrometer interferogram during the Gemini V flight (California coastal land).

Figure 9-6.- Interferometer measurements.

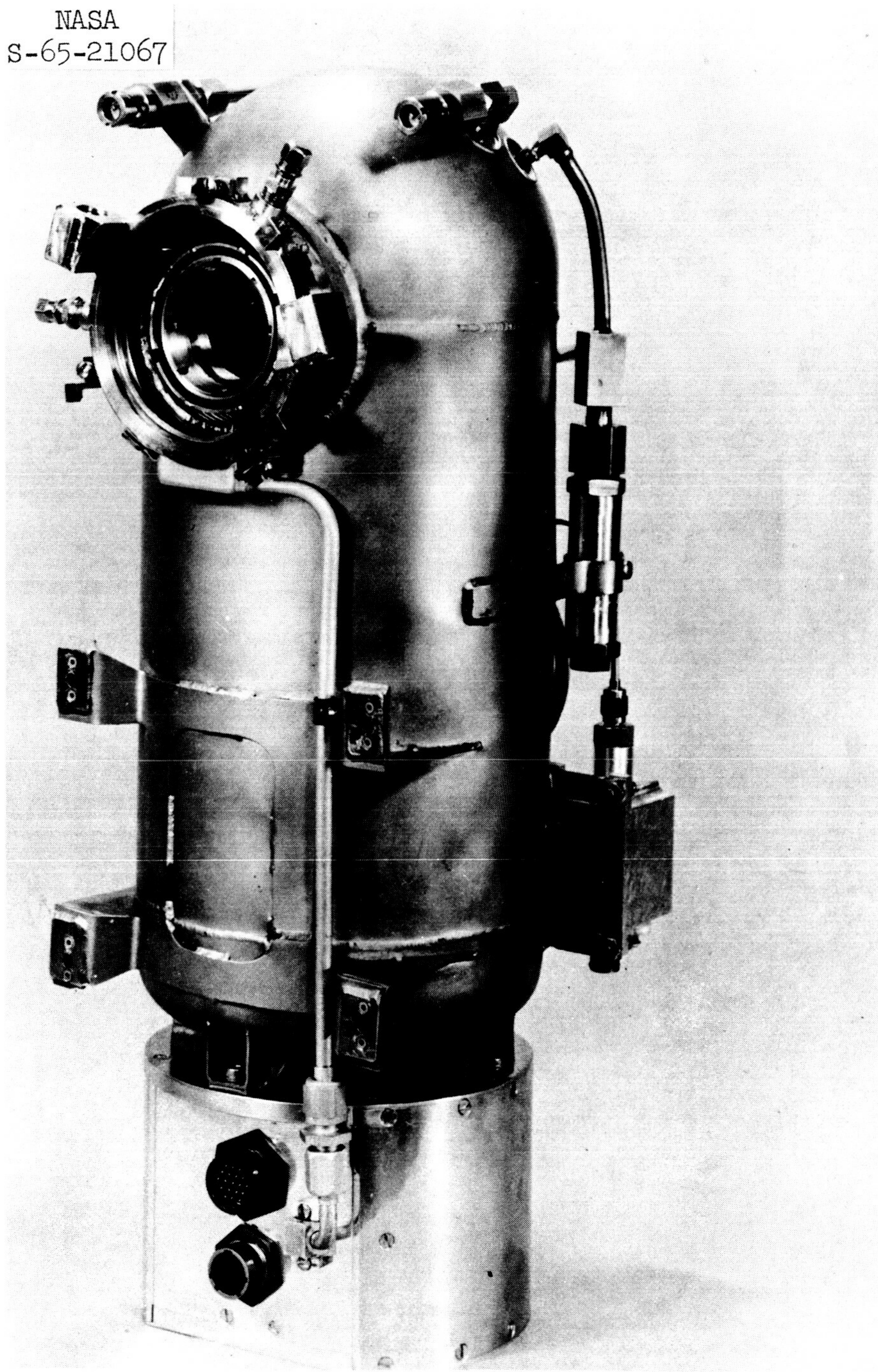

Figure 9-7.- Cryogenic interferometer spectrometer.

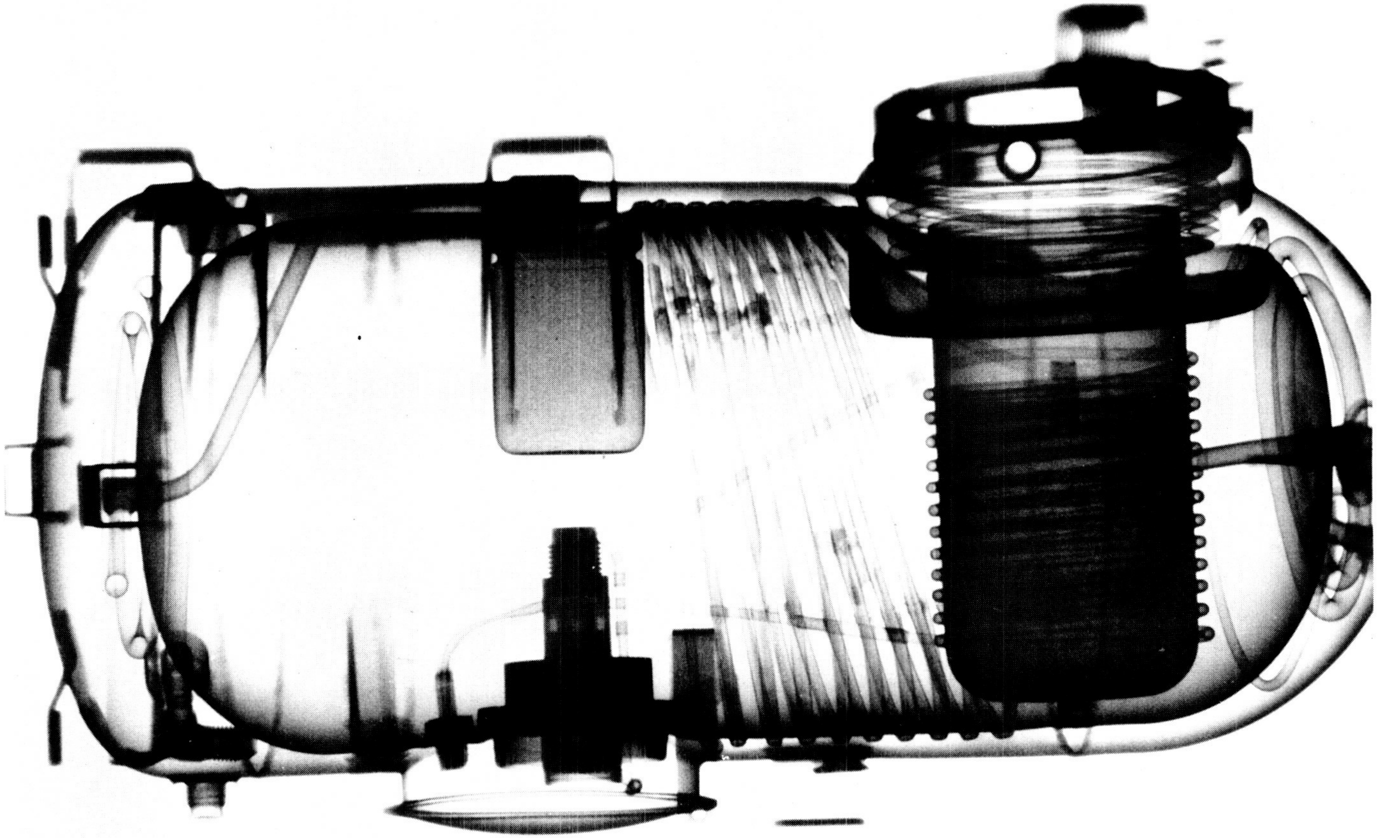

Figure 9-8.- Cryogenic tank and instrument well.

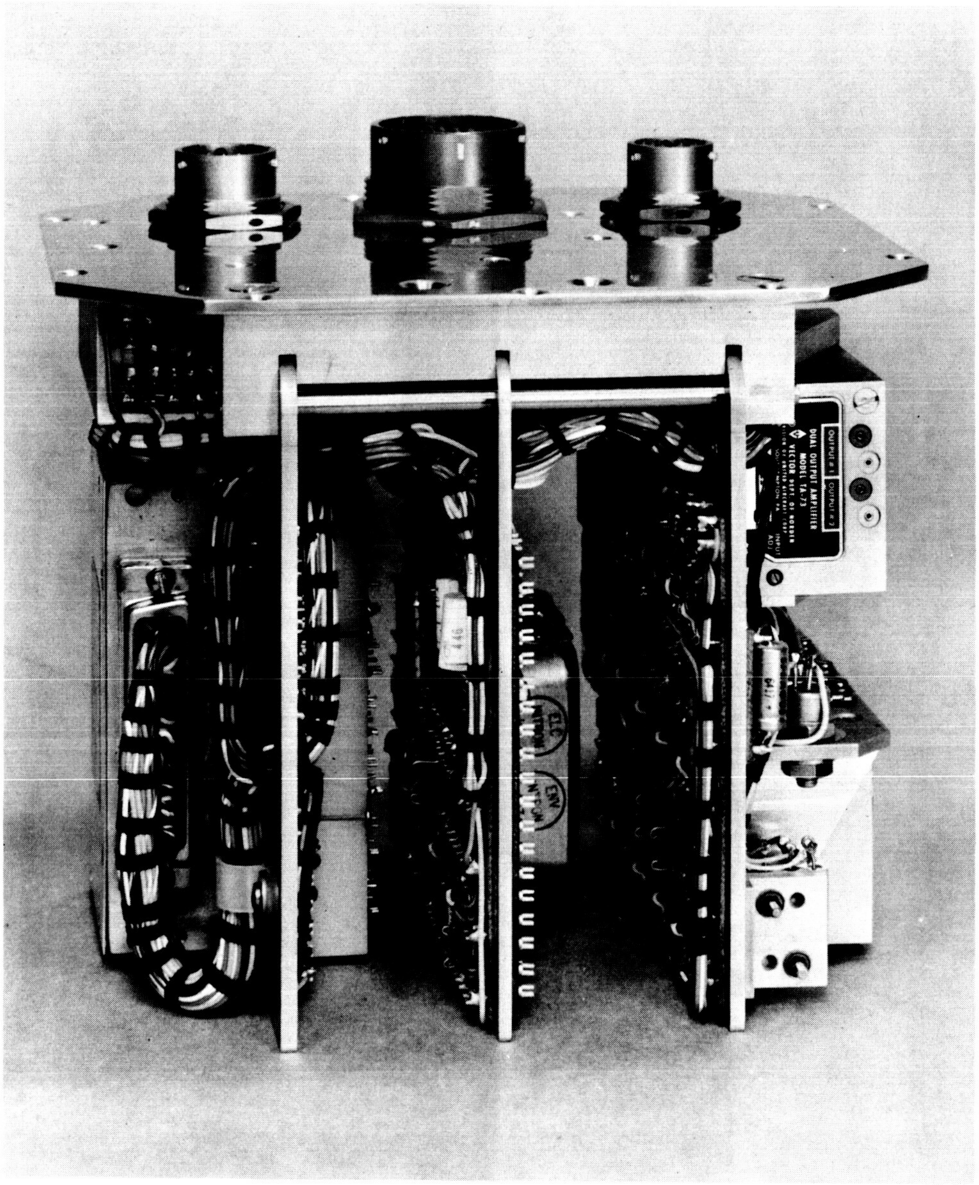

Figure 9-9.- D4/D7 Electronic unit.

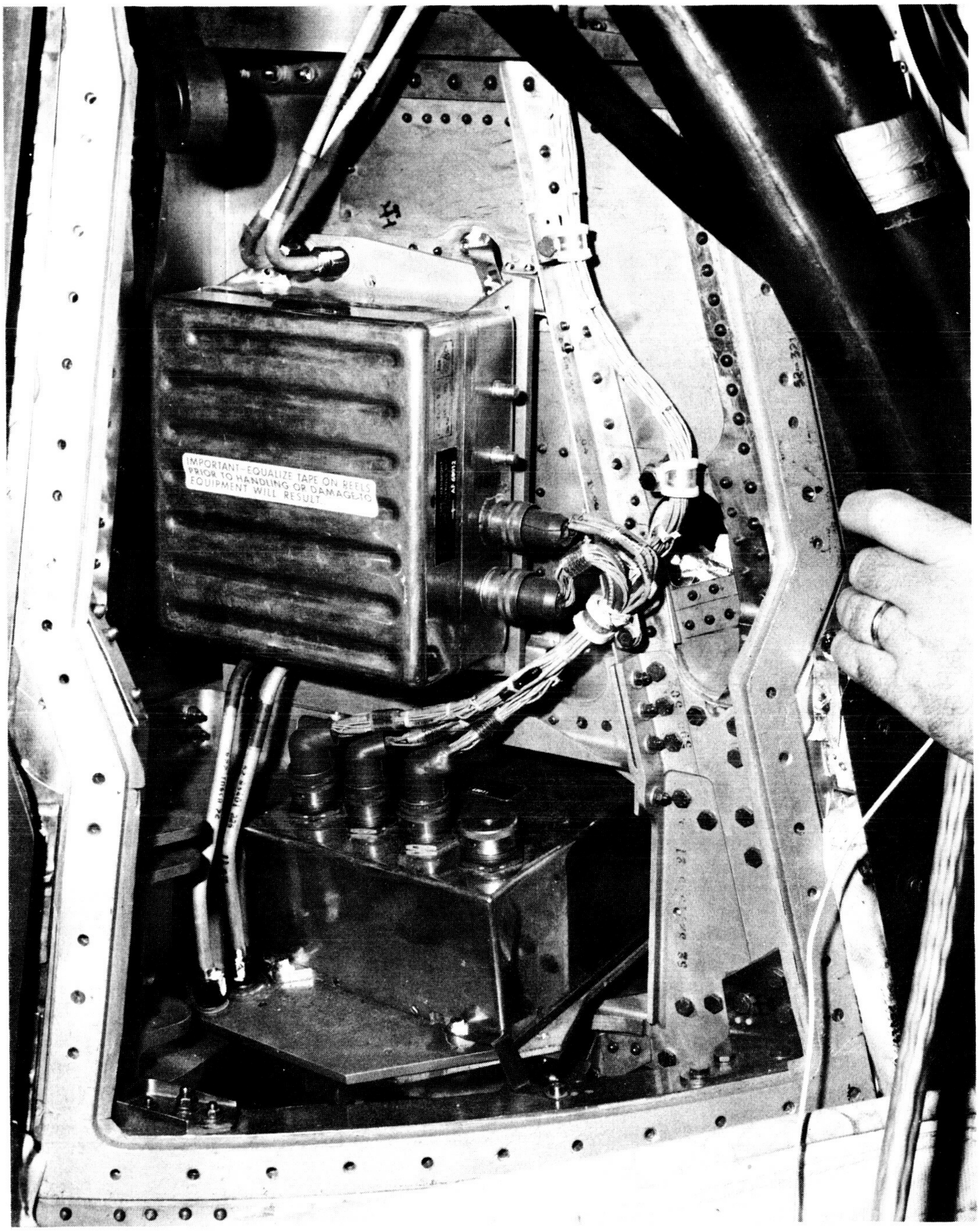

Figure 9-10.- Position of tape transport and recorder electronics on Gemini reentry vehicle.

NASA
S-65-16310

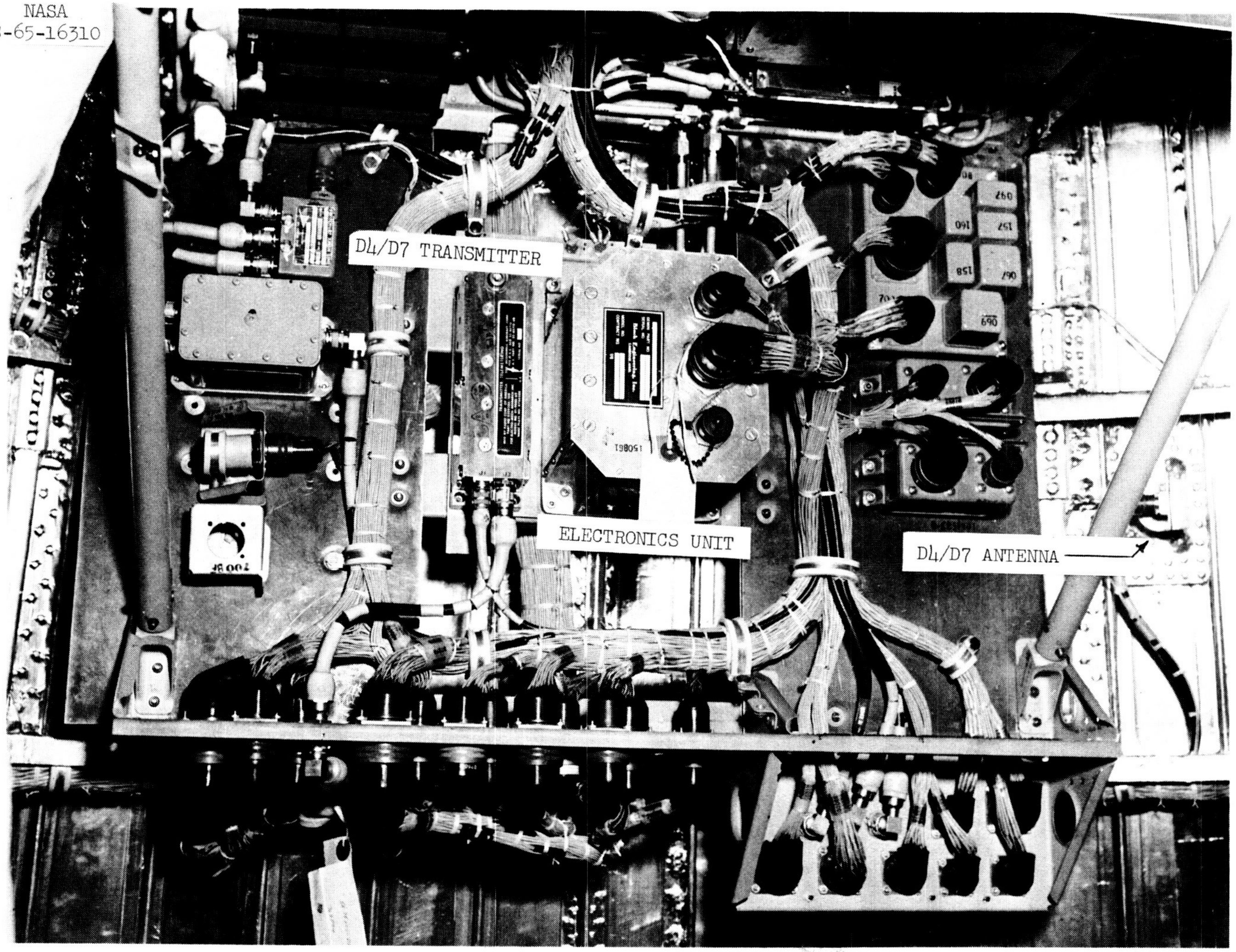

Figure 9-11.- D4/D7 electronics module showing electronics unit, transmitter, and antenna.

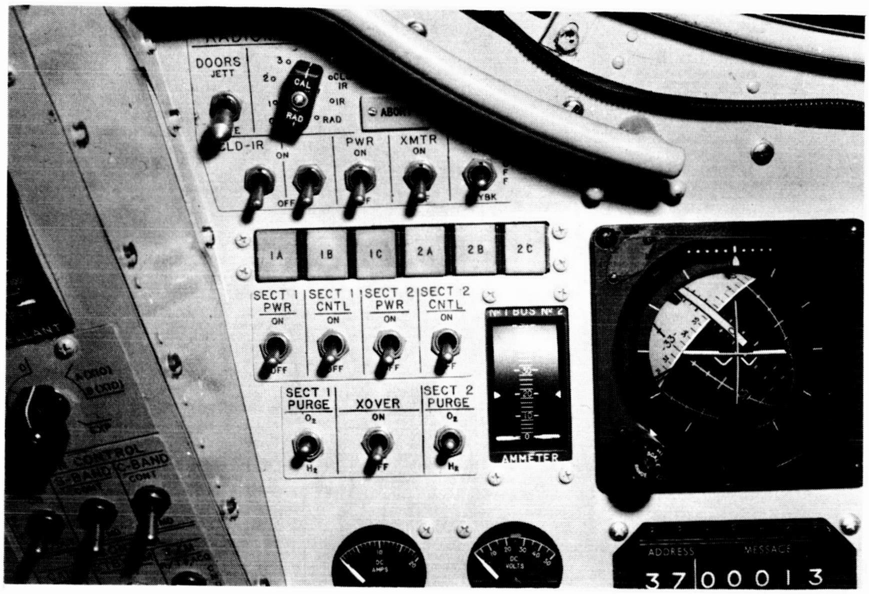

Figure 9-12.- D4/D7 experiment instrument panel.

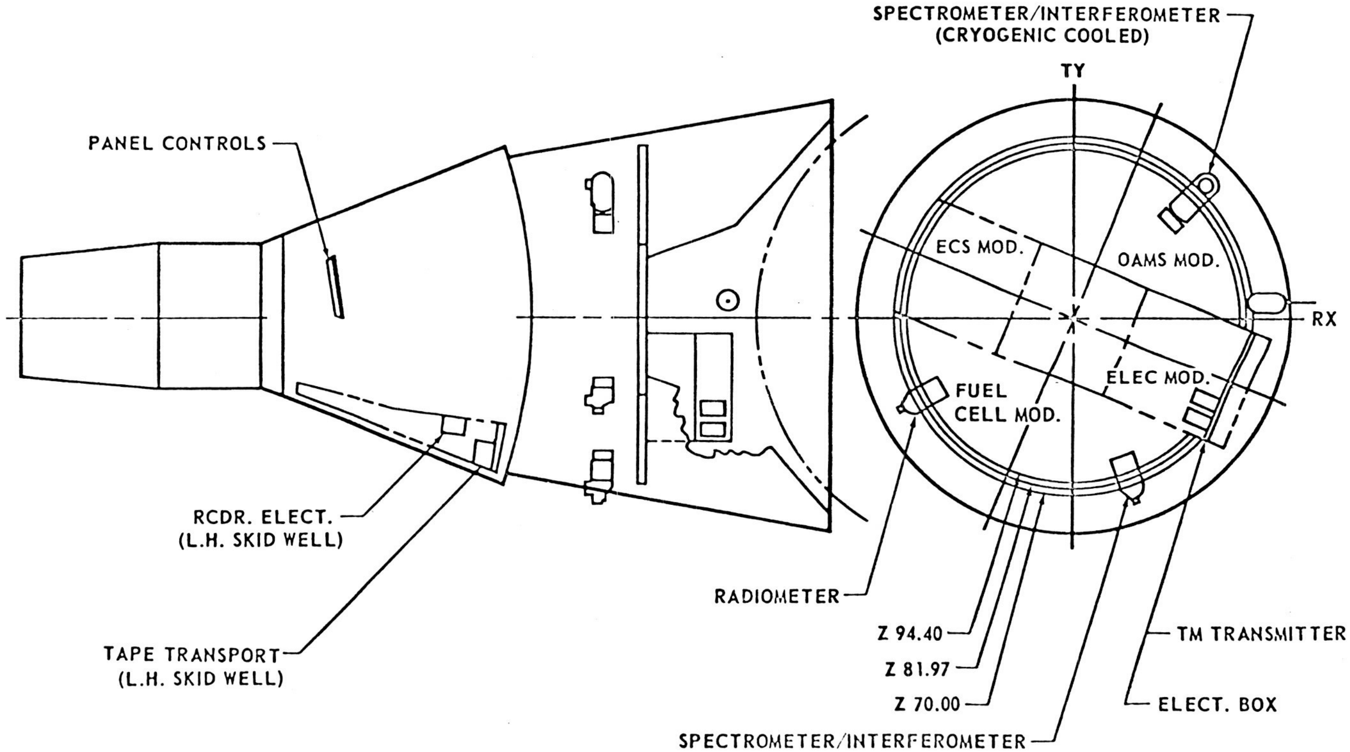

Figure 9-13.- Components and spacecraft position of D4/D7 equipment.

NASA
S-65-16309

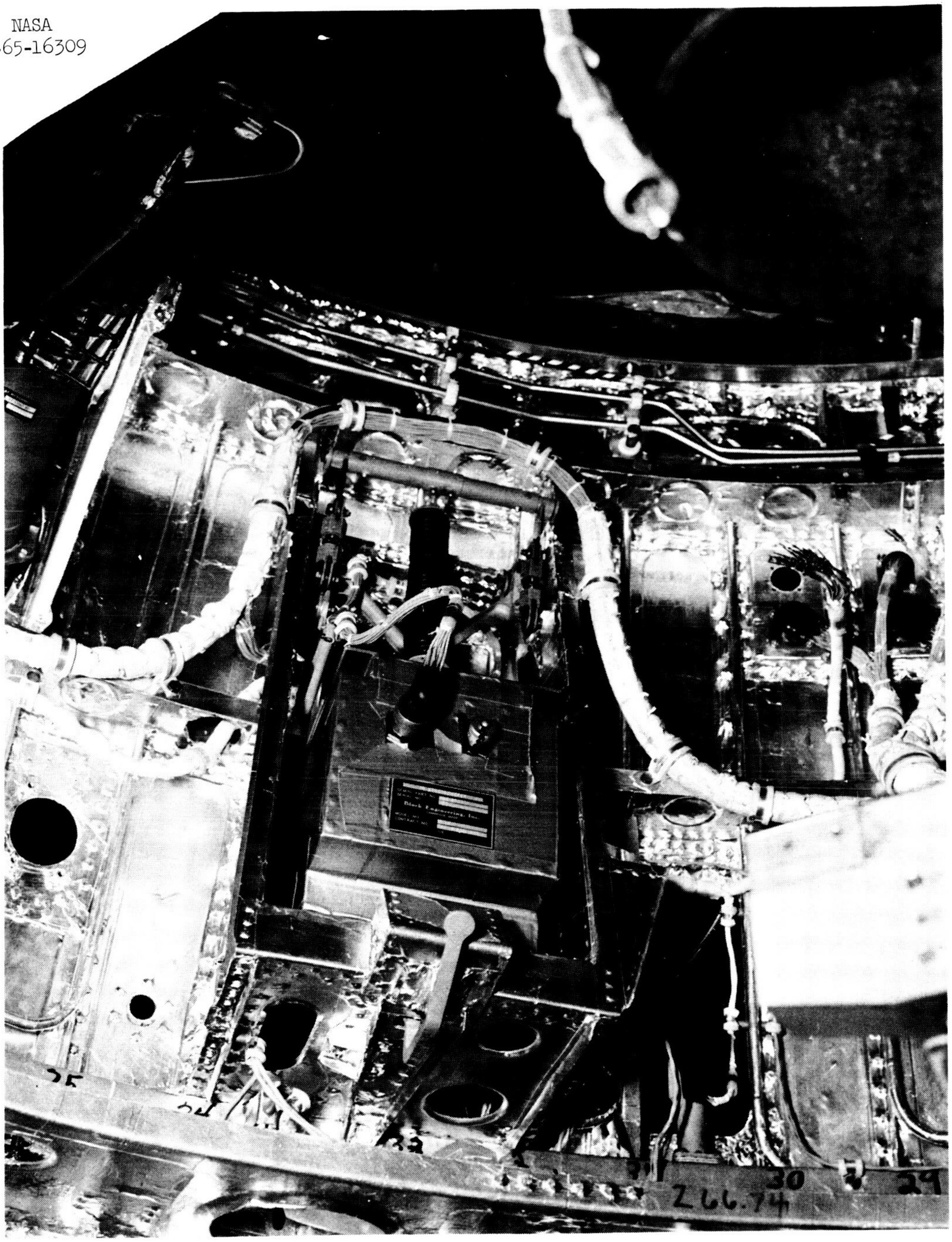

Figure 9-14.- D4/D7 spectrometer and radiometer stowed in retro adapter.

NASA
S-65-12339A

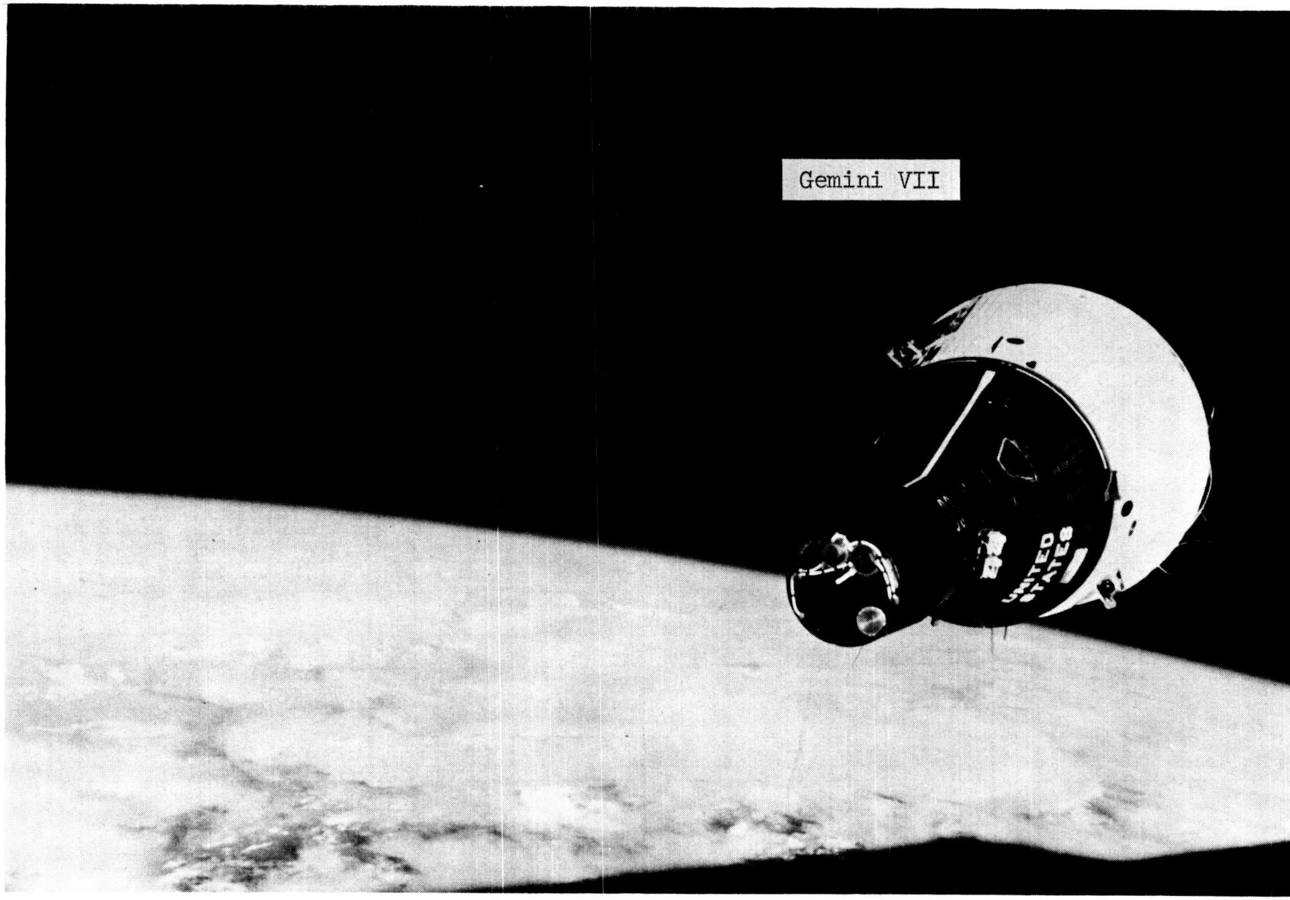

Figure 9-15.- D4/D7 cryogenic spectrometer and radiometer erected.

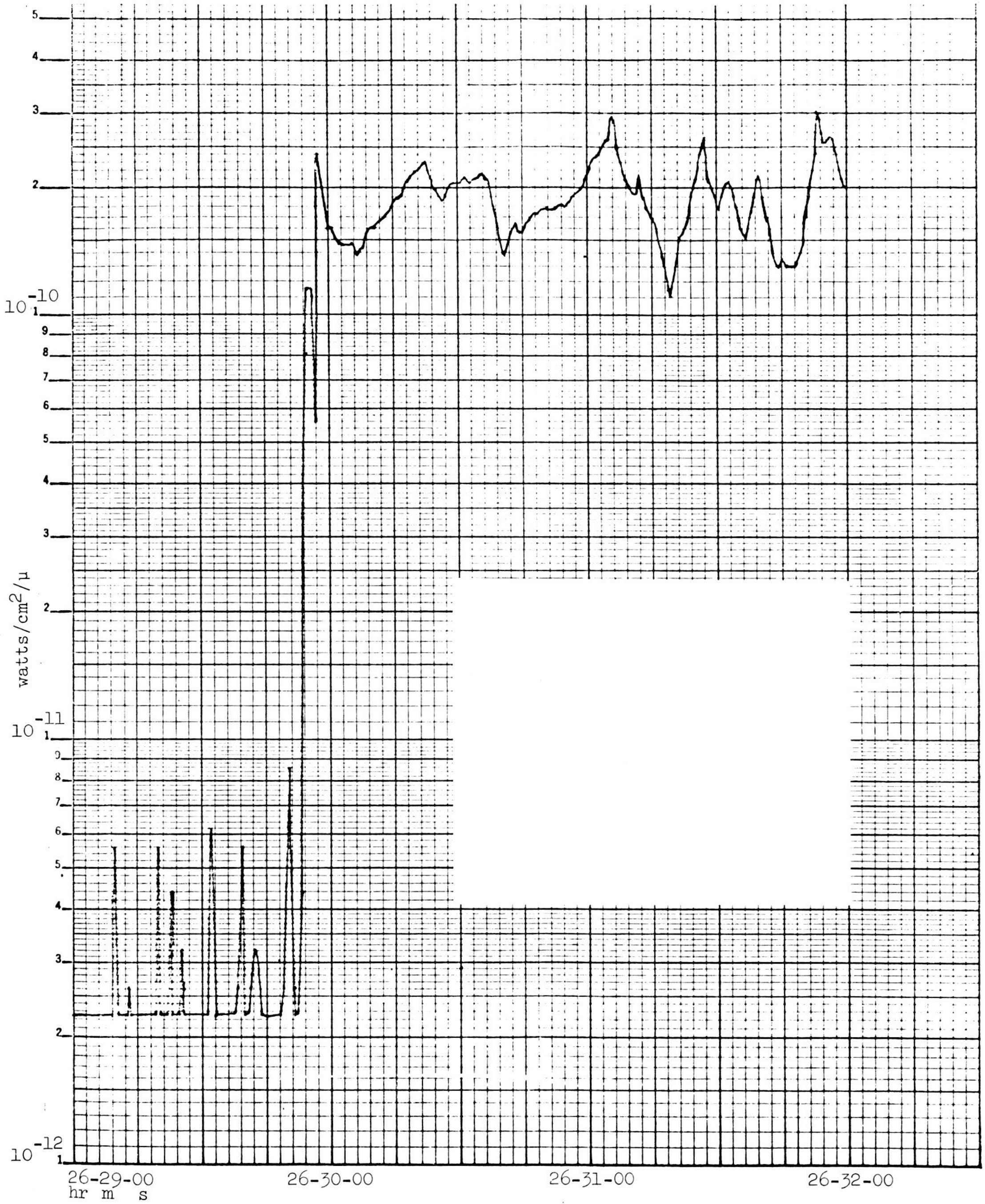

(a) Moon measurements (4000 Å), made on Gemini V, revolution 17.

Figure 9-16.- Radiometer data from moon measurements.

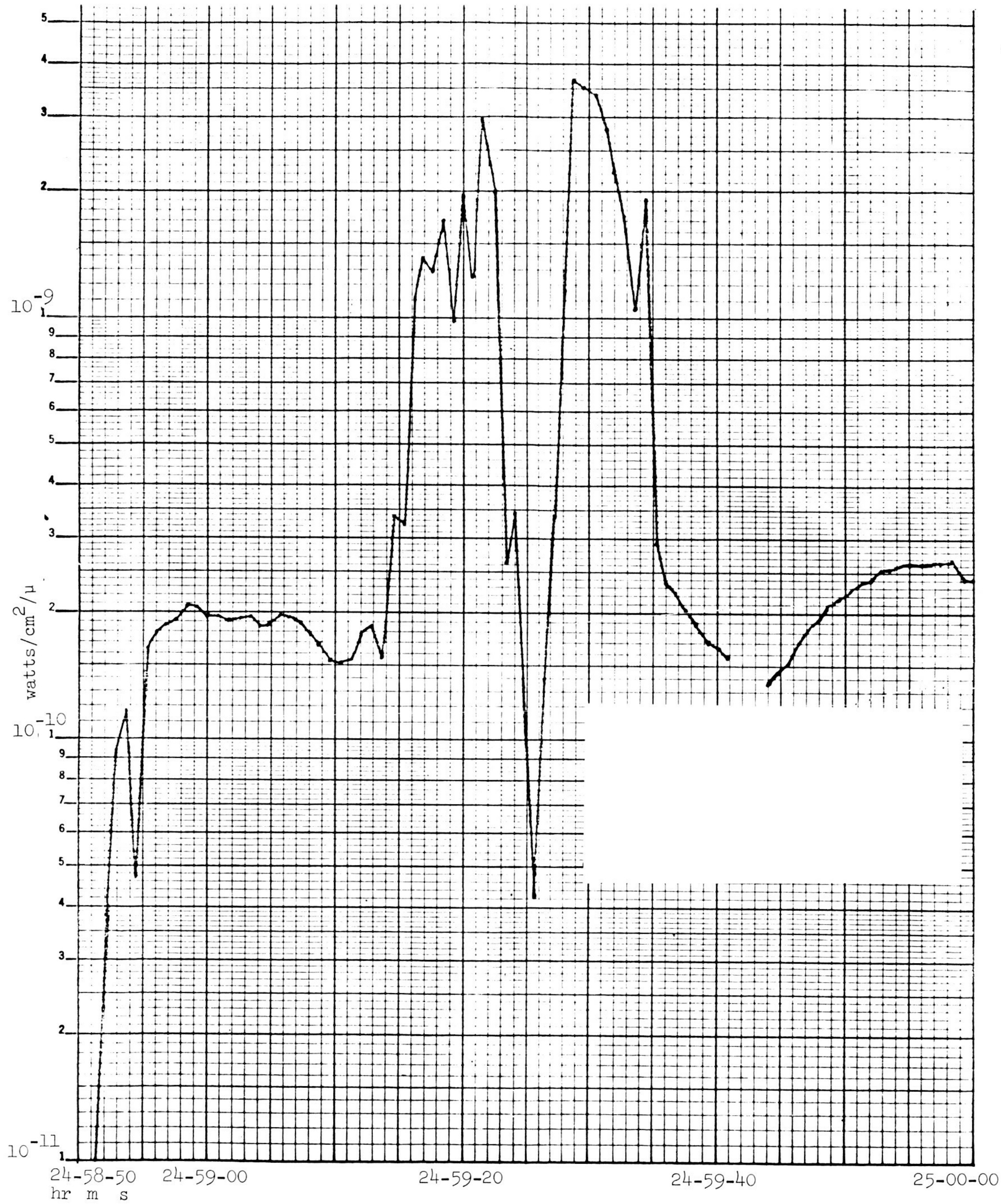

(b) Moon measurements during alinement check (4000 Å), made on Gemini V, revolution 16.

Figure 9-16.- Radiometer data from moon measurements.

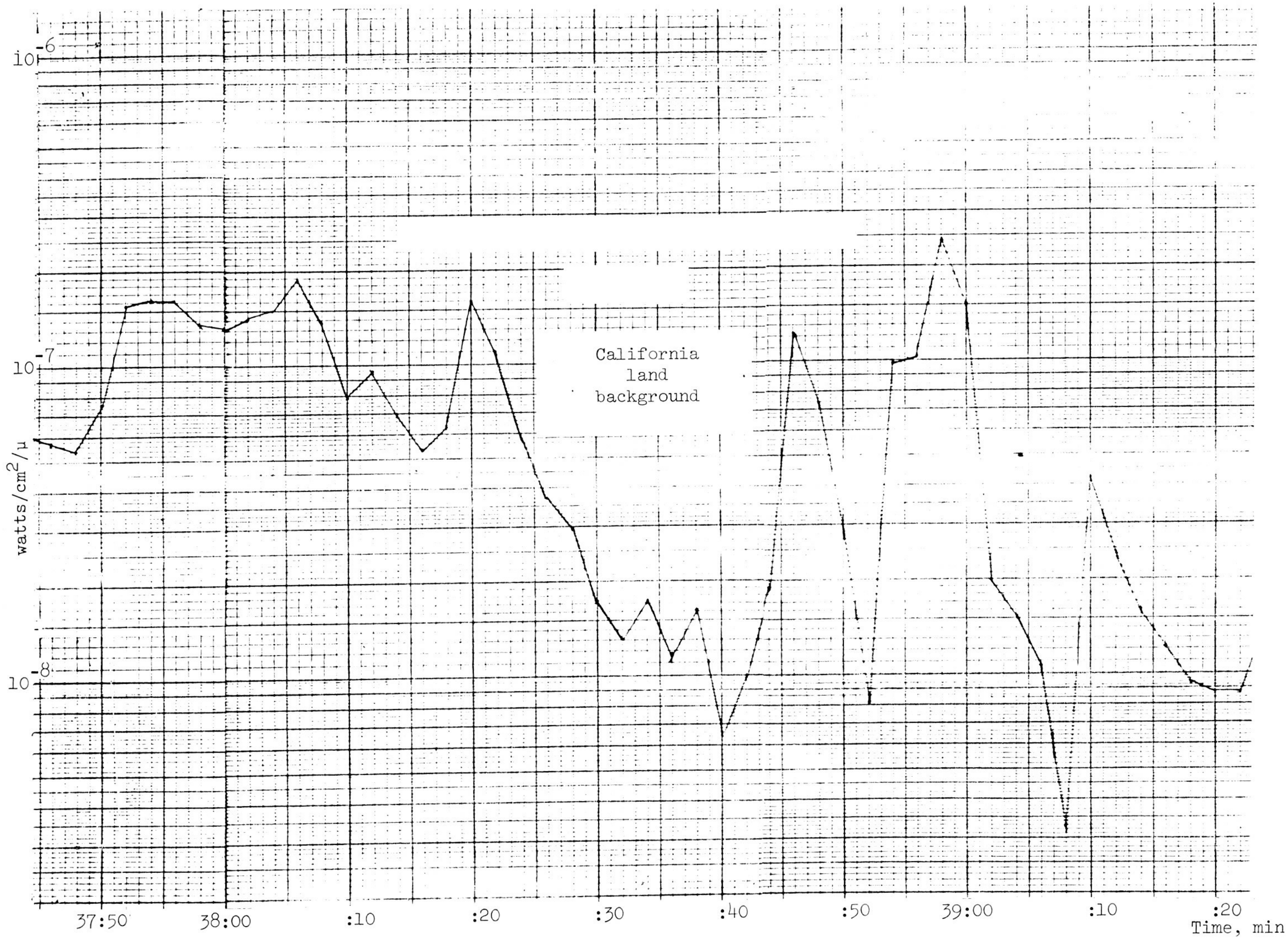

Figure 9-17.- Interoferometer spectrometer data (1.88μ).

10. EXPERIMENTS D1, D2, AND D6; BASIC OBJECT, NEARBY OBJECT, AND SURFACE PHOTOGRAPHY

By Col. D. McKee
Air Force Systems Command
NASA Manned Spacecraft Center

The purpose of Experiments D1, D2, and D6 is to investigate man's ability to acquire, track, and photograph objects in space and objects on the ground from earth orbit. These three experiments use the same equipment, and the experiment numbers primarily designate the type of object which serves as an aiming point. In Experiment D1 the aiming points were celestial bodies and the Rendezvous Evaluation Pod (REP), at relatively long photographic range. Experiment D2 designated the short-range tracking and photographing of the REP, and the D6 aiming points were objects on the ground.

The photographic system was designed to provide precise data on techniques of acquisition and tracking for possible future application to manned space flight. The equipment was selected to explore several techniques using different operational modes, different types of film, and lenses with different fields of view.

The equipment included the components shown in figure 10-1. The camera was a 35-mm Zeiss Contarex Special, incorporating single-lens reflex viewing, focal plane shutter, lens interchangeability, and removable film backs. An adapter was designed for fixed mounting to the right-hand window of the spacecraft. Due to the limited space in the cockpit, the adapter also provided a means of mounting the equipment vertically rather than horizontally. The two lenses were the 200-mm Nikkor with a field of view of 12°, and the Questar lens with a field of view of 1.8° and a focal length of 56 inches (1270 mm) to cover the 35-mm film format. The photograph event timer was designed to activate the shutter, advance the film, and provide time correlation on the Gemini digital tape recorder.

Two types of viewing devices were available: a periscopic reflex viewer and a telescope. The periscopic reflex viewer was attached to the ground glass of the reflex camera body and extended upward along the lens barrel. The telescope was attached to the adapter mount and provided a magnification of 4× with a field of view of approximately 9°. The telescope contained an inscribed cross hair and a reticle corresponding to the 1.8-degree field of view of the Questar lens. The periscopic viewer served as a secondary viewer for the Questar lens to test the ability of an astronaut to track an object under limited (1.8°) field-of-view conditions.

The three film backs contained Type 3400 Kodak Panatomic-X Aerial Film, Type 3401 Kodak Plus-X Aerial Film, and Type 8443 Kodak Ektachrome Infrared Aerial Film.

In figure 10-2 the system with the 200-mm lens is shown attached to the right-hand window. The system with the 1270-mm lens is shown in figure 10-3.

Figure 10-4 shows the optical sight mounted in the left-hand window for use by the command pilot. This sight is standard Gemini equipment, but it is also an integral part of these experiments. The optical sight is alined with the longitudinal axis of the spacecraft and with the line of sight of the camera, so that acquisition and tracking may be accomplished by maneuvering the spacecraft.

Since investigation of acquisition and tracking techniques was the primary objective of these experiments, two acquisition modes and three tracking modes were available. The two acquisition modes were:

(1) Visual. In this mode the command pilot acquired the object to be photographed by viewing through the optical sight.

(2) Instrument. In this mode the acquisition was accomplished by the use of pointing information from the ground and from the spacecraft attitude indicator.

The three tracking modes were:

(1) Visual. To evaluate this mode, the pilot sighted through the periscope or telescope and gave verbal cues to the command pilot to maneuver the spacecraft.

(2) Periscope. In the periscope mode, the pilot sighted through the periscope and maneuvered the spacecraft himself to accomplish the desired tracking.

(3) Telescope. In the telescope mode, the pilot maneuvered the spacecraft while sighting through the telescope.

On the Gemini V flight, Experiment D1 was accomplished using celestial bodies as aiming points. Distant photography of the Rendezvous Evaluation Pod, however, was not possible because of the spacecraft electrical power difficulties which developed after REP ejection. The planned D2 close-range photography of the REP was not possible for the same reason. The D6 terrestrial photography was accomplished within the limitations dictated by weather conditions and by spacecraft electrical and thruster problems.

The photographs obtained were significant only as an element of the data to be used in the evaluation of techniques. The other elements of data were time-correlated position and pointing information, atmospheric conditions, sun angle, exposure settings, and astronauts' flight logs and verbal comments. Figures 10-5 through 10-10 are representative of the photographs which will assist in the evaluation of the acquisition and tracking techniques employed in these experiments.

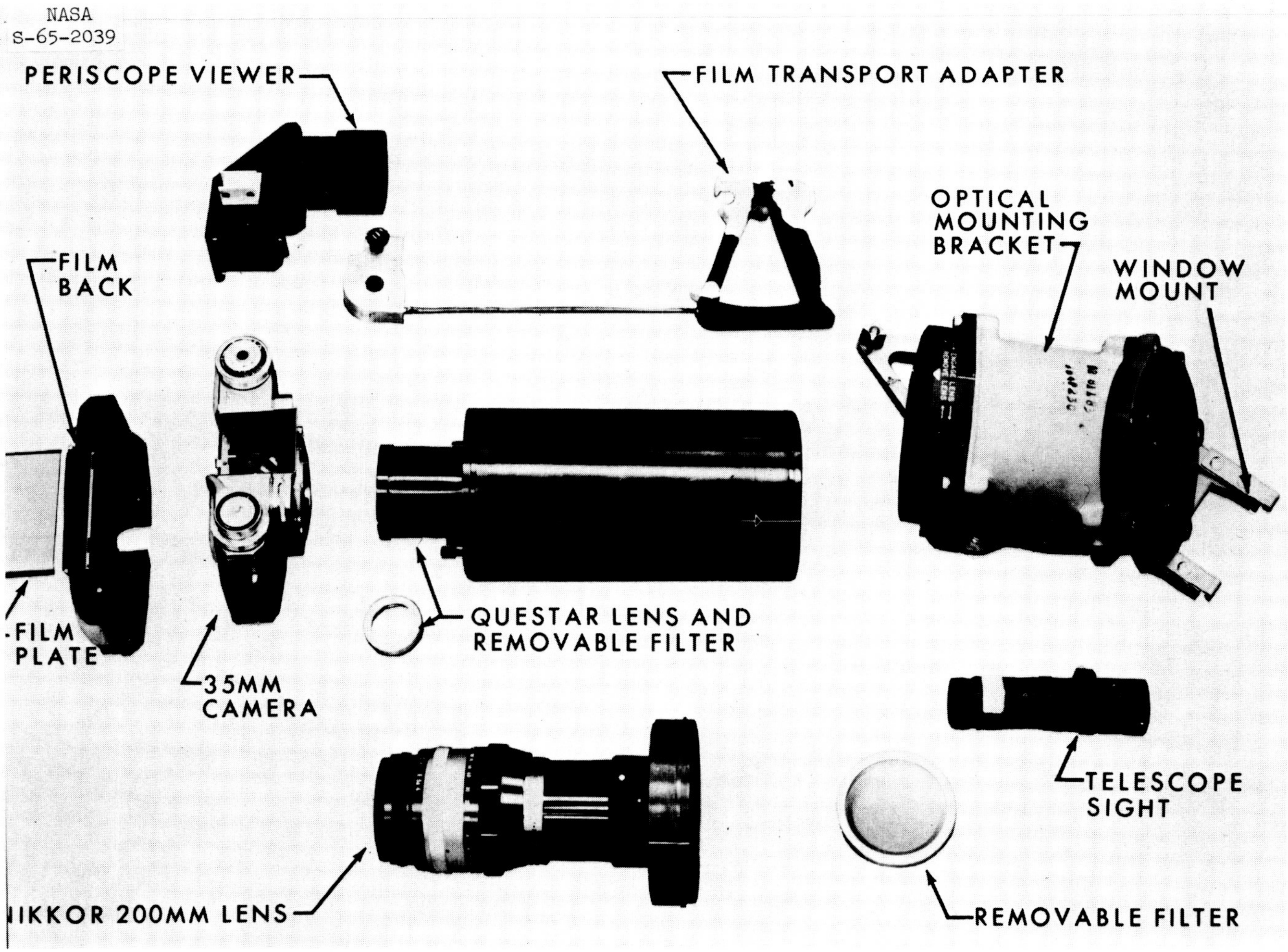

Figure 10-1.- Photographic equipment.

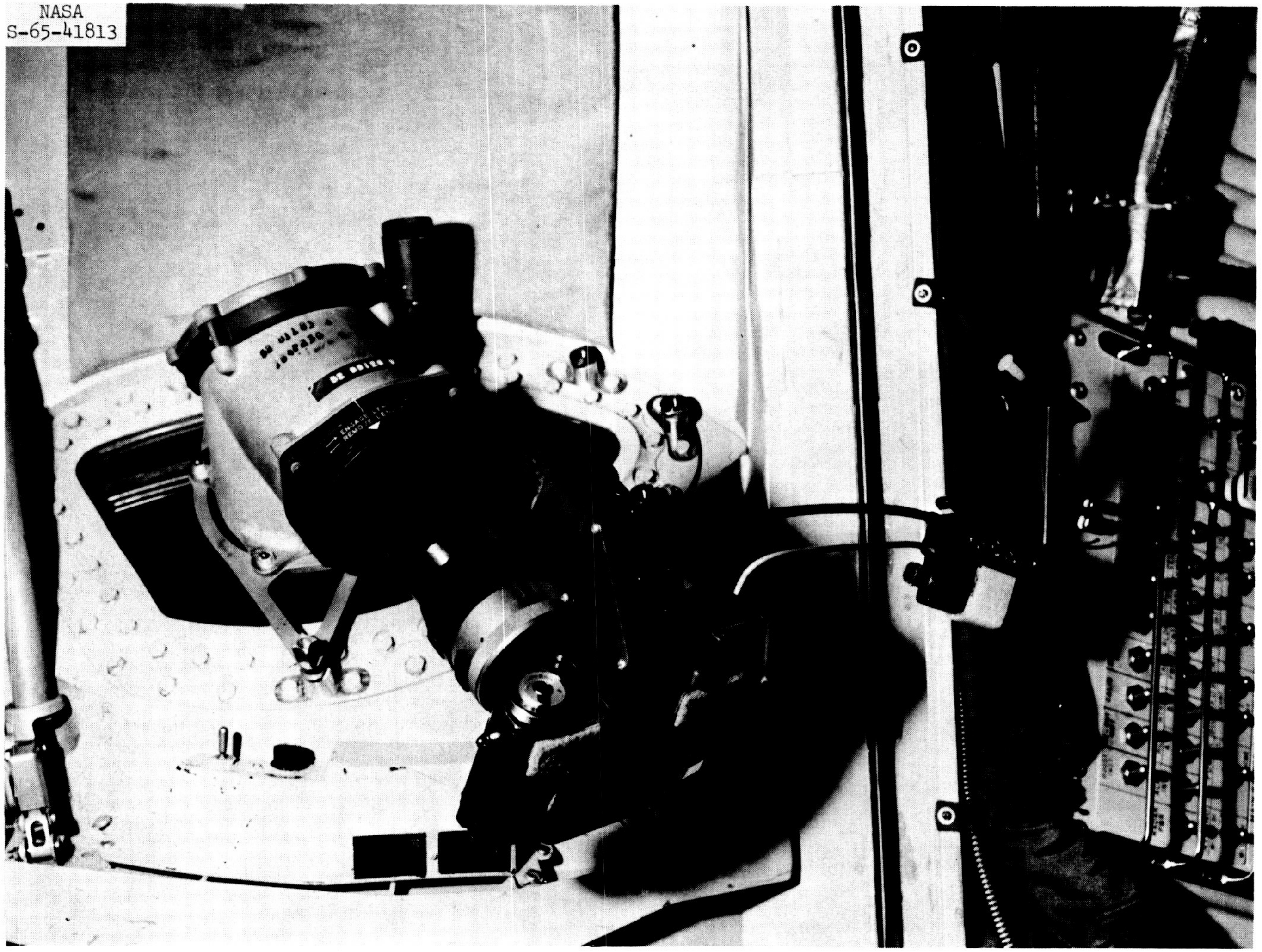

Figure 10-2.- Equipment installation with 20-mm lens.

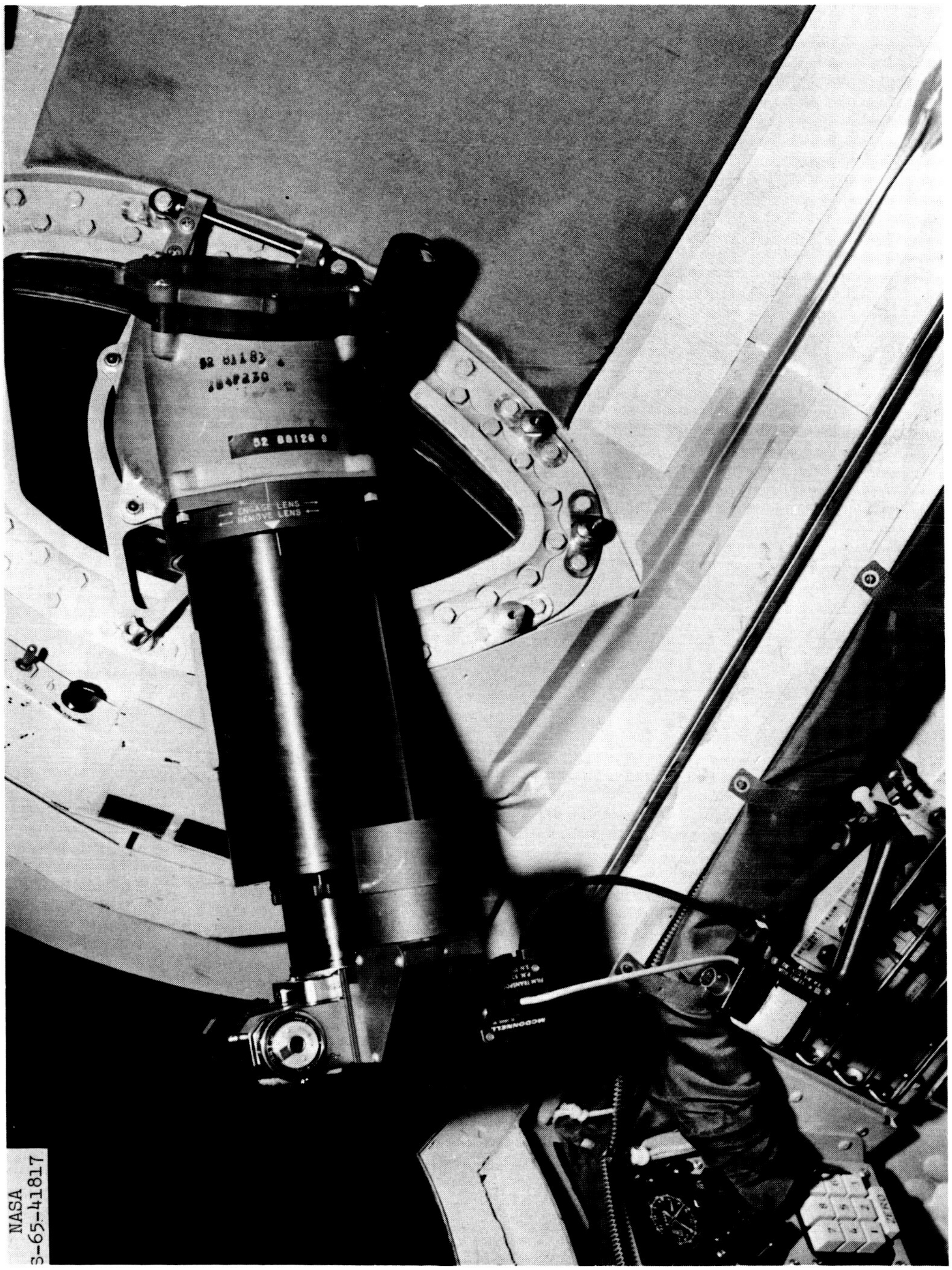

Figure 10-3.- Equipment installation with 1270-mm lens.

Figure 10-4.- Optical sighting device.

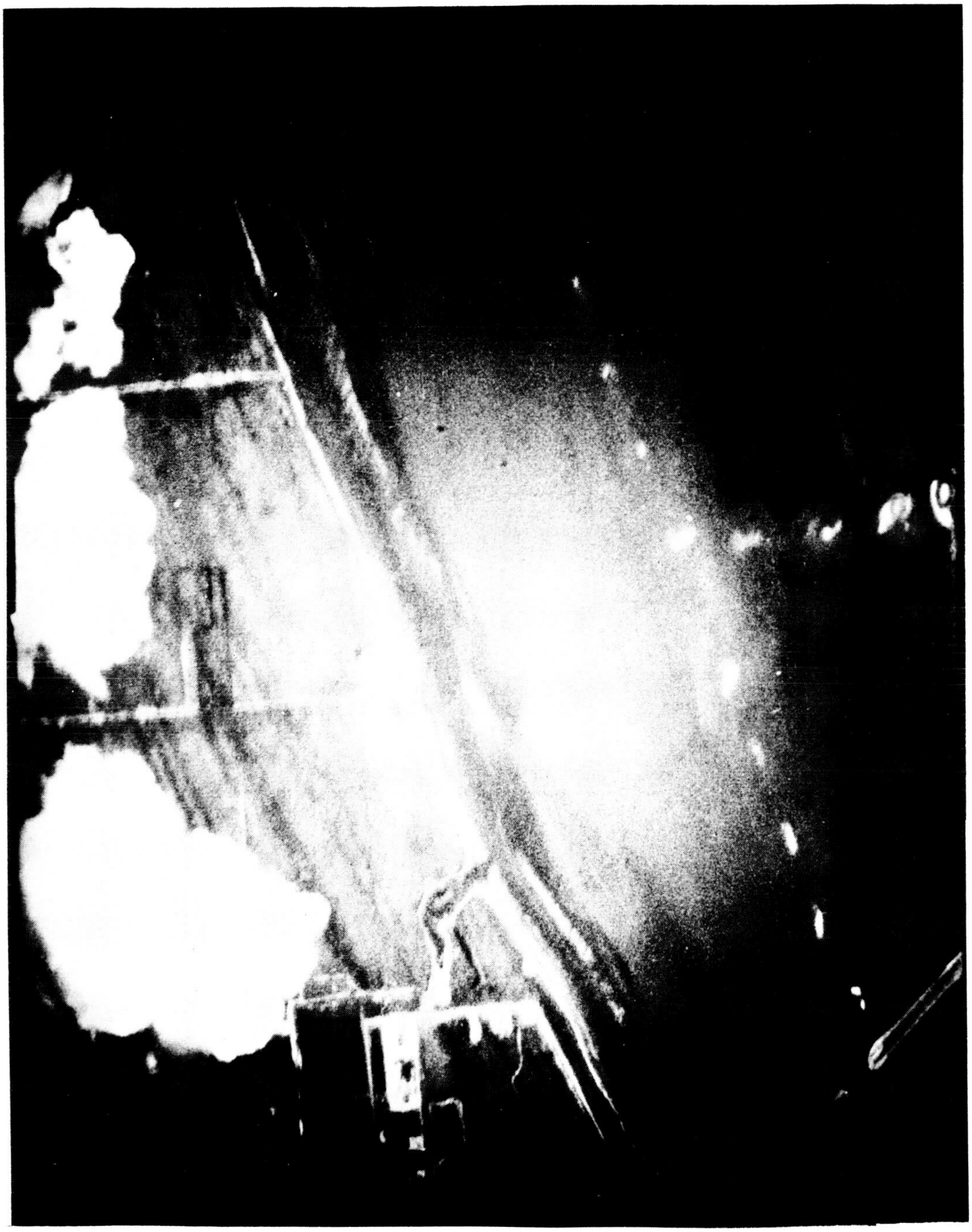

Figure 10-5.- Merritt Island, Florida.

Figure 10-6.- Rocas Island, Brazil.

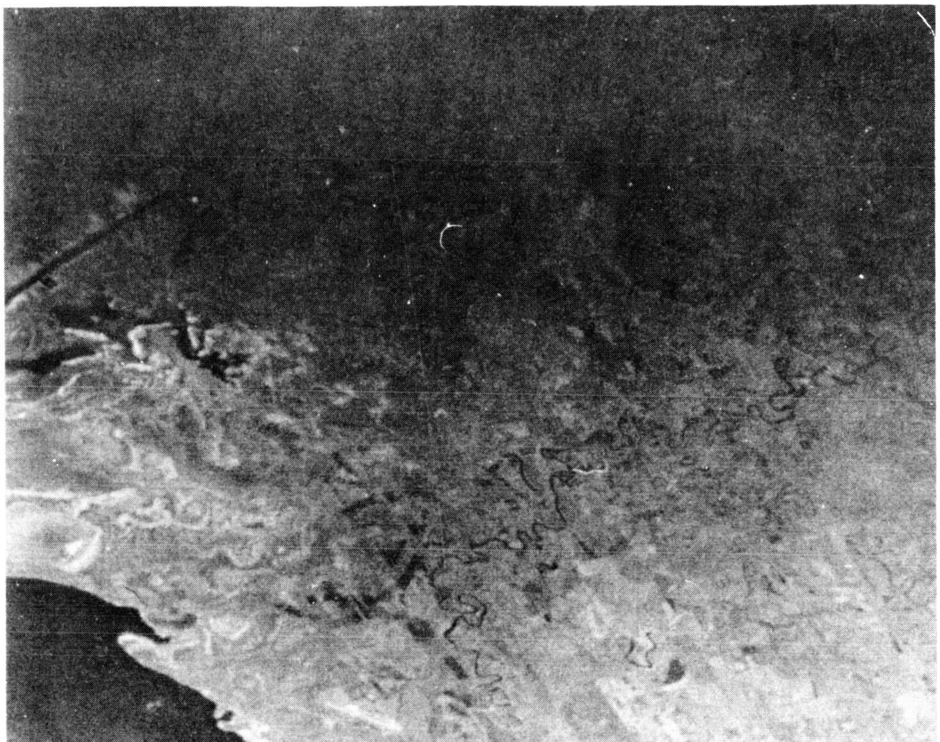

Figure 10-7.- Tampico, Mexico.

Figure 10-8.- Moon.

Figure 10-9.- Dallas, Texas.

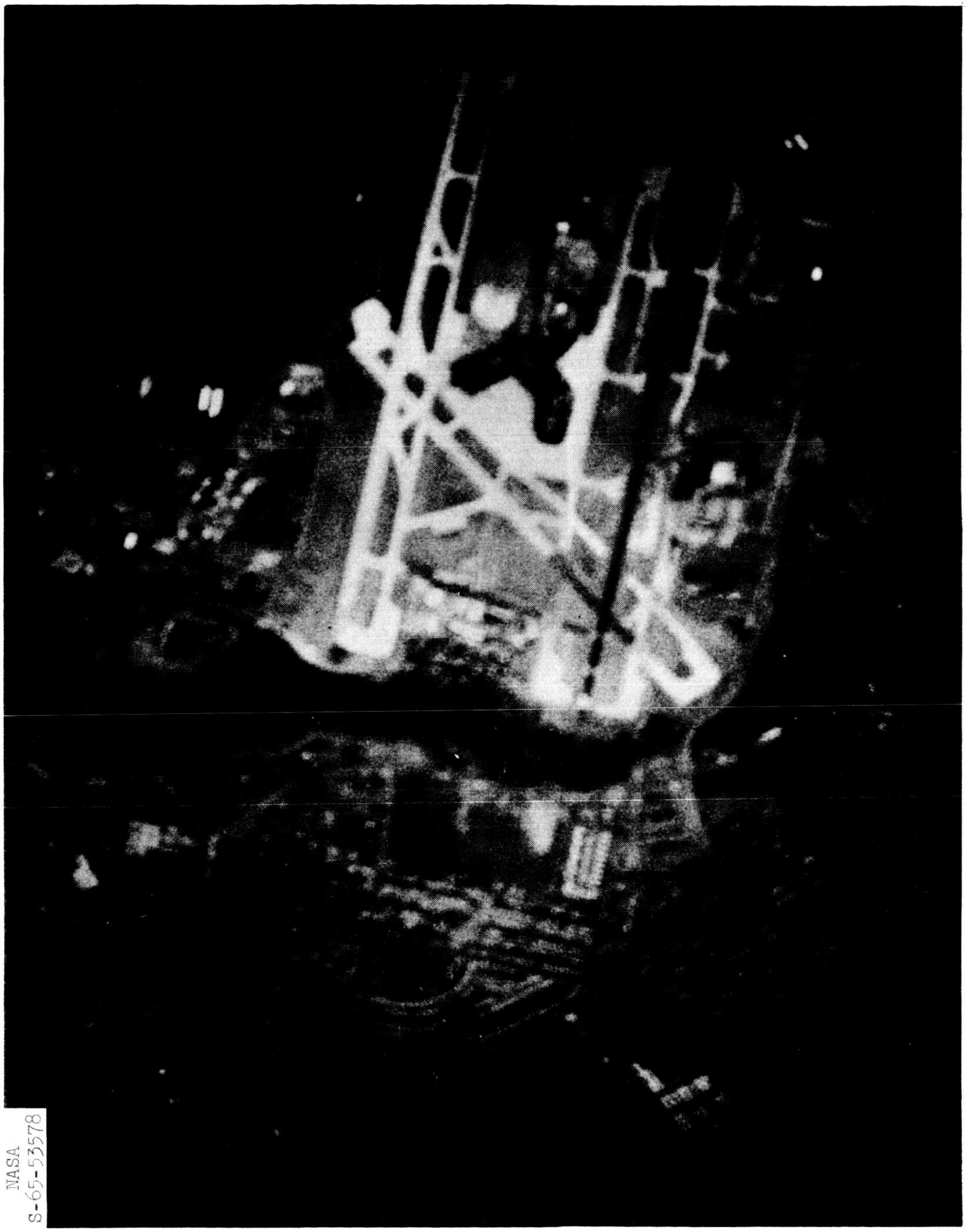

Figure 10-10.- Love Field, Dallas, Texas.